1

AN ALUMINUM SALVAGE STATION
FOR THE EXTERNAL TANK
(ASSET)

THESIS

GSE-90D

AFIT/GSE/ENY/90D-03

DISTRIBUTION STATEMENT A

Approved for public release;
Distribution Unlimited

DEPARTMENT OF THE AIR FORCE

AIR UNIVERSITY

AIR FORCE INSTITUTE OF TECHNOLOGY

Wright-Patterson Air Force Base, Ohio
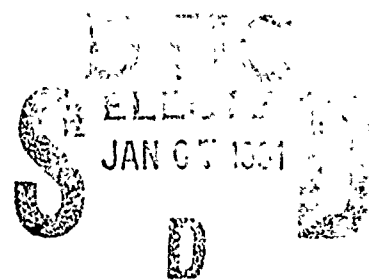
AFIT/GSE/ENY/90D-02

AN ALUMINUM SALVAGE STATION
FOR THE EXTERNAL TANK
(ASSET)

THESIS

GSE-90D

AFIT/GSE/ENY/90D-02

AN ALUMINUM SALVAGE STATION
FOR THE EXTERNAL TANK
(ASSET)

THESIS

Presented to the Faculty of the School of Engineering

of the Air Force Institute of Technology

Air University

In Partial Fulfillment of the

Requirements for the Degree of

Master of Science in Systems Engineering

James N. Haislip, Jr.
Captain, USAF

Roger E. Linscott
Captain, USAF

William C. Raynes, Jr.
Captain, USA

Michael A. Skinner
Captain, USAF

David L. Van Matre
Captain, USAF

December, 1990

Accesion For		
NTIS CRA&I		☑
DTIC TAB		☐
Unannounced		☐
Justification		
By		
Distribution /		
Availability Codes		
Dist	Avail a d / or Special	
A-1		

Preface

The purpose of this study was to determine whether the external tank of the Space Transportation System could be reduced to a form of readily usable construction material. Three methods of on-orbit reduction were developed and it is shown that low earth orbit salvage of the external tank is cost competitive with equivalent products launched from earth.

This study was sponsored by the Space Studies Institute (SSI), of Princeton, New Jersey. SSI has identified the need for ma erial at low earth orbit to support the construction of a demo platform to validate the design of a Solar Powered Satellite (SPS) and believed that salvage of a current throw-away item could provide a quicker, more cost effective means of providing the required m erial. We are indebted to Mr. Gregg Maryniak for the design topic, the initial zeal implanted in the design team, his thought provoking questions at design reviews, and, most importantly, for his ability to distance himself from the project and allow the design to be a product of our own creation.

Technical support was provided by Martin Marietta Manned Space Systems of New Orleans, LA., under contract number A71430, with SSI. Mrs. Faye Baillif, the Principal Investigator for External Tank Applications, proved to be an invaluable source of information. We are indebted to Faye for our tour of the New Orleans facilities, her support at the various design reviews, for obtaining answers from numerous sources throughout Martin Marietta, and, most importantly, for her quick response to every request we made. Clearly, we could not have maintained our schedules without the super efforts Faye consistently provided.

We wish to thank our principal advisor, Dr. Curtis H. Spenny, for his patience, guidance, and absolute accessibility. You were always there when we needed you and, for that, we are deeply indebted. We also thank the members of our Faculty

DEDICATION:

This effort is dedicated in memory of **Erica Michelle Haislip**, (13 February 1987 - 13 April 1990). Little Erica was struck by a car on the afternoon of 12 April, and passed away the following day. God has given the Haislip family the strength to carry on and we look forward to the day when Jim and Debbie can hug their little girl again.

GSE-90D

Table of Contents

List of Figures

List of Tables

AFIT/GSE/ENY/90D-02

Abstract

The external tank is currently the only non-reusable portion of the Space Transportation System. The tank already has 98% of the energy required to be placed in orbit at the point where it is jettisoned. The purpose of this study is to develop techniques which would transform a current throw-away item into a source of construction material at low earth orbit.

A SLAM simulation is developed to verify the reduction timelines and peak power requirements for both manual and automated reduction. The required tools to accomplish the tasks of initial cutting, piece part transport, spray on foam insulation (SOFI) removal, and product storage are developed. A trade study is conducted to determine the proposed method of power generation. Orbit models are developed to project the annual facility fuel requirements, predict the orbital decay of the facility, and estimate the orbital decay rates of any debris which may be generated during the salvage operation. A thermal model is developed and the thermal impacts of on-orbit salvage are included in all scenarios.

A probabilistic cost model is developed and life cycle costs are projected based upon reducing four tanks per year. It is shown that more than 52,000 lbs of readily usable construction material in the form of I-beams and plate can be salvaged on an annual basis in a manner that is cost competitive when compared to equivalent products launched from earth.

AN ALUMINUM SALVAGE STATION
FOR THE EXTERNAL TANK
(ASSET)

I. INTRODUCTION

The continued evolution of manned space flight will be dependent on a host of enabling technologies. Further major advances in manned space operations will continue to be hampered though, unless a way is found to lower the cost of transporting large quantities of material and equipment from Earth to orbit. The purpose of this thesis is to show the feasibility of using the National Space Transportation System (NSTS) External Tank (ET) to develop some of these enabling technologies, and answers a recent call by the National Space Council for innovative ways to lower the cost of conducting business in space.

The Space Studies Institute (SSI), a non-profit research organization founded by the physicist Gerard K. O'Neill, regularly promotes the use of such innovative concepts as solar power satellites (SPS) (29), mass drivers (3), and the on-orbit utilization of spent Space Shuttle external tanks (28). Early research has led SSI to believe that the economic viability of the SPS concept requires the use of non-terrestrial resources and initial emphasis was placed on the use of lunar materials to supply the raw materials required to build these massive structures. Further analysis has prompted SSI to investigate the use of the external tank (ET) as a potential source for some of this material or for the construction of a SPS demonstration platform.

SSI, in identifying the need for construction material at low Earth orbit (LEO), approached the Air Force Institute of Technology's Aeronautics and Astronautics Department with the question:

Can an ET be reduced to a useful raw material in a cost competitive manner when compared with launching the same material from the Earth's surface?

By taking a systems engineering approach to this question, a design team of one Army and four Air Force Officers have answered that question with a resounding yes.

The external tank is currently the only non-reusable portion of the NSTS. The tank reaches roughly 98% of the velocity required for orbital insertion when it is jettisoned for a splashdown in the Pacific Ocean. Neglecting the residual fuels at the jettison point, the ET has a mass of over 69,000 pounds, 80% of which is in the form of aerospace grade aluminum. While the idea of salvaging the ET is not new, the techniques developed in this study represent a fresh look and a novel approach at actual tank reduction. Three scenarios are developed to allow on-orbit salvage of the ET aluminum. Although all three scenarios presume the existence of Space Station Freedom (SSF), only one scenario demands SSF hardware for its success.

An overall system level study was initiated to identify the key technologies and hardware components required to carry out the salvage operation. These included cutting technologies, the provision of power for all phases of the operation, orbital maintenance hardware requirements, Extra-Vehicular Activity (EVA) technologies, and other special tooling requirements.

A process simulation, using SLAM II as the simulation language, is developed to estimate the tank reduction timelines and peak power requirements. A trade study is then conducted to identify viable candidates as sources of power generation. A

thermal model is developed and the thermal impacts of on-orbit salvage are included in all scenarios.

The necessary tools to accomplish the tasks of initial cutting, product/tool transportation, spray on foam insulation (SOFI) removal, and product storage are developed. The tool design is straightforward and well within today's state of the art. An orbital mechanics model is developed to estimate the orbital decay of the facility and the orbital lifetime of any debris which may be generated during the salvage operation. The model also produces estimates of the facility's annual fuel requirements.

A probabilistic cost model is developed and life cycle costs are projected based upon reducing four tanks per year. It is shown that more than 52,000 pounds of readily usable construction material in the form of I-beams and plate can be salvaged on an annual basis in a manner that is cost-effective when compared with equivalent products launched from Earth.

II. SYSTEMS ENGINEERING APPROACH

2.1 Introduction

The systems engineering approach is a systematic application of problem solving techniques that is employed to solve complex problems that span a wide range of disciplines (57:12). There is no standard framework for the systems engineering approach, although many methods have been proposed. We chose to structure this systems engineering study following Hall's Morphology (after Arthur D. Hall) (82:3-4), a problem solving technique that decomposes the system into three dimensions: time, logic, and knowledge. The time dimension represents the life of a system from its inception to its retirement. The logic dimension consists of seven problem solving steps, from problem definition, through decision making, to implementation of the decision. Together, the time and logic dimensions are described by what is known as Hall's activity matrix, shown in Figure 2.1, (82:69). The third dimension refers to the knowledge from various professions or disciplines required to solve the problem (81:499).

2.2 Value System Design

A critical step in following Hall's Morphology is the development of '...the set of interacting elements which provide a basis for decision making (82:69).' This is known as value system design. The value system is comprised of five elements: needs, alterables, constraints, objectives, and objective measures. Needs are qualities of the system that are required or desired in the final design, alterables identify the design variables to be optimized, while constraints define the range of the design variables. A sixth element is sometimes used to describe the societal effects on the system; these players are formally called societal sectors (33:613).

Steps of the fine structure — Logic → / Phases of the coarse structure — Time ↓	Problem definition	Value system design	System synthesis	Systems analysis	Rank (optimize) alternatives	Decision making	Planning for action
Program planning							
Project planning							
System development							
Production							
Distribution							
Operations							
Retirement							

Figure 2.1. Hall's Activity Matrix

2.2.1 Needs. There are two type of needs; something required, useful, or desired in the design of the system, or a condition that requires supply or relief (82:79). The following list of needs were developed as the problems associated with reducing the ET were analyzed.

1. A source of construction material at LEO.

2. A facility to convert the ET to a source of construction material.

3. Feasible methods of converting the ET to construction material.

4. Cost effective methods of converting the ET to construction material.

5. Quantify the amount of construction material available from an ET.

2.2.2 Alterables. Alterables are those items pertaining to the needs which can be changed as the system design evolves (82:81). The alterables identified in this study are:

1. Level of autonomy of the salvage facility.

2. Life span of the system.

3. Tank reduction methods.

4. Methods to minimize debris.

5. Methods of power generation for the facility.

6. Orbit and location of the facility.

7. Methods of residual fuel removal and storage.

8. EVA time required for the initial setup of the facility.

9. Methods of stabilization and control.

10. Methods of aluminum and scrap storage.

11. Percentage of shuttle payload required for initial setup.

12. Methods of SOFI removal, containment, and storage.

13. Methods of converting aluminum to a finished product.

2.2.3 Constraints. Constraints define the range over which the alterables can be varied or the requirements under which the needs can or must be satisfied (82:82). The constraints identified in this study are:

1. The facility will not be permanently manned.

2. The facility will be setup and operational in one shuttle mission.

3. EVA will not exceed eight hours per every 24 hours of mission time.

4. No more than four external tanks will be available for salvage per year.

5. No high risk or undeveloped technologies will be considered in the design.

6. Minimal pre-flight modifications will be made to the ET.

7. Total orbiter mission time will not exceed ten days.

8. Initial facility orbit and location is dependent upon the orbiter's capabilities.

2.3 Development of Objectives and Objective Measures

The process of designing the value system includes three important steps which are critical to the decision making process. First objectives must be defined and placed in a hierarchy, as shown in Figure 2.2. Second, the objectives must then be related to the needs, alterables, and constraints. Finally objective measures must be developed to determine how well objectives are satisfied (82:71). Objective measures allow the various alternatives being considered to be compared in a quantifiable way; each alternative is evaluated based on how well it meets the objectives established for the system. A common set of objective measures forms the baseline by which all alternatives can be evaluated and the best can be chosen. Figure 4.1 explains the interactions between the various models used in our analysis of the three reduction scenarios in terms of how well each scenario met our objectives. The primary objective of this study is to develop the best possible salvage operation which allows the ET to be a viable source of construction material at LEO. With this objective in mind, and considering the needs described above, the following system level objectives were developed:

- Minimize the technical complexity of the facility.

- Minimize the amount of debris produced during salvage.

- Maximize the net present value of the reduction facility.

- Minimize the life cycle costs of the reduction facility.

- Maximize the amount of salvaged construction material.
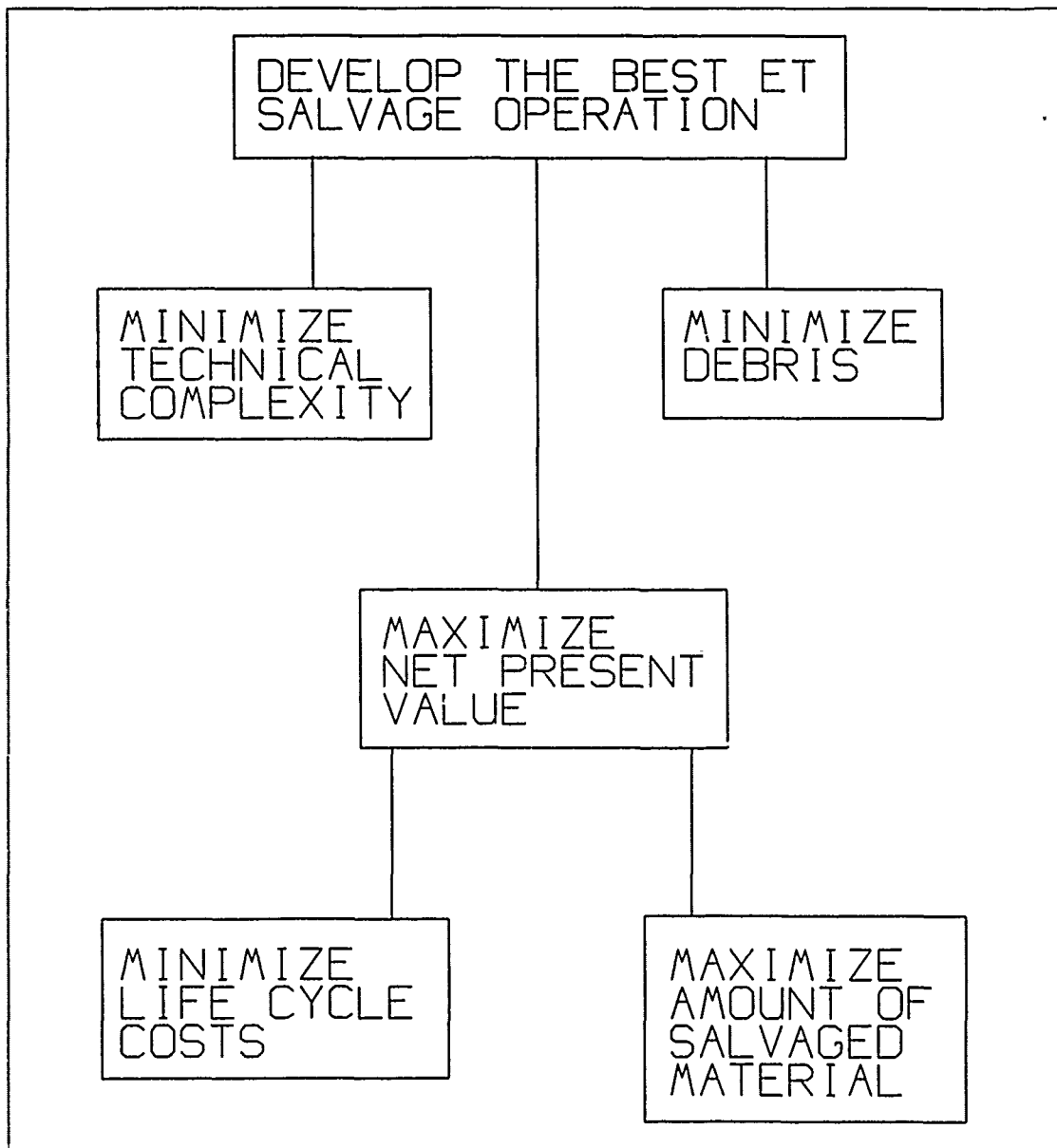
Figure 2.2. Objective Hierarchy

2.3.1 Minimum Technical Complexity. The objective to minimize technical complexity is based on the need for cost effective salvage methods. Keeping the facility design simple will help keep design and development costs lower as well as allow for improved reliability. Technical complexity can be loosely translated as technological risk. Technological risk includes the risk of using unproven or undeveloped technologies, and the risk of using a complicated design for a given reduction scenario. The model developed in Chapter VIII is the tool used to measure the technical complexity associated with each reduction alternative.

2.3.2 Minimum Debris. Debris is a concern due to the possibility of damage to space based platforms, such as the orbiter, space station, and other satellites, as well as to the ASSET reduction facility. A 'dirty' reduction operation is not as likely to be accepted as feasible. The objective, to minimize debris, is measured for each reduction scenario based on four criteria:

- Facility orbit/altitude where reduction is conducted.

- Cutting methods used to reduce the ET.

- SOFI removal, storage, and disposal methods.

- Storage and disposal methods of unsalvaged portions of the ET.

2.3.3 Maximum Net Present Value. The need for a cost effective method of converting the ET to construction material translates into the objective to maximize the net present value of the reduction facility. For our analysis, the net present value of the facility is based on the difference between the life cycle costs of the facility and the expected launch cost of the construction material produced by a given scenario. The launch cost of the product is used as an effective revenue stream. The cost model developed in Chapter IX measures the net present value of the reduction facility for each scenario. The life cycle cost and amount of construction material produced by a given scenario are direct inputs into the cost model.

2.3.4 Minimum Cost. The objective to minimize lifecycle costs is based on the need for a cost effective means of converting the ET to a source of construction material. It is directly related to the objective to maximize the net present value of the reduction facility. The cost model developed in Chapter IX is the tool used to measure the life cycle costs of the three alternative reduction scenarios and to determine the net present value of each reduction scheme. This is done for each scenario, using the expected launch cost of the product as an effective revenue stream. The overall measure of comparison for each scenario is to determine if the costs associated with producing construction material in LEO, with the ASSET concept, are less than the costs associated with transporting the same amount to LEO from earth.

2.3.5 Maximum Product. The amount of readily usable construction material from each scenario is an easily measured item that allows for a fair assessment of how efficient each scenario is in terms of the amount of material produced. The expected launch cost of the product is used as the effective revenue stream for each scenario. It is a direct input into the cost model(see Chapter IX). The more products available from an ET, the more efficient the scenario.

III. EXTERNAL TANK DESCRIPTION

The External Tank (ET) is the only expendable element of the Space Shuttle vehicle. The ET not only contains and supplies the liquid hydrogen (LH$_2$) and liquid oxygen (LO$_2$) for the Orbiter's main engines, it has also been designed to act as the structural backbone of the Space Shuttle during launch operations.

The External Tank, 153.8 feet long by 27.6 feet in diameter, weighs just under 69,000 pounds empty and nearly 1,660,000 pounds when fully loaded with propellants. The surface of the tank is coated with a Spray-On Foam Insulation (SOFI), giving the ET its characteristic burnt-orange appearance. The tank is composed of three primary structural elements: the LO$_2$ tank, the intertank, and the LH$_2$ tank (see Figure 3.1, (50)). The basic structure of the tank is made primarily of 2024, 2219, and 7075 aluminum alloys.

3.1 LO$_2$ Tank

The LO$_2$ tank (see Figure 3.2, (50)), with a volume of 19,563 ft^3, is a thin-wall monocoque shell structure designed to contain approximately 1.4 million pounds of oxidizer. It measures roughly 655 inches in length with an outside diameter of 331 inches. The tank is a fusion-welded assembly of machined and formed panels and rings, consisting of an aft dome, a slosh baffle, a barrel section, a T ring, forward and aft ogive sections, and a nose cone. Being the forwardmost element of the ET, the LO$_2$ tank has been designed with an ogive shape to reduce aerodynamic drag. The ogive shape is joined at its aft edge to a short cylindrical section, which is in turn joined to a modified 0.75 ellipsoidal dome.[1] This basic dome shape is also used for both the forward and aft LH$_2$ domes. The ogive nose section is capped by a removable cover plate and nose cone. The cover plate is mated to the ogive forward

---

[1]An 0.75 ellipsoid is one where the ellipse of revolution has a height x to radius y ratio of 0.75.
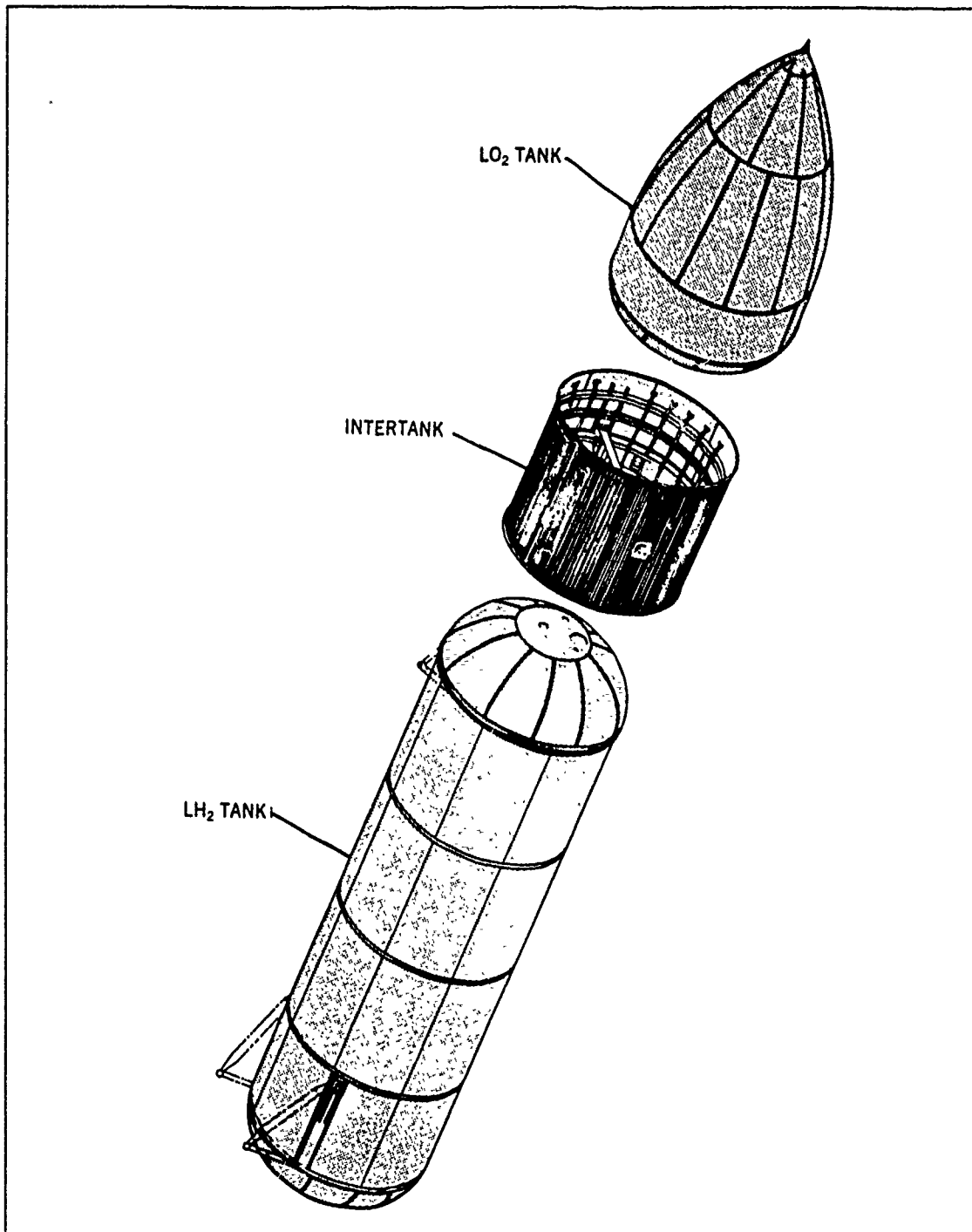
Figure 3.1. External Tank Structure

fitting with ninety two 5/16-inch diameter bolts, while the nose cone is attached with seventeen 5/16-inch bolts.

The LO_2 tank also includes a manhole in the dome cap for tank access, an internal slosh baffle to minimize fuel slosh, and a vortex baffle at the LO_2 outlet. The manhole provides a 36-inch diameter clear access to the tank interior. Additionally, a cable tray and pressurization lines are mounted external to the LO_2 tank structure.

The cylindrical barrel section is 98.2 inches long and is fabricated from four chem-milled and formed panels welded together. The skin thickness on the two side panels are tailored to accommodate the Solid Rocket Booster (SRB) thrust loads; in general, skin thickness tapers longitudinally (with the heavier gauges toward the aft end of the tank) in order to withstand both hydrostatic and ullage loads. The reduction of this section of the LO_2 tank appears to be a viable option, given certain mission planning assumptions.

3.2 Intertank

The intertank (Figure 3.3, (50)) is the structural connection between the LO_2 and LH_2 tanks. It is a skin/stringer/frame structure of cylindrical shape with external stringers and internal frames. The intertank's primary functions are to receive and distribute all thrust loads from the SRBs and transfer loads between the propellant tanks. The intertank consists of eight 45 degree mechanically joined panels, a main ring frame, four intermediate ring frames, and an SRB beam assembly. Weighing roughly 12,200 lbs, the only non-aluminum components of the intertank are steel fasteners and SRB fitting socket inserts.

Additionally, the intertank serves as a compartment for housing instrumentation and range safety components. Access into the intertank compartment can be gained through a nonstructural 52 inches high by 46 inches wide access door.[2] Prior

---

[2]The opening measures 48 inches high by 42.7 inches wide.
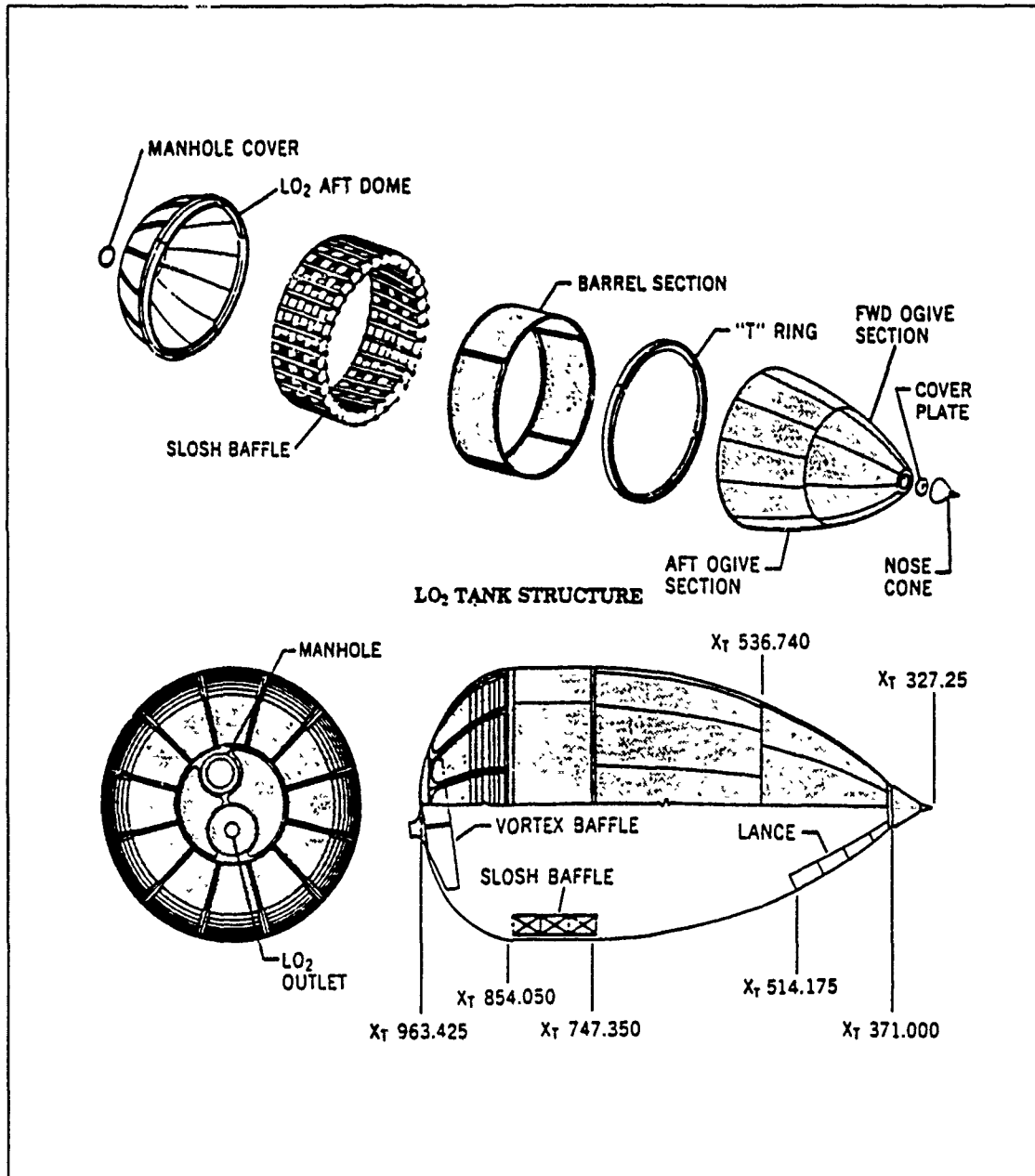
Figure 3.2. LO$_2$ Tank Structure

AFT FLANGE

SKIN/STRINGER PANEL (6)

FORWARD FLANGE

THRUST PANEL (2)

MAIN RING FRAME

SRB BEAM

INTERMEDIATE RING FRAME (4)

SRB THRUST FITTING (2)

FWD

ACCESS DOOR
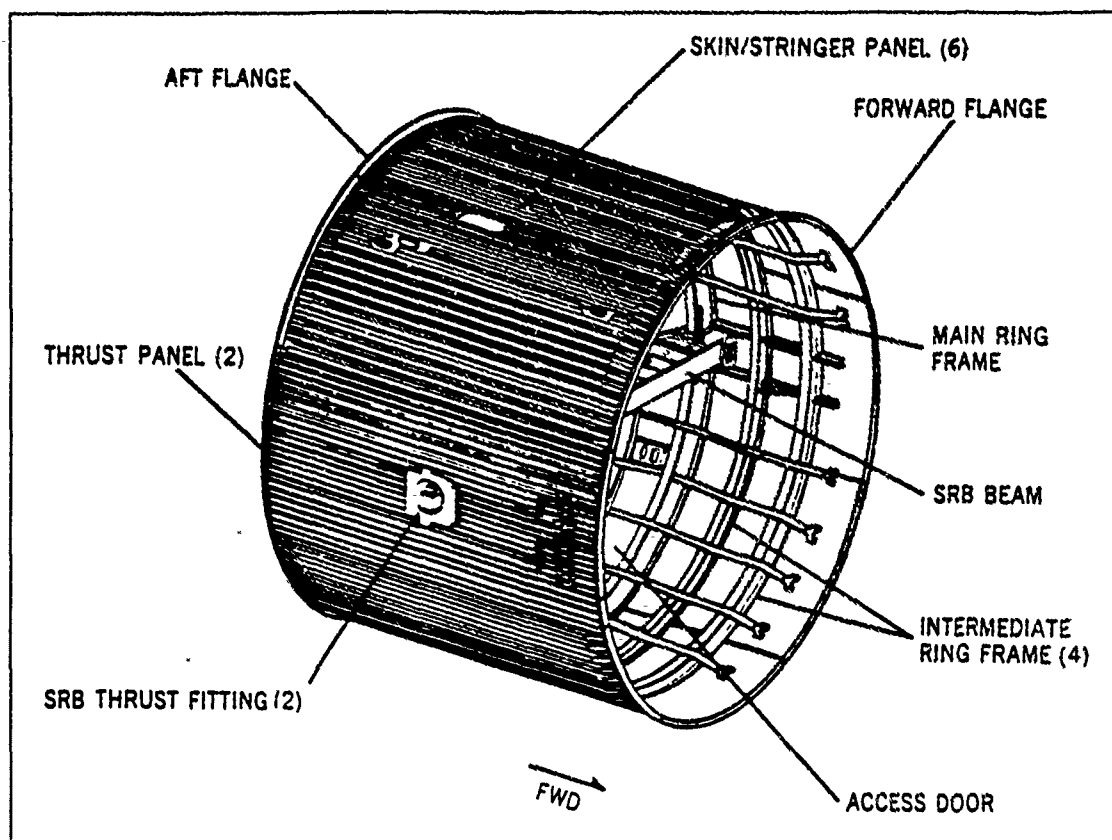
Figure 3.3. Intertank Structure

to launch, the intertank compartment can be outfitted with operational hardware so that requirements for cargo space in the Orbiter payload bay can be minimized.

The intertank will serve as a strongback for the ASSET facility. Solar arrays and orbital maintenance hardware will be attached to the intertank, taking advantage of its structural rigidity. Attachments will be made at the SRB thrust fitting. Subsequent tanks identified for salvaging must be outfitted with orbital deboost hardware (54); the hardware will be physically attached to the intertank assembly prior to launch. This will allow for the deorbiting of any unusable scrap material and it is assumed that a single structure will be deorbited.

3.3 LH_2 Tank

The LH_2 tank (Figure 3.4, (50)) is a fusion-welded assembly consisting of forward and aft domes, four barrel sections, and five major ring frames. Designed to contain some 227,000 pounds of propellant, the LH_2 tank weighs approximately 28,000 pounds and has a volume of over 53,000 ft^3. It is over 1160 inches long with an outside skin diameter of 331 inches. Eight intermediate ring frames serve to stabilize the barrel skins, while two longerons are installed in the aft barrel section to receive Orbiter thrust loads.

The LH_2 barrel sections, fusion-welded assemblies made from eight integrally stiffened skin panels, are joined by fusion butt welds at the five major ring frames. The skin panels are machined from plate stock with longitudinal stiffeners remaining as an integral part of each skin panel. The barrel sections of the LH_2 tank provide the vast bulk of readily recoverable aluminum during the salvage operation.

One can see how the barrel sections readily lend themselves to some form of automated reduction. Figure 3.5 (50) clearly shows the relationship between the integral T-shaped stringers and barrel skin sections. Cutting the skin out from between the T-stringers, and then making circumferential cuts at either end of the barrel[3] section produces two rather interesting products: slightly curved $\frac{1}{8}$" thick plate,[4] and 1.25 inch by 1.25 inch I-beams.[5] This observation had a major impact on the direction our study would take.

---

[3]The specifics of the reduction process are covered in Chapters 4-7.

[4]Roughly 9.5 inches wide by 182 inches long, depending upon the barrel section.

[5]Web thickness of 0.1", flange thickness of 0.125", and length of 182".

Figure 3.4. LH$_2$ Structure

Figure 3.5. LH$_2$ Barrel Section
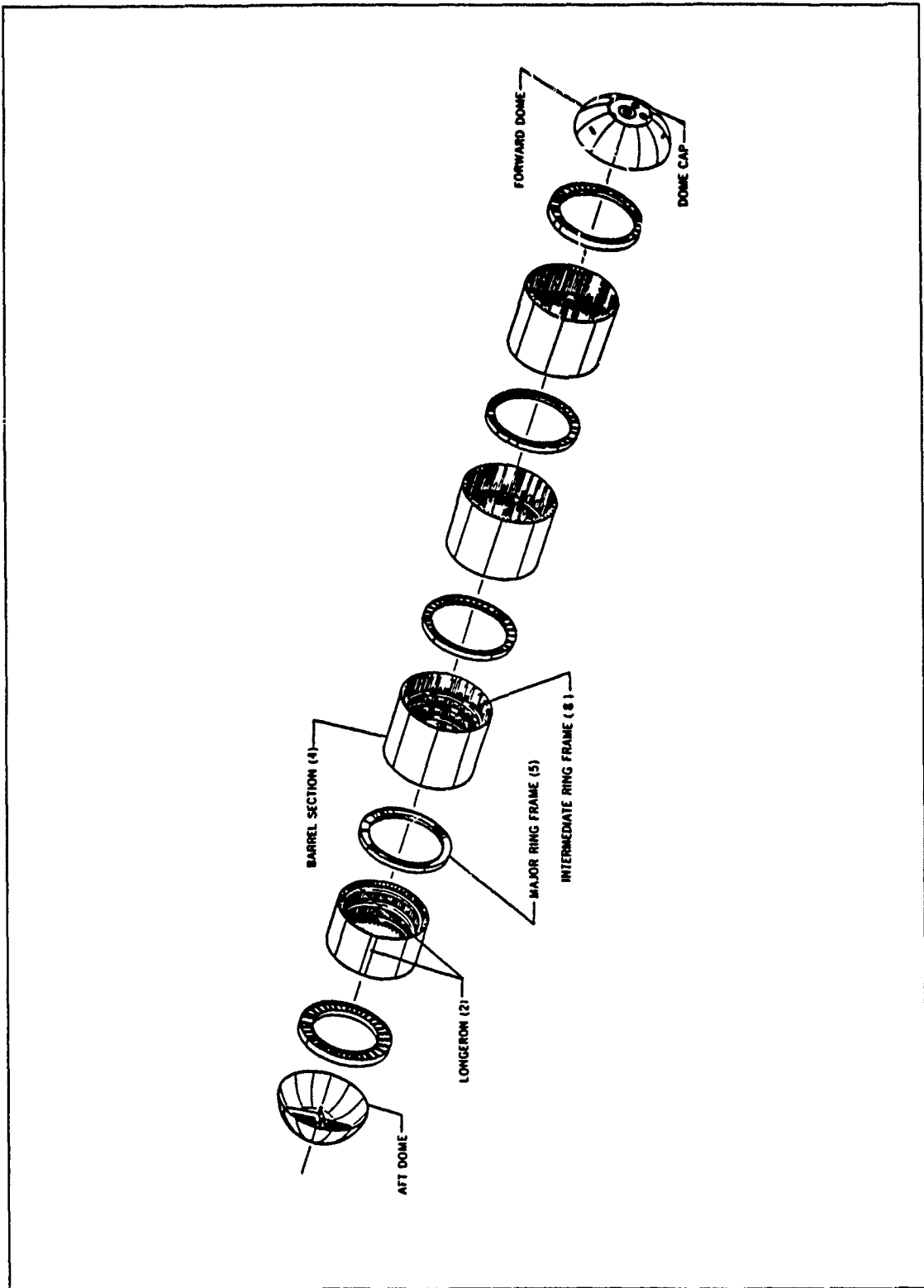
IV. SCENARIO DEVELOPMENT - OVERVIEW

4.1 Introduction

This chapter is intended to briefly preview the three scenarios which will be developed in detail in the following three chapters. In the interest of brevity, the emphasis here will be placed on the distinguishing characteristics of each scenario. One unique distinction of the ASSET concept (from other groups which have contemplated tank reduction (17, 28)) is that all scenarios accomplish the initial reduction from the inside of the tank.

4.2 Scenario 1 - Automated Reduction

The distinguishing characteristics of Scenario 1 are the pre-installation of a centerline track down the middle of the LH_2 tank and the absence of astronauts during the actual reduction operation. A cutter rides the stringers within the LH_2 tank and cuts out pieces of stringer and plate (which will still have the SOFI attached). An extending (prismatic-revolute-prismatic [PRP]) robot arm is attached to a trolley mounted on the centerline track to provide product/tool transport. The robot arm initially picks up the composite (plate, I-beam, and SOFI) strips as they are cut out and carries them to the SOFI workstation. The SOFI workstation removes the SOFI, stores the removed SOFI, provides a secondary cut to separate the stringers from the plate, and stores the separated products in their respective containment equipment.

The process is repeated until an entire barrel section of the LH_2 tank has been cut up into a predesignated number of pieces. Portions of each barrel section will be left to maintain the structural integrity of the overall facility. It will be shown that some 6,125 linear feet of stringers and 4,859 ft^2 of plate can be salvaged from a single tank within 40.8 hours of actual reduction time over the course of a 6.3 day

4-1

orbiter mission. The 40.8 hours would be preceded by 16 hours of 2 man EVA and the peak power required during the salvage operation would not exceed 11.5 kW.

4.3 Scenario 2 - Manned Reduction

The distinguishing characteristics of Scenario 2 are the absence of a centerline track and the presence of astronauts to perform the actual reduction operation. EVA crews of three persons will be required. Astronauts are used instead of automated tools to perform all tasks associated with product/tool transport.

Two primary cutters are used instead of one and two barrel sections of the LH_2 tank are reduced simultaneously. Astronauts will transport the composite strips, load the piece parts into the workstation, and store the products in separate containers at the output of the SOFI workstation.

With minor exceptions, the same basic products will be salvaged; however, the salvage task is much more EVA intensive. The actual reduction time is 23 hours, but (due to the required rest time between EVA's) the overall orbiter mission extends to 8.3 days. A total of 63 equivalent 2 man EVA hours would be required and the peak power requirement during the salvage operation would increase to 18.85 kW.

4.4 Scenario 3 - Rendezvous With SSF

The distinguishing characteristic of Scenario 3 is the rendezvous and subsequent sale of electrical power at Space Station Freedom. Scenario 3 incorporates salvage at a lower altitude (via Scenario 1 or 2) prior to rendezvous. The only physically distinguishable features of Scenario 3 are the duplication of a SSF power module on the external tank and the effects this larger system (from a weight and drag standpoint) has on the overall ASSET facility.

Table 4.1. Product Yield From LH$_2$ Tank Reduction

LH$_2$ Tank Reduction			
Products	Material	Weight	Description
Plates	2219 Al	9082 lbs	81 pieces 163" long 89 pieces 225.7" long 178 pieces 225.95" long
I-beams	2219 Al	3123 lbs	81 pieces 163" long 89 pieces 225.7" long 178 pieces 225.95" long
Centerline track	2219 Al	276 lbs	One 76.33' piece
T-beams	2219 Al	150 lbs	4 pieces 126" long 4 pieces 155.5" long
Int. Ring Frames	2024 Al	414 lbs	32 pieces of quarter ring frame sections

4.5   Product Summary

The baseline product yield for Scenario 1 is shown in Table 4.1. The yield for Scenario 2 is very similar except there are no centerline track or cross bars (T-beams) to salvage. Additional yield from the LO$_2$ tank was also considered and that data is provided in Chapter X.

4.6   ASSET System Model

The system level interfaces for the ASSET facility are shown in Figure 4.1. Figure 4.1 is intended to show the relationships between the various models and will be used here to explain how a reduction scenario selection drives the ASSET facility design.

The reduction scenario selection is fed into the SLAM reduction model which performs the following functions:

- Simulates the LH$_2$ tank reduction.

- Incorporates variable tool rates for adjustable reduction timelines.

Figure 4.1. ASSET System Level Interfaces

- Tracks power consumption on a per tool basis.

- Provides histogram outputs for peak power requirements and total timelines required for reduction.

The simulation is varied to minimize either of two conflicting outputs: reduction time and peak power required. The reduction time is minimized (by running the tools at as high a rate as a particular design will support) at the expense of a higher peak power requirement. This tradeoff is defended in later chapters and is shown to maximize the net present value for the facility. Details of the reduction model are provided in Appendix B.

Once the tool rates have been determined, the tool design can be solidified. The tool design is straightforward and is based on the joint objectives to minimize the technical complexity and minimize debris. Various sizes of potential debris (which may escape the confines of the ASSET facility) are sent to the orbital model and estimates are made on the debris orbital lifetime. Complexity estimates for a scenario design are used to trade one scenario against another to see which scenario yields the minimum technical complexity. Scenario specific tool designs are provided in their respective chapters and calculations are provided in Appendix A.

The thermal model incorporates the radiant heat present during the sunlit portion of the orbit with the internal heat generated during the reduction operation to quantify the thermal environment as a function of time. The thermal model is used to perform the following functions:

- Determines the internal LH_2 tank temperature at initial ingress.

- Quantifies the ambient tool environment during the eclipse portion of the orbit.

- Predicts the local and average temperature of composite strips as they are cut out of the tank.

No thermal problems were anticipated and the model verified that hypothesis. Details of the thermal model are provided in Appendix E.

The EPS design accepts the peak power requirement from the SLAM reduction model and generates a scenario specific design to provide the requested power. The EPS is the primary drag contributor to the facility and the total drag which must be offset is input into the orbital model. The array area is also an input to the cost model. Scenario specific EPS designs are included in their respective chapters and calculations and trade studies performed to support EPS design are provided in Appendix C.

The orbital model accepts the total drag input (from the EPS) and the reduction time from SLAM and incorporates these with a total facility weight to calculate orbital altitude loss and fuel consumption during the reduction operation. A detailed discussion is provided in Appendix D.

The cost model accepts various inputs (array area, EVA requirements, fuel consumption, and subsystem weights) and generates a life cycle cost. The model also uses the salvaged products to generate a revenue stream. Life cycle costs are compared to the revenue stream to generate a net present value (NPV). Initially, the focus was to minimize cost inputs to the cost model, but it was determined the facility would operate at a loss over a 15 year period. Additional salvage was then investigated (to maximize the amount of product salvaged), cost inputs were adjusted to incorporate additional salvage, and it was determined that the ASSET facility could be operated at a profit (when compared to products launched from earth) over a 10 year operational life. Detailed discussion on the cost model is included in Appendix G.

V. SCENARIO 1 - AUTOMATED REDUCTION

5.1 Overview

Scenario 1 features automated reduction. Tools have been developed to carry out all aspects of the salvage operation and the ASSET facility will be unmanned during the actual reduction operation. The distinguishing characteristics of Scenario 1 are the pre- flight installation of a centerline track (mounted longitudinally down the center of the LH$_2$ tank) and the absence of astronauts during the actual reduction operation.

Reduction starts in the aft barrel section (see Figure 5.1) between station 2058 and 1871. A primary cutter rides the stringers (I-beams) and cuts out a composite strip composed of plate, I-beam, and SOFI. The centerline track is utilized to mount a robot arm/trolley combination which moves the primary cutter in the radial direction and transports the composite strips (see Figure 5.2) in the longitudinal direction once they have been cut out. The robot arm will insert the composite strips into the SOFI workstation.

The SOFI workstation (see Figure 5.3) removes the SOFI, stores the removed SOFI, provides a secondary cut to separate the I-beam from the plate, and stores the I-beam and plate in separate storage/containment equipment.

An overall view of the Scenario 1 operation is shown in Figure 5.4. The pre-installed centerline track provides power to the primary cutter by means of a free-sliding power truck. The trolley receives its power from the forward area of the tank via a cable fed through an inertia reel device. This power connection to the trolley is attached to the non-rotating portion of the trolley. The extending robot arm, attached to the rotating portion of the trolley, will pick up the composite strips as they are cut out of the LH$_2$ barrel and insert them into the SOFI workstation input funnel which is approximately 4 feet inward from the outer surface of the tank.
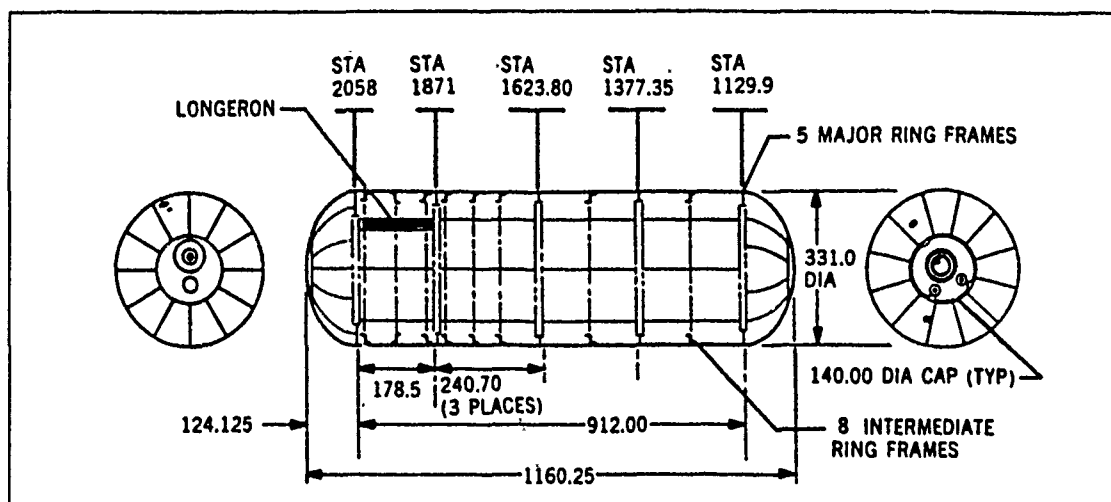
Figure 5.1. LH$_2$ Tank Profile
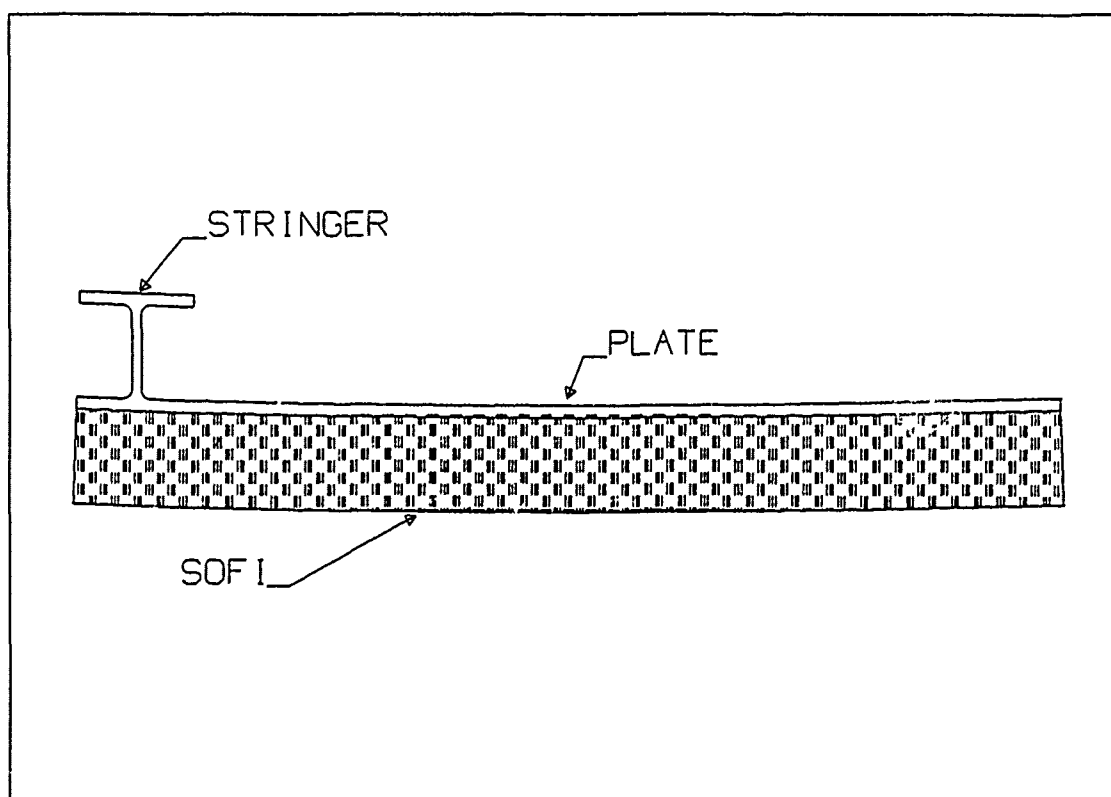
Figure 5.2. Pre-processed Composite Strip
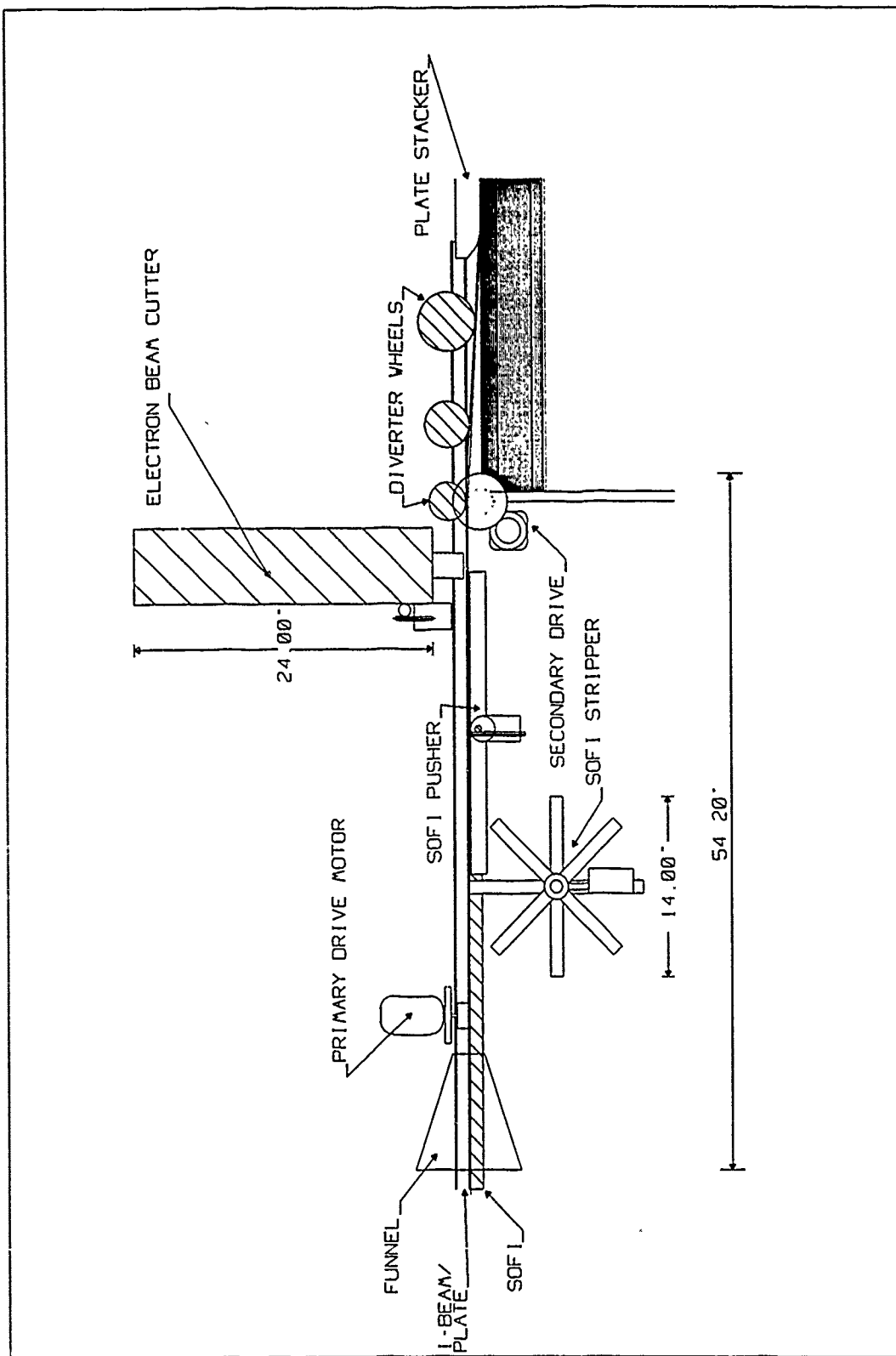
Figure 5.3. SOFI Workstation

5-3

Once the SOFI has been removed and secondary cuts have been made to separate the I-beam from the plate, the separated products are stored between the two major ring frames as shown.

The LH$_2$ tank is reduced to a 'birdcage' structure (see Figure 5.5) in 1.7 days (40.77 hours). The peak load demand is 11.5 kW and 13,045 pounds of readily usable aluminum have been salvaged.

5.2 Pre-flight Modifications

There are two categories of pre-flight modifications to the External Tank. The first category involves those modifications which any ET user would need in order to exploit the tank on orbit (henceforth to be called general pre-flight modifications) and the second category are modifications peculiar to the task at hand.

In their study exploiting the space shuttle external tank on orbit (52:185-193), Martin Marietta suggested the following general pre-flight modifications:

- Tumble Valve Deactivation

- Range Safety System Safing

- LO$_2$ and LH$_2$ Tank Depressurization

At present, the External Tank of the Space Shuttle is configured for jettison shortly after Main Engine Cut Off (MECO). The current jettison trajectory would de-orbit the ET for splashdown in the Indian or Pacific Ocean. In order to keep the ET aloft for use as the ASSET facility platform, systems which cause de-orbit must be disarmed. Deactivation of the tumble valve system will accomplish this task. According to the Gamma Ray Imaging Telescope (GRIT) study (52:185-193), the following modifications will be necessary:

- The pyrotechnic valve and nozzle must be removed.
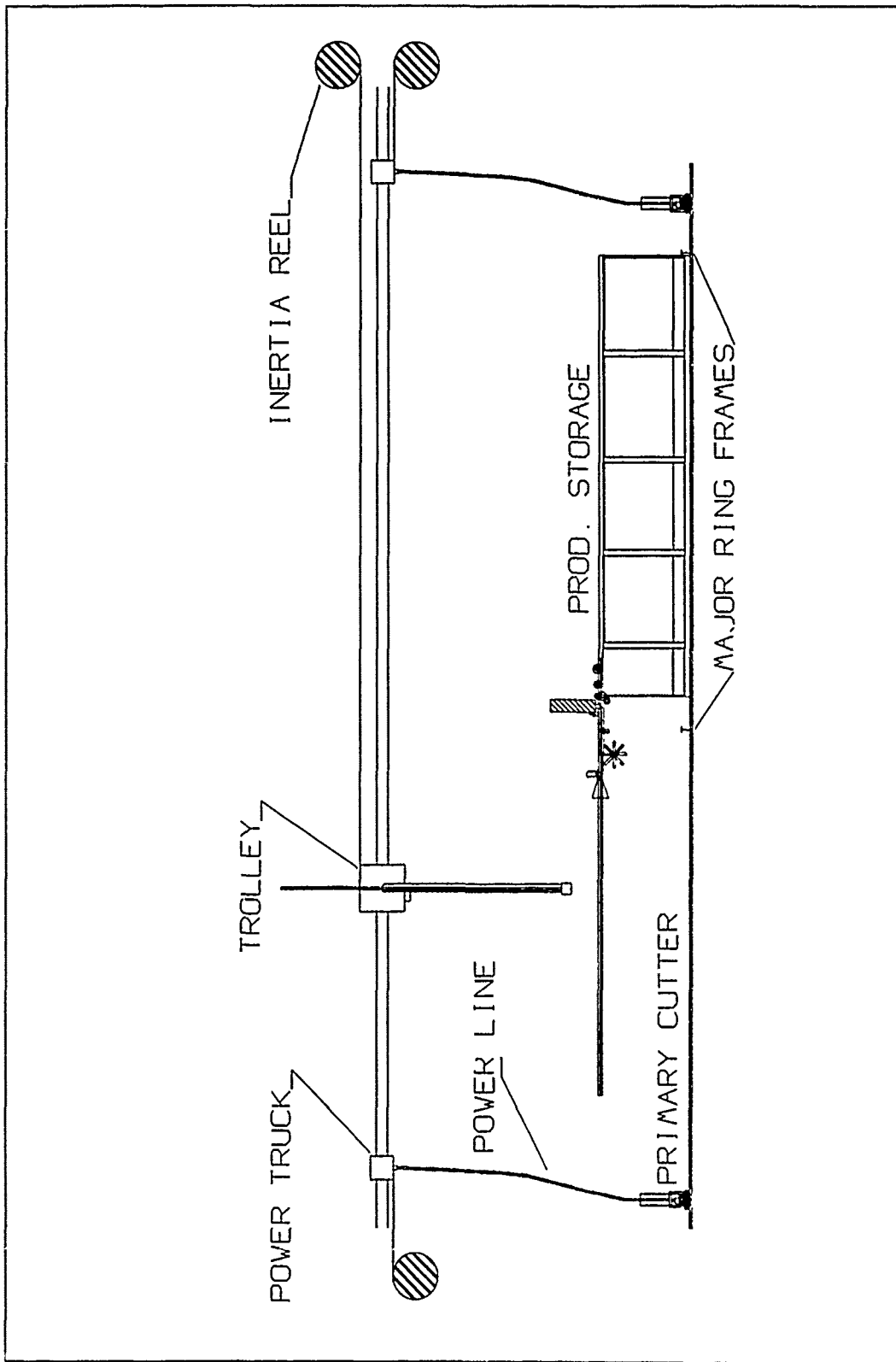
Figure 5.4. Overall View of Scenario 1
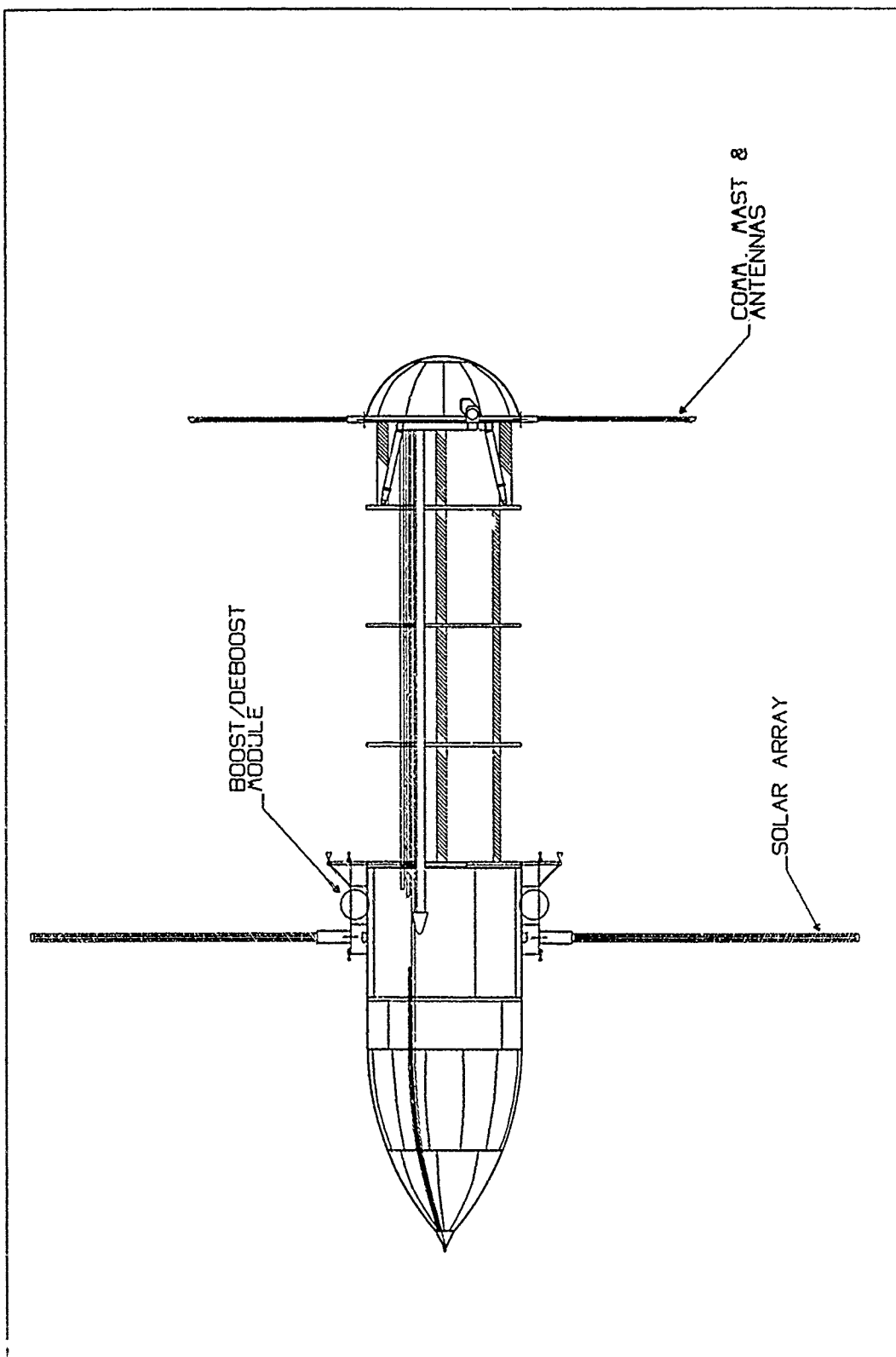
Figure 5.5. ET Bird Cage, Top View

- A new cover plate, using existing hardware, should be installed to cover the hole left by the removal of the pyrotechnic valve.

- A cover plate should be installed to cover the hole left by nozzle removal.

- The tumbling switch module and its associated wire bundle and connector should be removed.

- The tumbling system wires should be coiled and stowed.

The Space Shuttle contains range safety devices which would be detonated by ground controllers should flight problems arise. Once on orbit, this range safety system should be disarmed. Required modifications to the range safety system follow:

- New wiring should be added in the range safety system (RSS) box enclosure.

- Using existing cabling from the ET Orbiter I/F, the safing circuitry should be connected to the RSS box enclosure.

Earlier in the study, it was thought that the residual cryogenic fuels which the ET will contain after MECO, could be scavenged for on orbit use. Subsequent consultations with the External Tank's manufacturer, Martin Marietta, made it clear that the plumbing modifications to the Orbiter and the ET required to scavenge the cryogenic fuels would be prohibitively expensive. Therefore the LO_2 and LH_2 tanks must be vented on orbit. Currently, the LO_2 tank is vented in an asymmetric fashion to induce tumbling in the ET as it deorbits. This tumbling facilitates the disintegration of the ET as it deorbits and insures that most of its components burn up before splashdown. The purpose of one of the preflight modifications is to provide for symmetric, on orbit venting of the cryogenics. Even with such pre-flight mods, the orbiter will need to be attached to the ET during venting in order to compensate for the reaction forces that can not be designed out of the venting system. Required ET modifications follow:

- A gaseous helium bottle approximately $1.75 ft^3$ in volume is installed in the intertank.

- A non-propulsive gaseous hydrogen duct is installed in the LH_2 tank.

- On orbit, astronauts would be required to close the 17 inch and the 2 inch disconnects after MECO.

- They would also need to dump the LH_2 and LO_2 from the orbiter manifolds.

- Two new steps would be to:

    1. Actuate the gaseous hydrogen and gaseous oxygen from the intertank helium bottle.

    2. Periodically close and open the vent valves to assure all the liquid has boiled off.

All of these activities are accomplished from inside the orbiter. No EVA would be required. Pre-flight modifications which are peculiar to ASSET facility requirements are as follows:

LH_2 TANK

- Addition of hand rails and foot restraints within the LH_2 tank to assist EVA operations.

- Pre-installation of centerline track in the LH_2 tank.

- Highlight internal 'birdcage' stringers.

- Install handle on aft manhole cover.

- Install mesh under SOFI on aft manhole cover.

- Install 'bar codes', for indexing, on major ring frames.

- Pre-tap holes for SOFI workstation mounts.

- Pre-tap holes for brackets and lights on major ring frames.

INTERTANK

- Install mesh under SOFI on access door.

- Install hinged access door.

Modifications to the LH_2 tank are required to facilitate the manual mounting of equipment by astronauts as well as to support the reduction equipment once it is in place. Intertank modifications are necessary to access power and power conditioning systems.

5.3 Initial Set-Up

Astronaut EVA is required for initial set-up and eight hour hard suits (which obviate the need for the current three hours of pre-breathing) are assumed. This would seem to be a safe assumption in view of suit improvements being developed to support operations at SSF (84). Two eight hour EVA's will be required during initial set-up of the facility. It is further assumed that the orbiter can initially deliver the ET at an altitude of 170 nautical miles.

The initial tank will be transformed into what will eventually become the AS-SET facility. Initial facility set-up will require a dedicated shuttle mission with an approximate 50,000 pound payload. The initial tank will be fitted with two boost/deboost modules (see Figure 5.6) to control all orbital functions. These modules are installed at the SRB thrust fittings on the intertank. Once the ET has been stabilized, the residual pyrotechnic charges in the LO_2 and LH_2 tanks will be removed in a parallel operation.

Electrical power system (EPS) installation can commence once the ET has been stabilized in orbit and rendered safe. Photovoltaic (PV) arrays will be installed at the SRB beam attach points. Orbital replacement units (ORU's) for the conditioning, regulation, and distribution can be mounted externally (similar to SSF) in
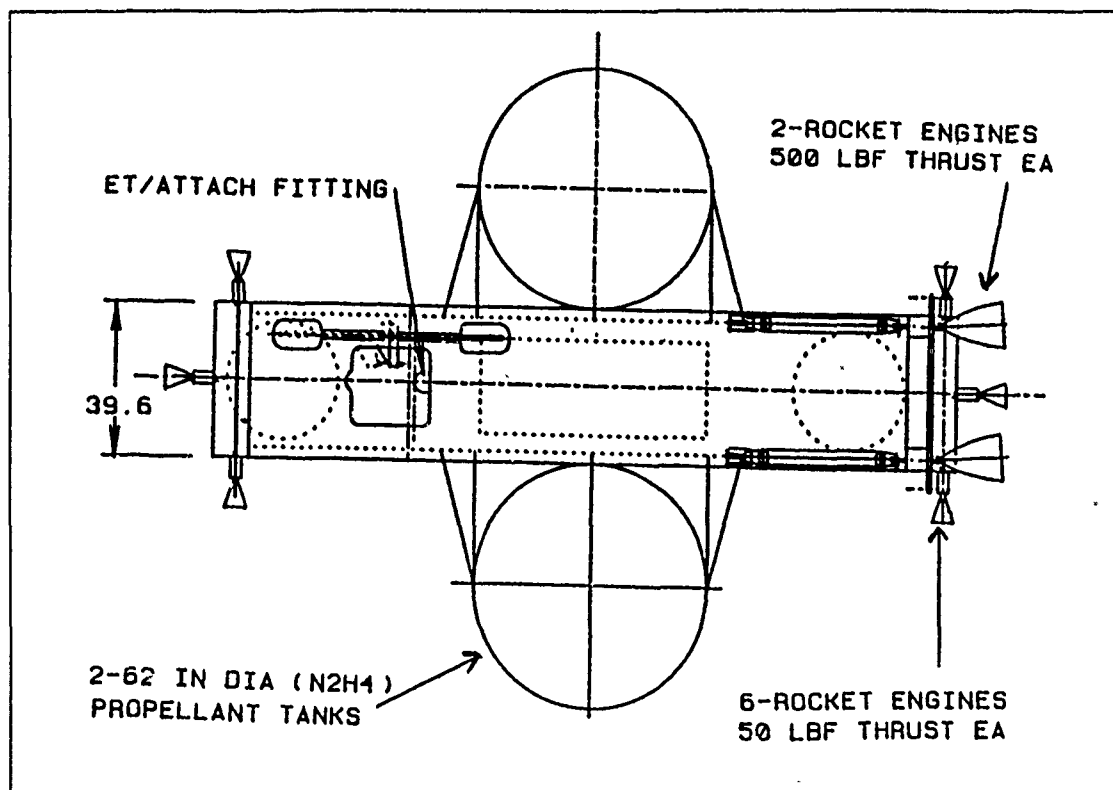
Figure 5.6. Boost/Deboost Module

the integrated equipment assembly (IEA) or internally in the intertank region of the ET.

Connecters for the three power distribution system. will be installed in the forward dome of the LH_2 tank. Installation will be accomplished from within the intertank. The astronauts will then ingress the LH_2 tank via the aft manhole cover. The ingress of all subsequent equipment will also be via the aft manhole on the LH_2 tank.

A portable electron beam cutter will be used to remove 7 of the 8 intermediate ring frames (see Figure 5.7). These ring frames are attached via t-clips and will be cut as shown in Figure 5.8. The eighth intermediate ring frame (station 1973.5) is installed via 108 bolts. Removed ring frames will be cut in four pieces (at the four splice plates; see Figure 5.9), bundled, and stored in the forward LH_2 dome.
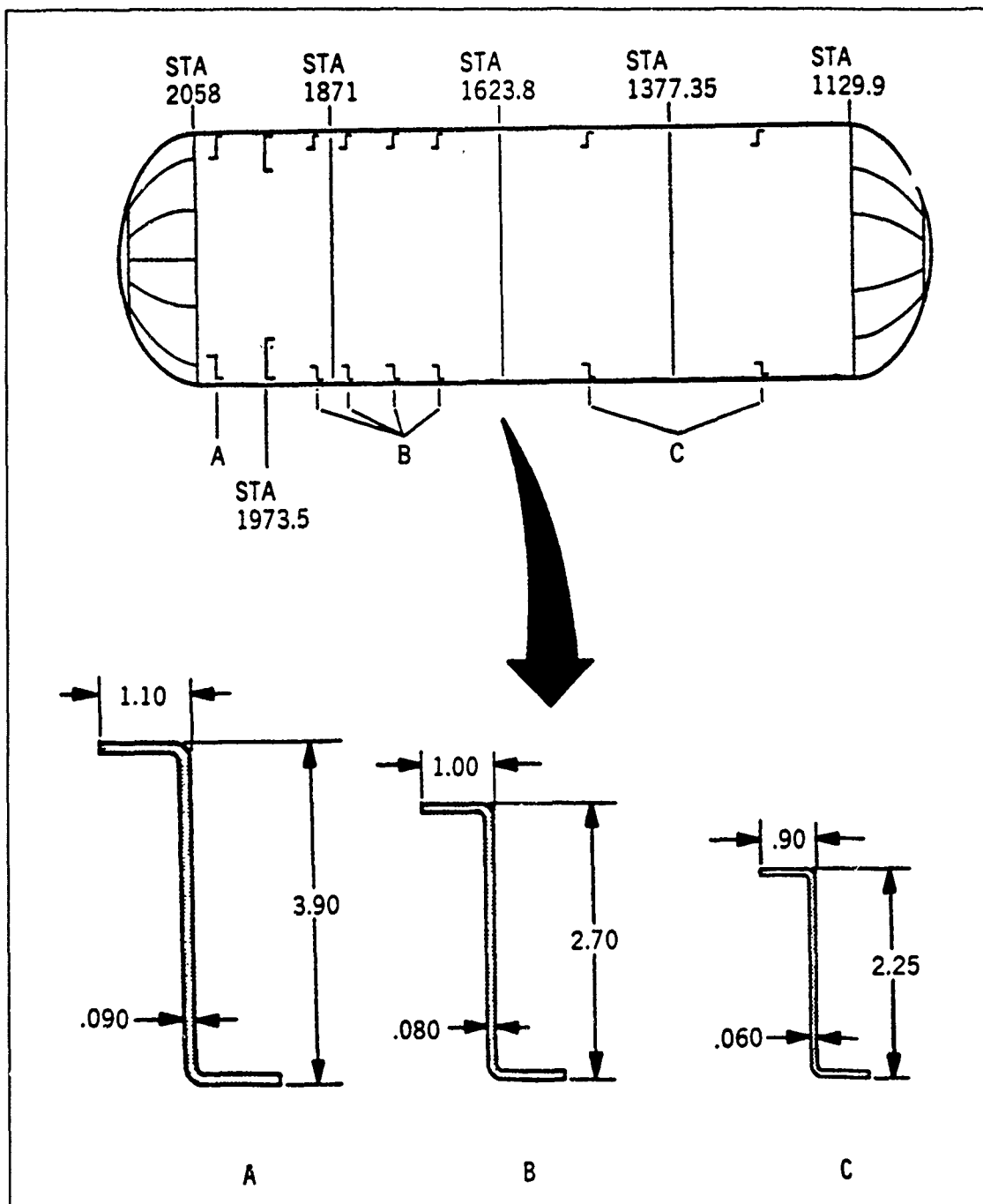
Figure 5.7. Intermediate Ring Frame Locations
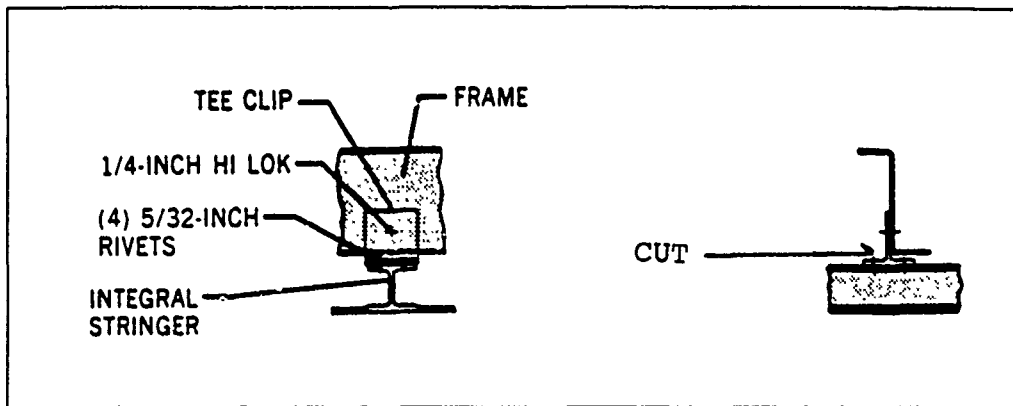
Figure 5.8. Typical Intermediate Ring Frame Attachment
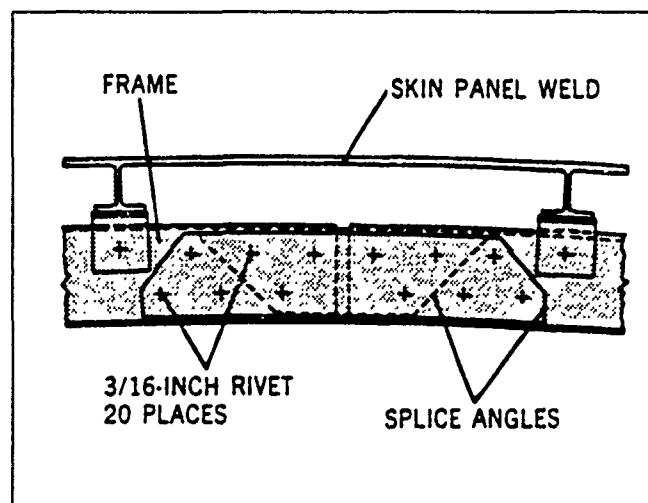
Figure 5.9. Intermediate Ring Frame Splices

Following removal of the intermediate ring frames, the internal LH_2 power distribution cables can be installed. Cables will be installed in the interior of the LH_2 tank for each of the three distribution networks. Network one will supply power for the communications equipment, on-board avionics, lights, cameras and sensors. Network two will supply the SOFI workstation. Network three will supply the centerline trolley and the primary cutter.

Lights, camera mounts, and cameras will then be installed. The SOFI workstation (which includes SOFI removal, SOFI storage, a secondary cutter, and product storage/containment equipment) will then be installed. Internal installation is concluded upon the installation of the center arm trolley, the primary cutter, and a spare cutter (which may be utilized in either the primary or secondary position).

Facility set-up is concluded upon the installation of the control masts and antennas at the aft orbiter attach points, and the storage of electrical umbilical cables for subsequent tanks in the intertank area. At this point, the tank is in a state to start reduction, all EVA tasks are concluded, and the orbiter could (in theory) vacate the premises. It is recommended that the orbiter remain in the vicinity in the event troubles arise during initial tank reduction.

5.4 Tools

The entire automated reduction system is illustrated in Figure 5.10 (end view) and Figure 5.4 (side view). A detailed description of the tool strength and motor power calculations is included in Appendix A.

5.4.1 Centerline Track. A pre-installed centerline track solves the problem of automated product/tool transport. The track is made of 6" X 6" X 0.125" thick square 2219 aluminum tubing and extends from the forward most major ring frame to the aft most major ring frame (912" total). T-beam crossbar supports (Figure 5.11) attach the track to these ring frames. The forward and aft T beam crossbars are
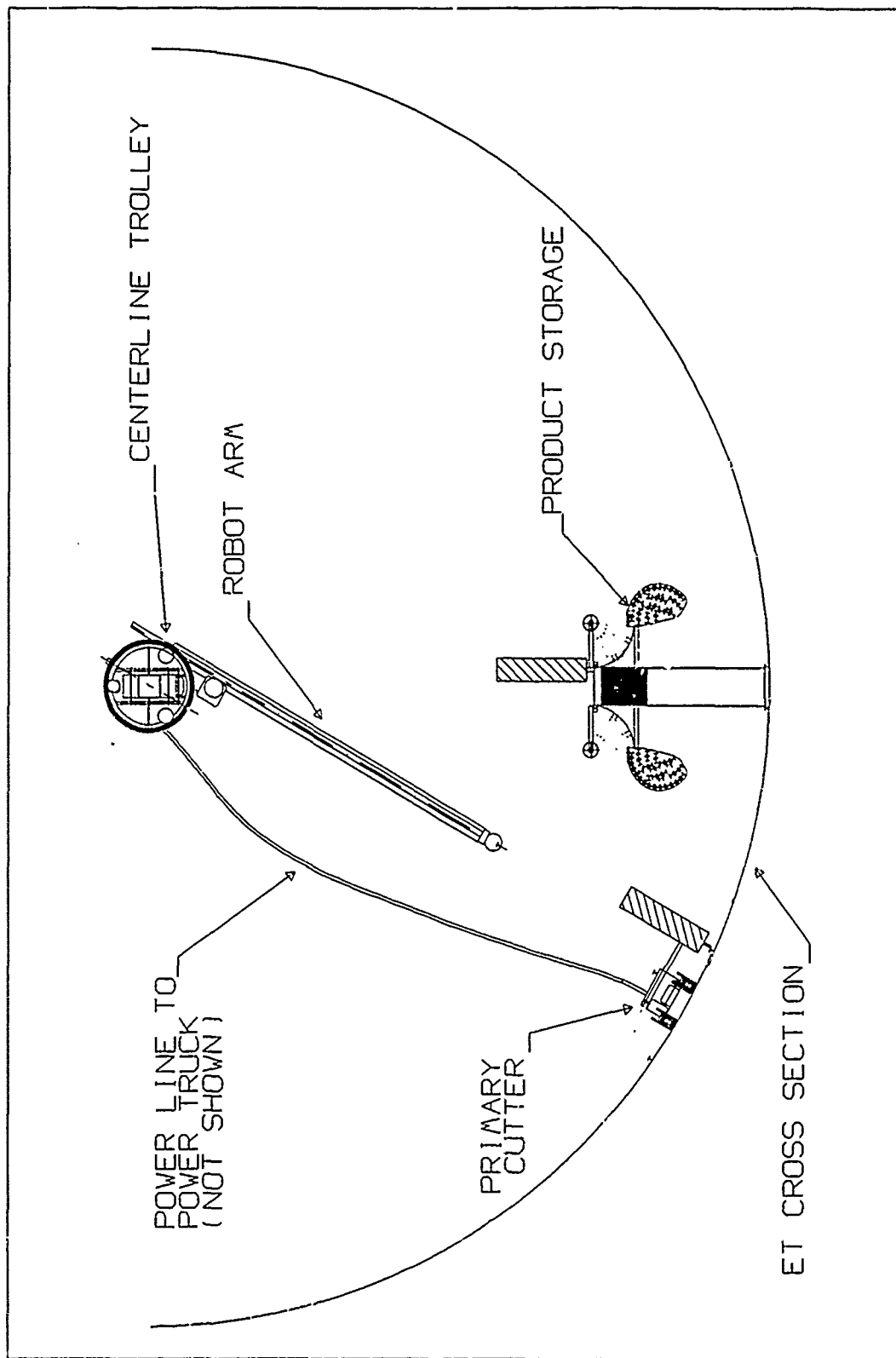
Figure 5.10. ET Reduction Tools, End View

made of 6" X 3.5" X 0.25" and 6" X 6" X 0.25" thick 2219 aluminum respectively. This entire pre-installed structure weighs 426 lbs.

5.4.2 Centerline Trolley. Actual material transport is accomplished by the centerline trolley (Figure 5.12). The trolley is capable of radial (angular motion about the centerline track), lateral (perpendicular to the track), and longitudinal (along the track) motion.

Radial motion is provided by dual redundant drive motors (Figure 5.13). Through a series of reduction gears the motor delivers torque to the external housing which supports the arm. The radial motor is equipped with a tachometer to measure the radial displacement of the arm ensuring proper radial indexing.

Lateral movement is accomplished by the arm extension (Figure 5.12). The arm extension is attached to a shaft which is operated by the extension drive motor, rack, and pinion (Figure 5.14). Through a series of reduction gears, the extension motor turns a pinion which moves a rack that is attached to the extension shaft. This motor is also equipped with a tachometer to provide lateral indexing.

Longitudinal motion is made possible by dual redundant drive motors which, through a series of reduction gears, pass torque to the drive wheels (Figure 5.13). The drive wheels, along with the track, are geared to ensure good traction and longitudinal indexing. The longitudinal drive motor is equipped with a tachometer to complete the indexing capability.

Installation of the trolley is completed during the setup EVA. The internal and external trolley housings can be opened and placed around the track (Figure 5.14). The internal and external housings are then sequentially closed and fastened together.

Power and control is provided to the trolley by cables coming from an inertia reel mounted to the forward track crossbar (Figure 5.15). The inertia reel is attached to the forward track crossbar and maintains proper cable length, thus eliminating
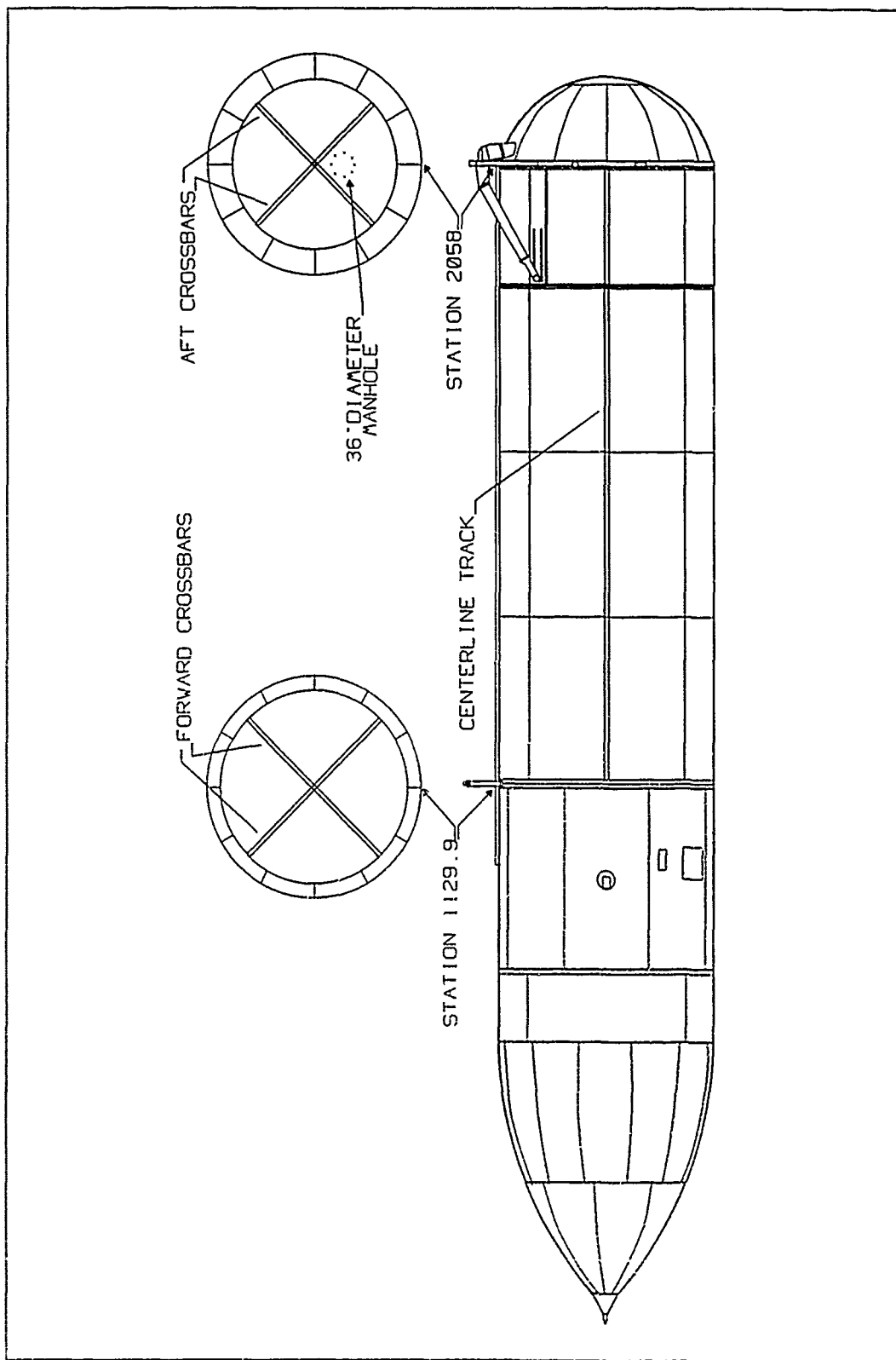
Figure 5.11. Centerline Track Layout
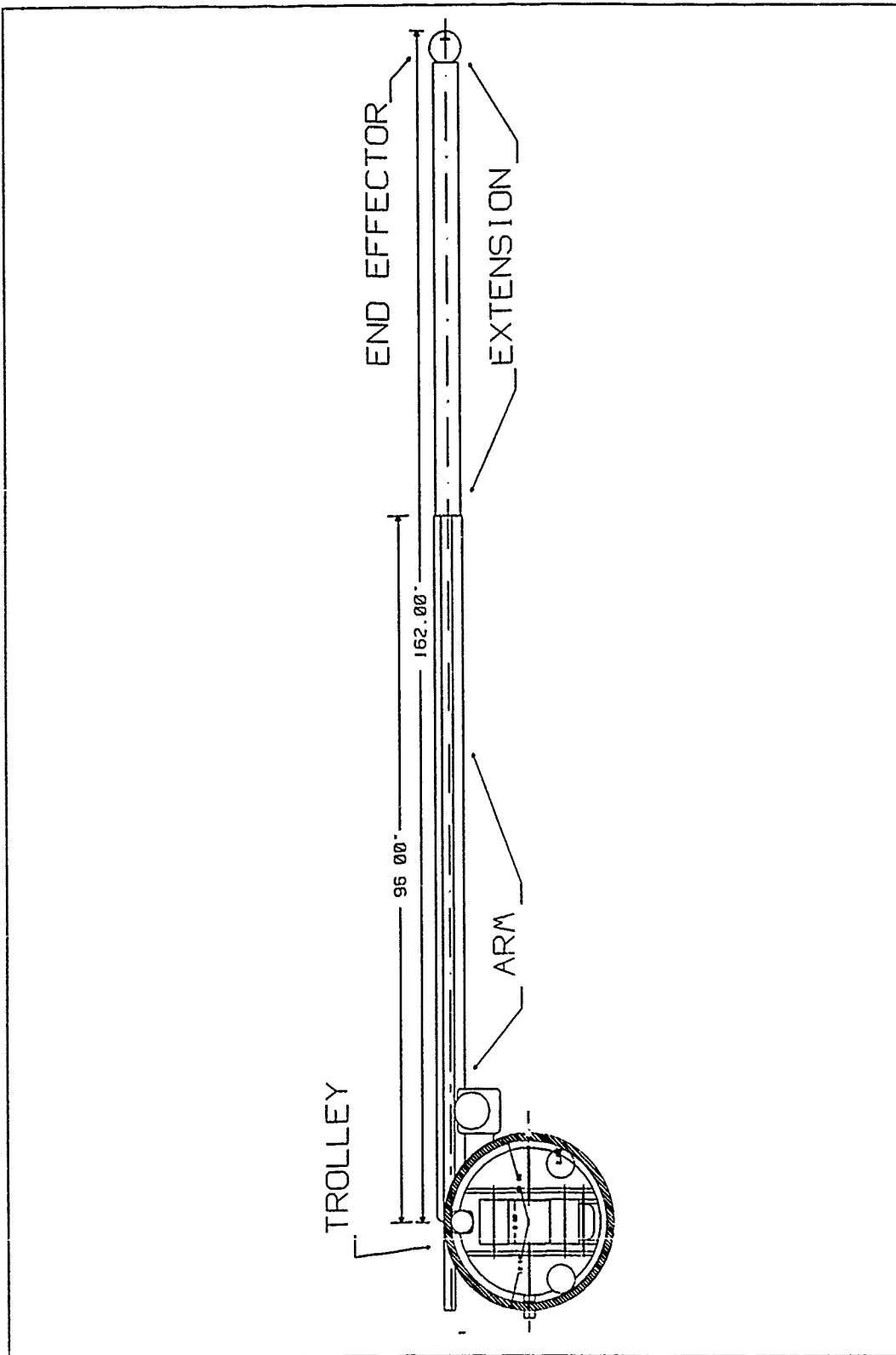
Figure 5.12. Centerline Trolley
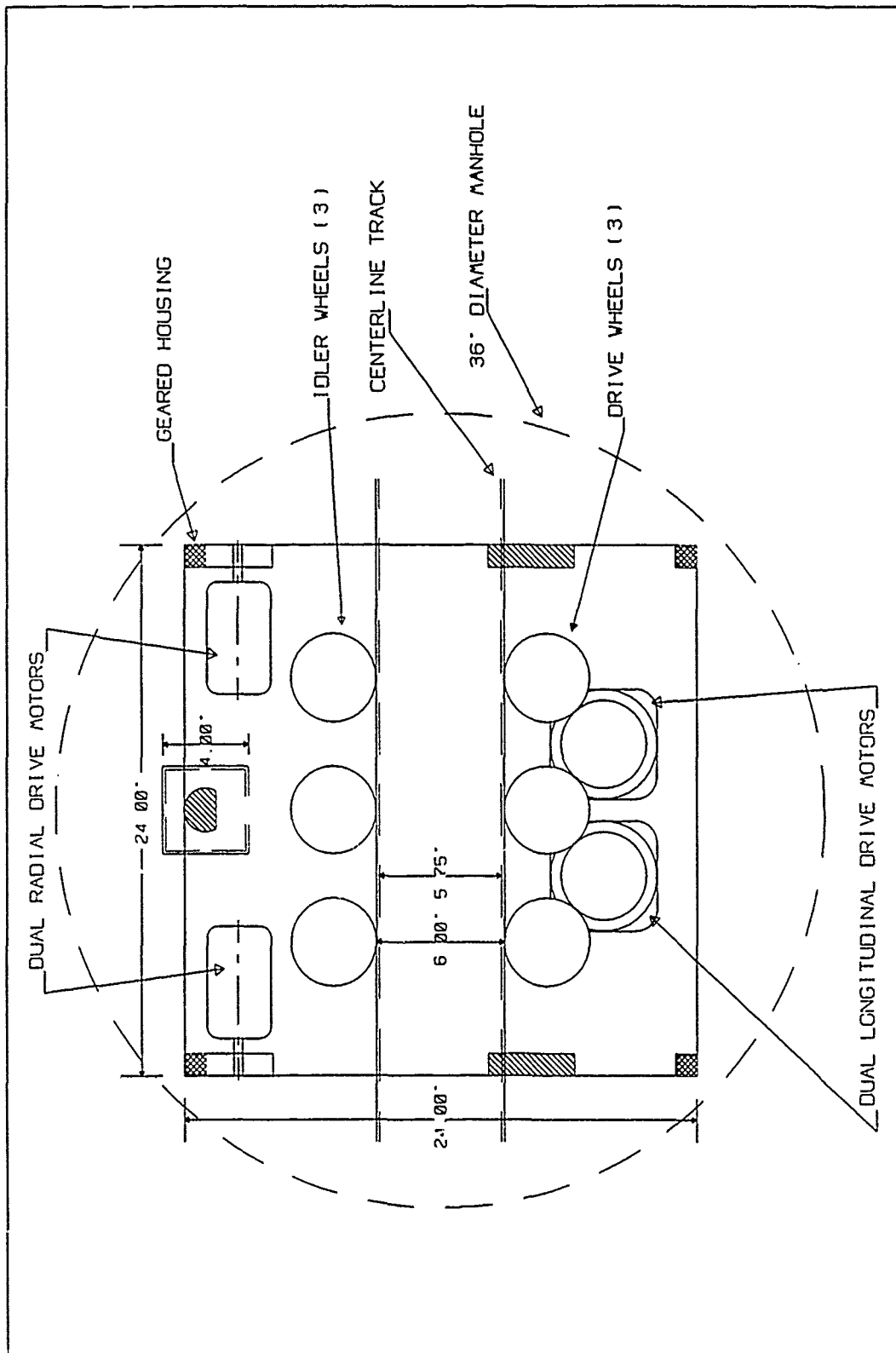
Figure 5.13. Trolley End View
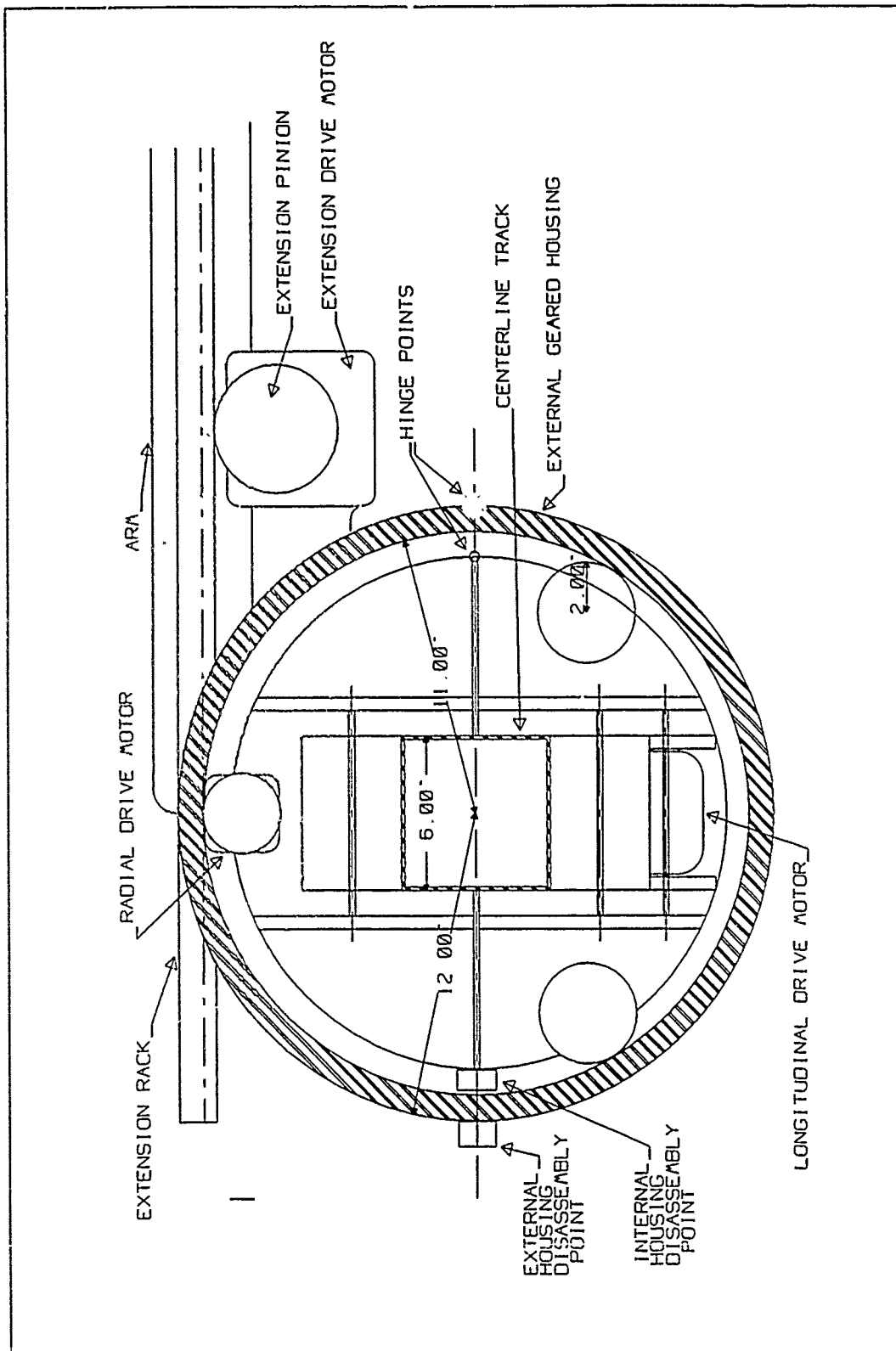
Figure 5.14. Trolley Side View

5-19

possible cable incidents (Figure 5.15). The power and control cable is attached to the non-rotating internal housing.

The end effector (Figure 5.12) is a simple open and close device capable of grasping the T-shaped grips on the materials and tools.

5.4.3 Primary Cutter. Automated ET reduction is initiated by the Primary Cutter (Figure 5.16). The actual material cutting is performed by an electron-beam cutter (see Appendix A). The primary cutter moves the electron-beam cutter longitudinally and laterally to cut out composite strips of plate, I-beam (stringer), and SOFI.

The primary cutter attaches itself to pairs of adjacent stringers with four sets of retractable guide wheels. Each guide wheel is positioned below the stringer flange thus holding the primary cutter to the stringer. The wheels are spring mounted to allow for irregularities such as intermediate ring frame support clips. The drive wheels are configured to allow the primary cutter to get as close to the major ring frames as possible.

Longitudinal motion is generated by the longitudinal drive motor which, through a series of reduction gears, provides power to the drive wheels. Lateral motion is accomplished by the slide drive motor. The electron-beam cutter is attached to a shaft that is moved in and out by the rack driven by the slide drive motor pinion. This permits cross cutting of the plate/I-beam sections.

The centerline trolley/arm provides the radial motion. The top of the primary cutter is equipped with a T-shaped grip which allows the end effector to grasp it. When the primary cutter is secured by the arm, the guide wheels automatically retract. The trolley/arm is then free to move the primary cutter to another set of stringers.

Power is provided to the primary cutter from a power truck located on the centerline track (Figure 5.4). The power truck is connected to the primary cutter
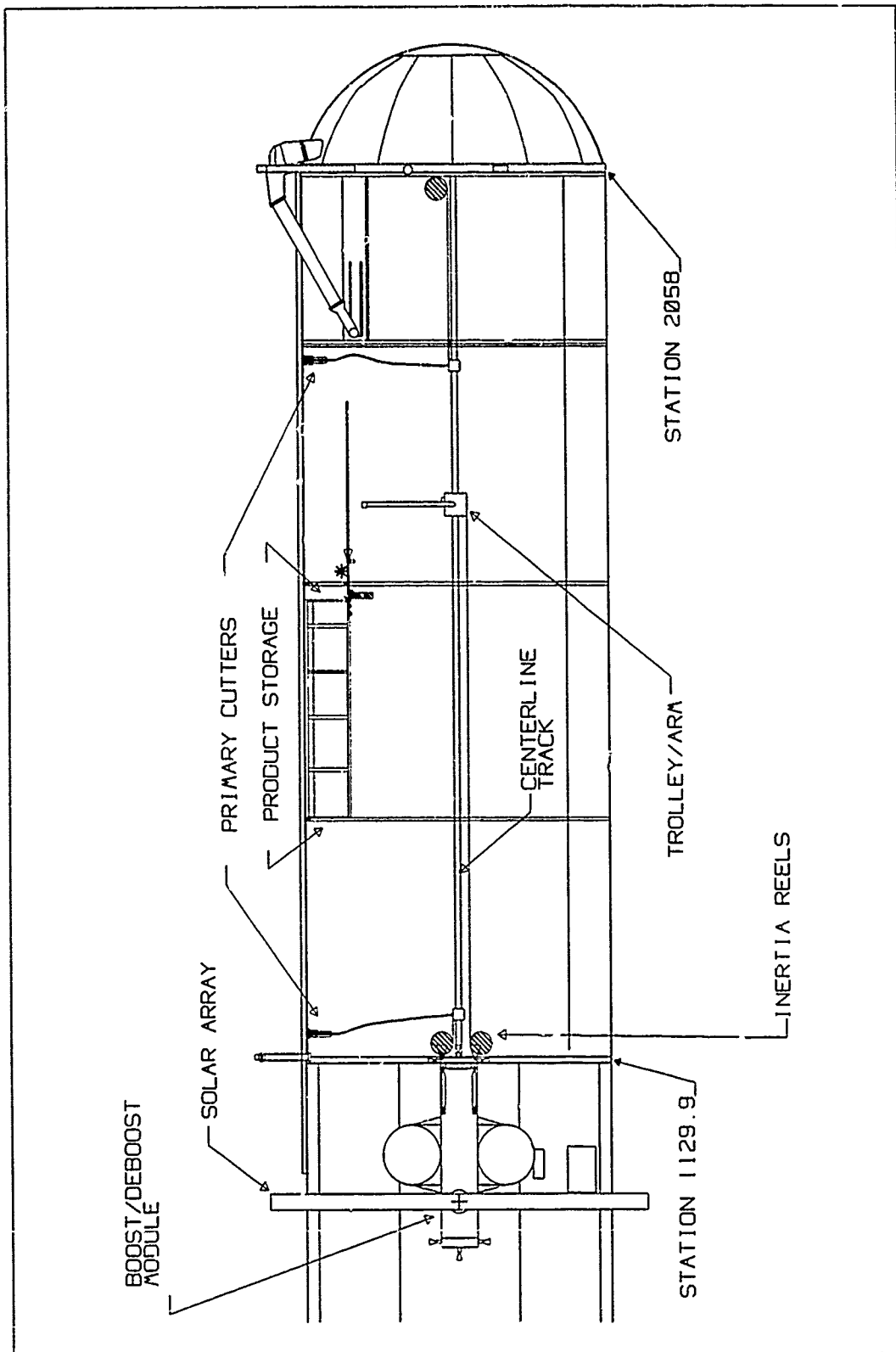
Figure 5.15. Trolley Power and Control
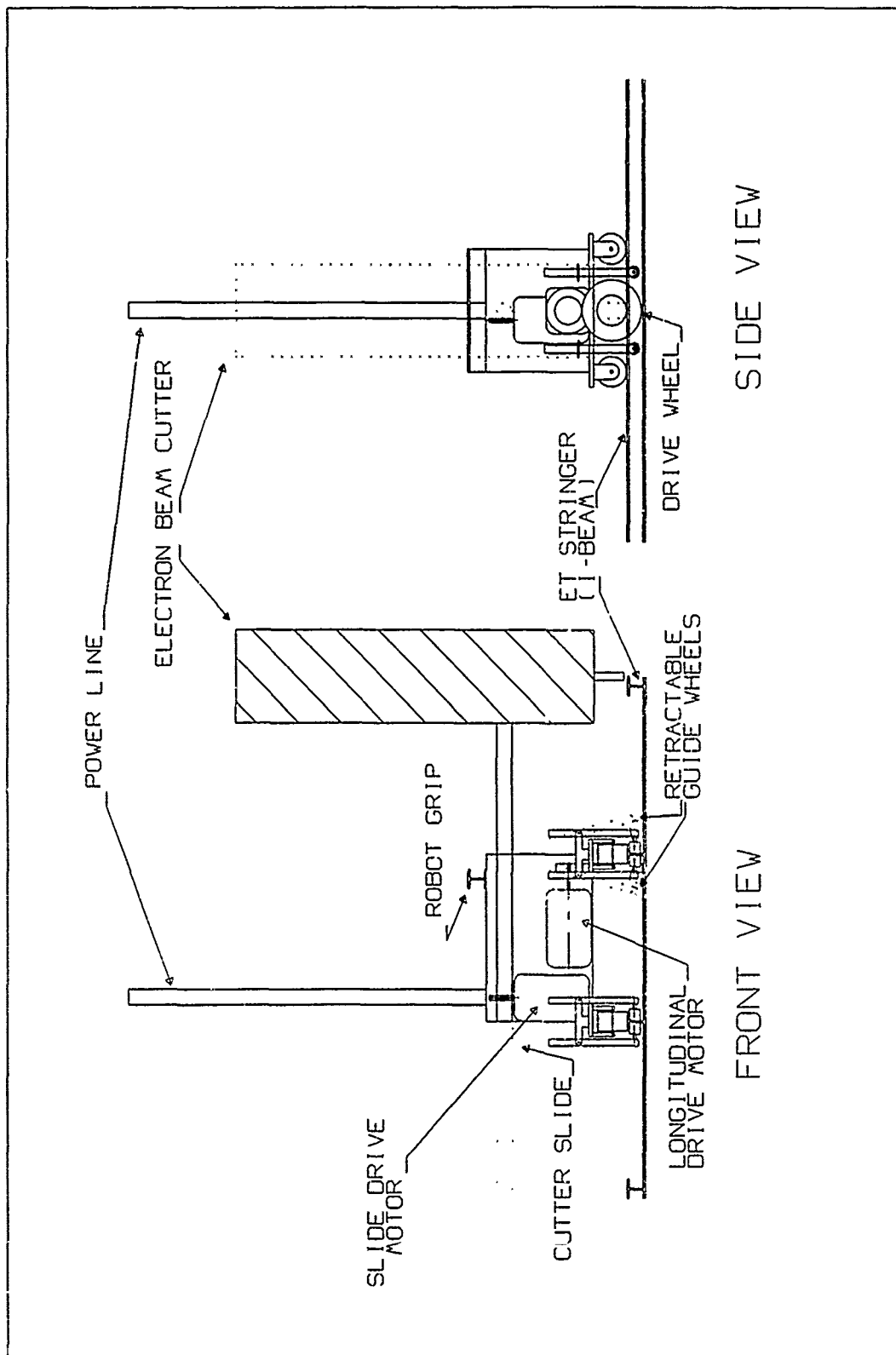
Figure 5.16. Primary Cutter

5-22

by a flexible coiled power line which allows both angular and lateral displacements. When the lateral displacements are great enough, the power truck is free to roll along the centerline track. The coiled power line attach point to the power truck rotates freely as the primary cutter is moved radially about the tank. The power truck obtains power from an inertia reel in the same manner as the trolley.

5.4.4 SOFI Workstation. When a skin/stringer combination has been completely cut free, the trolley/arm will move it to the SOFI workstation. The initial workstation interface is the funnel (Figure 5.3). The funnel allows for small deviations in the trolley/arm's placement of the material (up to 4.5" in any direction). These deviations (see Appendix A) can be caused by indexing errors or play in the trolley/arm system. The material is then pushed through the funnel until it engages the primary drive wheels. Dual primary drive wheels are located on both sides of the workstation to allow for stringers on either side (Figure 5.17, left). The primary drive wheels move the material first to the SOFI stripper.

5.4.4.1 SOFI Stripper. The SOFI stripper is comprised of eight wires capable of cutting through the SOFI. As one wire breaks it is replaced by a simple rotation of the SOFI stripper device (Figure 5.3). The stripper actuators (Figure 5.17, center) make cuts through the SOFI by moving up or down. The SOFI is then cut from the aluminum skin as the material is pushed through. The device remains in its upper position until two feet pass by; then it cuts down through the SOFI creating a two foot piece of SOFI. The SOFI pusher then engages the freshly removed SOFI and moves it laterally through the SOFI funnel.

5.4.4.2 Electron-Beam Cutter. As the material continues through it engages the electron-beam cutter which separates the stringer from the skin creating an I- beam/plate combination (Figure 5.18). The electron-beam is attached to a shaft that moves it from side-to-side to allow for stringers on either side. This side-to-side
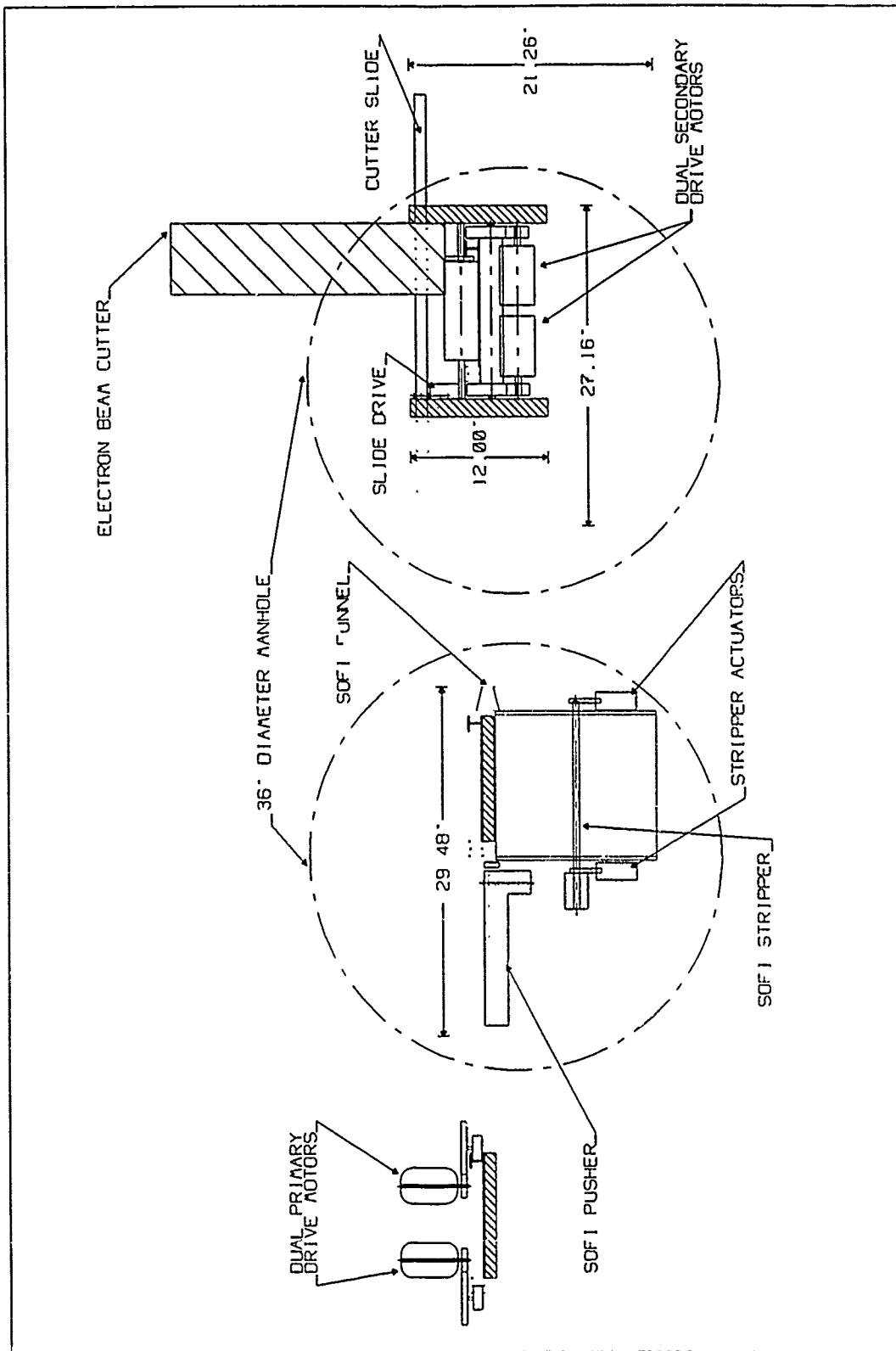
Figure 5.17. SOFI Workstation Cross-sectionals

motion is provided by the cutter slide and slide drive motor (Figure 5.17, right).

5.4.4.3 Plate Stacker. As the I-beam/plate combinations emerge from the electron-beam cutter, the plate is engaged by the secondary drive motor (Figure 5.3). The diverter wheels then gently bend the plate downward until they enter the plate stacker. The plate is wedged between the stacker structure and the previous plate. The plate stack is held in place by a spring-loaded frame which holds the plates firmly to the upper structure (Figure 5.3).

The I-beams continue until they are free from the secondary drive wheels. Once free, they are engaged by the I-beam stacker (Figure 5.19). The stacker moves the I-beam along a circular arc until the I-beams are secured in the Bungee restraint. As the I-beams enter the restraint a spring-loaded door closes smartly behind it, thus ensuring its immobility. The stacker actuator then returns to its original position.

Upon completion of the cutting process, the Bungee cord restraint can be disconnected from the product storage system and then interconnected creating a tightly bundled package of I-beams. The Bungee cord restraint and plate stacker are sufficiently sized to hold the total products salvaged from the LH_2 tank. Figure 5.19 shows that the 348 total plates that are salvaged can be stored in a single stack 43.5 inches high.

5.5 Scenario One Reduction Model

Reduction of the LH_2 tank was simulated using the SLAM II simulation language and FORTRAN subroutines. The primary objectives of the reduction model were to develop reduction timelines for the reduction of one LH_2 tank and to determine the peak power requirements for the reduction facility. Appendix B gives a detailed description of the reduction model.

5.5.1 Tool Work Rates and Power Consumption. Establishing tool work rates was a primary step in determining the overall power consumption of the facility as
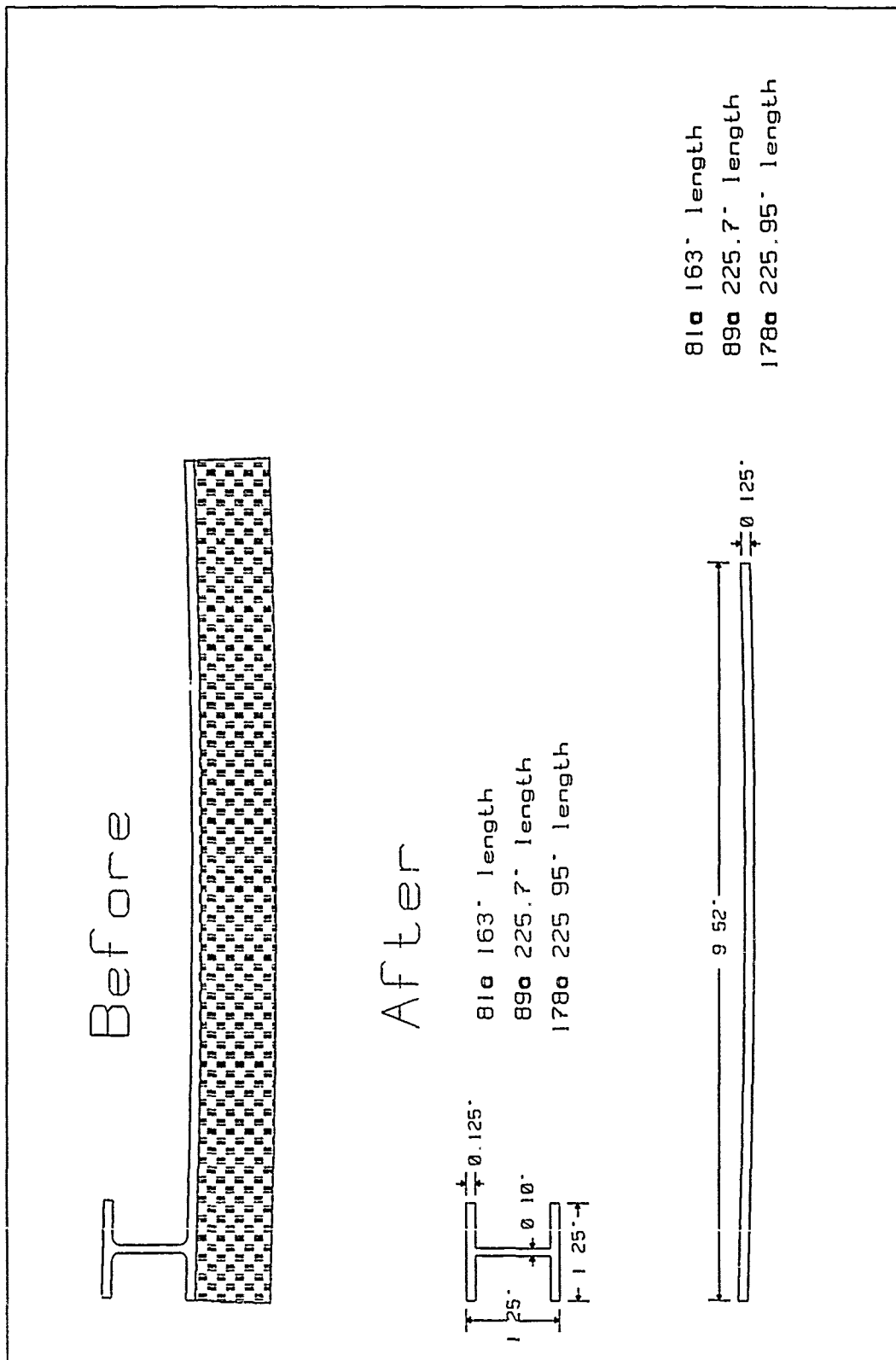
Figure 5.18. Pre and Post Processed Products
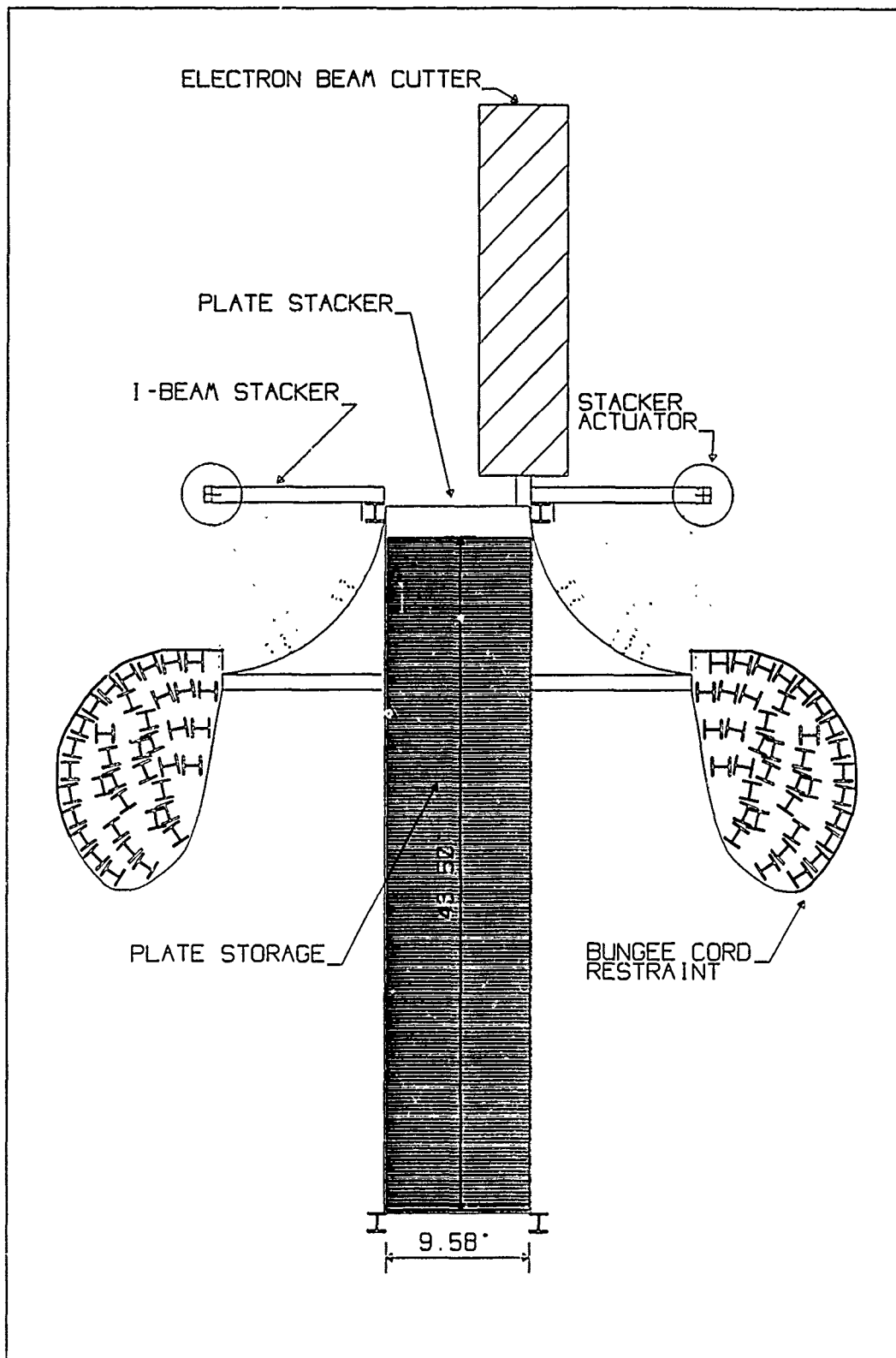
Figure 5.19. Product Storage System

Table 5.1. Primary Cutter Design, Scenario 1

MATERIAL	CUT RATE	POWER REQUIRED
Stringer	10 inches/minute	7.05 kW
Plate	80 inches/minute	4.05 kW

well as the total time required to reduce the tank. Work rates and power use were varied for the primary and secondary cutters, the transport arm, and the SOFI work station in order to assess their affect on power consumption and reduction times. The critical design variable was found to be the primary electron beam cutter. Once this was established, other tool work rates and power requirements were held constant and the electron beam cut rate and power use were optimized in order to minimize the tank reduction time while staying below a self imposed peak power constraint of 12 kW. The EB cutter requires the most power (especially when cutting through stringers) and is directly related to the cut rate; the faster the cut, the more power required for a given depth of cut. Following several iterations the primary cutter design was determined to be as shown in Table 5.1.

5.5.2 Results. Once tool work rates and their power needs were established, the simulation was conducted again to determine the facility power requirements and the total tank reduction time. Figure 5.20 illustrates typical facility power use over a series of cuts for scenario one. Each phase of the reduction model is explained below. A base power of 2 kW is used by the facility for communications, cameras, and lights. The sections labeled with a 2 indicate when a stringer is being cut. The sections labeled with a 3 indicate when plate is being cut.

1 The transport arm moves the stringer/plate piece, then the cutter (0.2 kW), plus a base power of 2 kW. Total power = 2.2 kW

2a The cutter cuts I-beam (7.05 kW), while the arm moves into position to grasp the stringer/plate piece (0.2 kW), plus a base power of 2 kW.

Total power = 9.25 kW.

3a The cutter cuts plate (4.05 kW), while the arm moves (0.2 kW), and the SOFI stripper (1.25 kW) and the secondary cutter operate (4 kW), plus base power (2 kW). Total power = 11.5 kW.

3b The cutter cuts plate (4.05 kW), while the SOFI stripper (1.25 kW) and the secondary cutter (4 kW) operate, plus base power (2 kW). Total power 11.3 kW.

3c The cutter cuts plate (4.05 kW), while the storage drive motors operate (0.2 kW), plus base power (2 kW). Total power = 6.25 kW.

3d The cutter cuts plate (4.05 kW), plus base power (2 kW). Total power = 6.05 kW.

2b The cutter cuts I-beam (7.05 kW), plus base power (2 kW). Total power = 9.05 kW.

4 No tools are operating, base power only (2 kW). The cutter and the piece are waiting to be moved by the arm.

Figure 5.21 shows the facility power use for the first 500 minutes of reduction. Each square wave represents one complete stringer/plate piece cut from the aft barrel section. The peak power required for Scenario 1 is 11.5 kW; 1.70 days of continuous operation are required to reduce the ET to the 'bird cage' configuration. A more detailed description of the reduction model and the tool interfaces is included in Appendix B.

5.6 Electrical Power Subsystem (EPS)

5.6.1 Introduction. The first task taken to support this subsystem design effort was to perform a trade study between viable candidates as sources of power generation. Photovoltaic (PV) arrays augmented with nickel hydrogen (NiH$_2$) batteries
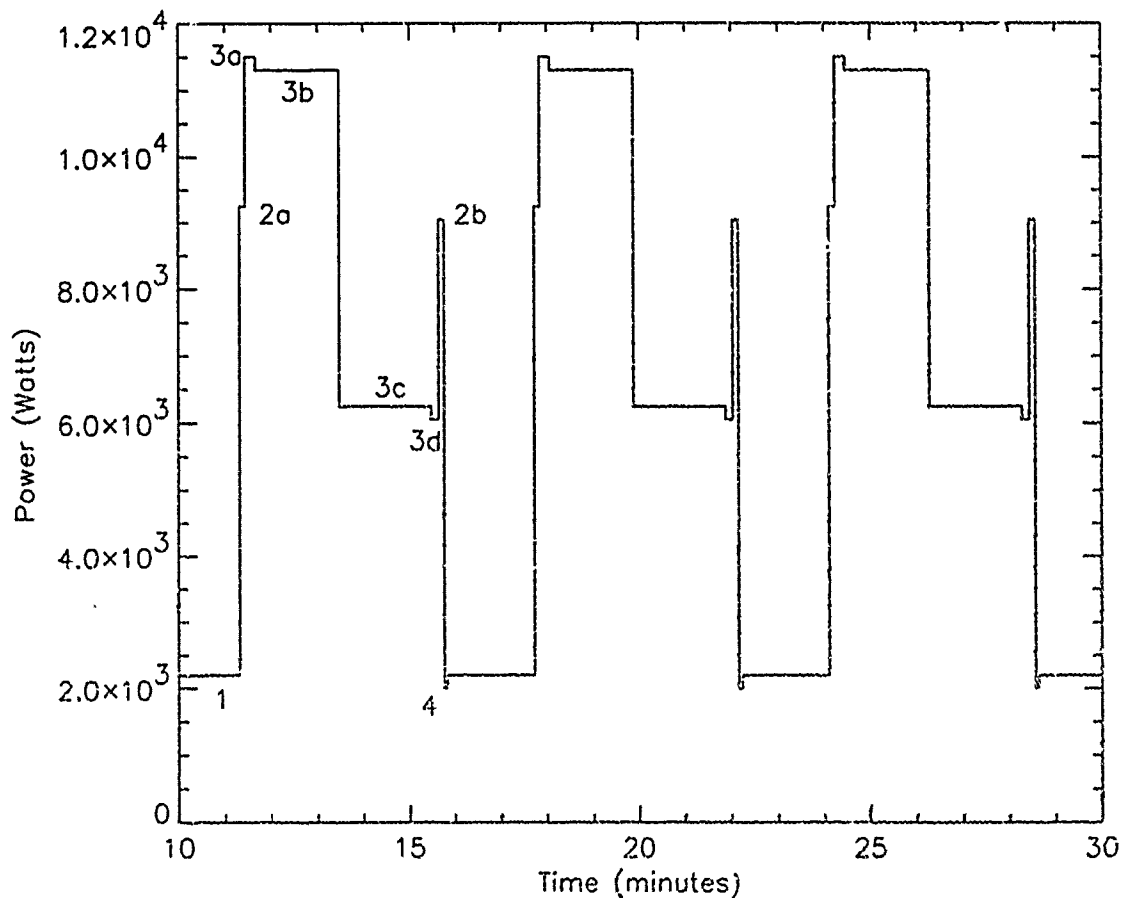
Figure 5.20. Typical Power Use - Scenario One

were chosen as the power generation source and the justification for this decision is provided in Appendix C.

Since the initial power budget was estimated to be 25 kW, and PV arrays were selected, it seemed a natural extension to study the SSF EPS to see if it could be adapted or exploited for our use. The baseline SSF EPS is explained in Appendix C. The ASSET EPS design is, essentially, a derivative of the SSF design.

5.6.2 ASSET EPS Design. The ASSET EPS is basically a modified version of a single PV module of SSF. The baseline SSF configuration is composed of 8 PV arrays as shown in Figure 5.22. The PV arrays are built up in pairs via a station
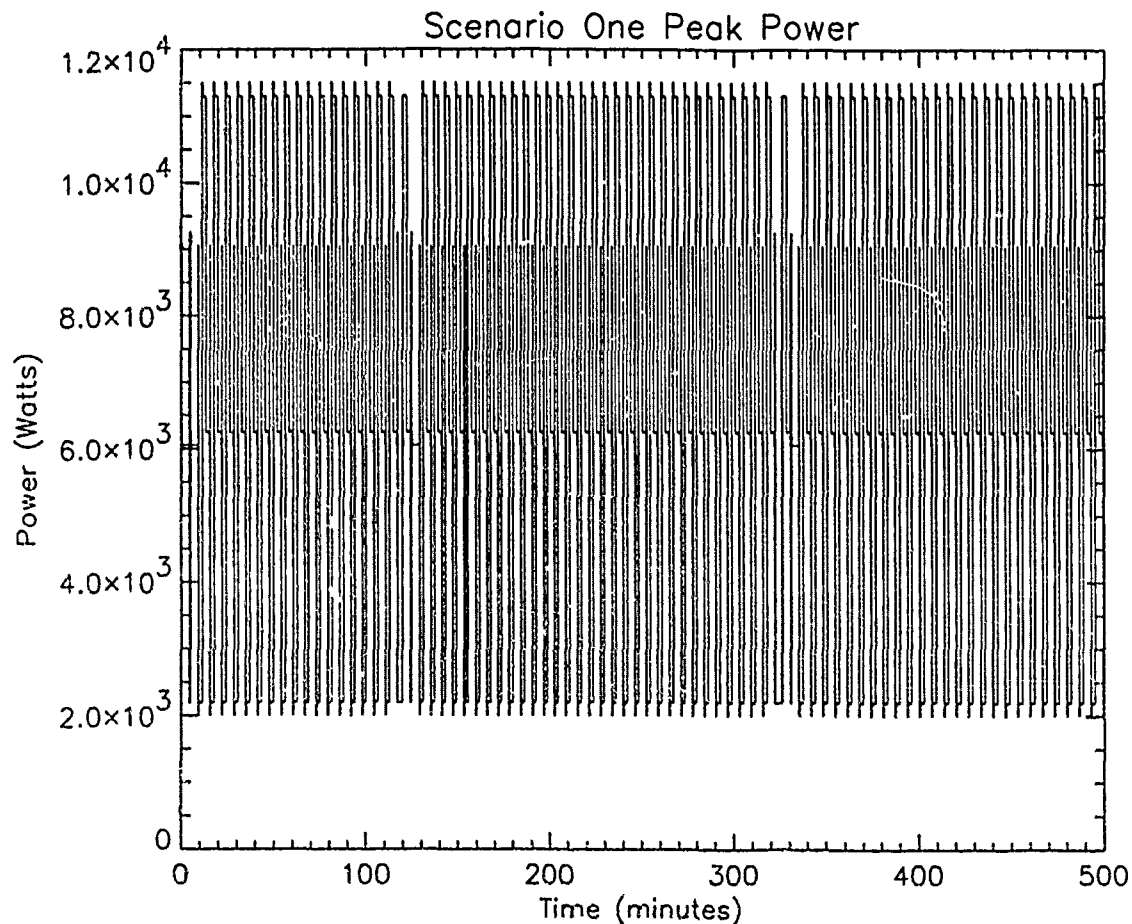
Figure 5.21. Peak Power Required - Scenario One

PV Power Module as shown in Figure 5.23.

The principle difference between the SSF design and the ASSET design is that the SSF design incorporates orbital averaging (as explained in Appendix C) while the ASSET design delivers a constant load power. The ASSET EPS design is shown in Figure 5.24. A constant load power system offers significant reduction in the design complexity for load scheduling (as compared to SSF) and is consistent with our objective to minimize technical complexity. The ASSET facility will simply not ask for more power than can be generated. It will be shown that this design can be implemented consistent with the objective to minimize life cycle costs.
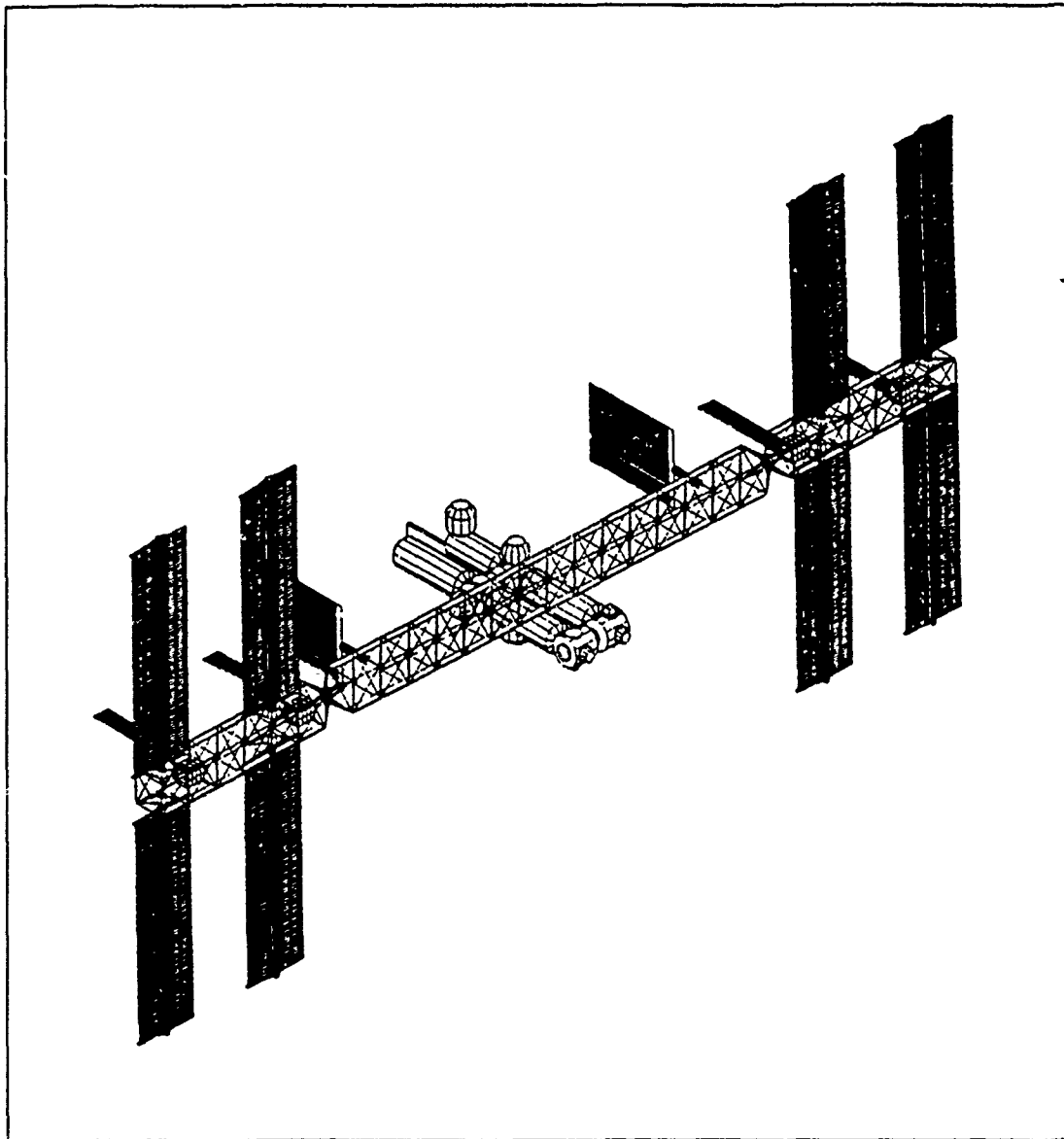
Figure 5.22. Space Station Phase 1 Baseline Configuration
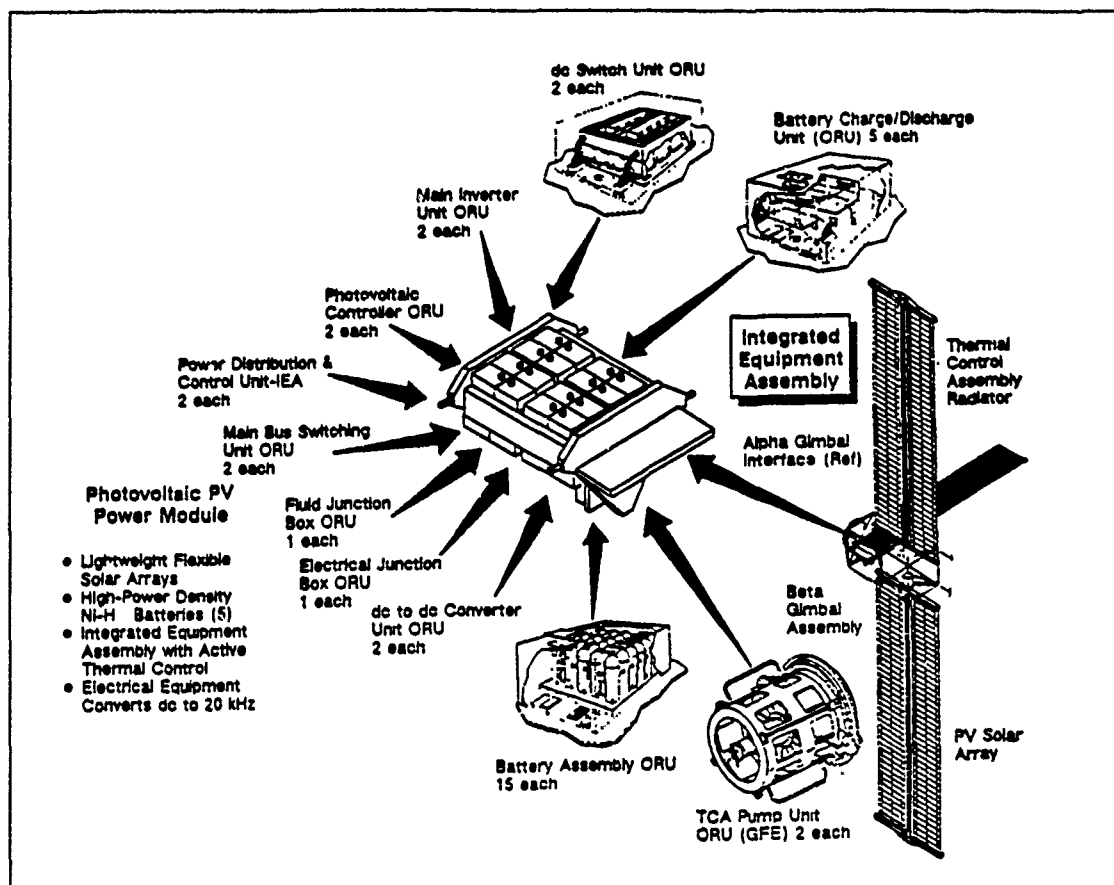
Figure 5.23. Station PV Power Module

Since the peak load demand does not exceed 12 kW, one can work from right to left (through Figure 5.24) to determine the sizes of the PV arrays. Given the efficiencies of the electrical equipment subsystem (EES) and power management and distribution (PMAD) equipment, one can determine the input to the EES. Knowing that the EES receives 51% of the base of array (BOA) power (the other 49% being used for battery charging during the sunlit portion of the orbit), one determines the required BOA power.

Once the BOA power has been determined, the actual array blanket sizes can be determined. Since an individual circuit (two array panels) delivers 160 vdc @ 2.4 watts, it is found that 82 circuits are required to supply the required BOA power.
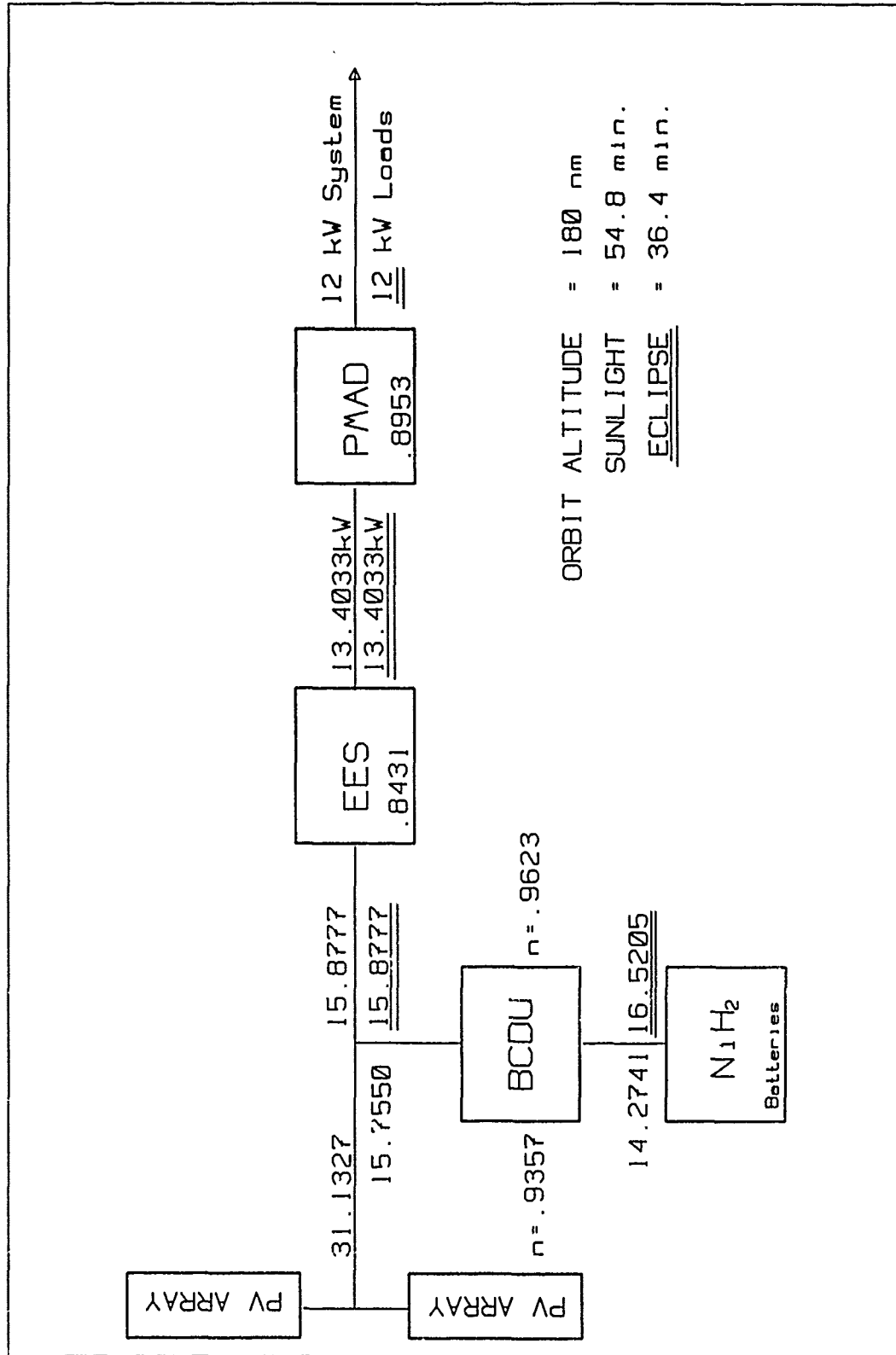
Figure 5.24. ASSET EPS Design: Scenario 1

Table 5.2. ASSET Battery Optimization, Scenario 1

# Batt.	kW/Batt.	Dischg Amps	DOD	Life (yrs)	Weight (lbs)
5	3.3041	29.3698	.3626	7.3315	2689.5
4	4.1301	36.7122	.4532	4.6425	2151.6
3	5.5068	48.9496	.6043	1.3699	1613.7
2	8.2603	73.4244	.9065	0.1113	1075.8

The number of circuits, in turn, can be used to determine the actual blanket area of the PV arrays (82 circuits x 2 panels/circuit x 1.6842 m^2 /panel = 276.2088 m^2 of panel area). The blanket area is summed with the mast, blanket boxes, and thermal control subsystem radiator area to determine a maximum drag area of 424 m^2.

The number of batteries (to supply the required 16.5205 kW of power during the eclipse period) is determined by balancing the requirements for weight, depth of discharge (DOD), life length, and reliability. The ASSET facility makes approximately 16 orbits per day which, in turn, implies 5,840 charge/discharge cycles of the batteries per year. Figure 5.25 is used to determine the number of charge/discharge life cycles as a function of DOD.

Life tests conducted at 100% DOD yield 300 to 500 charge/discharge cycles (85) before failure occurs. Conservative life data was generated by using the line projected to 300 cycles in Figure 5.25. Life length data, as a function of the number of batteries available, is presented in Table 5.2.

The life length of a battery may or may not be equivalent to a set number of calendar years. Life is only extracted from the batteries while they are cycling and the data in column 5 of Table 5.2 was generated under the assumption of a continuous cycling (24 hours per day 365 days a year) operation. Scenario 1 will typically require battery cycling for 10 days (a very conservative estimate) during the salvage operation.

Using Table 5.2, it is determined that 4 batteries is the optimum number of
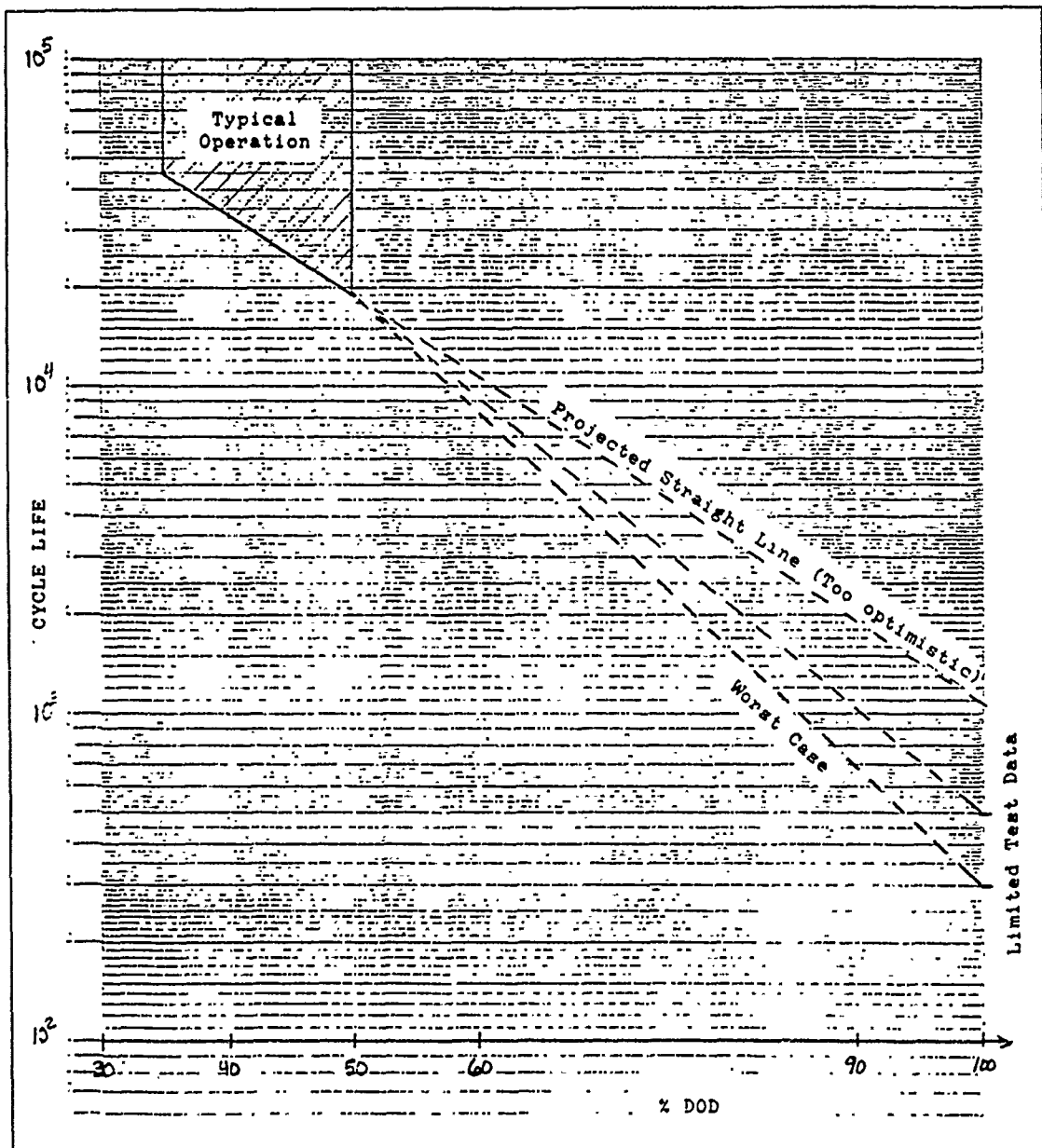
Figure ɔ.25. Cycle Life vs. % DOD

batteries to support Scenario 1. This choice represents the best balance between weight savings, and life length in the event of the loss of 1 battery. Even if a battery fails on day one of the initial tank to be salvaged, the three remaining batteries have sufficient life to allow the salvage of 50 tanks over a period of 12.5 calendar years.

In summary, the ASSET EPS design is a SSF EPS derivative which is implemented as a constant (as opposed to orbital averaging) load source. This decision simplifies the load scheduling problem and reduces the technical complexity of the facility. The batteries are driven at a higher DOD than normal, but it has been shown that sufficient cycle life is available to salvage 50 tanks (even after the loss of a battery) over a period of 12.5 calendar years. No battery maintenance is required, which is consistent with the objective to minimize life cycle costs.

5.7 Orbit Analysis Discussion

One of the prime drivers behind the technical feasibility of the ASSET operation is the issue of orbital maintenance. In the interest of public safety, any organization or company wishing to deploy space-based structures must minimize the risk of an uncontrolled deorbit. Additionally, economic considerations require positive control and long orbital lives for all space assets. By virtue of the nature of the ASSET mission, these issues are more significant and difficult to manage than would generally be the case.

Fortunately, studies have been conducted of the orbital maintenance requirements of the external tank for several scenarios involving the adaptation of the ET for on orbit applications (55, 52). Many of the orbital maintenance recommendations herein are adapted from these studies and from communications with the authors. In addition, much of our analysis is adapted from a study of orbital decay by Miner (61). He studied the orbital decay characteristics of the external tank with the use of an advanced orbit predictor program called *The Artificial Satellite Analysis Program (ASAP)*. His efforts laid the foundation for the analytical work

performed in this section.

Appendix D explains the assumptions and mathematical model used to describe the orbital dynamics of the ASSET facility. ASAP has been used to model the orbital decay of the ASSET structure (tank, Boost/Deboost Module, solar panels, etc.) and any debris generated during the operation. The development of a model that quantifies the fuel requirements for the ASSET mission scenarios is also explained in Appendix D. The following sections present the results of the fuel consumption and orbital lifetime trade studies between the Scenario 1 design alternatives.

5.7.1 Hardware Considerations. One of the constraints placed on the ASSET facility design was that it could not rely on outside stationkeeping support (orbital transfer vehicles, etc.). In other words, ASSET had to be self-sufficient in the areas of attitude and altitude control. Martin Marietta faced the same constraint during their design of the proposed ET Gamma Ray Imaging Telescope (ET GRIT) (55); their solution was to design a Boost/Deboost module (Figure 5.26), complete with built-in avionics and propulsion hardware to effect altitude and attitude control. Given the similarities between ASSET and ET GRIT, it became clear that this Boost/Deboost module (or a variant thereof) would meet our stationkeeping needs quite well. We therefore have adopted the ET GRIT Boost/Deboost Module as the baseline for all three scenarios.

Martin Marietta investigated a number of alternative rocket motors for use on the Boost/Deboost Module (52). We have simply adopted their recommendations here, thereby establishing the performance parameters of the module. All calculations assume the use of four 500 lb_f main thrusters with a specific impulse (I_{sp}) of 230 seconds.

5.7.2 Facility Orbit Decay. Figure 5.27 depicts a typical six-month altitude history of the ASSET system. A preliminary analysis has shown that due to the
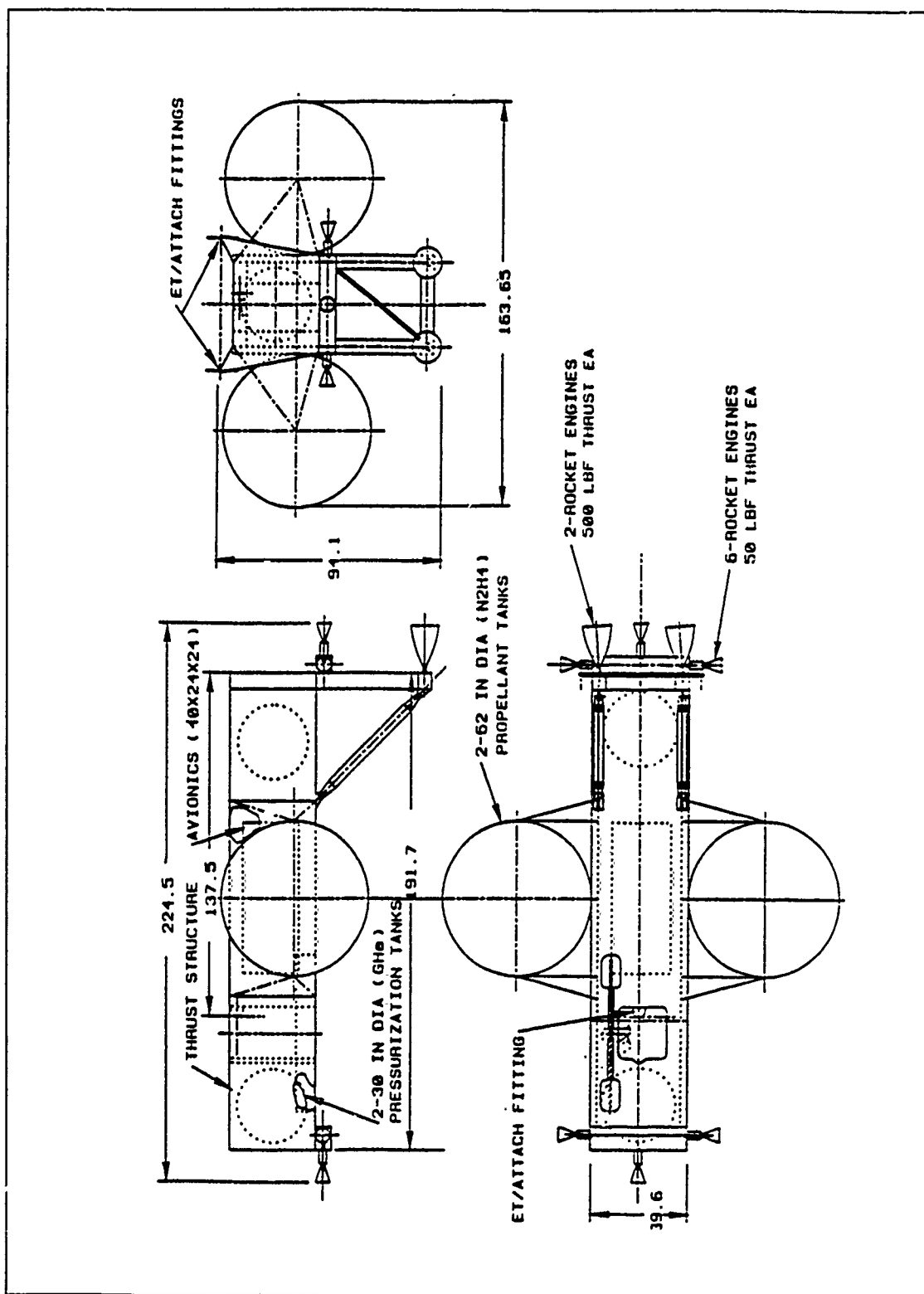
Figure 5.26. Candidate ET GRIT Boost/Deboost Module.
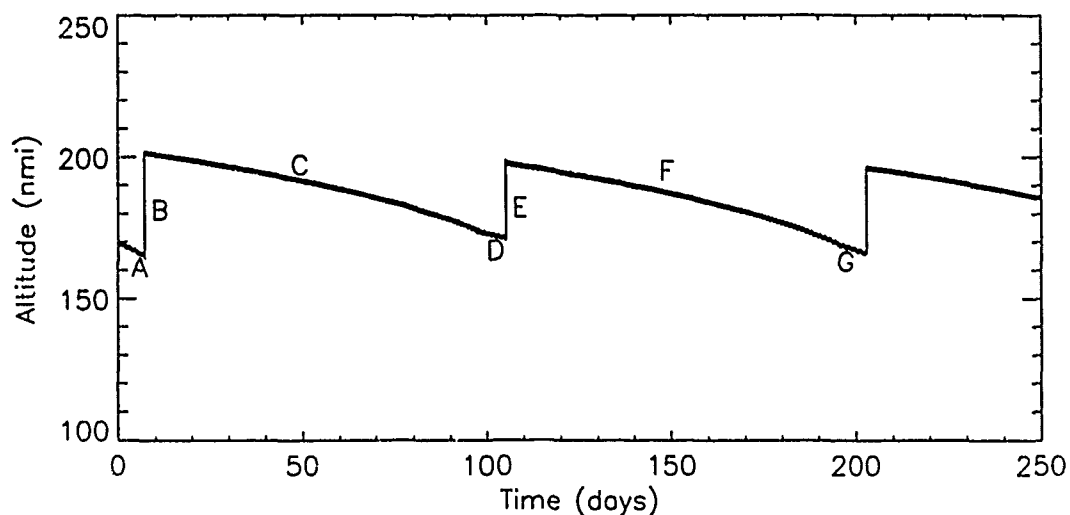
Figure 5.27. Altitude History, Scenario 1

required mission timelines, each reduction cycle (rendezvous, setup, cutting, etc.) must begin at an altitude of 170 nautical miles (nmi) or higher. Early mission plans called for a setup/rendezvous altitude of 160 nmi due to STS payload constraints and debris concerns. This proved to be unacc̲ able since the orbital life of the ASSET facility at that altitude was shown to ˙ less than 12 days. In fact, the altitude starts to drop off rapidly after only 7-8 days. By starting at 170 nmi, the altitude does not begin to decay rapidly until after 13 days or so. This provides the needed margin for any schedule slips or other unforeseen circumstances.

The six month altitude history of an ASSET mission plan is divided into seven phases labeled A through G. Phase A represents the initial setup of the facility, and includes the reduction of that first tank to its 'bird-cage' configuration. Phases B and E represent the Hohmann transfers that boost the facility into a pseudo parking orbit. [1] Phases D and G represent the periods during which the ASSET facility docks with and reduces subsequent tanks.

---

[1] This maneuver places the ASSET facility at an altitude such that after 90 days, the altitude losses due to drag will bring the facility back down (Phases C and F) to the rendezvous altitude of 170 nmi.

Referring to Figure 5.27, one finds that Phases F and G are virtually identical to Phases C and D. This cyclical feature of the ASSET altitude history is shared by all scenarios under consideration (with a slight modification for Scenario 3). The only difference between the cycles is the ballistic coefficient, β, of the facility (see Appendix D). Upon completion of each cycle, the mass of the ASSET facility is increased by an amount equal to the mass of the aluminum salvaged from the previous tank. Therefore, due to the improvement of the facility's ballistic coefficient, the altitude decay rate will decrease with time.

Note that after the initial setup and tank reduction at the end of Phase A, the facility experienced an altitude loss of approximately 5.0 nmi. During Phase D, when ASSET is docked with a second tank, the system has a longer orbital life due to its improved ballistic coefficient (see Appendix D). Over an eight day period, the docked tanks experience only a 3.7 nmi loss of altitude.

The fuel consumption calculations shown in Table 5.5 indicate that the ASSET facility propellant tanks must be recharged annually; this scenario dependent O&M cost could run as high as $50 million per year. It is clear that over the expected life of the system, a smaller array can save a great deal of fuel. A trade study was performed to measure the impact of competing solar array designs on the system life cycle cost. However, as we shall see, the lower efficiency solar arrays proved to be more cost effective despite their greater size.

Table 5.3 highlights the physical differences between the alternative solar array technology designs. Shown are the effective facility drag area A_d, mass M, and ballistic coefficient β. The impact these parameters have on the altitude at the end of each phase, h_f, is readily apparent. Notice the 3 nmi (average) altitude differences between the two options; fuel savings are proportional to these differences.

5.7.3 Debris. During the initial investigation of this concept, debris was identified as a major area of concern. Since one of our assumptions declared that the

Table 5.3. Orbit Parameters, 12% vs. 21% Solar Arrays.

Phase	12% Efficiency				21% Efficiency			
	h_f (nm)	A_d (ft^2)	M (lbs)	β ($\frac{lbs}{ft^2}$)	h_f (nm)	A_d (ft^2)	M (lbs)	β ($\frac{lbs}{ft^2}$)
A	165.0	4563.8	101,088	10.1	165.8	3229.1	99,156	14.0
B	201.4	4563.8	101,088	10.1	198.2	3229.1	99,156	14.0
C	174.4	4563.8	99,088	9.9	171.2	3229.1	97,172	13.7
D	171.2	5134.3	168,612	14.9	168.5	3800.0	166,696	19.9
E	201.4	4563.8	111,844	11.1	193.8	3229.1	109,928	15.5
F	169.5	4563.8	109,644	10.9	172.2	3229.1	107,745	15.2
G	165.8	5134.3	179,168	15.9	169.8	3800.0	177,270	21.2

ASSET facility would operate in the same orbital plane as Space Station *Freedom* (but at a lower altitude), debris management affected all aspects of the system design. The desire to minimize debris hazards drove the mission planning phase of the study; the cutting operations are carried out at a low altitude by design, primarily to enable the atmosphere to 'pull' the debris back down to Earth as rapidly as possible. Figure 5.28 shows the projected orbital life of a typical section of SOFI that has been removed from a plate/I-beam section.

The three curves represent the maximum, median, and minimum drag orientations of the SOFI debris. This plot shows that in the event debris of this type (24" long x 9.5" wide x 1" thick) escapes the ASSET facility, it should deorbit within a matter of days. Smaller pieces of SOFI should deorbit within 12-24 hours. Operating at this altitude then essentially eliminates the concern that the cutting operation might contaminate the environment of Space Station *Freedom*.

5.7.4 Fuel Consumption. The data presented in Table 5.3 is used to determine the amount of fuel consumed during the orbital maneuvers required to establish the altitude profile in Figure 5.27. These maneuvers include main thruster burns for the Hohmann transfers, plus RCS jet burns for attitude adjustments. Table 5.4
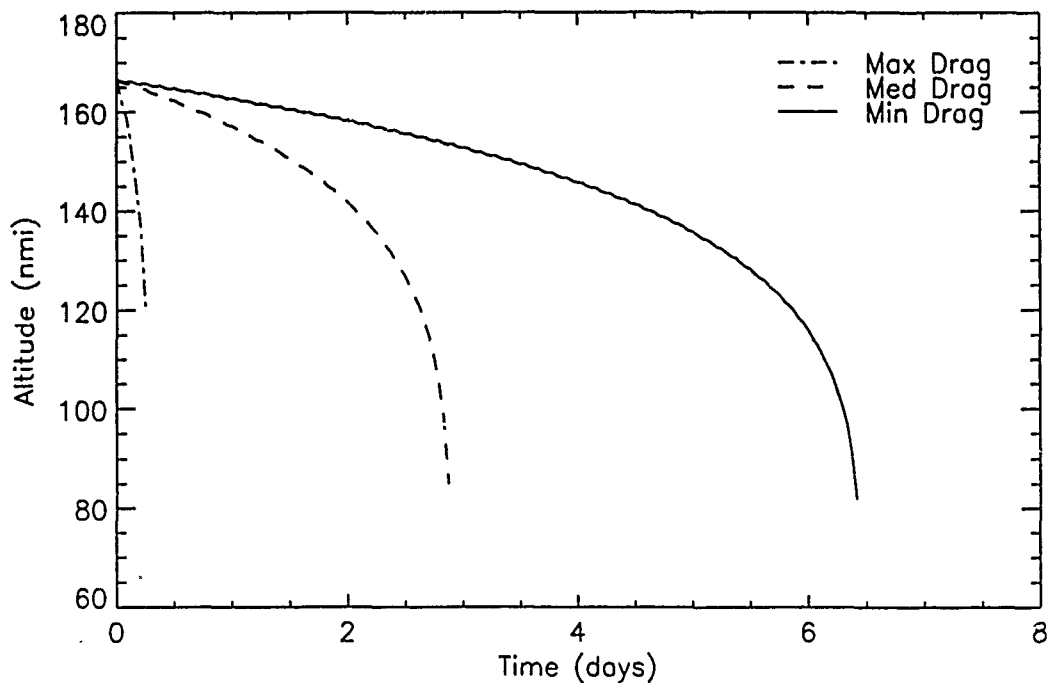
Figure 5.28. SOFI Debris Orbital Life.

presents the total ΔV's and thruster burn times required for those maneuvers per-
formed each year for both the 12% and 21% efficient solar array systems. Table 5.5
lists the fuel requirements for the Hohmann maneuvers. The total quantity of fuel
consumed is adjusted to include a 20% allowance for RCS fuel and a 10% allowance
for management reserve requirements (54:45). Notice that there is a substantial
fuel savings realized when the higher efficiency (smaller surface area) solar arrays
are used. However, our cost model has shown the fuel savings to be of insufficient
magnitude to offset the added development costs associated with the more efficient
arrays.

From Table 5.5. one can see that the propellant tankage for the 12% efficiency
EPS system must be designed to house at least 9,784 *lbs* of fuel. Notice that for the
21% efficient EPS system the tanks need hold only 7,521 *lbs* of fuel.

Table 5.4. Annual ΔV Requirements, Scenario 1.

Hohmann Transfer	12% Array		21% Array	
	ΔV_t (ft/sec)	t_b (sec)	ΔV_t (ft/sec)	t_b (sec)
#1	126.8	199.2	101.5	156.5
#2	105.2	182.8	88.5	151.1
#3	118.6	225.5	88.4	165.6
#4	118.6	244.8	89.4	182.0
Total	469.2	852.3	367.8	655.2

Table 5.5. Annual Fuel Consumption, Scenario 1.

Hohmann Transfer	12% Array m_f (lbs)	21% Array m_f (lbs)
#1	1,732	1,361
#2	1,590	1,314
#3	1,961	1,440
#4	2,129	1,583
Subtotal	7,412	5,698
20% RCS	1,482	1,140
	8,894	6,838
10% Res	889	684
Total	9,784	7,521

Since the bulk density of hydrazine, ρ_h, is $\approx 74.92 \ \frac{lb}{ft^3}$ (7), the approximate volume of the propellent tanks can be calculated:

$$V_{12\%} = \frac{m_f}{\rho_h} = \frac{9784 lbs}{74.92\frac{lbs}{ft^3}} \approx 131 ft^3$$

The ASSET Boost/Deboost Module requires four spherical tanks to house the hypergolics, therefore

$$V_{sph} \approx 32.65 = \frac{4}{3}\pi r^3 \Rightarrow r = 1.98 ft$$

or, for the 12% EPS, each tank must have a minimum diameter of about 4 ft. Similarly for the 21% EPS, each tank requires a minimum diameter of roughly 3.6 ft. However, to keep the fuel *resupply* costs down, one would want to maximize the size of the tanks, subject to the geometric constraints of the Space Shuttle payload bay. Clearly then, the lower efficiency EPS system will require more frequent refuelings. These results are reflected in the ASSET life cycle cost model.

5.7.5 Other Considerations. A great number of assumptions and simplifications have been made in order to reduce the complexity of this analysis (see Appendix D). As far as calculating rough order of magnitude fuel consumption numbers are concerned, these simplifications are justifiable. However, there are several key issues that have been neglected in this study which require further consideration.

We have assumed a steady supply of four tanks per year (due to *Freedom* crew exchanges) for our life cycle cost model. However, should there be an interruption in the STS schedule, contingency plans would have to be put into effect, and the facility placed in a 'holding pattern' until scheduling issues are resolved. This would result in higher fuel costs, increased operations costs, etc. No such contingencies have been incorporated in our cost model.

Even if we could assume a regular exchange of *Freedom* personnel, there remains the issue of Space Shuttle Orbital Maneuvering System (OMS) fuel constraints. Depending upon the payload manifest of the Shuttle Orbiter, any given resupply mission could be deemed 'OMS Critical'.[2] Missions deemed OMS critical would not be able to support the deployment of an ET, unless waivers could be negotiated. An OMS critical mission would have the same impact on our cost model as a schedule slip.

From a technical standpoint, the Achilles heel of the ASSET facility is the proposed manner in which it will dock with future tanks. The need to perform an

---

[2]STS-32, the Long Duration Exposure Facility (LDEF) retrieval mission was 'OMS Critical' (56)

automated, three point dock as shown in Figure 5.32 presents two major problems. First, the U. S. has little experience with automated docking maneuvers,[3] second, no-one has ever designed a three-point docking system. However, by designing an appropriate interface structure between the two tanks, a single point dock can be realized. Martin Marietta has recommended the use of the CTV (Cargo Transfer Vehicle [4]) to stabilize the passive 2nd tank while the ASSET facility performs the rendezvous/docking maneuvers. The projected cost of leasing a CTV for each docking maneuver has been incorporated in the cost model.

Finally, the most serious problem confronting the ASSET concept is the possibility of having different rates of orbital precession between *Freedom* and ASSET. Having to cope with plane change ΔV's could quickly jeopardize the economic viability of this project. This issue is discussed in more detail in Appendix D. However, the effect of the orbit precessions has not been evaluated in this study due to time constraints.

5.8   Facility Monitoring and Control

Scenario one minimizes the amount of manned control required to reduce the ET. For normal operations, no manned interface is necessary; the facility is totally automated. The reduction sequence is predetermined and all machines operate independent of any external control. This requires that all tools be controlled using simple sensors and switches. The reduction tools primarily use two types of sensors:

- Tactile or touch sensors.

- Force/torque sensors.

Tactile sensors are activated when the sensor comes in direct contact with another surface. It is a binary type device that indicates contact or no contact. A

---

[3]The Soviets perform automated dockings regularly with their Mir Space Station (91).

[4]Some Space Station planners are calling for a CTV type vehicle for space station operations.

simple microswitch is an example. They are usually used to stop motion or to define the bounds of a tool(44:230).

Force/torque sensors measure magnitude and direction of reaction forces or moments imparted to a given item. They use piezoelectric transducers or strain gauges on the compliant sections to detect the force or moment applied(44:245). The sensoring employed to control each tool and for detecting equipment failures will be discussed separately.

5.8.1 Cutter Control. Control of the cutter and platform is critical to the reduction of the ET. The cutter and platform are required to interact with the transport arm and the geometry of the LH_2 tank in order to move throughout the tank without external control. The cutter and platform must be capable of:

1. Grasping or releasing the stringers when moved by the transport arm.

2. Starting and stopping the cut at the proper location.

3. Differentiating between cutting stringers and plate and adjusting the cut rate and power level accordingly.

4. Determining when to cut radially or longitudinally.

5. Determining when to make a box - cut or c - cut.

5.8.2 Cutter Sensoring. The sensoring required to control the cutter and platform is fairly simple, since the cutter and platform follow a regular sequence of cuts. The most common cut sequence is a radial cut of plate and stringer, followed by a longitudinal cut of plate the length of the barrel section, ended by a radial cut of stringer and plate. This type of cut is called a c - cut. A less frequent cut, called a box - cut, consists of two radial cuts and two longitudinal cuts. The box - cut is used to complete a series of c - cuts. The cutter itself moves while making radial cuts; the platform moves for longitudinal cuts. Figure 5.29 illustrates the sensoring employed

by the cutter and platform throughout each phase of the cutting operation. Each number indicates a sensoring operation.

1. Once the transport arm brings the cutter in contact with the stringers a tactile sensor in the base of the platform activates a switch which causes the platform to grasp the stringers.

2. When the transport arm releases the cutter, a tactile sensor switches the cutter power on, initially set to cut plate, and the first radial cut begins.

3. A switch on the cutter adjusts the cut rate and power level to cut stringer as the cutter is extended to within 1.25 inches of its total reach.

4. A switch senses the end of the radial cut when the cutter is extended at its full reach, and adjusts the cut rate and power to begin a longitudinal cut of plate.

5. When the cutter and platform reach the end of the longitudinal cut, another tactile sensor contacts the major ring frame and indicates the start of the second radial cut, and the cut rate and power are adjusted to cut stringer.

6. As the cutter clears the stringer, a sensor loses contact with the stringer and adjusts the cut rate and power level to cut plate.

7. When the cutter retracts to its shortest length, a tactile sensor turns off the cutter and the cut is complete, or

8. A mechanical counter indicates that a box - cut is to be made, and the cutter and platform continue, cutting a longitudinal cut and returning to the other end of the barrel section where a tactile sensor contacts the major ring frame and turns off the cutter.

9. When the transport arm grasps the cutter, a microswitch is activated that releases the platform's grip on the stringers and allows the arm to move the cutter to the next stringer.
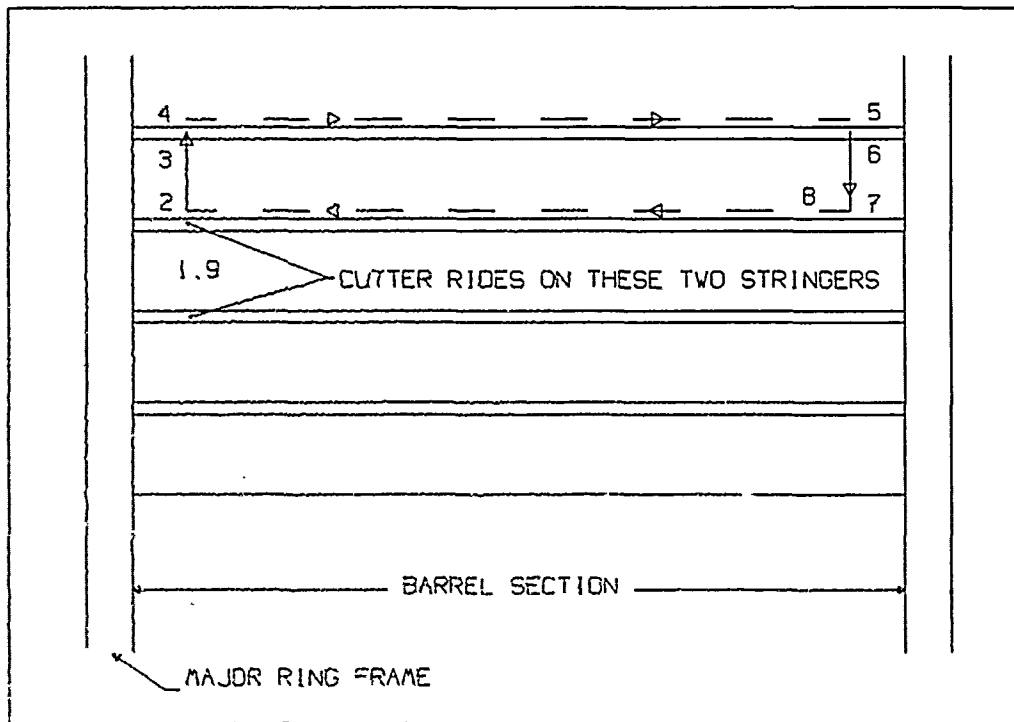
Figure 5.29. Sensoring for the Cutter and Platform

5.8.3 Transport Arm Control. The transport arm must be 'aware' of its location within the LH$_2$ tank at all times. This requires that the arm be accurately indexed to maintain the correct geometric relationships to the other tools within the tank. This is done two ways. First, the arm is geared on the centerline track to maintain accurate distances longitudinally and radially within the tank. The second way the arm is kept correctly oriented is by using static sensing. This requires a linear array type camera on the arm to scan a photosensitive element and provide location feedback to the arm(44:235). In this case, the photosensitive element is a simple bar coded strip located at several locations within the tank that provides an exact radial and longitudinal location to the arm. The transport arm corrects for any error in its location after each series of cuts in a barrel section. Another capability the transport arm requires is the ability to distinguish between grasping a stringer and grasping the cutter. This is easily taken care of by the use of tactile sensors. The arm grasps the cutter on a grip identical to that of a section of stringer. By using

tactile sensors on the transport arm gripper that extend beyond the dimensions of the cutter grip but not beyond those of a stringer, the arm can determine whether it is gripping a stringer or the cutter.

5.8.4 SOFI Work Station Sensoring and Control. The SOFI work station must be capable of accomplishing three tasks which require sensoring:

1. Turn on the work station drive motors when a piece is fed into the stripper.

2. Determine which side the stringer is located on the piece and adjust the secondary cutter accordingly.

3. Turn off the drive motors when the product has been stored.

All three tasks are easily accomplished using tactile sensors. As the piece contacts sensors on the inlet guide to the SOFI stripper, the drive motors are turned on. Sensors in contact with each side of the piece determine which side the stringer is located on and position the secondary cutter accordingly. As the products are pushed into storage they no longer contact sensors located at the work station exit and the drive motors are turned off.

5.8.5 Fault Detection and Correction. System failures for the Scenario 1 AS-SET facility can be divided into three categories:

1. Simple failures which can be detected with sensors and corrected automatically.

2. Failures which can be detected by sensors and can be corrected by teleoperation of the transport arm.

3. All other failures which may or may not be detected by sensoring and require that the facility be repaired by EVA.

Simple failures will be discussed first. Two simple failures can be detected and corrected automatically: a broken stripper wire at the SOFI work station, and an

incomplete cut. A broken stripper wire is detected when an electrical signal is interrupted by the broken wire. This causes stripping to stop and the stripper wire cartridge to be rotated to expose a new wire. The stripping operation can then resume. An incomplete cut is detected by the transport arm, using a force sensor. If there is any reaction force detected by the arm as it attempts to move a stringer/plate piece to the SOFI work station, the arm will release the piece and, once the cutter stops, move the cutter to recut the piece. If the arm detects an incomplete cut in three consecutive cuts, a primary cutter failure has occurred and the cutter must be replaced by teleoperation of the transport arm. One spare cutter is mounted in the tank upon initial set up of the facility. Teleoperation of the transport arm is also required if a stringer or plate becomes jammed at the SOFI work station. Torque sensors on the drive motors of the work station detect if a jam has occurred and signal that teleoperation is required. Teleoperation of the transport arm can be conducted from the space station, the orbiter, or the ASSET ground base. If any fault cannot be corrected by teleoperation of the transport arm, the facility will be shut down and the fault will be corrected by EVA.

5.8.6 Communications. The degree of monitoring and control necessary for the reduction facility to operate according to Scenario 1 has a direct impact on its required communications capabilities(52). The following communication requirements were established for Scenario 1:

1. Ability to receive uplink commands and messages and transmit video communication and data via the Tracking and Data Relay Satellite System (TDRSS).

2. Backup communications capability through the space station or the orbiter.

3. Ability to teleoperate the transport arm and remotely control the extension and retraction of the solar arrays.

4. Ground command shutdown and boost/deboost capability.

5. Data encryption of uplink commands.

6. Ability to remotely monitor the reduction operation from a ground based control center.

5.8.7 Camera Equipment. The capability to teleoperate the transport arm implies that sufficient lighting and video equipment is installed within the tank. Camera requirements were based on the desire to view the entire LH_2 tank at any stage of the reduction operation and to provide enough correctly positioned cameras to provide depth perception during teleoperation of the transport arm. A minimum of two cameras are required to adequately control the transport arm during teleoperations; one mounted on the arm itself to provide a close up view of the gripper, and one to provide an overall view of the work area. Two cameras, each with 60-70 degrees field of view, positioned to provide an orthogonal view of the work area is the optimal configuration for controlling the trans, ort a...n(35:59). Since a majority of the teleoperation of the arm will be conducted in the vicinity of the SOFI work station, it was determined that a total of four fixed vidicon cameras positioned on the bird cage structure at the second and fourth major ring frames and oriented toward the work station would be adequate for most teleoperations. Any product jams could be viewed and corrected by the arm using these cameras. Two cameras are mounted on each major ring frame. A fifth vidicon camera mounted on the transport arm truck provides the capability to view the remaining area of the tank not in the field of view of the four fixed cameras. All the cameras required for the facility are black and white. A summary of the Scenario 1 camera requirements is provided in Table 5.6.

5.8.8 Light Fixtures. The primary considerations in selecting and positioning light fixtures were to provide light to all areas within the tank that require video monitoring and to minimize shadowing in areas that the arm is required to teleoperate. Light fixtures were positioned evenly throughout the tank, three per major ring frame, at the junction of the bird cage and the major ring frame. Power cables for

Table 5.6. Scenario One Camera Requirements

CAMERA TYPE	NUMBER
Fixed wide angle black and white vidicon (mounted on major ring frames)	4
Mobile wide angle black and white vidicon (mounted on the transport arm truck)	1
Mobile telephoto black and white vidicon (mounted on the transport arm)	1
Linear array, for indexing arm position (mounted on the transport arm)	1

Table 5.7. Scenario One Lighting Requirements

NUMBER	LOCATION	POWER
15	3 per major ring frame	60 watts each
1	Transport arm truck	100 watts
		1000 watts total

the lights, as well as the camera equipment, are routed along each major ring frame. Another light fixture located on the transport arm provides lighting when required to teleoperate the arm. Estimates for the weight and volume of light fixtures were: 10.0 pounds per light and 1.25 cubic feet each(35:59). A summary of the Scenario 1 lighting requirements is shown in Table 5.7.

5.9 Thermal Analysis

There will be little variation in the thermal conditions from scenario to scenario. For this reason most thermal considerations will be dealt with in this section and in Appendix E. Thermal conditioning for power and avionics are treated in Appendix C.

5.9.1 LH_2 Thermal Conditions. Shortly after all the liquid hydrogen is vented, the walls of the LH_2 tank will be at a temperature of $-423°F$. Since the astronaut's

spacesuits are only rated at temperatures down to $-180°F$, the initial LH_2 tank temperature would be too cold for work. However, in Scenario 1 (as with all the scenarios), the astronauts would not be required to enter the LH_2 tank until 24 hours after the liquid hydrogen is vented. By this time, sufficient heat will leak through the spray on foam insulation to warm up the tank to approximately $-117°F$ (See calculations in Appendix E). Once the LH_2 tank is warmed up to $-117°F$, it will get no colder than $-131°F$ during the eclipse period.

To cope with the cold of the initial temperature of the LH_2 tank, motors and robotic joints should be equipped with small, hot coil heaters. The heaters should be thermostatically controlled so that they can be automatically turned on and off when conditions warrant.

5.9.2 Heat Sources. There were two potential sources of elevated temperature problems. Heating due to solar radiation, and heating due to the electron beam cutter.

For both the interior and exterior surfaces of the LH_2 tank, heating due to solar radiation would not be a problem. The principle reason for this is the thermal properties of the insulation on the surface of the LH_2 tank and the thermal properties of the 2219 Aluminum which comprises the interior structure. For both the spray on foam insulation (SOFI) and the 2219 aluminum, the ratio of the thermal absorptivity to the thermal emissivity is 1.0 (one). The solar thermal equilibrium temperature of any surface in space is determined by this ratio. The equilibrium temperature is reached when the flow of heat energy into a surface is equal to the flow of heat energy out of a surface. The thermal equilibrium temperature for SOFI and 2219 Aluminum is 40.85°F (as explained in Appendix E). If the sun were the only heat source, one would estimate that, at worst, both the SOFI and the 2219 would eventually achieve a temperature of 40.85 and would go no higher. A fundamental principle in the theory of heat transfer is that heat flow can not exist unless a difference in temperatures

exists. This is true for both radiative and conductive effects. If only solar radiation effects are considered, neither the 2219 Aluminum nor the SOFI can cause objects around them to reach temperatures above $40.85°F$.

The electron beam cutter cuts a path 157,079 inches long and .125 inches wide as the LH_2 tank is disassembled. The aluminum represented in this cut strip ·s heated to a temperature of $1220°F$ during this operation. If the tank were perfectly insulated, none of the heat energy would be lost. If the effects of thermal energy were averaged out over the interior surface of the LH_2 tank, the temperature would rise from $40.85°F$ to $60.02°F$. This temperature rise would not be a problem for astronauts or machinery.

The thermal radiation effects from the electron bombarded aluminum don't present a problem either. The reason for this is that the total surface area heated by the cutter is only $136.35 ft^2$ while the interior surface area of the LH_2 tank, minus dome caps, is $8384 ft^2$. Even if the solar radiation and the worst case electron beam radiation effects were combined, the hottest equilibrium temperature they could produce in concert would be $90.52°F$. Since spacesuits are rated to $235°F$, this temperature would not be a problem for astronauts.

The final source of heat for this scenario is the SOFI Workstation. The SOFI removal process itself generates no appreciable thermal energy. However, the plate/I-beam separator contains an electron beam cutter. The electron beam in the SOFI work station concentrates energy in a small area so the average temperatures are larger. For a typical 9.582 inch by 163 inch plate, the average temperature due to the electron beam would be $56.23°F$. An I-beam associated with this plate would be .125 inches by 163 inches. Its average temperature after cutting would be $148.4°F$. Since the astronauts suits are rated to $235°F$, these temperatures would present no problems either. All of the SOFI Workstation components that handle the I-beams and all of the stacking elements for the I-beams should be designed to take into account elevated temperatures. This should not be a problem since terrestrial

machinery exists which operates at much higher temperatures.

The radiative effects of the heated aluminum in the SOFI Workstation are largely mitigated by the fact that a plate/I-beam combination spends at least 9 seconds in the machine after it is heated. As analysis in the Appendix E shows, 9 seconds after they are heated, both the plate and I-beam can be considered to be at their average temperatures with no hot spots. The size of the hot spot at the SOFI Workstation is at worst, $.0052 ft^2$. The exposed surface area in the interior of the stripper machine would be at least $3.61 ft^2$. The heat flux which would flow from the hot spot to the machine surface could produce temperatures no greater than $-241.54°F$. Since the surface of the SOFI Workstation is likely to be closer to $40.85°F$, the radiative flux is small enough to neglect.

5.10   Products

Our initial desire was to reclaim the entire mass of the ET. However, we quickly came to the realization that this would be both impractical and cost prohibitive. We then began an investigation into reducing the ET into pieces that could be refined into structural material (for use in the Grumman Beam builder). Grumman Aerospace (see Chapter XI) has developed a beam builder that uses 10 mil. aluminum rolls and assembles large structural beams. Our goal was to produce the 10 mil. aluminum by either melting aluminum pieces and then extruding the 10 mil. sheet or rolling the .125" ET skin to a 10 mil. thickness. Both methods proved to be cost prohibitive. The best use of the ET as a resource is to use integral parts of the tank structure with only minimal refinements. The process involves cutting sections of the skin and stringers, then separating them to produce a nearly flat plate and an I-beam.

The plates are 2219 aluminum, 9.52" wide and .125" thick. The radius of curvature is 165.5" which results in a maximum .3" overall deflection in each plate. The plate lengths vary from 163" to 225.95" (see Figure 5.18 and Table 4.1). The I-

beams are 2219 aluminum that are 1.25" tall and 1.25" wide. They have .125" thick flanges and .10" thick webs. The I-beam lengths also vary from 163" to 225.95".

The automated nature of our tank reduction process permits additional material to be salvaged. The centerline track and the crossbar supports will be available (for use as products) beginning with the second tank.

The centerline track is 6" X 6" square 2219 aluminum tubing with a .125" wall thickness (Figure 5.30). The track is 912" long and can be easily removed from a reduced tank with a portable electron-beam cutter.

The crossbar supports are T-beam structures of 2219 aluminum. The forward supports are 6" X 3.5" with a .25" flange thickness and 155.5" length (Figure 5.30). The aft supports are 6" X 6" with a .25" flange thickness and 126" length.

The intermediate ring frames will be cut and quartered during the initial setup EVA. During the automated tank reduction period, the 32 intermediate ring frame pieces will be stored in the forward hydrogen tank dome. Upon completion of the reduction process these pieces will be available for construction use. While their uses in their present form are not as readily apparent as the I-beam and plates, they do provide 414 lbs. of additional material. The quarter ring frames are 234" long and varying widths and thicknesses (Figure 5.31).

5.11 Rendezvous With Subsequent Tanks

The problems of actually effecting a rendezvous with subsequent tanks has previously been discussed. Once rendezvous has been accomplished, tool transfer must be effected. For tank #2 only, the initial products from tank #1 will have to be bundled and stored (or delivered) prior to tool transfer. Once the initial products have been stored, tool tear-down and transfer will commence. Tools are transferred via the LH_2 aft manholes (just like the first tank; the difference being that tools now come from tank #1 instead of the orbiter cargo bay.
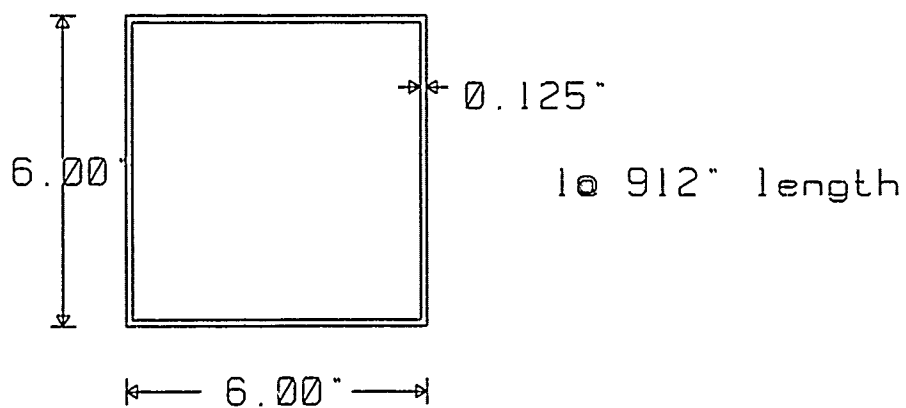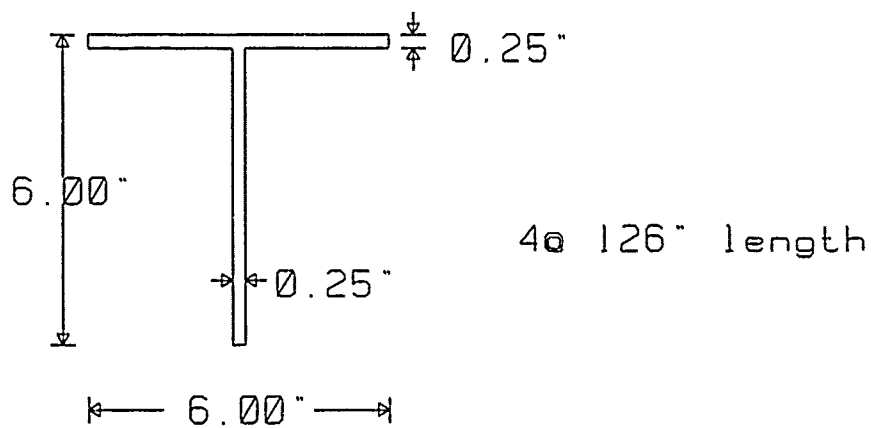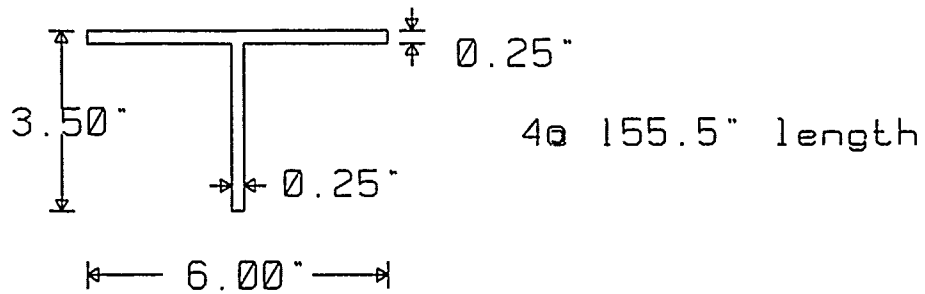
Figure 5.30. Centerline Track as a Product
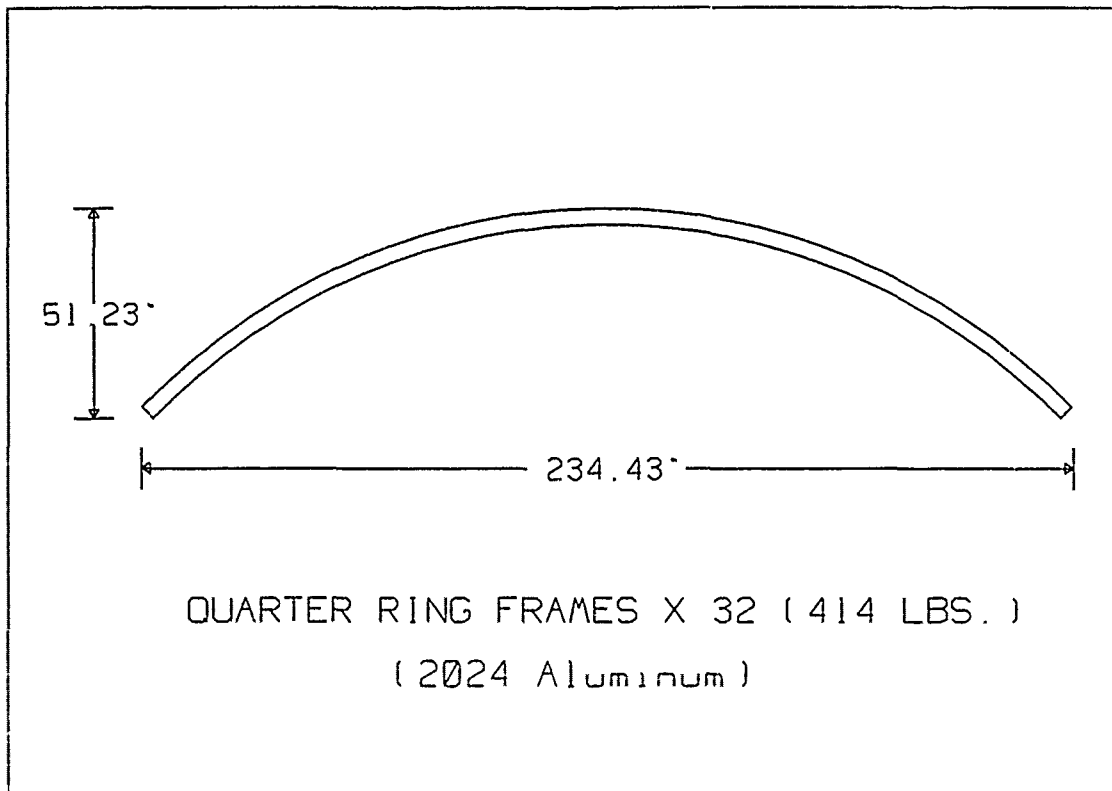
Figure 5.31. Quarter Ring Frames

Electrical umbilicals will be run between the two intertank access doors. Connectors for power distribution will be installed in the tank #2 LH$_2$ forward dome (as in tank #1). Distribution networks will be removed from tank #1 and reused in tank #2. Essentially, the only equipment from tank #1 that is not transferred to tank #2 is the boost deboost module (for orbital maintenance) and the solar arrays (for power generation). All tool tear down and transfer is accomplished via EVA and detailed timelines for such tasks are provided in Appendix F.

Actual reduction for the second and subsequent tanks is accomplished exactly like the initial reduction. All subsequent tanks will have pre-installed centerline tracks, and the same tools will process the same piece parts and salvage the same products. The orbiter would be free to leave during the actual reduction process, but EVA will again be required once the reduction is finished.

Once the second (or subsequent) tank has been reduced, EVA is required to transfer products and tools back to the initial tank. This task will be somewhat easier than the original tool transfer since both tanks have now been reduced to a 'bird cage' structure as shown in Figure 5.32. Transferred tools will be stored in the aft LH_2 dome area of the original tank to facilitate quicker transfer to subsequent tanks.

Subsequent tanks which have been reduced will either be sold (customer would have to provide his own orbital maintenance and power generation systems) or de-orbited. The increased drag effects during actual reduction of the second tank and the delta fuel consumed as a function of salvaged products aboard are included in fuel calculations. Fuel consumption to include boosting ASSET (with a subsequent tank still attached) was not considered.

5.12 Mission Timelines

For the initial tank, which will be a dedicated NSTS mission, five days will be required. This mission timeline assumes that NASA will grant a waiver to allow ASSET employees to conduct an initial EVA 24 hours after launch (current NASA guidelines require 72 hours after launch prior to first EVA). This timeline also assumes that the orbiter remains on station during the 40.8 hours (1.7 days) of actual reduction. Two 480 minute EVA's would be used to set up the initial facility. Sixteen hours of rest time are assumed to be required between EVA's. Detailed task lists per EVA are provided in Appendix F.

For subsequent tanks, which will not be dedicated missions, 6.3 days will be required. This mission timeline again assumes NASA will grant a waiver to allow EVA 24 hours after launch. Two 480 minute EVA's would be used to bundle previously salvaged products, transfer tools, and ready the subsequent tank for reduction. The orbiter could leave for the 1.7 days of actual reduction. Two more EVA's (of 480 and 380 minutes duration) would be required after reduction to move salvaged
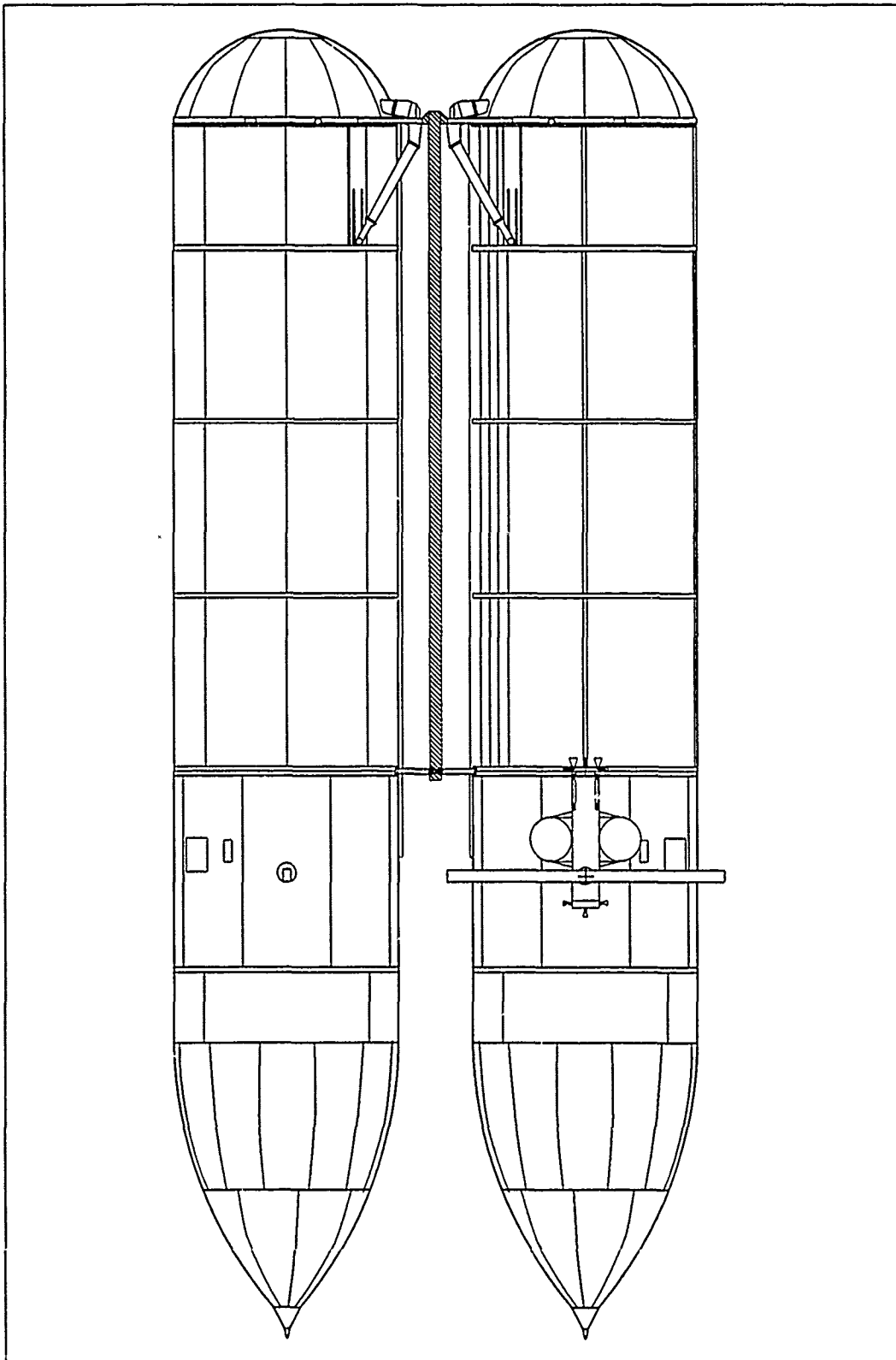
Figure 5.32. Rendezvous and Subsequent Tank Reduction

products and the facility tools back to the original ASSET tank. Sixteen hours of rest time are assumed to be required between EVA's. Detailed task lists per EVA are provided in Appendix F.

5.13 Evolution and Optimization

5.13.1 Ideas Considered But Rejected. Automated reduction was always the focus of Scenario 1. While other attempts at reduction focused on cutting up or melting the tank from the outside, our view of the uniform nature of the interior of the LH_2 tank led us to develop tools which reduce the tank from the inside out. The uniformity of the interior, especially if the intermediate ring frames were removed, led us to believe that automated reduction would be a low risk development.

Our initial idea was to develop a sophisticated cutter which could provide it's own radial and longitudinal mobility. This early device would have cut out several plate/I-beam strips, stacked them on itself, and eventually carried the parts to a workstation which would remove the SOFI and store the salvaged aluminum products.

This initial cutter was discarded for various reasons; the foremost being the level of sophistication required to accomplish such a task. Positive control of the parts, from cutting to transport to storage, has always been a design driver and this concept was viewed as requiring sophisticated robotics (which was in conflict with our objective to minimize the technical complexity). Not only would the robotics required to pick up and initially store the plate/I-beam strips be complex, it appeared that a second 'machine' would be required at the workstation to unload our products.

Clearly, such a device would not be very efficient (although it was originally thought that such an automated process could be a very slow, less power intensive operation). Radial mobility did not seem to be an insurmountable problem and the ability to 'step' over the integral major ring frames was a relatively straightforward design (remnants of which survived on the primary cutter).

Aside from the facts that such a device would require a sophisticated robotics design and would not be very efficient, there remained the very large problem of how to power a device with almost unlimited freedom of movement. The principal problem (which could not be resolved in an efficient manner) was how to keep power cables free from other obstructions within the tank (such as the SOFI workstation). This concept was abandoned in favor of a simpler design which helped minimize technical complexity and offered a lower cost development effort.

Another idea originally considered but abandoned was the concept of an automated tool to remove the intermediate ring frames from the interior of the LH_2 tank. The motivation for removal stemmed from the fact that a more efficient cutting operation (fewer pieces to handle, transport, and store) could be conducted once they were removed. Equally as important, was the fact that much longer products could be salvaged. We envisioned a camera equipped tool that would locate the t-clips which fasten the intermediate ring frames to the I-beams. A cutter (probably a pulsed electron beam gun) would then cut through the t-clip flanges. We considered a tool which either straddled or worked on one side of the intermediate ring frame.

This idea was abandoned since something still had to be done with the intermediate ring frames once they had been removed. The intermediate ring frames would need subsequent cuts, some form of bundling, and transportation to an area not planned for reduction. Debris was also a contributor to the abandonment of this concept since 1 of the 8 intermediate ring frames is attached via 108 bolts. The level of sophistication required to solve this problem was judged to be in conflict with the objectives of minimizing technical complexity and life cycle costs.

5.13.2 Lessons Learned/Changed Perceptions. The foremost lesson learned was that a slower, less power intensive operation was not a valid candidate to handle subsequent tank reduction. Not only would a slow reduction effort be fuel intensive (to maintain orbit during reduction), but EVA is also required to remove products

and tools after reduction. An assumed 10 day maximum mission for orbiter support would clearly be a severe constraint and it was deemed necessary to operate within NASA guidelines whenever possible. Clearly, the demand for orbiter support (in terms of EVA) drove the development toward a design which salvaged as much of the ET as possible, as quickly as possible.

5.13.3 Scenario Level Trade Studies. The trade between facility drag (dominated by the surface area of the PV arrays) and the fuel consumed to maintain orbit was examined. The initial PV array design was an off-the-shelf concept using the same array design as SSF. These arrays have an efficiency of 12%. A more efficient array design (state-of-the-art is approximately 21%) would present a considerably smaller drag area and would offer significant fuel savings. The question to resolve was whether the increased research and development costs (for a more efficient array) could be offset by reduced fuel consumption and fuel resupply costs.

The trade between the number of batteries required to supply power during the eclipse portion of the orbit was also examined. The number of batteries determines how hard each battery is driven, which, in turn, determines battery life length, which, in turn, drives maintenance costs. The data presented in section 5.6 represented the best balance between weight, life length, and reliability.

Attempts to optimize the weight of the ASSET facility were also conducted. Neglecting the boost/deboost module (whose weight is clearly dominated by the expendable fuels it contains), the principal driver to the ASSET facility lies within the EPS. Weight savings (as functions of the number of batteries and projected estimates for weight savings realized by pursuing more efficient arrays) were compiled. Basically, the EPS impacts (as a function of ASSET weight and ASSET drag) were traded against the fuels expended (to maintain orbit) to determine a more cost effective method of facility operation.

A trade study to determine potential candidates for primary and secondary

cutters was also carried out. This trade study is documented with the rest of the tools in Appendix A.

The results of the remaining scenario level trades are presented (and contrasted with other scenarios) in Chapter IX where the various system level trades between scenarios are explained.

5.13.4 Cut Rate Optimization. Most earth based electron beam metal processing use is restricted to welding and drilling applications; very seldom is it used for large scale metal cutting. This is due to the high cost compared to other cutting methods and due to the requirement for the work piece to be enclosed in a vacuum for the electron beam to be most efficient. In space, the electron beam is in its optimum environment and can meet our needs for large scale metal cutting. Because of its limited use on earth, there is little published data on electron beam cutting, especially in a zero gravity environment. The electron beam cut rates used in the ET reduction model are based on research done by Richard D. Engquist on electron beam welding of 6061 aluminum (25). Unlike on earth, where gravity aids in removing the molten metal from the area of the cut, in space the primary force that allows electron beam metal cutting to take place is the surface tension of the molten metal. Surface tension is the force that tends to minimize the area of the surface of the molten metal. As the metal is melted, its surface tension pulls it away from the cut, creating a void in the workpiece. For successful EB cutting to take place, the width of the cut must be greater than the thickness of the workpiece in order for the surface tension of the metal to aid in removing the molten metal from the cut (77:310).

5.13.4.1 Power Versus Cut Rate. The cut rate, power level, and depth of cut are three parameters of electron beam cutting that are very closely related. The depth of the cut is directly related to power level; a deeper cut requires more power. For our application, depth of cut is a known constant: 0.125 inches while

Table 5.8. Initial Power and Cut Rate

MATERIAL	POWER	CUT RATE
Plate	3 kW	40 inches/min
Stringer	7 kW	10 inches/min

Table 5.9. Final Power and Cut Rate

MATERIAL	POWER	CUT RATE
Plate	4 kW	80 inches/min
Stringer	7 kW	10 inches/min

cutting plate and 1.25 inches for stringer. The power level of the cutter and cut rate can be varied. In developing the reduction model, the power level of the EB cutter and the EB cut rate were optimized to cut at the fastest rate (which can only be accomplished at the expense of a higher peak power requirement). The power level of the EB cutter and cut rate are inversely related; the faster the cut the more power is required. The reduction facility's initial power budget was set at 25 kW and EB cut rates were constrained between 10 - 100 inches per minute, in order to remain within the range of available data.

5.13.4.2 Simulation Results. The Scenario 1 reduction scheme was simulated with the initial values for power and cut rate shown in Table 5.8.

Simulation results conducted at the rates shown in Table 5.8 yielded a facility peak power of 14.5 kW. Analysis of histogram data showed that by managing when stringers were being cut, this peak power could be lowered to 10.5 kW with no change in the cutter power levels or cut rates. Since the peak power was well below the maximum level of 25 kW, the power level, and therefore the cut rate, for the cutter could be increased. Using the regression data from Engquist(25), the power level and cut rate for the cutter were increased to the values shown in Table 5.9.

Simulation results conducted at the rates shown in Table 5.9 yielded a facility

peak power of 11.5 kW. Since the tool rates were already near their maximum value (for the material thicknesses being cut), the 11.5 kW peak power requirement was established at the Scenario 1 baseline. A slight margin was added and 12 kW became the baseline requirement for the EPS design. The values in Table 5.9 were used in the final Scenario 1 reduction simulation.

VI. SCENARIO 2 - MANNED REDUCTION

6.1 Overview

Scenario 2 features manned reduction. The distinguishing characteristics of Scenario 2 are the absence of a centerline track and the fact that astronauts will be present during the actual salvage operation. In fact, EVA crews of three persons are required during the salvage operation.

The major change in philosophy between Scenario 1 and Scenario 2 is that astronauts now perform all transport tasks. Humans are used to move cutters, transport piece parts, load SOFI workstations, and store products. The three crew members will be designated as cutter, loader, or stacker and their functions are explained below.

The same basic tools developed for Scenario 1 will be used again for Scenario 2. There is no change to the design of the primary cutter, but Scenario 2 uses two primary cutters and will reduce two barrel sections of the LH_2 tank simultaneously. Although the cutter design is unchanged, the cutting scheme had to be modified. The cutters from two barrel sections must end up at a common point so they can be moved (radially) by a single person. This person is designated as the cutter.

The input side of the SOFI workstation is unchanged, except the piece parts are now loaded manually by an astronaut appropriately designated as the loader. The actual stripping operation is unchanged, but the output to the SOFI workstation has been simplified. The separated I-beams and plate are no longer automatically stored; rather an astronaut (appropriately designated as the stacker) will place the products in separate storage containers.

One new device was developed to support Scenario 2, a seat which is installed on one of two major ring frames. The seat is shown in Figure 6.1. Input power is routed into the rear of the seat and distributed out to the two primary cutters

(one on either side of the major ring frame). An astronaut (who may or may not be strapped into this seat) will move the cutters (radially) and hand off piece parts as they are cut out to one of the two remaining astronauts. A brake is provided to lock the seat at a certain location. The astronaut releases the brake and provides his own power to move in the radial direction.

Reduction starts in the two forward barrel sections of the LH_2 tank as shown in Figure 6.1. As piece parts are cut out, the astronaut (cutter) in the work seat (initially installed at major ring frame 1377.35) will pick up and hand off piece parts to the astronaut (stacker) stationed at the output of the SOFI workstation (approximately station 1500.58). The part is then handed off to the 3rd astronaut (loader) stationed at the input to the SOFI workstation (approximately station 1711.46) who, in turn, will load the piece part into the SOFI workstation.

The stacker will move the parts into storage containers very similar to those used in Scenario 1. This person will be required to handle all piece parts twice while the two forward barrels of the LH_2 tank are being reduced. The stacker has the highest workload, but could trade off with the loader if fatigue becomes a factor. The stacker is required even if the output of the SOFI workstation had been left in its Scenario 1 configuration since pieces cut out of the forward barrel sections are of insufficient length to be handed directly to the loader.

Once the two forward barrels of the LH_2 tank have been reduced, the workseat will be moved from station 1377.35 to station 1871. Power cables to the two primary cutters are disconnected prior to transport. The workseat is only moved once in the longitudinal direction during Scenario 2 reduction. When the workseat has been reinstalled, the two primary cutters moved from barrels three and four to barrels one and two, and power cables reconnected to the primary cutters, reduction of the two aft barrels of the LH_2 tank is ready to begin.

As piece parts are cut out of the two aft barrels, the astronaut in the workseat (cutter) picks them up and hands them off to the loader at the input to the SOFI
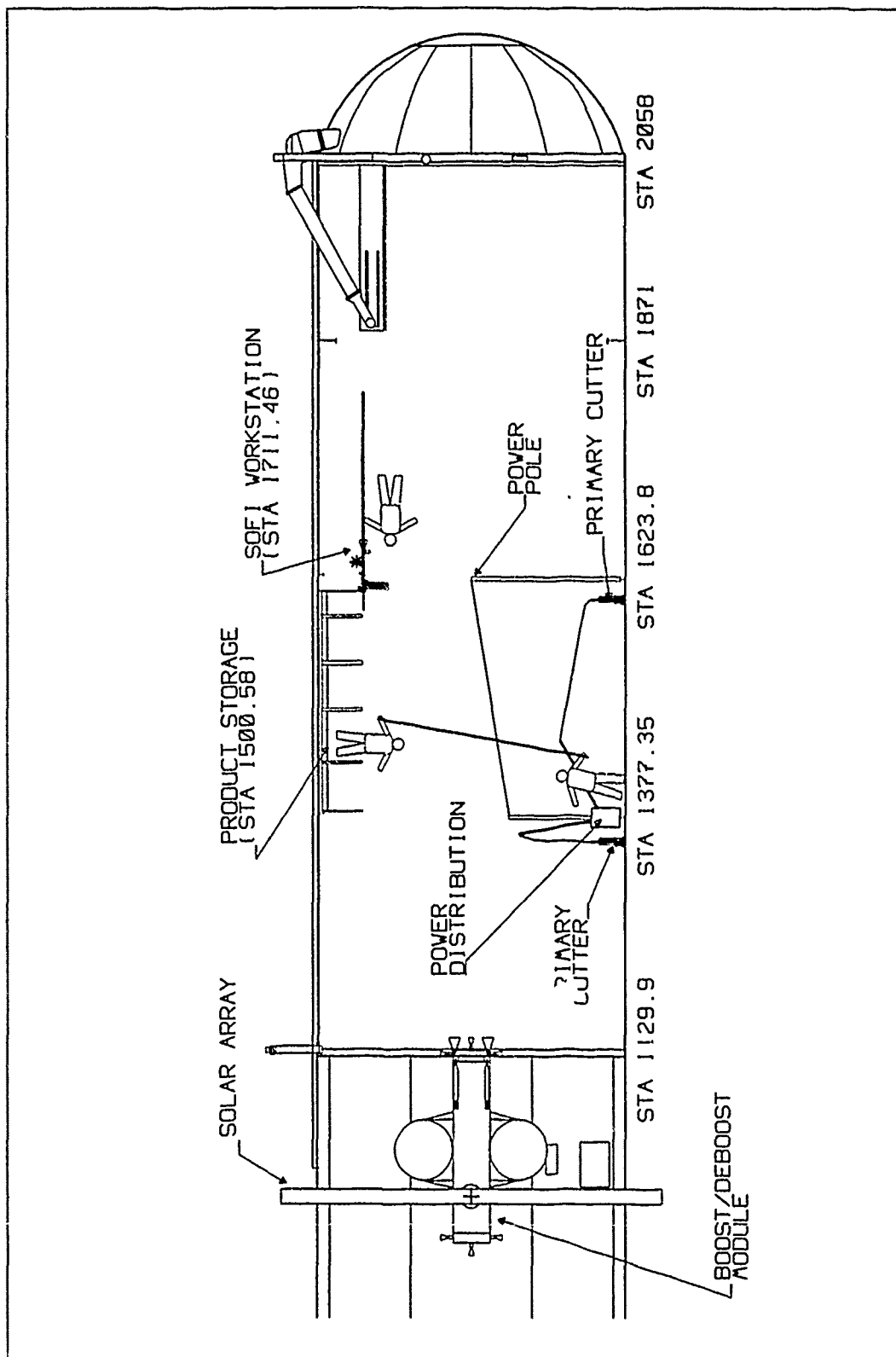
Figure 6.1. Scenario 2 Overview

workstation. Although the piece parts from barrel one are shorter, they are still of sufficient length to be handed off from the workseat. The stacker is not required to handle piece parts twice while the the aft barrels are being reduced.

The LH2 tank is again reduced to a 'bird cage' structure (as in Scenario 1) as shown in Figure 5.5. The actual reduction time for Scenario 2 is 23 hours (as opposed to 40.77 hours for Scenario 1). However, since crew rest is required between EVA's, the actual mission timeline is longer in Scenario 2. Eight hour EVA's with 16 hours of rest between EVA's are assumed.

The peak power requirements for Scenario 2 are higher since multiple cutters are operated simultaneously. The peak load demand is 18.85 kW (as opposed to 11.5 kW for Scenario 1). Scenario 2 yields 12,618.7 lbs of salvaged aluminum, (as opposed to 13,044.7 lbs for Scenario 1), due to the fact that no centerline track and associated cross bars are available for salvage.

6.2 Pre-flight Modifications

During manned reduction of the ET, astronauts would do most of the work. For this reason, the robot arm and its associated center line track would not be necessary. Since the astronauts will need greater mobility and flexibility, even more handrails and foot restraints may be required. In addition, some of the support structure of the mobile work seat should be pre-installed. There will be less need for a sophisticated comm/camera/lights network since the astronauts will be on site as they work. Bar codes and and other means to designate particular areas of the tank should be retained. Although these markers may not be as necessary as for the automated reduction scenario, it would still be of some help to an astronaut to be able to instantly orient himself.

6.3 Initial Set-Up

Initial set-up for Scenario 2 is very similar to Scenario 1. The initial facility is fitted with boost/deboost modules, the residual pyrotechnic charges are again removed, and solar arrays are installed as before. The intermediate ring frames are again removed prior to the start of the actual salvage operation.

There is a minor change in one of the three power distribution systems. Scenario 2 features a 'power pole' mounted on the middle major ring frame (station 1623.80). The power distribution system for the primary cutters will be routed up the power pole and over to the workseat initially installed on major ring frame station 1377.35. The input connection to the workseat is also via a pole mount and the primary power cable will remain essentially in the radial center of the tank while the workseat travels radially around the tank.

Other than this slight change to 1 of the 3 power distribution systems and the installation of a second primary cutter, the Scenario 2 initial set-up is the same as for Scenario 1.

6.4 Tools

The unique aspect of Scenario 2 is the use of human labor in the reduction process. Piece-part/tool transport and product storage are accomplished by physical labor (Figure 6.1). A detailed description of the tool strength and motor power calculations are included in Appendix A.

6.4.1 Primary Cutter. The basic design of the Primary Cutter is unchanged from the design for Scenario 1. The principal difference for Scenario 2 is concerned with how the cutter is transported in the radial direction and an astronaut provides this capability. The top of the primary cutter is slightly modified; the stringer which was present in the Scenario 1 design has been replaced with an astronaut grip

(see Figure 6.2). When the primary cutter is moved to a new set of stringers, the astronaut must squeeze a lever for the guide wheels to retract.

Power is provided to the primary cutters by means of a power distribution box (Figure 6.1). The power distribution box is mounted on a major ring frame and can be moved radially by an astronaut as the cutters are moved. Power from the forward LH_2 dome is routed along the skeleton structure to the power pole. The power pole maintains the power cable centered and away from possible incidents. The power cable is then routed to the distribution box from which two cutters are powered. Two spring mounted arms are attached to the distribution box which maintain a slight cable tension to the cutters. The cables to the cutters are coiled to allow for varying travel distances.

6.4.2 SOFI Workstation. When a skin/stringer combination has been completely cut free, an astronaut will grasp the T-shaped stringer and pass it to the astronaut at the SOFI workstation. The astronaut at the SOFI workstation will insert the material into the funnel (Figure 6.3). The funnel allows for small deviations in the placement of the material (up to 4.5" in any direction). The material is then pushed through the funnel until it engages the primary drive wheels. Dual primary drive wheels are located on both sides of the workstation to allow for stringers on either side (Figure 5.17, left). The primary drive wheels move the material first to the SOFI stripper.

6.4.2.1 SOFI Stripper. The SOFI stripper design for Scenario 2 remains unchanged from Scenario 1. It was originally believed that the same device could be used to remove SOFI in much longer lengths. It was believed that up to 20 foot sections of SOFI could be removed without stopping the SOFI workstation to make numerous cuts (recall Scenario 1 cut the removed SOFI into 2 foot sections). This idea was abandoned for two reasons.

The primary reason that single strip SOFI removal was abandoned was driven
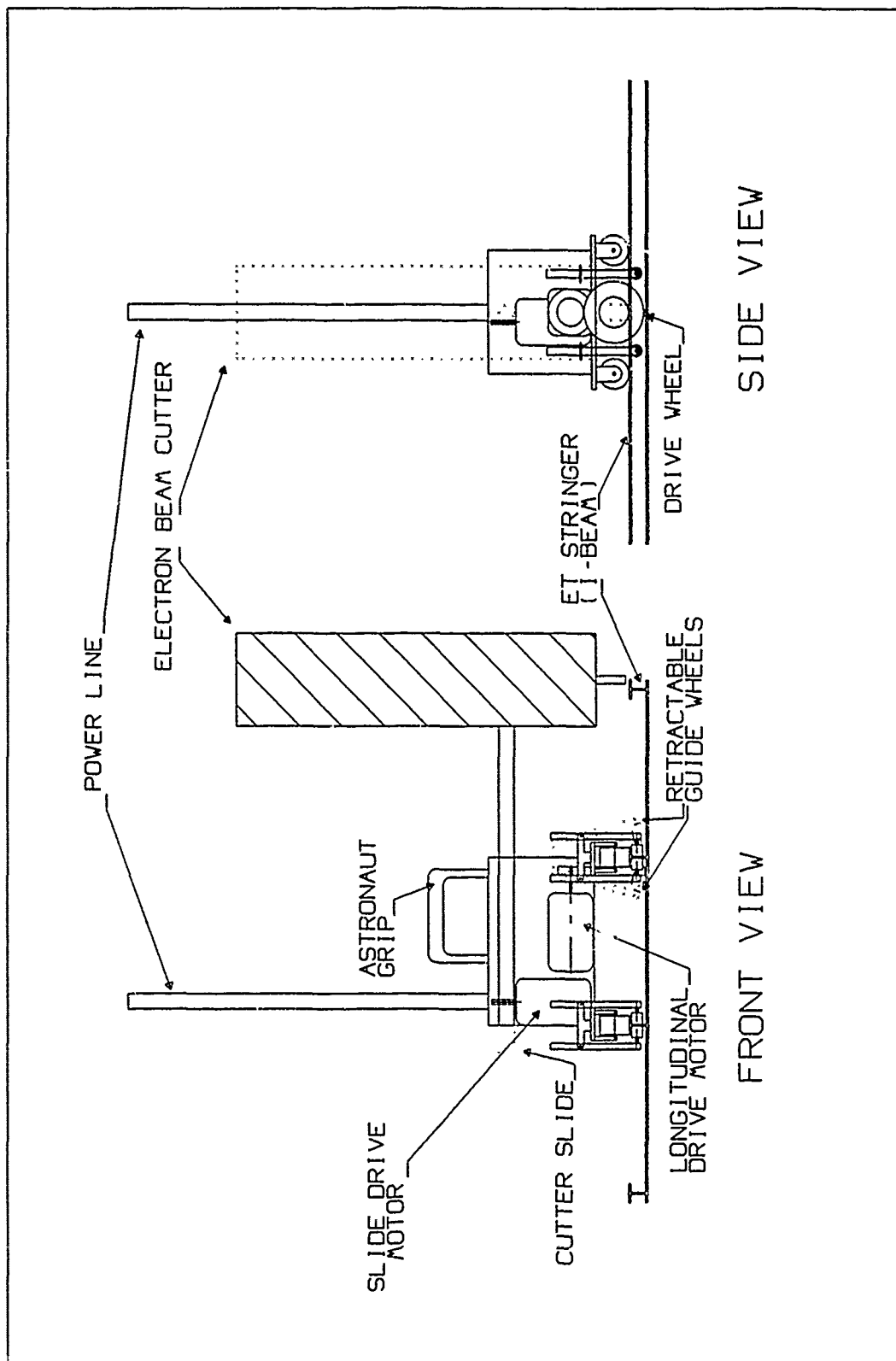
Figure 6.2. Primary Cutter, Scenario 2
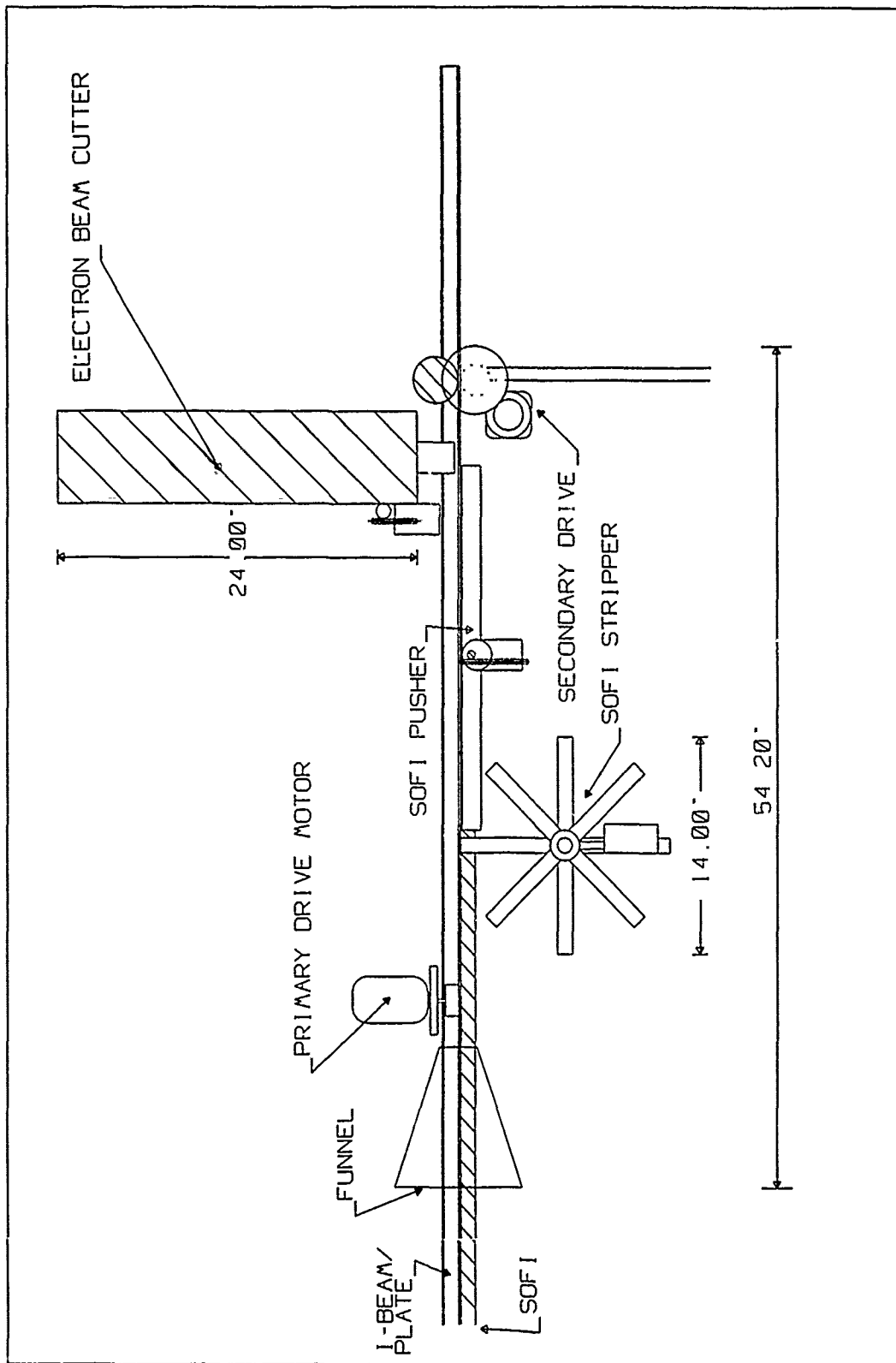
Figure 6.3. SOFI Workstation

by the workload of the stacker. The stacker would be simultaneously trying to store the I-beam, store the plate, and store the SOFI. The astronaut serves as a force source and if he should 'bump' one of the pieces while he's trying to store another, it was not clear that positive control of the pieces could be maintained.

The secondary reason that single strip SOFI removal was abandoned was due to the orbital life lengths of a 20 foot piece of SOFI if it happened to escape the confines of the ASSET facility. The worst case orbital life is evaluated (see Figure 6.7) and shown to last on the order of 50 days.

6.4.2.2 Electron-Beam Cutter. The only change to the secondary cutter for Scenario 2 is that it is run at a higher rate (with a slight increase in power consumption). As the material continues through the workstation, it engages the electron-beam cutter which separates the stringer from the skin creating an I-beam/plate combination (Figure 5.18). The electron-beam is attached to a shaft that moves it from side-to-side to allow for stringers on either side. This side-to-side motion is provided by the cutter slide and slide drive motor (Figure 5.17, right).

6.4.3 Product Storage. The product storage for Scenario 2 has been slightly modified. The diverter wheels at the output of the SOFI workstation have been removed and the automatic storage capability is no longer available. As the I-beam/plate combinations emerge from the electron-beam cutter the plate is engaged by the secondary drive motor (Figure 6.3). The plate and I-beam are then grasped by an astronaut who places the product in the appropriate storage bins.

6.5 Scenario Two Reduction Model

Reduction of the LH_2 tank was simulated using the SLAM II simulation language and FORTRAN subroutines. The primary objectives of the reduction model were to develop reduction timelines for the reduction of one LH_2 tank and to de-

termine the peak power requirements for the reduction facility. Appendix B gives a detailed description of the reduction model.

6.5.1 Tool Work Rates and Power Consumption. Establishing tool work rates was a primary step in determining the overall power consumption of the facility as well as the total time required to reduce the tank. Work rates and power use were varied for the primary and secondary electron beam cutters, and for the SOFI work station, in order to assess their affect on power consumption and tank reduction times. All astronaut activities were modeled as normally distributed random variables. The critical design variable was found to be the secondary electron beam cutter, located at the SOFI work station. Once this was established, other tool work rates and power requirements were held constant and the electron beam cutters were designed in order to minimize the tank reduction time while staying below the peak power budget of 25 kW. The power required by an EB cutter is directly related to its rate of cut; the faster the cut, the more power required for a given depth of cut. The cut rate of the secondary cutter limits the rate at which the SOFI work station can accept stringer/plate pieces. Since there are two primary cutters producing stringer/plate pieces, the SOFI work station and secondary cutter must work at a rate approximately twice as fast as the primary cutters to be most efficient. Following several iterations the primary and secondary cutter parameters were determined to be as shown in Table 6.1. The iterative process and intermediate results are included in section 6.13.

Table 6.1. Electron Beam Cutter Design

CUTTER	MATERIAL	CUT RATE	POWER REQUIRED
Primary	Stringer	10 inches/minute	7.05 kW
Primary	Plate	50 inches/minute	3.55 kW
Secondary	Plate	100 inches/minute	4.00 kW
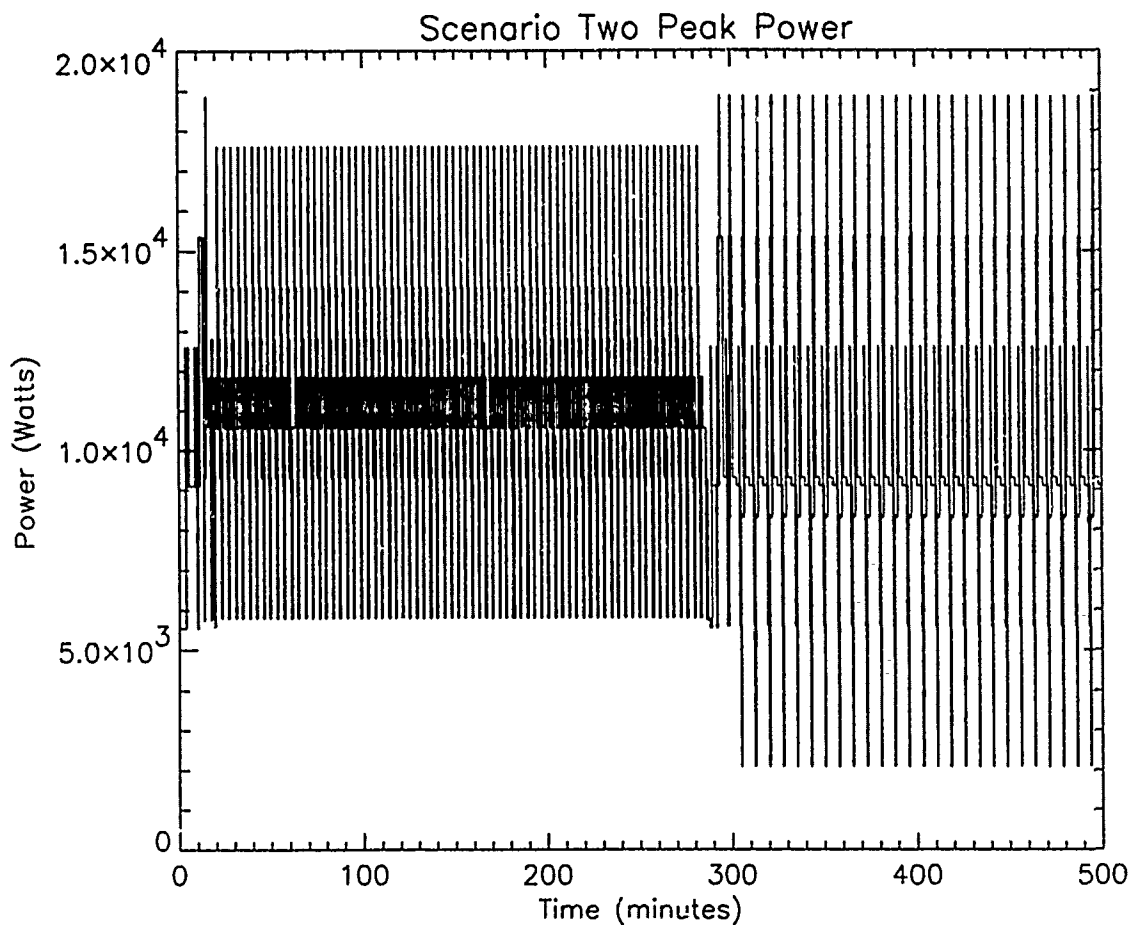
Figure 6.4. Peak Power Required - Scenario Two

6.5.2 Results. Once tool work rates and their power needs were established, the simulation was conducted again to determine the facility power requirements and the total tank reduction time. Figure 6.4 shows the facility power use for the first 500 minutes of reduction. The first series of 37 cuts for the two forward barrel sections can clearly be seen between 0 - 290 minutes of the simulation. The peak power required for Scenario 2 is 18.85 kW and 23 hours of EVA are required to reduce the ET to the 'bird cage' configuration. The simulation output file is included in Appendix B.

6.6 Electrical Power Subsystem (EPS)

6.6.1 ASSET EPS Design. The ASSET EPS is basically a modified version of a single PV module of SSF. The baseline SSF configuration is composed of 8 PV arrays as shown in Figure 5.22. The PV arrays are built up in pairs via a station PV Power Module as shown in Figure 5.23. The principal difference between the SSF design and the ASSET design is that the SSF design incorporates orbital averaging (as explained in Appendix C) while the ASSET design delivers a constant load power. The ASSET EPS design is shown in Figure 6.5. A constant load power system offers significant reductions in the design complexity for load scheduling (as compared to SSF). The ASSET facility will simply not ask for more power than can be generated.

Since the peak load demand does not exceed 20 kW, one can work from right to left (through Figure 6.5) to determine the sizes of the PV arrays. Given the efficiencies of the electrical equipment subsystem (EES) and power management and distribution (PMAD) equipment, one can determine the input to the EES. Knowing that the EES receives 51% of the base of array (BOA) power (the other 49% being used for battery charging during the sunlit portion of the orbit), one determines the required BOA power.

Once the BOA power has been determined, the actual array blanket sizes can be determined. Since an individual circuit (two array panels) delivers 160 vdc @ 2.4 watts, it is found that 136 circuits are required to supply the required BOA power. The number of circuits, in turn, can be used to determine the actual blanket area of the PV arrays (136 circuits x 2 panels/circuit x 1.6842 m^2 /panel = 458.1 m^2 of panel area). The blanket area is summed with the mast, blanket boxes, and thermal control subsystem radiator area to determine a maximum drag area of 612 m^2.

6.6.2 Battery Optimization. The number of batteries (to supply the required 27.534 kW of power during the eclipse period) is determined by balancing the requirements for weight, depth of discharge (DOD), life length, and reliability. The
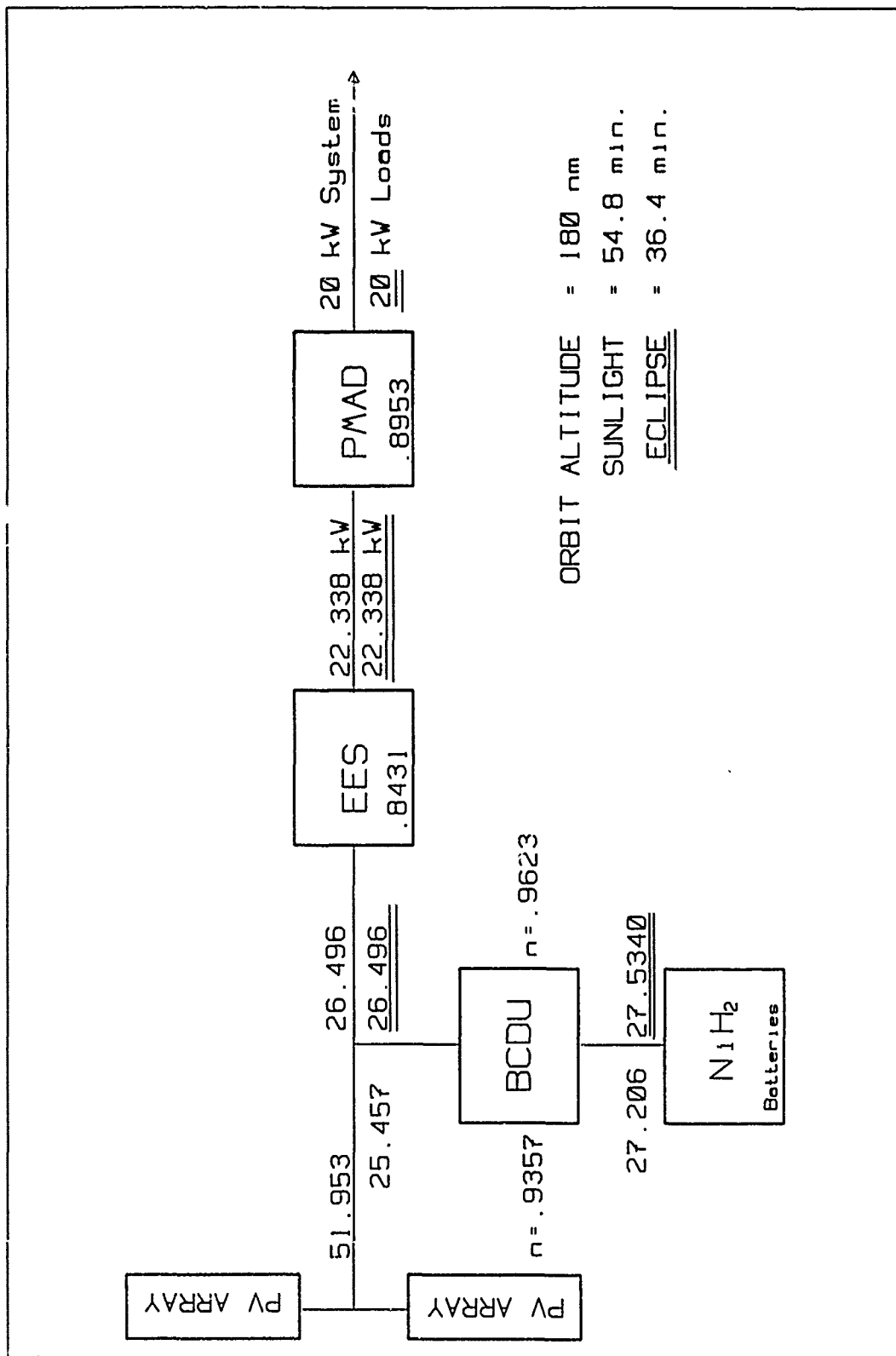
Figure 6.5. ASSET EPS Design: Scenario 2

Table 6.2. ASSET Battery Optimization, Scenario 2

# Batt.	kW/Batt.	Dischg Amps	DOD	Life (yrs)	Weight (lbs)
6	4.5890	40.7911	.5036	3.5509	3227.4
5	5.5068	48.9493	.6043	1.3699	2689.5
4	6.8835	61.1867	.7554	0.7406	2151.6
3	9.1780	81.5822	n/a	n/a	1613.7

ASSET facility makes approximately 16 orbits per day which, in turn, implies 5,840 charge/discharge cycles of the batteries per year. Figure 5.25 is used to determine the number of charge/discharge life cycles as a function of DOD. Life tests conducted at 100% DOD yield 300 to 500 charge/discharge cycles before failure occurs (85). Conservative life data was generated by using the line projected to 300 cycles in Figure 5.25 and life length data, as a function of the number of batteries available, is presented in Table 6.2.

Using Table 6.2 it is determined that five batteries is the optimum number of batteries to support Scenario 2. This choice represents the best balance between weight savings, and life length in the event of the loss of a battery. Adding a sixth battery would incur additional design costs while starting with a normal complement of five would still allow the salvage of 27 ET's even if a battery failed on the 1st mission.

6.7 Orbit Analysis Discussion

The discussion of the Scenario 2 orbit dynamics follows the same outline found in Section 5.7. However, the differences between the scenarios will be emphasized here. Again, Appendix D explains the assumptions and mathematical model used to describe the dynamics of the ASSET facility.

6.7.1 Hardware Considerations. As mentioned in Section 5.7.1, some variation of the ET GRIT Boost/Deboost Module has been identified as the baseline
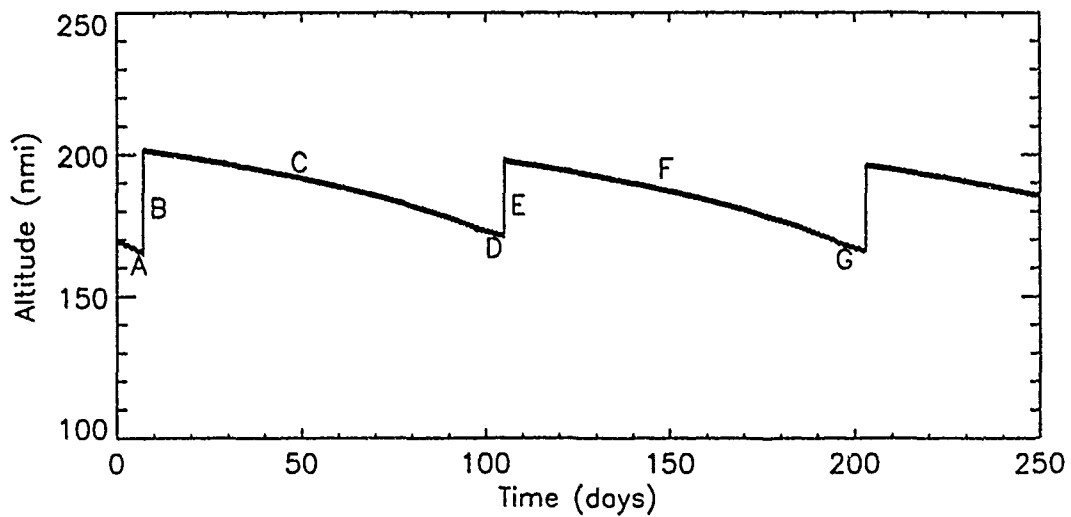
Figure 6.6. Altitude History, Scenario 2.

RCS/Propulsion design. There are, however, no differences between the propulsion modules of Scenario 1 and Scenario 2.

6.7.2 Facility Orbit Decay.   Figure 6.6 depicts a typical six-month altitude history of the Scenario 2 facility. This altitude history is virtually identical with Scenario 1, except that the salvage operation lasts longer (approximately 10 days). [1]

The mission flight plan is again divided into seven phases labeled A through G. Notice now that after the initial setup and tank reduction at the end of Phase A, the facility experiences an altitude loss of 6.9 nmi. During Phase D, when ASSET is docked with the second tank, the system experiences only a 4.9 nmi loss of altitude. Those additional two days of orbit decay at less than 170 nmi results in a substantial increase in fuel consumption. This phenomenon proves to have a major impact on the cost effectiveness of the Scenario 2 designs.

Table 6.3 highlights the physical differences between the alternative solar array technology designs for this particular scenario. The effective facility drag area A_d,

---

[1] Versus eight days for Scenario 1.

Table 6.3. Orbit Parameters, 12% vs. 21% Solar Arrays.

Phase	12% Efficiency				21% Efficiency			
	h_f (nm)	A_d (ft^2)	M (lbs)	β ($\frac{lbs}{ft^2}$)	h_f (nm)	A_d (ft^2)	M (lbs)	β ($\frac{lbs}{ft^2}$)
A	163.1	5683.2	102,831	8.2	165.2	3831.9	101,174	12.0
B	204.6	5683.2	102,831	8.2	197.2	3831.9	101,174	12.0
C	170.6	5683.2	100,803	8.1	170.1	3831.9	99,170	11.8
D	165.2	6253.7	170,327	12.4	166.0	4402.3	168,692	17.4
E	203.0	5683.2	113,559	9.1	195.2	3831.9	111,925	13.3
F	172.5	5683.2	111,337	8.9	169.5	3831.9	109,714	13.0
G	167.6	6253.7	180,861	13.1	165.8	4402.3	179,236	18.5

mass M, and ballistic coefficient β for the design alternatives are presented.

6.7.3 Debris. As far as debris is concerned, there is only one minor difference between Scenario 1 and 2. Since astronauts can now handle the SOFI, the design of the SOFI Workstation can be simplified. The hardware used to cut the SOFI into two foot sections could be deleted. The astronauts could dispose of the entire, 19 foot strips of SOFI individually or temporarily store them until a large bundle can be deorbited. The three curves in Figure 6.7 again represent the maximum, median, and minimum drag orientations of the SOFI debris. Unfortunately, the minimum drag orientation in this case has a relatively large ballistic coefficient as reflected in the 50+ day orbit life. Although the probability is low that a 19 ft long strip of SOFI will ever attain and remain in a minimum drag orientation, such a large piece of debris could remain in orbit much longer than desired. Our recommendation is to process the SOFI in a manner that will:

- produce relatively small SOFI strips,

- minimize loose debris, and

- can be deorbited in large bundles.
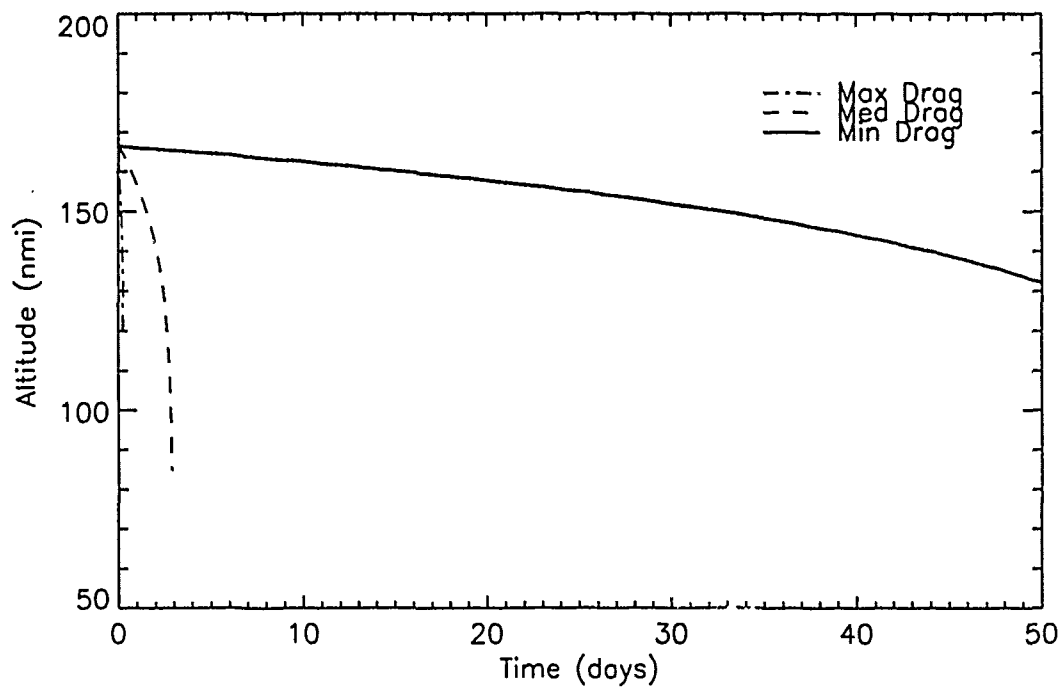
Figure 6.7. SOFI Debris Orbital Life.

Table 6.4. Annual ΔV Requirements, Scenario 2.

Hohmann Transfer	12% Array		21% Array	
	ΔV_t (ft/sec)	t_b (sec)	ΔV_t (ft/sec)	t_b (sec)
#1	144.8	231.4	111.1	174.6
#2	131.6	232.3	101.7	176.8
#3	114.9	221.6	99.8	189.9
#4	118.5	247.7	90.4	186.6
Total	509.8	933.0	403.0	729.9

Table 6.5. Annual Fuel Consumption, Scenario 2.

Hohmann Transfer	12% Array m_f (lbs)	21% Array m_f (lbs)
#1	2,012	1,518
#2	2,020	1,538
#3	1,927	1,652
#4	2,159	1,623
Subtotal	8,113	6,331
20% RCS	1,623	1,266
	9,736	7,597
10% Res	974	760
Total	10,709	8,357

6.7.4 Fuel Consumption Table 6.4 presents the annual total ΔV's and burn times required for the four Hohmann transfers for both Scenario 2 design options. Table 6.5 presents the fuel consumption data associated with the burn times in Table 6.4. Again, the total quantity of fuel consumed includes a 20% allowance for RCS fuel and a 10% allowance for management reserves (54:45). As expected, more fuel is required to offset the altitude losses of the low efficiency EPS.

6.7.5 Other Considerations. Here again, the ASSET orbit will have a different precession rate than that of *Freedom*. However, the Scenario 2 alternatives could have even greater ΔV penalties than Scenario 1 due to the larger swing in relative altitudes.

6.8 Facility Monitoring and Control.

Scenario 2 is almost exclusively controlled by the astronauts conducting the reduction operation, although the monitoring requirements are more critical since lives are involved. For normal operations, control of the cutter and platform is accomplished much the same as in Scenario 1 except an astronaut takes the place of the transport arm and physically attaches and detaches the cutter platform to and from the stringers each time the cutter is moved. The cutter platform does not have to sense the arm grasping and releasing the cutter. The actual cutting operation is fully automated and the same sensoring and control mechanisms are required. Control and sensoring of the SOFI work station is identical to the Scenario 1 configuration.

6.8.0.1 Fault Detection and Correction. System failures for the Scenario 2 ASSET facility can be divided into two categories:

1. Simple failures which can be detected with sensors and corrected automatically.

2. All other failures which may or may not be detected by sensoring and require that the facility be repaired by EVA.

Simple failures will be discussed first. One simple failure can be detected and corrected automatically; a broken stripper wire at the SOFI work station. A broken stripper wire is detected when an electrical signal is interrupted by the broken wire. This causes stripping to stop and the stripper wire cartridge to be rotated to expose a new wire. The stripping operation can resume. This is the same as Scenario 1. All other failures require that astronauts repair the equipment by EVA.

6.8.0.2 *Communications and Monitoring.* The communication requirements for Scenario 2 are identical to Scenario 1 with the exception of the added requirement for the facility to transmit and receive voice communication, and no requirement for teleoperation. Without the transport arm, camera and lighting equipment is comprised of hardware mounted directly to the bird cage. Rather than four fixed cameras, the Scenario 2 configuration requires four cameras that can pan to view the entire LH₂ tank, two at each end of the tank, mounted to the first and fifth major ring frames.

6.9 Thermal Analysis

When the astronauts enter the External Tank, 24 hours after the liquid hydrogen has been vented, temperature of the walls should be $-117°F$. Since their suits will function down to $-180°$ the astronauts should have no thermal problems. The lowest temperature the astronauts might experience during the eclipse period is $-131°F$. This low temperature is very conservative. To reach it a good portion of the ET would have to be removed just before the eclipse period, without adding significant energy to the tank. It is very unlikely that this juxtaposition of circumstances could ever arise.

Thermal considerations for machinery were dealt with in section 5.9 and Appendix E. The current focus will be on the one aspect that differs from Scenario 1 to Scenario 2: the men in the loop.

The chief problem the astronauts could face is in their proximity to working electron beam cutters. In order to cut aluminum, the beam cutter must heat it to $1220°F$. When the electrons strike metal, x-rays are produced. The two potential hazards are: heat and X-rays.

When a portion of a metal strip is heated to a high temperature and then allowed to cool, a transient thermal condition can be said to exist. There is no closed form solution to this transient thermal problem. Numerical methods, shown

in detail in Appendix E, were used to find how soon a spacesuited astronaut could safely touch a piece of hot metal. These transient thermal methods showed that 1.1 seconds after the electron beam cutter has melted a strip of aluminum, the hottest part of metal will be $231.1°F$. After two seconds the hottest spot will be $162°F$. Since the astronauts are not required to touch the metal for approximately 4.5 minutes after it has been cut, they will be in no danger.

Terrestrial workers are protected from the x-ray radiation produced by the electron beam cutter by shielding and goggles. In Scenario 2, it will not be necessary for the astronauts to visually inspect a surface while it is being cut. An opaque lead shield surround the beam housing should minimize any potential x-ray effects. Since this lead shielding will be quite close to the cut surface, it should be clad in a heat resistant material like the tile on the space shuttle. If this cladding material is extended several inches from the x-ray shield, it can also serve as a visual shield so that the astronauts won't suffer adverse effects from any bright visible light generated from the electron beam.

The analysis of the SOFI workstation in section 5.9 and in Appendix E showed that the hottest object it produces would be I-beams and that they would be about $148°F$. Since space suits are rated to $235°F$, this temperature should not be a problem. The electron beam portion of the SOFI workstation should be shielded so that no x-rays or bright light can escape. If an astronaut wished to adjust the machine, he should turn off the electron beam cutter and allow the workpiece to cool before doing so.

6.10 Products

The products derived from Scenario 2 are less than those from Scenario 1. The manual reduction of Scenario 2 eliminates the track and crossbars as byproducts.

6.11 Rendezvous With Subsequent Tanks

The actual rendezvous with subsequent tanks for Scenario 2 is virtually the same as for Scenario 1. There is a slight change to the installation of the power distribution network for the primary cutters. A power pole is installed on the central major ring frame, but this is a rather trivial task.

Initial reduction for the second and subsequent tanks is accomplished exactly like the initial tank. The same tools will process the same piece parts and salvage (essentially) the same products. The orbiter would not be free to leave during the actual reduction process since EVA support is required during the salvage operation in Scenario 2. EVA will again be required once the reduction is finished.

Once the second (or subsequent) tank has been reduced, EVA is required to transfer products and tools back to the initial tank. This task will be somewhat easier than the original tool transfer since both tanks have now been reduced to a 'bird cage' structure as shown in Figure 5.32. Transferred tools will be stored in the aft LH_2 dome of tank 1 to facilitate quicker transfer to subsequent tanks.

6.12 Mission Timelines

For the initial tank, which will be a dedicated mission, 6.3 days (as opposed to 5.0 days for Scenario 1) will be required. This mission timeline assumes that NASA will grant a waiver to allow ASSET employees to conduct an initial EVA 24 hours after launch (current NASA guidelines require 72 hours after launch prior to first EVA). This scenario also assumes that 3 man EVA teams can be supported by the orbiter.

Two 480 minute 2 man EVA's would be used to set up the initial facility. Three 3 man EVA's (of duration 480 minutes, 480 minutes, and 420 minutes; 23 hours total) would be required for the actual tank reduction. Sixteen hours of rest time are assumed to be required between EVA. Detailed task lists per EVA (excluding

actual reduction) are provided in Appendix F. The total equivalent EVA required for tank #1 in Scenario 2 is 50.5 hours (as opposed to 16 hours for Scenario 1).

For subsequent tanks, which will not be dedicated missions, 8.3 days (as compared to 6.3 days for Scenario 1) will be required. This mission timeline again assumes NASA will grant a waiver to allow EVA 24 hours after launch. This mission timeline also assumes that 8.3 days can be allotted to ET salvage during 'other' primary missions.

Two 2 man 480 minute EVA's would be used to bundle previously salvaged products, transfer tools, and ready the subsequent tank for reduction. Three 3 man EVA's would be required for the actual reduction and two more 2 man EVA's (of 480 and 380 minutes duration) would be required after reduction to move salvaged products and the facility tools back to the original ASSET tank. Sixteen hours of rest time are assumed to be required between EVA. Detailed task lists per EVA are provided in Appendix F. The total equivalent EVA required for tank #2 in Scenario 2 is 63 hours (as opposed to 30.3 hours for Scenario 1).

6.13   Evolution and Optimization

6.13.1   Ideas Considered But Rejected.   Manned reduction has always been the focus of Scenario 2. In contrast with Scenario 1 (which utilized the pre-installed centerline track to radially move the primary cutters and longitudinally move the piece parts), Scenario 2 utilizes astronauts to resolve all mobility problems. This approach simplifies the tool design since men are present during the reduction to supervise and resolve any problems that may arise. It was initially envisioned that multiple astronaut teams would swarm all over the tank and try to reduce it in 1 or 2 days.

Since the operation was viewed as being carried out within 1 or 2 days, the SOFI removal was viewed such that it may have to become a very 'quick and dirty' operation. Since debris minimization was a factor, the concept of 'wrapping' the en-

tire LH$_2$ tank with blankets (supported by an EVA installed structure to provide a standoff distance between the tank exterior and the interior of the blankets) was considered. It was not clear that the time saved by 'quick and dirty' SOFI removal could be recovered within the timelines required to install such a containment structure.

A simplified piece part transport system (consisting of a clothesline assembly secured by pulleys on either end) was briefly considered and rejected. The concept was geared toward attaching piece parts to the clothesline and letting the clothesline carry the piece parts to the SOFI workstation. The clothesline concept was initially plagued by the fact that multiple cutter teams were envisioned and that the clothesline needed to be accessed from almost any radial location within the LH$_2$ tank. Providing power (to essentially any location within the tank interior) for the device was another problem unless the clothesline was to be operated by astronaut supplied hand-over-hand power.

The problems of SOFI removal and clothesline operation were resolved when the method of Scenario 2 was modified to reduce the number of astronauts required. It was determined that a similar SOFI workstation (compared to Scenario 1) could be used and that removal of the intermediate ring frames prior to the start of the reduction operation yielded piece parts of sufficient length to accommodate the physical hand-off of piece parts (thus eliminating a piece part transport system) when 3 astronauts are used.

Since Scenario 2 was always envisioned as an EVA intensive task, we briefly considered a 'man-in-the-can' (see Figure 6.8, (26)) concept as a way to extend the EVA time. Man-in-the-can is a self-contained system which takes care of life support, mobility, communications/cameras, and incorporates tool fixtures (either via 'gloved extenders' or joystick operated robot arms) to accomplish a variety of tasks. This idea was abandoned since the development of such a device (from the drawing board concepts found in the literature to a concept deemed acceptable from the cost and risk point of view) could easily consume the time alloted for the entire ASSET thesis
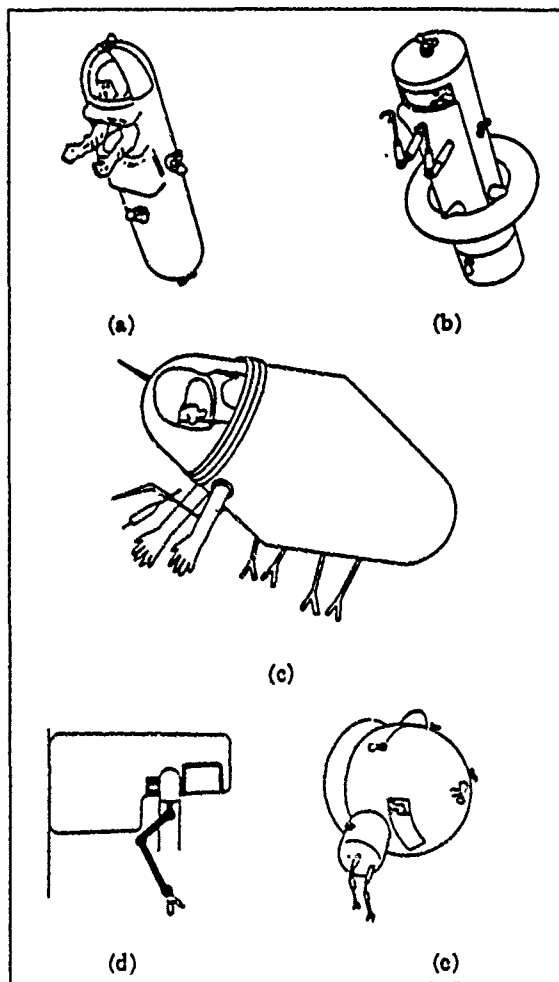
Figure 6.8. Typical Man-In-The-Can Concepts

project.

6.13.2 Lessons Learned/Changed Perceptions. The foremost lesson learned was that our fears of an EVA intensive task were quickly justified. EVA timelines for initial set-up (provided in Appendix F), the actual reduction operation (provided in Appendix B), and facility tear down after salvage (also provided in Appendix F) quickly convinced us that the only way to make Scenario 2 a viable option was to reduce the tank as quickly as possible and minimize the EVA required to accomplish both initial and subsequent reduction.

An assumed 10 day maximum mission for orbiter support would clearly be a severe constraint for initial tank reduction and it was deemed necessary to operate within NASA guidelines whenever possible. Clearly, the demand for orbiter support (in terms of EVA) would be a problem area for NASA since subsequent tank reductions are not viewed as 'primary' missions.

6.13.3 Scenario Level Trade Studies. The trade between facility drag (dominated by the surface area of the PV arrays) and the fuel consumed to maintain orbit was examined. In order to salvage equivalent products (compared to Scenario 1), and stay within reasonable EVA timelines, the EPS had to be scaled up to provide more power to the facility. This was required to provide power for multiple primary cutters and to operate the tools at increased rates.

The initial PV array design was an off-the -shelf concept using the same array design as SSF. These arrays have an efficiency of 12%. A more efficient array design (state-of-the-art is approximately 21%) would present a considerably smaller drag and would offer significant fuel savings. The question to resolve was whether the increased research and development costs (for a more efficient array) could be offset by reduced fuel consumption and fuel resupply costs.

The trade between the number of batteries required to supply power during the eclipse portion of the orbit was also examined. The number of batteries determines how hard each battery is driven, which determines battery life length, which, in turn, drives maintenance costs. The data presented in section 6.6 represented the best balance between weight, life length, and reliability.

The results of the scenario level trades are presented (and contrasted with other scenarios) in Chapter IX where the various system level trades between scenarios are explained.

6.13.4 Cut Rate Optimization. Selecting the optimum EB cut rate is a trade between minimizing the facility peak power level and maximizing the rate of reduction of the ET. Maximizing the cut rate of the EB cutter is more important for Scenario 2 than for Scenario 1 since EVA costs are directly related to the total time to reduce the tank.

6.13.4.1 Power Versus Cut Rate. In developing the reduction model for Scenario 2, the power level of the three EB cutters and their cut rates were optimized to cut at the fastest rate while remaining below the facility's peak power constraint. The reduction facility's peak power was initially set at a maximum of 25 kW. This constraint limits the power level on the cutters. EB cut rates were constrained to be between 10 - 100 inches per minute, in order to remain within the range of available data.

6.13.4.2 Simulation Results. The Scenario 2 reduction scheme was simulated with the initial values for power and cut rate as shown in Table 6.6.

Table 6.6. Initial Power and Cut Rate

CUTTER	MATERIAL	POWER	CUT RATE
Primary	Plate	3 kW	40 inches/min
	Stringer	7 kW	10 inches/min
Secondary	Plate	4 kW	80 inches/min

The cutter parameters of Table 6.6 yield a facility peak power of 21.35 kW. Analysis of histogram data revealed that managing when stringers were being cut would allow the peak power to be lowered to 17.35 kW with no change in the cutter power levels or cut rates. Since the peak power was well below the maximum level of 25 kW, the power level (and therefore the cut rate) for the cutters could be increased. Using the regression data from Engquist (25), the power level and cut rate for the cutters was increased to the values shown in Table 6.7.

6-27

Table 6.7. Final Power and Cut Rate

CUTTER	MATERIAL	POWER	CUT RATE
Primary	Plate	3.5 kW	50 inches/min
	Stringer	7.0 kW	10 inches/min
Secondary	Plate	5.0 kW	100 inches/min

The cutter parameters of Table 6.7 yield a facility peak power of 18.85 kW, still below the design level of 25 kW. The secondary cutter is the critical tool since it operates at the maximum rate allowed, 100 inches per minute, and limits the two primary cutters to a cut rate of 50 inches per minute. This is because both primary cutters are feeding stringer/plate pieces to the secondary cutter simultaneously. Since the cut rate could not be increased any further the peak power constraint was lowered to 20 kW. This allowed the Scenario 2 power system to be sized 20 percent smaller than the 25 kW power budget. The values in Table 6.7 were the final values used for the Scenario 2 reduction model simulation.

VII. SCENARIO 3 - RENDEZVOUS WITH SPACE STATION FREEDOM

7.1   Overview and Evolution

Scenario 3 is a by-product of the previously described scenarios. The original concept was that initial reduction could be carried out at a lower altitude (thus lowering the concern over debris), subsequent rendezvous with SSF would then be effected, and further reduction of the tank could be accomplished at SSF. Thus, the initial concept was to salvage even more aluminum products.

The initial idea was modified due to two problems. The first has been previously discussed and deals with the excess fuel costs associated with carrying subsequent tanks to SSF. The second dealt with the problem of generating debris at SSF. The combination of these two problems led to the abandonment of further salvage after arrival at SSF.

It was also realized that either Scenario 1 or 2 would be carried out within a period that is short compared to the time between resupply missions. This left the ASSET facility in a status of simply maintaining orbit for approximately 325 days out of the year. There are claims that SSF is a power limited facility, (23:30) and realizing that ASSET has a sizable power source, we decided to augment our salvage business by providing power to SSF during the downtime between resupply missions. This is consistent with our objective to maximize the net present value of our facility. This idea assumes that excess available power at SSF (supplied by the ASSET facility) will be purchased at the same rate as the normal NASA supplied power. By the same token, the ASSET facility would need to pay for the delta fuel required to maintain SSF orbits with ASSET attached. An additional benefit of rendezvous with SSF is that this allows the ASSET facility to offload products, saving fuel during Hohmann transfers of the reduction facility.

One way to insure compatibility between the two electrical power subsubsystems is to emulate the SSF EPS design in the ASSET facility. Thus, the EPS envisioned to support Scenario 3 is a single PV module from the SSF baseline design. Other than this change for the EPS, Scenario 3 creates no new problems to be solved. Scenario 1 or 2 would be conducted at a lower orbit (prior to rendezvous) and the pre-flight modifications, set-up requirements, tools installed, and products salvaged would be unchanged.

7.2 Electrical Power Subsystem (EPS)

7.2.1 Introduction.
Recall that the Scenario 3 EPS will be used at a lower orbit for automated (Scenario 1) or manned (Scenario 2) reduction. Thus, the Scenario 3 design must provide adequate power for either of the other two scenarios.

The EPS developed to support Scenario 3 is a single PV module from the SSF baseline design. Such a design will have higher weight (19,018.4 lbs) and drag penalties (714 m^2) than the other two scenarios. This fact will be traded against the revenue stream generated by selling power at SSF to see which scenario is the most cost effective and those results will be presented in Chapter IX. One consideration for scenario 3 is that the battery life length will have to be maximized.

7.2.2 ASSET EPS Design: Scenario 3.
The configuration of a PV module, complete with arrays, batteries, and supporting hardware is shown in Figure 5.23. Orbital averaging (as explained in Appendix C) is the normal mode of operation for SSF and a typical power cycle for the ASSET EPS is shown in Figure 7.1.

The orbital average power is obtained (as in Appendix C) as

$$\text{Orbital Avg. Power} = \frac{54.8}{91.2}(24.2334) + \frac{36.4}{91.2}(11.5833) = 19.1845 \text{kW}.$$

Figure 7.1 shows that the power available during the sunlit portion of the orbit
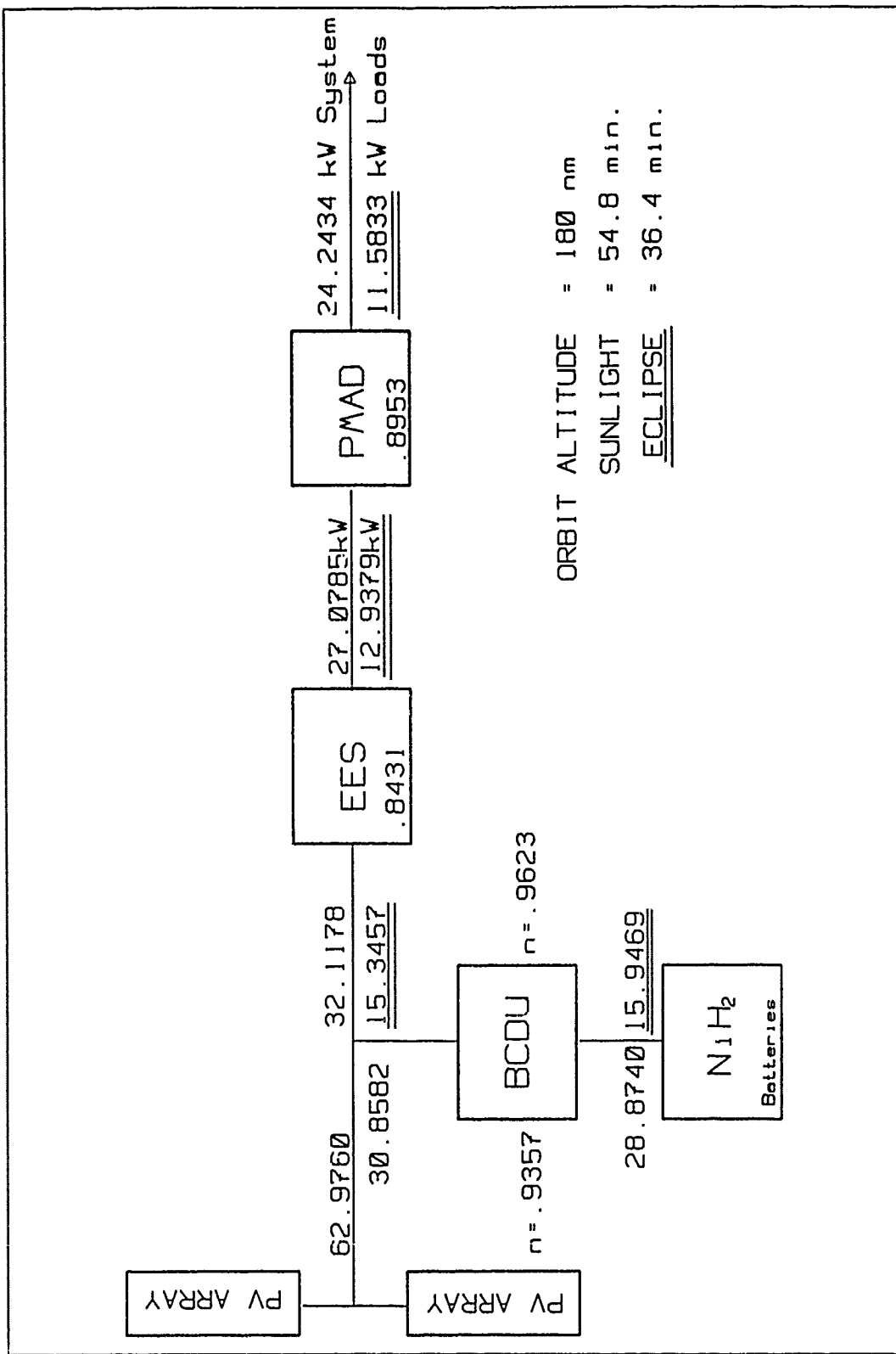
Figure 7.1. Scenario 3 Orbital Average Power Flow Diagram

is more than twice the value of the available power during the eclipse portion of the orbit. This does not present a problem when this EPS is used for autonomous reduction (Scenario 1 requires a peak power of 11.5 kW).

This design could not be operated as an orbital averaging power system and still provide the peak power requirements (18.85 kW) for Scenario 2 since only 11.58 kW is available during the eclipse portion of the orbit. Thus, the Scenario 3 EPS must have the capability to operate as an orbital average power system (for normal operation approximately 325 days per year while attached to SSF) and as a constant power system (for contingency operation during the approximate 40 days per year of salvage via Scenario 2).

As pointed out in Appendix C, the complement of 5 batteries is operated at 35% DOD to deliver 15.95 kW to the BCDU's during the eclipse portion of the orbit. To supply the required power to operate as a constant power system, a 5 battery complement would have to be operated at 73.25% DOD. Driving the batteries at this DOD has severe impacts on the battery life length, but the batteries are only operated in this fashion for approximately 40 days per year (under the assumption that Scenario 2 is the reduction method used). Thus, operating at 35%DOD (as the normal mode of operation) for the majority of the time will maximize the battery life.

7.3   Orbit Analysis Discussion

7.3.1   Hardware Considerations.   The most significant difference between the ASSET configuration of Scenario 3 and those of Scenarios 1 and 2 is the requirement to outfit the nose of the ASSET LO_2 tank with the appropriate docking hardware. However, with an estimated weight of roughly 300 lbs, the effect on the facility's ballistic coefficient is negligible. Another important distinction is that the EPS for Scenario 3 is based on the SSF design. This requires a larger solar array which translates to more weight and drag.

Table 7.1. Orbit Parameters, Scenario 3.

Phase	h_f (nm)	A_d (ft^2)	M (lbs)	β ($\frac{lbs}{ft^2}$)
A	161.2	8255.7	104,780	5.8
B	190.0	8255.7	104,780	5.8
C	170.6	8255.7	90,882	5.0
D	163.9	8826.2	160,404	8.3
E	190.0	8255.7	103,636	5.7
F	170.1	8255.7	90,384	5.0
G	163.1	8826.2	159,906	8.2

7.3.2 Facility Orbit Decay. The altitude history of the Scenario 3 facility is similar to Scenarios 1 and 2 except that after the salvage operation, ASSET docks with *Freedom*. The space station then assumes station keeping responsibilities. AS-SET is then released at the appropriate time to rendezvous with the next external tank. Table 7.1, above, highlights the physical characteristics of the facility at different phases of the operation. Again, A_d represents the effective facility drag area, M is the facility mass, and β the ballistic coefficient. (Refer to Figure 5.27 for a definition of phases A through G.)

7.3.3 Debris. As far as the cutting operations are concerned, Scenario 3 is no different than either Scenarios 1 or 2. Therefore, the SOFI debris issues have already been addressed. However, during the early stages of the evolution of this scenario, we had planned to continue disassembling the tank while attached to *Freedom*. However, we soon realized that debris containment measures would constrict our operation so severely, salvaging would soon become impractical. We therefore rejected the concept of space station-based salvaging.

7.3.4 Fuel Consumption. Table 7.2 presents the total ΔV's and burn times required for the Scenario 3 Hohmann transfers.[1] Table 7.3 presents the total fuel consumed during the maneuvers. Again, the quantity of fuel consumed includes a 20% allowance for RCS fuel and a 10% allowance for management reserves (54:45).

Table 7.2. Annual ΔV Requirements, Scenario 3.

Hohmann Transfer	ΔV_t (ft/sec)	t_b (sec)
#1	100.6	163.8
#2	91.1	147.0
#3	94.0	150.6
#4	91.1	145.4
Total	376.8	606.8

Table 7.3. Annual Fuel Consumption, Scenario 3.

Hohmann Transfer	m_f (lbs)
#1	1,464
#2	1,319
#3	1,355
#4	1,317
Subtotal	5,455
20% RCS	1,091
	6,546
10% Res	654
Total	7,200

7.3.5 Other Considerations. The major concern of Scenario 3 is the requirement to physically dock ASSET with *Freedom*. The technical issues related to automated docking maneuvers are addressed elsewhere in the study, but the concern here is the potential risk of damaging the space station during the maneuver.

---

[1]Assumes ASSET and *Freedom* rendezvous at an altitude of 190 nmi.

VIII. TECHNICAL COMPLEXITY

The final scenario decision needs to be made based on more than cost alone. While cost may indeed be the overriding factor, other factors play a very important role in final decision making. To aid future decision makers in making informed decisions we have included additional factors which we have termed "Technical Complexity".

Technical complexity is a measure of the degree of development necessary to produce a given design. It may be that the technology has never been tried in space, but proven on earth. Or perhaps an area seems simple to develop but is only at the conceptual stage. In all cases our designs were made with simplicity in mind and therefore the technical complexities are low.

Table 8.1 reveals our evaluations of the technical complexities associated with the most important aspects of this study.

1. Pre-flight Mods - the complexities associated with modifications to the ET prior to launch. These might include; wiring, centerline track, brackets and attach points, and internal tank markings for indexing. Scenarios with fewer required pre-flight mods have lower technical complexities.

2. EVA - the complexities associated with the development of space suits capable of performing the tasks necessary. Scenarios with shorter EVA's will have lower chances of necessary further development. EVA's requiring 3 man teams are viewed as having higher technical complexity than 2 man EVA teams.

3. Video/Communications - the complexities associated in the application of video/communication technology. Scenarios requiring more autonomy will be more dependent on video/communications and therefore have higher technical complexity.

Table 8.1. Technical Complexity

	Scenarios		
	1	2	3
1. Pre-flight Mods	0.100	0.050	0.100
2. EVA	0.050	0.150	0.050
3. Video/Communications	0.150	0.050	0.150
4. Piece-part Transport	0.100	0.050	0.100
5. Primary Cutter	0.150	0.100	0.150
6. SOFI Workstation	0.120	0.080	0.120
7. Plate/I-beam Stacker	0.100	0.010	0.100
8. Orbit Maintenance	0.200	0.200	0.250
Net Technical Complexity	0.648	0.522	0.670

1 - Automated reduction, 12kW arrays
2 - Astronaut Tended reduction, 20kW arrays
3 - Automated reduction, 23.4kW arrays (SSF)

4. Piece-part Transport - the complexities associated with the tools that move materials around the tank. The automated scenarios requiring machines to be developed for piece-part transport will have larger technical complexities.

5. Primary Cutter - the complexities associated with the reliability of the primary cutter. The scenarios with human supervision require less development to obtain an acceptable level of reliability.

6. SOFI Workstation - the complexities associated with the reliability of the SOFI workstation. The scenarios with human supervision require less development to obtain an acceptable level of reliability.

7. Plate/I-beam Stacker - the complexities associated with the development of automated plate and I-beam stackers. The automated scenarios will require much more development to achieve an acceptable level of dependability.

8. Orbit Maintenance - the complexities associated with the development of a orbit maintenance device capable of performing the necessary tasks of each

scenario. Scenarios requiring many orbit changes or close maneuvering (i.e. docking) are technically more complex.

The net technical complexity (T_i) calculation shown in Table 8.1 is given by:

$$T_i = \left[1 - \prod_k (1 - t_{k,i})\right] \qquad (8.1)$$

where $t_{k,i}$ is the technical complexity due to the kth characteristic.

The numbers in Table 8.1 were developed by starting with the upper left-hand corner (Pre-flight Mods; Scenario 1). Based on our understanding, as the system designers, we believe 0.1 is good representation of the amount of development necessary. From there we looked horizontally and considered the relative complexity of the other scenarios. We then looked vertically and considered the relative importance of each aspect within the scenario. For example, Orbit Maintenance has a higher technical complexity than piece-part transport because if orbit maintenance fails the entire complex could be lost, where if piece-part transport fails operations would be curtailed temporarily.

The net technical complexity given in Table 8.1 passes a reasonableness test in that Scenario 2 is the least complex; Scenario 1 is more complex, due to its automated nature; and Scenario 3 is most complex, due to the additional orbital maintenance problems.

IX. COST ANALYSIS

Before any development efforts can proceed beyond the preliminary design stage, decision makers must have at their disposal relatively accurate cost estimates of the competing designs. The ASSET cost model quantifies the three system level objectives: maximize *net present value* (NPV), minimize life cycle costs (LCC), and maximize product yield for each reduction scenario. This allows the life cycle costs of the design alternatives to be compared, and options singled out for further consideration.

9.1 Assumptions

A NASA space station cost model (LCCM) (68), developed in 1977 for the George C. Marshall Space Flight Center, forms the foundation of the ASSET cost model. It provides life cycle costs for all Design, Development, Test, and Evaluation (DDT&E), Flight Hardware Production (FH), and Operations expenditures.

The NASA cost model makes use of historical data dating back to the mid-1960's. Both manned and unmanned spacecraft systems are represented. Typical examples include the Mariner, Landsat, and Lunar Orbiter spacecraft, as well as the Apollo, Gemini, Skylab and early Space Shuttle programs.

Due to the similarities between Space Station *Freedom* and the ASSET facility, the NASA LCCM proved to be a useful starting point from which ASSET cost estimates could be forecasted. Both facilities:

- serve as infrastructures for space-based operations,

- require similar power generation equipment,

- require similar altitude and attitude control hardware,

- and incur similar operations costs.

On the other hand, *Freedom* has been designed to house a permanent crew of a dozen or so astronauts while the ASSET facility is designed to be man-tended only. An argument could be made that costs for a man-rated system should not be used to estimate the costs of an unmanned facility. However, this conceptual difference is taken into account when the existing NASA cost model is adapted to meet our needs.

The ASSET design team strove to use off-the-shelf technologies wherever possible during this study. The NASA cost model however assumes the use of state-of-the-art technologies, but provides the means with which the user can adjust the cost estimates to allow for commonality, inheritance, and use of off-the-shelf hardware. 'Cost complexity factors' are used to make these adjustments, and will be discussed in more detail later.

The initial cost analysis of the ASSET facility made use of a NASA supplied $100 Million (1989$) cost estimate for a dedicated STS flight (73). This cost element is by far the most important single element of the cost model. A presentation of preliminary cost figures at our Critical Design Review prompted a re-evaluation of that cost figure. Our sponsor observed during this meeting that the true cost of a dedicated shuttle flight is not necessarily what NASA charges commercial customers. Their recommendation was to use a more realistic and market based estimate of $150M to $250M for a dedicated flight. This recommendation was adopted, and the cost results presented in our study reflect this update. In the discussions that follow, note that all calculations are made in 1978$ and escalated to 1990$ for the system level trade studies.

9.2 Model Development

9.2.1 Cost Elements. The system LCC is generated from 23 random variable cost elements and seven Cost Estimating Relationships (CER) Table 9.1 categorizes the cost elements in terms of classification (DDT&E, FH Production, Operations,

or Revenue) and type (CER or Random Variable (RV)). A life cycle cost computer program (MLCC[1]) is used to sample the random variables and CERs to provide a population of LCC data points upon which a statistical analysis can be performed.

MLCC produces 750 LCC data points which are then processed by a statistical analysis program (SAS) to produce an empirical probability density function (pdf) for the life cycle cost. SAS provides, among other things, the mean and standard deviation of the empirical pdf; it then becomes a simple matter to find a mean and upper LCC value (with confidence statements) from the empirical pdf. SAS also provides a histogram that displays the general shape of the underlying LCC pdf.

9.2.2 Time Value of Money. The MLCC user specifies how disbursement and revenue streams are timed over the life of the system. Figure 9.1 portrays the assumed cash flow timeline for the three scenarios, and includes the three major cost categories mentioned earlier[2] along with an 'effective' revenue stream. Although year zero can coincide with any year, we have assumed a project start date of 1990. MLCC calculates the present (year zero) value of the expenses and revenue stream as discussed in Appendix G.

Notice that DDT&E costs are assumed to increase linearly to some constant level during the first year (phase-in), remain constant for two years, then eventually decrease to zero during the fourth year. FH costs follow a similar pattern. Operational costs are projected to start at the beginning of year four and increase to some constant level beginning with year five. They then remain constant throughout the life of the system. The launch cost of the ASSET facility is projected to occur at the end of year five. The 'effective' revenue stream comes on-line during year five. ASSET is given an operational life, somewhat arbitrarily, of 10 years. However, this is a reasonable estimate since many military weapon systems are projected to have at least a 10 year mission life.

---

[1] Modified Life Cycle Cost program (15).
[2] DDT&E, FH Production, and Operations.

Table 9.1. Cost Model Variables.

Class	Cost Element	Type
DDT&E	Structure	RV
	Docking Adapter	RV
	Electrical Power	CER
	Environmental Control	RV
	Data Management/Communications	CER
	Stabilization & Control	RV
	RCS/Propulsion	CER
	System Test & Evaluation	RV
	Integration, Assembly & C/O	RV
	Ground Support Equipment	RV
	Systems Engr. & Integrations	RV
	Program Management	RV
FH	Structure	CER
	Docking Adapter	RV
	Electrical Power	CER
	Environmental Control	RV
	Data Management/Communications	CER
	Stabilization & Control	RV
	RCS/Propulsion	CER
	Electron Beam Cutter	RV
	Integration, Assembly & C/O	RV
	Systems Engr. & Integration	RV
	Program Management	RV
OPS	EVA, Initial Setup	RV
	EVA, Operations	RV
	Misc. Operations	RV
	Consumables	RV
	Launch Cost	RV
REV	Effective Revenue	RV
	EPS Revenue	RV
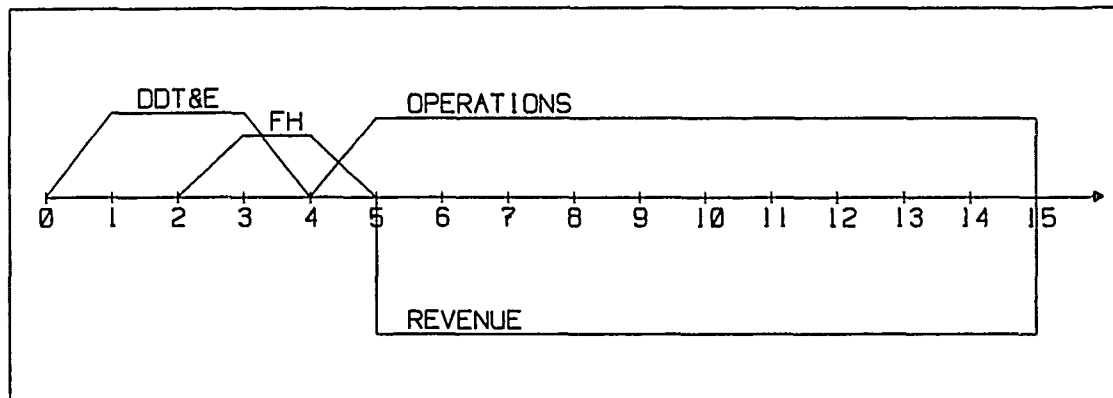
Figure 9.1. Cash Flow Timeline Assumptions.

An 'effective' revenue stream here means the costs an agency could reasonably expect to incur assuming they:

- require the same ASSET I-beam/plate deliverables,

- in the same amounts provided by normal ASSET operations,

- and use the launch services of the NSTS (Space Shuttle) to haul the material up from the Earth's surface.

This 'revenue stream' is subtracted from the life cycle costs,[3] producing the *net present value* of the cash flow stream. This turns out to be the only practical way with which to evaluate the cost competitiveness of the ASSET concept, as there are no customers today looking for structural aluminum at low Earth orbit.

9.3 LCC Input Data - Random Variables

The MLCC program uses random variables and cost estimating relationships to generate system life cycle costs. CERs require very little in the way of refinements in order to be used by MLCC. However, the user must specify several parameters before the random variables can be used:

---

[3]Revenue is assumed to be a negative quantity here since MLCC was originally designed for expenditures, which are entered as positive numbers.

- the lowest anticipated cost

- the highest anticipated cost, and

- the spread of the cost estimate between these extremes.

The first two items are either generated by hand calculations or through the use of NASA CERs and cost complexity factors. Since MLCC assumes an underlying Beta pdf to describe the distribution of the random variable cost between those extremes, the user simply specifies a 'type' of Beta pdf to take care of item three.[4] These intermediate results are presented in the tables below, and prove to be useful in the scenario level trade study discussions.

9.3.1 Scenario 1 Random Variables. The expected minimum and maximum costs associated with a given cost element for both the 12% and 21% EPS systems are presented Figures 9.2 and 9.3. 'Tendency' implies the shape ('type') given the underlying Beta distribution to accommodate the user's judgement of how the cost should be skewed (see Figure G.4[5]).

The cost extremes shown in Tables 9.2 and 9.3 are generated by direct application of the CER's provided in the Space Station cost model. The CER estimate is used as the maximum value, while the low value is generated by multiplying this unadjusted CER by a cost complexity factor f_c, where

$$0 < f_c \leq 1.0.$$

The complexity factor is a measure of the designer's use of 'off-the-shelf' technology for that particular subsystem design. The complexity factors assigned to the subsystem cost elements were generated by the ASSET design team after a thorough literature search and by comparisons with Space Station *Freedom* hardware designs.

---

[4]See Appendix G for details.

[5]'Low' $\Rightarrow$ skew left, 'High' $\Rightarrow$ skew right. As a result, cost will tend to be concentrated at high or low end respectively.

Table 9.2. Scenario 1a Random Variable Cost Data.

	Cost Element (12% EPS)	1978$ (Millions)		Tendency	f_c
		Min	Max		
DDT&E	Structure	1.897	18.975	low	.1
	Environmental Control	4.342	14.474	low	.3
	Stabilization & Control	3.759	9.398	low	.4
	Docking Adapter	0.425	4.245	high	.1
	System Test & Evaluation	12.102	60.512	low	.2
	Integration, Assembly & C/O	1.574	15.738	low	.1
	Ground Support Equipment	5.193	10.387	low	.5
	Systems Engr. & Integration	4.863	9.725	low	.5
	Program Management	2.547	8.579	low	.3
FH	Environmental Control	0.671	0.745	high	.9
	Stabilization & Control	4.986	5.540	high	.9
	Docking Adapter	0.354	0.393	high	.9
	Electron Beam Cutter	0.355	0.462	high	—
	Integration, Assembly & C/O	1.722	2.460	low	.7
	Systems Engr. & Integration	1.643	3.287	low	.5
	Program Management	0.722	2.408	low	.3
OPS	EVA, Initial Setup	0.758	1.137	central	—
	EVA, Operations	50.400	59.120	high	—
	Misc. Operations	24.480	244.780	low	.1
	Consumables	104.938	174.897	central	—
	Launch Cost	71.056	118.427	central	—
REV	Effective Revenue	-642.710	-1109.080	central	—

The generally low complexity factors assigned to the DDT&E cost elements reflect our optimism regarding the use of off-the-shelf technology. With the exception of the tools required for the cutting operations, all other hardware elements are either already fielded and require little in the way of modifications to meet our needs, or are at an advanced stage of development. We therefore felt justified in using low complexity factors for many of the DDT&E cost adjustments.

On the other hand, we did not feel quite as optimistic about adjusting the costs associated with flight hardware production. The design team was in agreement that the production costs for ASSET hardware would be on the high side of the NASA

CER results. High unit costs were expected due to low-volume production runs.

The cost complexity factors for the Mission Support[6] and Operations cost elements were used to model the relative complexities of the ASSET and *Freedom* missions. Space Station *Freedom* is an inherently more complex facility than ASSET because humans play a large role in the mission and design of the station. Much more emphasis must be placed on safety and human factors issues. These concerns drive up the complexity of the system, in turn driving up the costs associated with integration, testing, operations, and overall program management. ASSET is a simple concept in comparison. Although safety is still of paramount concern, fewer humans will be involved and for shorter periods of time than with *Freedom*. The comparatively small-scale operation of ASSET will require a smaller 'standing army' for ground and flight operations than will *Freedom*. It seemed plausible then that both the Mission Support and Operations costs would be on the low side of the NASA cost estimates, hence the low complexity factors. However, note that the complexity factors assigned to the Miscellaneous Operations costs for Scenario 3 (Space Station offloading of products) are much higher than for the other scenarios not requiring direct space station support (see Tables 9.6 and 9.7).

Referring to Table 9.2, it is clear that with the exception of the System Test & Evaluation costs, the individual DDT&E and FH cost estimates prove to be relatively minor players in the composite LCC calculations.[7] The primary cost drivers turn out to be the operations costs, and are explained in more detail below.

The EVA costs are subdivided into two major categories: Initial Setup and Operations. The initial setup EVAs involve the deployment of the Boost/Deboost Module, the EPS system, the tools and other support hardware. The sustaining

---

[6]Includes the system test and evaluation, integration, assembly, GSE, and program management costs.

[7]Note however that in the aggregate, the DDT&E and FH costs do have a substantial impact on the LCC due to the time value of money. The DDT&E and FH costs are weighted more heavily than the operations costs since they occur earlier in the cash flow timeline.

Table 9.3. Scenario 1b Random Variable Cost Data.

	Cost Element (21% EPS)	1978$ (Millions)		Tendency	f_c
		Min	Max		
DDT&E	Structure	1.784	17.840	low	.1
	Environmental Control	4.182	13.939	low	.3
	Stabilization & Control	3.759	9.398	low	.4
	Docking Adapter	0.425	4.425	high	.1
	System Test & Evaluation	11.418	57.089	low	.2
	Integration, Assembly & C/O	1.532	15.321	low	.1
	Ground Support Equipment	8.365	16.731	low	.5
	Systems Engr. & Integration	7.349	14.699	low	.5
	Program Management	3.623	12.075	low	.3
FH	Environmental Control	0.620	0.689	high	.9
	Stabilization & Control	4.986	5.540	high	.9
	Docking Adapter	0.354	0.393	high	.9
	Electron Beam Cutter	0.355	0.462	high	—
	Integration, Assembly & C/O	1.640	2.344	low	.7
	Systems Engr. & Integration	1.529	3.059	low	.5
	Program Management	0.676	2.253	low	.3
OPS	EVA, Initial Setup	0.758	1.137	central	—
	EVA, Operations	50.026	59.118	high	—
	Misc. Operations	23.130	231.300	low	.1
	Consumables	80.666	134.444	central	—
	Launch Cost	71.056	118.427	central	—
REV	Effective Revenue	-642.710	-1109.080	central	—

EVA operations include the transfer of tools and other support equipment from the ASSET facility to the tanks docked with the facility. Also, upon completion of the reduction operation, these tools and the newly salvaged products must be transferred from the secondary tank back to the ASSET facility. The initial setup EVA is a one-time-only event and occurs at the beginning of year five. On the other hand, the sustaining EVA Operations occur each time ASSET docks with a secondary tank. Therefore, EVA Operations costs are incurred four times per year throughout the

life of the system.[8]

The Miscellaneous Operations costs (those costs associated with NASA support) includes such support functions as flight operations, ground operations and sustaining engineering. The spread of this cost estimate reflects the high level of uncertainty associated with this estimate. However, the cost estimate is shifted to the lower end of this range (i.e. low tendency) since minimal NASA support is expected for this scenario.

'Consumables' costs represents those expenditures associated with resupplying the ASSET facility with orbital maneuvering fuel. Chapter VI discussed the development of the annual fuel requirements for Scenario 1. The mass of the consumed fuel, when multiplied by the expected cost of transporting the fuel to ASSET, produces the 'Min' and 'Max' values in the tables.[9] At a transportation cost ranging from $2800 to $4700 per pound, this cost element proved to be one of the more dominant factors in the system LCC.

'Launch Cost' is a one-time only cost incurred at the beginning of year five to cover the cost of the dedicated STS setup flight. As discussed earlier, the low and high estimates for this dedicated mission, $71.056-$118.427 M 1978$ ($150-$250 M 1990$), was recommended by our sponsor.

The 'Effective Revenue' stream is generated by multiplying the product yield from each salvaged tank[10] by the estimated cost of delivering similar cargo to Earth orbit ($2800 to $4700 per pound). This 'revenue' is subtracted from the other cost elements (hence the negative sign), producing the system *net present value* alluded to earlier.

---

[8]This explains the drastic difference between the magnitudes of the EVA Setup and EVA Operations costs ($0.758-$1.137 million versus $50.4-$59.12 million). MLCC spreads the EVA Operations cost over the 10 year program life of ASSET.

[9]Sample calculations for this and other random variable cost estimates can be found in Appendix G.

[1] Roughly 12-13,000 lbs, depending on the scenario.

9.3.2 Scenario 1 Trade Stuay. The major difference between Scenario 1a (12% EPS) and Scenario 1b (21% EPS) is found in the Consumables cost category. The cost of consumables for the 12% EPS system is substantially higher than that for the 21% EPS system. This is a direct consequence of the fuel consumption data presented in Table 5.5. As expected, the operations costs for the more efficient (hence smaller) solar arrays are lower than the costs associated with the less efficient arrays. The question of whether or not this savings pays for the added cost to develop the higher efficiency EPS is addressed in the CER cost discussion.

9.3.3 Scenario 2 Random Variables. A brief discussion of the intermediate Scenario 2 cost estimates follow. Again, with the exception of the System Test & Evaluation costs, the individual DDT&E and FH cost estimates are relatively small when compared with the cost of operations. Notice also that the cost complexity factor associated with Miscellaneous Operations has been adjusted from .1 for Scenario 1 to .5 for Scenario 2. This is done to capture the expected cost increase for additional NASA support due to the increased reliance on astronauts.

9.3.4 Scenario 2 Trade Study. The major trade study in Scenario 2 is again between the 12% and 21% EPS systems. As was the case for Scenario 1, the higher efficiency arrays prove to be the least expensive to operate in terms of the consumables costs.

However, the most significant findings are realized when comparing the Scenario 2 operations expenses with those of Scenario 1. First, the Scenario 2 sustaining EVA Operations expenses are roughly twice those of Scenario 1 ($50.026-$59.118 versus $97.820-$132.022 M). This can be traced back to the Scenario 1 and 2 EVA timelines established in Appendix F where one can see that the total EVA hours required for Scenario 2 are roughly twice the hours required for Scenario 1.

Second, a close examination of the Consumables expenses between Scenarios 1 and 2 provides additional useful information. Comparing the cost of consumables

Table 9.4. Scenario 2a Random Variable Cost Data.

	Cost Element (12% EPS)	1978$ (Millions)		Tendency	f_c
		Min	Max		
DDT&E	Structure	1.829	18.293	low	.1
	Environmental Control	4.518	15.060	low	.3
	Stabilization & Control	3.759	9.398	low	.4
	Docking Adapter	0.425	4.245	high	.9
	System Test & Evaluation	12.197	60.984	low	.2
	Integration, Assembly & C/O	1.579	15.795	low	.1
	Ground Support Equipment	5.072	10.143	low	.5
	Systems Engr. & Integration	4.746	9.527	low	.5
	Program Management	2.530	8.434	low	.3
FH	Environmental Control	0.729	0.810	high	.9
	Stabilization & Control	4.986	5.540	high	.9
	Docking Adapter	0.354	0.393	high	.9
	Electron Beam Cutter	0.474	0.616	high	—
	Integration, Assembly & C/O	1.733	2.476	low	.7
	Systems Engr. & Integration	1.659	3.318	low	.5
	Program Management	0.729	2.430	low	.3
OPS	EVA, Initial Setup	0.758	1.137	central	—
	EVA, Operations	97.820	132.022	low	—
	Misc. Operations	121.470	242.940	high	.5
	Consumables	114.859	191.932	central	—
	Launch Cost	71.056	118.427	central	—
REV	Effective Revenue	-642.710	-1109.080	central	—

between Tables 9.2 and 9.4, one finds that for a given solar array efficiency (12% in this case) the cost of consumables is greater for Scenario 2 than for Scenario 1. This can be explained by the EVA constraints imposed on the work crew in Scenario 2. Since only eight EVA hours are allowed in a 24 hour period (see Appendix F), it turns out that the total mission time required to dock with and reduce the secondary tanks is 6.3 days for Scenario 1 versus 8.3 days for Scenario 2. Recovering the same amount of material over an additional two day period means that the Boost/Deboost Module must compensate for the altitude loss that will occur over that period. Sections 5.7.4 and 6.7.4 discuss the fuel consumption requirements for Scenarios 1 and 2

Table 9.5. Scenario 2b Random Variable Cost Data.

	Cost Element (21% EPS)	1978$ (Millions)		Tendency	f_c
		Min	Max		
DDT&E	Structure	1.705	17.049	low	.1
	Environmental Control	4.463	14.876	low	.3
	Stabilization & Control	3.759	9.398	low	.4
	Docking Adapter	0.425	4.425	high	.1
	System Test & Evaluation	11.333	56.667	low	.2
	Integration, Assembly & C/O	1.527	15.269	low	.1
	Ground Support Equipment	8.608	17.215	low	.5
	Systems Engr. & Integration	7.533	15.067	low	.5
	Program Management	3.697	12.325	low	.3
FH	Environmental Control	0.710	0.789	high	.9
	Stabilization & Control	4.986	5.540	high	.9
	Docking Adapter	0.354	0.393	high	.9
	Electron Beam Cutter	0.474	0.616	high	—
	Integration, Assembly & C/O	1.630	2.329	low	.7
	Systems Engr. & Integration	1.515	3.031	low	.5
	Program Management	0.670	2.234	low	.3
OPS	EVA, Initial Setup	0.758	1.137	central	—
	EVA, Operations	97.820	132.022	low	—
	Misc. Operations	112.886	225.772	high	.5
	Consumables	89.633	149.388	central	—
	Launch Cost	71.056	118.427	central	—
REV	Effective Revenue	-642.710	-1109.080	central	—

respectively. These sections show that more fuel is required to maintain the orbit of the Scenario 2 ASSET facility than for Scenario 1. As a result, we have the increased consumables expenses between the scenarios mentioned earlier.

Finally, the Miscellaneous Operations expenses for Scenario 2 are substantially larger that those for Scenario 1. The increase in the cost complexity factor (from .1 to .5) for this scenario has been discussed earlier in this section. However, notice also that the underlying probability distribution describing this cost element has been shifted from a low expected value tendency to a high tendency. This was done to model the logistical complexities and scheduling impacts this particular scenario

would have on the nominal NASA STS mission.[11]

9.3.5 Scenario 3 Random Variables.   Table 9.6 details the expected ranges of the Scenario 3 cost random variables for the automated mode of tank reduction, while Table 9.7 presents the estimates for the astronaut-tended mode. The major difference between this scenario and the others is that an additional revenue stream is incorporated in Scenario 3. Recalling the overview discussion in Chapter IV, the third scenario called for the docking of ASSET with Space Station *Freedom*. This provides two immediate benefits:

1. The I-beam/plate product bundles can be off-loaded onto the space station truss structure, thereby minimizing the amount of mass the Boost/Deboost Module must haul around.

2. During the 80 some days that the ASSET facility lies dormant, we could potentially sell power to NASA and its customers.

The cost savings associated with the first item is reflected in the Consumables cost estimate. However, the concept of selling power to NASA assumed a bartering agreement between ASSET and NASA that allows for the exchange of ASSET supplied power for *Freedom* supplied stationkeeping propellant expenditures.[12] Fully half of the forecasted revenue stream from selling power has been allocated to NASA in exchange for services rendered. Decreased fuel expenses and increased revenue are evident in the tables below.

Notice also that the cost complexity factor associated with Miscellaneous Operations has been adjusted from .5 for Scenario 2 to .6 for Scenario 3. This increase attempts to capture the additional cost complexity associated with docking ASSET with *Freedom*.

---

[11]We have assumed a 'background' role for ASSET operations for all subsequent tank reductions. However, Scenario 2 requires an inordinate amount of EVA support during these missions. Such a tremendous use of NASA resources justifies this increase in the cost complexity factor.

[12]Sample calculations can be found in Appendix G

Table 9.6. Scenario 3 (Automated) Random Variable Cost Data.

| | Cost Element (12% EPS) | 1978$ (Millions) | | | |
		Min	Max	Tendency	f_c
DDT&E	Structure	2.046	20.460	low	.1
	Environmental Control	4.518	15.060	low	.3
	Stabilization & Control	3.759	9.398	low	.4
	Docking Adapter	0.546	5.455	high	.1
	System Test & Evaluation	13.554	67.772	low	.2
	Integration, Assembly & C/O	1.658	16.582	low	.1
	Ground Support Equipment	6.314	12.628	low	.5
	Systems Engr. & Integration	5.759	11.519	low	.5
	Program Management	2.961	9.869	low	.3
FH	Environmental Control	0.729	0.810	high	.9
	Stabilization & Control	4.986	5.540	high	.9
	Docking Adapter	0.444	0.493	high	.9
	Electron Beam Cutter	0.355	0.462	high	—
	Integration, Assembly & C/O	1.892	2.703	low	.7
	Systems Engr. & Integration	1.890	3.781	low	.5
	Program Management	0.822	2.961	low	.3
OPS	EVA, Initial Setup	0.758	1.137	central	—
	EVA, Operations	50.026	59.118	high	—
	Misc. Operations	163.766	272.944	high	.6
	Consumables	74.703	124.505	central	—
	Launch Cost	71.056	118.427	central	—
REV	Effective Revenue	-642.710	-1109.080	central	—
	EPS Revenue	-139.380	-170.360	central	—

9.3.6 Scenario 3 Trade Study. Scenario 3 is unique in that there was no trade study performed between differing solar array efficiencies. The same solar array efficiency was assumed for the Scenario 3 design alternatives, so the major tradeoffs are found by comparing the cost implications of the automated versus the astronaut-tended modes of operation. Although the same type of cost implications discussed in Section 9.3.4 apply here as well, the most significant factor worth considering in Scenario 3 is the cost of sustaining EVA Operations. The $50-$132 M cost differential (low estimates) reflects the EVA operations costs for an automated versus astronaut-tended facility.

Table 9.7. Scenario 3 (Man-tended) Random Variable Cost Data.

	Cost Element (12% EPS)	1978$ (Millions)		Tendency	f_c
		Min	Max		
DDT&E	Structure	1.941	19.415	low	.1
	Environmental Control	4.518	15.060	low	.3
	Stabilization & Control	3.759	9.398	low	.4
	Docking Adapter	0.546	5.455	high	.1
	System Test & Evaluation	13.174	65.870	low	.2
	Integration, Assembly & C/O	1.637	16.366	low	.1
	Ground Support Equipment	5.945	11.891	low	.5
	Systems Engr. & Integration	5.467	10.934	low	.5
	Program Management	2.836	9.452	low	.3
FH	Environmental Control	0.729	0.810	high	.9
	Stabilization & Control	4.986	5.540	high	.9
	Docking Adapter	0.444	0.493	high	.9
	Electron Beam Cutter	0.474	0.616	high	—
	Integration, Assembly & C/O	1.848	2.640	low	.7
	Systems Engr. & Integration	1.825	3.650	low	.5
	Program Management	0.796	2.653	low	.3
OPS	EVA, Initial Setup	0.758	1.137	central	—
	EVA, Operations	97.820	132.022	low	—
	Operations	159.144	265.240	high	.6
	Consumables	74.703	124.505	central	—
	Launch Cost	71.056	118.427	central	—
REV	Effective Revenue	-642.710	-1109.080	central	—
	EPS Revenue	-139.380	-170.360	central	—

9.4   LCC Input Data - Cost Estimating Relationships.

9.4.1   General Discussion.   Some of the system LCC estimates are generated using Cost Estimating Relationships (CERs) of the form:

$$C_i = k_i \beta_0 W_i^{\beta_1}.$$

In general, cost is presumed to be a function of subsystem element weight. Therefore, in the equations above, W_i represents the weight of the subsystem and C_i the LCC. For the case of estimating the LCC of the electrical power subsystem, cost is assumed

to be a function of the surface area of the solar panels. The term k_i represents the cost complexity factors for the CERs. Both k_i and W_i are used as random variables here.

The CERs used in the ASSET cost model differ somewhat from those used in the NASA Space Station Cost model. ASSET uses a natural logarithm based CER while the Space Station Cost model uses a base 10 logarithm. This explains why some of the DDT&E and FH cost elements are used as random variables instead of CERs. When the historical data was analyzed using a natural log based CER for the linear model, only seven of the CERs proved statistically valid (see Table 9.8).[13]

Table 9.8. ASSET CER List.

CER	Description	Class
#1	Structure	FH
#2	Electrical Power	DDT&E
#3	Electrical Power	FH
#4	Data Management	DDT&E
#5	Data Management	FH
#6	RCS/Propulsion	DDT&E
#7	RCS/Propulsion	FH

Weight estimates for these subsystem components were arrived at through literature searches or through preliminary sizing calculations. For instance, most of the weight estimates for the RCS/Propulsion and Stabilization & Control CERs were derived from the ET Gamma Ray Imaging Telescope (ET GRIT) study(55). On the other hand, the weight estimates for ASSET unique hardware were produced through simple hand calculations. The sizes of the hardware components were estimated and then converted to rough order of magnitude weight estimates. See Appendix G.4 for a detailed listing of the cost complexity factors and weight estimates used for the CERs.

---

[13]The seven remaining CERs were converted to random variables. See discussion in Appendix G.

9.4.2 CER Impacts on Trade Studies. A discussion of the tradeoffs between using 'off-the-shelf' versus 'state-of-the-art' hardware for the electrical power system requires an understanding of the interplay between DDT&E costs, cost complexity factors, and the time value of money.

Appendix H provides, among other things, the array sizes of the ASSET EPS design options. Scenario 1 data shows that the 12% efficient array requires roughly 4564 ft^2 of blanket area while the 21% array requires only 3229 ft^2. Although the higher efficiency provides a 71% reduction in blanket area, the cost to develop this technology (represented by the cost complexity factor) offsets any potential savings seen in the EPS CER.

Referring to Tables G.1 and G.2, one can see that the DDT&E cost complexity factor used for the 12% efficiency solar arrays ranged from .1 to .3 (skewed towards .1) while the complexity factor used for the 21% efficient array ranged from .4 to .6 (skewed towards .5). In other words, for a given array surface area, the 21% efficient array development cost would be roughly five times that of the 12% array cost. This difference in the cost complexity factors can be attributed to the additional effort required to address the following design considerations:

1. Further flight test and integration work is required before a 21% array can be deployed.

2. The solar array packing factor changes since the 21% efficient solar cells will be smaller.

3. Changing the packing factor forces a redesign of the array blanket and support structure.

4. Changes in the array structure also impacts the design of sun tracker control mechanisms.

Since we are trying to recover this increase in DDT&E costs through fuel savings, the time value of money also becomes a factor. Table 9.1 shows that the

bulk of the DDT&E outlays are realized by the end of year 3, while fuel savings are not realized until year 6. An 8% rate of interest implies that the year 6 money is discounted by a factor of .794 relative to year 3. Year 15 money is discounted by a factor of .397 (30:538). As the data in Table 9.9 will show, the fuel savings were not of sufficient magnitude to overcome this discounting effect.

9.5 Results/System Level Trade Studies

After running the MLCC program with an assumed 8% opportunity cost of money, the 750 sampled life cycle cost estimates for each scenario are then analyzed by SAS to generate the empirical probability density functions. SAS provides a variety of statistical information pertaining to the pdfs, the two most important being the expected value (or mean) and the 90th percentile value of the system NPV.

9.5.1 LH$_2$ Reduction, Median Launch Cost.

Table 9.9 summarizes the relative merit of each scenario for LH$_2$ tank reduction only:

Table 9.9. Net Present Value, 1990$.

Scenario	Mean	90th Percentile
#1, 12% EPS	-105.916	29.554
#1, 21% EPS	-67.648	80.218
#2, 12% EPS	65.323	202.656
#2, 21% EPS	97.219	255.431
#3, Automated	-83.435	67.552
#3, Man Tended	-39.132	113.994

Keep in mind that a negative value here means that revenue exceeds expenses. Clearly, the automated scenarios[14] are more cost-effective than the man-tended scenarios, while the lower efficiency solar cell electrical power system is more cost competitive than the higher efficiency system. Notice though, at the 90% confidence level, none of the design options are cost competitive with transporting the same material from Earth to Earth orbit.

However, the NPV data presented in Table 9.9 are very sensitive to launch costs. Due to the uncertainty in the actual costs of launching a payload on the

---

[14]Scenarios 1 and 3 (automated).

NSTS to low Earth orbit, the most cost effective scenario (Scenario 1) has been re-evaluated at the two launch cost extremes provided by our sponsor. Table 9.10 gives an indication of how the launch cost estimate can affect the NPV calculations:

Table 9.10. Scenario 1 NPV Sensitivity, 12% EPS System, 1990$ (Millions).

Launch Cost ($/lb)	Mean	90th Percentile
Low (2800)	-62.981	54.886
Median (3750)	-105.916	29.554
High (4700)	-175.323	-51.720

Notice that at the high end of the launch cost range, the ASSET concept becomes cost competitive with Earth based suppliers. For a given opportunity cost of money, several iterations of the MLCC program could provide the launch cost necessary to break even over the 15 year program.

9.5.2 LH$_2$ Tank and LO$_2$ Barrel Reduction, Median Launch Cost. Table 9.11 documents how salvaging the barrel section of the LO$_2$ tank impacts the two most cost competitive design alternatives at the median launch cost:

Table 9.11. NPV, LH$_2$ Tank and LO$_2$ Barrel Reduction, 1990$ (Millions).

Scenario	Mean	90th Percentile
#1, 12% EPS	-222.575	-111.883
#3, Automated	-215.567	-44.331

The ASSET concept *with* LO$_2$ barrel reduction is clearly cost competitive with Earth based suppliers. The numbers indicate that the time invested in salvaging the barrel section of the LO$_2$ tank is well worth the additional effort.

9.6 Other Considerations

The ASSET LCC model does not include any of the maintenance costs that one would expect to see over the facility's 10 year life. However, a preliminary investigation of the EPS has revealed that many of the electrical power components have lifelengths of at least 7 to 10 years (with the notable exception of batteries). Also, should any of the specialized tools break, repairs can readily be performed during system setup. [15] On the other hand, little can be said about the mean time between failure (MTBF) for most of the remaining ASSET components. We have chosen to overlook the costs associated with maintenance actions due to the high level of uncertainty in the subsystem MTBFs.

The residual value of the facility is another aspect of the cost model worth considering. The life cycle costs assumed a completely depreciated facility after 10 years of operation. Plant or fixed assets are generally considered 'long-lived" and have life estimates ranging from 15, 30, to even 50 years, depending upon the type of property (70:237-241). It is reasonable to assume therefore that the ASSET facility wouldn't necessarily be completely depreciated after 10 years. However, since it is virtually impossible to establish a residual value here, we have chosen to ignore it.

There are many intangible benefits worth considering, two of which come immediately to mind. Although the LCC numbers shown in the results section do seem to indicate ASSET cost-competitiveness, one key element is being overlooked. The United States today does not have the launch capacity to deliver such large amounts of material to low Earth orbit as quickly as can be delivered by the ASSET concept. The NSTS is currently experiencing a launch backlog that could take years to clear; the expendable launch vehicle industry is also under pressure to clear its payload backlog. In short, even if one could afford to launch these materials in today's market, they can expect to wait five to seven years before the first shipment of

---

[15]EVAs are required for tool setup; it would be a simple matter then to bring up spares as needed to replace faulty components.

aluminum reaches Earth orbit, and another 5 to 10 years to match, pound for pound, the ASSET deliverables. In other words, since ASSET could begin providing large quantities of raw structural aluminum almost immediately (with little impact on current launch schedules), the opportunity cost associated with *not* taking advantage of this potential resource is staggering.

Another worthwhile benefit that does not show up in the 'bottom line' is the experience that will be gained in space-based operations. Many technological spin-offs are sure to come from such a venture, not to mention the experience of managing a 'factory in the sky'. EVA techniques and technologies are sure to improve as a result, while similar gains in other areas of space operations can be expected as well.

X. ADDITIONAL REDUCTION

The interior of the LH_2 tank is the largest most homogeneous volume in the External Tank. All other constituent parts are smaller and far less homogeneous. The External Tank is 64.44 percent 2219 aluminum alloy. Most of this 2219 is in the LH_2 Tank. After the LH_2 tank was 'played' out, the rest of the External Tank was be examined with an eye toward recovering 2219 aluminum as well as salvaging materials which are easily accessible.

10.1 Salvaging the Birdcage

The next logical step in salvaging the External Tank (ET) is to cut the remaining structural members into plate and I beams. There are two approaches to this process. Either leave an even more minimal structure in place than the birdcage or salvage to the point that the birdcage configuration is eliminated altogether.

To eliminate the birdcage configuration, uses for the remaining plate and I-beam, the major ring frames, the siphon assembly, and the aft dome cap, must be found. The benefits of plate and I-beam have been detailed in XI, but it is not entirely clear that items such as the aft dome assembly and the ring frames and the siphon assembly can be used cost effectively.

There are two main uses for unique components. Save them for as yet unforeseen contingencies or modify them for current contingencies.

Some forms of piece part modification will require end user specifications. There is however, a clear need for a diversity of metal shapes and tempers which could be produced from melted metal. As part of the long range plan for the ASSET facility, a work station should be built that can cut up odd sized pieces with electron beam or shear cutters and feed these pieces to a solar powered furnace.

Table 10.1. LO$_2$ Tank Materials

Element	Material	Condition
Nose Cone		
Lightning Rod	A356.0 Casting	T61
Major Cone		
Skin, Frames, and Stringers	2024 Sheet	T6
Mounting Frame	6061 Extrusion	T62
Ogive		
Gores;Cover Plate	2219 Plate	T87
Fwd. Fitting	2219 Forging	T6
T-Ring	2219 Extrusion	T8511
Barrel Panels	2219 Plate	T87
Int. and Ext. Lugs	2219 Sheet/Plate	T87
Dome		
Cap,Gore,Manhole Cover and Fitting	2219 Plate	T87
Suction Fitting	2219 Forging	T6
Ring Frame(Chords)	2219 Extrusion	T8511
Slosh Baffle		
Webs (All but Sta. 851)	2024 Sheet	T62
Webs(Sta. 851)	2024 Sheet/2219 Forging	T81/T652
Web Stiffeners;Tension Strap	2024 Sheet	T81
Chord Angle;Stiffener Angle and Stringer	2024 Extrusion	T8511
Vortex Baffle		
Splice;Caps and Stiffeners	2024 Extrusion	T8511
Web;Splash Plate and Straps	2024 Sheet	T81

When the birdcage configuration is eliminated, the intertank and LO$_2$ tank remain.

As Table 10.1, Table 10.2, Table 10.3 show, the LO$_2$ tank and the intertank are inherently more difficult to use than the LH$_2$ tank. The number and diversity of constituent components of the LO$_2$ and the intertank is larger than the LH$_2$ tank. Since the LO$_2$ tank and intertank are also smaller than the LH$_2$ tank, salvaging them represents a 'tight squeeze' operation.

Table 10.2. Intertank Materials

Element	Material	Condition
Thrust Panels	2219 Plate	T87
Skin/Stringer Panels		
Skins, Doublers	2024 Sheet	T81
Doublers	7075 Sheet	T6
Stringers, Rolled/Chem-milled	2024 Sheet	T81
Stringers, Extruded	2024 Extrusion	T8511
Buttstraps	2024 Sheet	T81
Attachment Flange	2024 Extrusion	T8511
Shims	6063 Extrusion	T6
Thrust Panel Longerons	7075 Extrusion	T73511
Ring Frames		
Chords	7075 Extrusion	T73511
Webs	7075 Sheet	T6 and T62
Stiffeners	7075 Extrusion	T73511
SRB Beam		
Chords	7075 Extrusion	T73511
Webs	7075 Sheet	T6
Stiffeners	7075	T73511
Bulkheads	7075 Sheet	T62
SRB Thrust Fittings	7050 Forging	T73

Table 10.3. LH$_2$ Tank Materials

Element	Material	Condition
Dome Sections		
Gores and Caps	2219 Plate	T87
Barrel Sections		
Skin Panel	2219 Plate	T87
Intermediate Ring Frames	2024 Extrusion	T8511
Longeron	2219 Forging	T6
Major Ring Frames		
Outer Chord	2219 Extrusion	T8511
Inner Chord	2024 Extrusion	T8511
Webs	2024 Sheet/2024 Plate	T81/T851
Fittings	2219 Forging/2219	Plate T6/T87
Stiffeners	2024 Extrusion	T8511
Frame Stabilizers	2219/2024 Extrusion	T81/T8511

10.2 Salvaging the LO$_2$ Tank

The LO$_2$ tank barrel section is physically and metallurgically similar to the barrel sections of the LH$_2$ tank. The LO$_2$ barrel section is composed of 2219 T87 Aluminum alloy just as the LH$_2$ barrel sections are. The LO$_2$ barrel section is 95.65 inches long. It is fabricated from four chemically milled and formed panels welded together. Skin thickness on two side panels are tailored in grid fashion to accommodate SRB thrust loads The other two panels are identical except for three thickened skin pads and weld tabs on one panel. These tabs support the cable tray and GO2 pressure line extending over the barrel. The barrel section skin is also tapered in a manner similar to the ogive gores.

Though eventual use of the LO$_2$ tank barrel section looks promising, there remain several problems. First, the thickness of the skin of the LO$_2$ barrel section is not uniform. Second, the characteristics of the SRB thrust load grid portions of the LO$_2$ barrel section are not known. Third, a portion of the barrel section, the part which contains three thickened skin pads and weld tabs is likely to be difficult to use.

DESCRIPTION

The LO₂ tank is a fusion-welded assembly of preformed, chem-milled gores and panels, and machined fittings and ring chords.

MANHOLE COVER

LO₂ AFT DOME

BARREL SECTION

"T" RING

FWD OGIVE SECTION

COVER PLATE

SLOSH BAFFLE

AFT OGIVE SECTION

NOSE CONE

LO₂ TANK STRUCTURE

MANHOLE

X_T 536.740

X_T 327.25

VORTEX BAFFLE

LANCE

SLOSH BAFFLE

LO₂ OUTLET

X_T 854 050

X_T 963.425

X_T 747.350

X_T 514.175

X_T 371.000

LO₂ TANK PROFILE
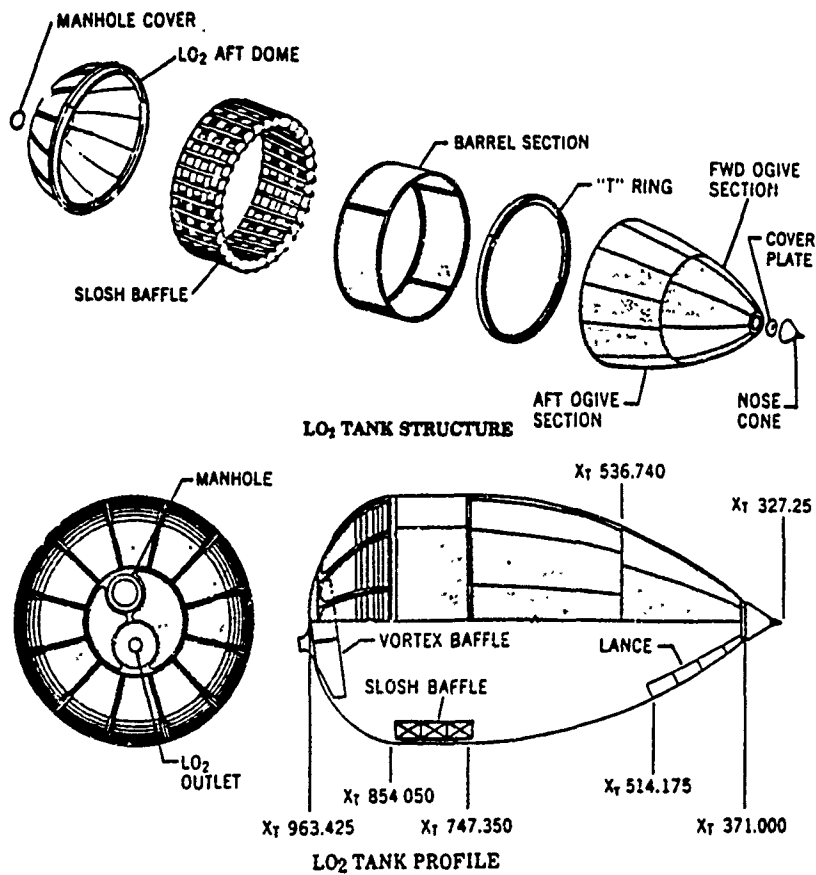
Figure 10.1. LO₂ Tank Structure

Fourth, the slosh baffle covers the barrel section and it may have to be removed.

Fortunately, the slosh baffle is not attached to the LO_2 barrel proper. Rather the slosh baffle is attached to a T-ring at the top of the barrel section and to the aft baffle support at the bottom of the barrel section. If the barrel section is salvaged from the exterior of the LO_2 tank, there will be no need to deal with the slosh baffle at all. The whole LO_2 section of the ET is fused welded together. The LO_2 barrel section can be cut away from the LO_2 tank from the exterior. To do this, SOFI must first be removed from the bolts joining the nose cone to the forward ogive. Then the 92 bolts in the forward ogive cover plate must be removed. Once the nose cone has been removed and stowed in the LH_2 tank, a ten foot section of scaffolding, brought by the space shuttle can be bolted into place. The rest of the scaffolding is compose of three additional sections, each of which is ten feet long. These are joined together by fasteners similar to those used in the Ease/Access experiment. This 40 foot 'truss' should be prestressed so that it has a tendency to press against the LO_2 tank. The truss should be equipped with roller wheels which make contact with the actual surface of the LO_2 tank. The base of the truss must have a joint that is free to rotate so that the truss can rotate rotate around the LO_2 tank. Lastly, an e-beam cutter must be placed on the truss/track so that it is free to ride on the track above the barrel section.

The LO_2 barrel section of the External Tank could add to the amount of available plate by approximately 709 square feet. The barrel can be cut up into 104 strips which are 10 inches wide by 95.65 inches long. The truss and cutter would take 3 EVA hours to be put into place. If the cutter cuts at the rate of 80 inches per minute, 5.0 EVA hours will be required to retrieve the cut pieces. Dismantling the LO_2 tank cutting operation would require 3 EVA hours. The total time for LO_2 salvage alone then, would be 11 EVA hours. The total amount of 2219 plate that would be salvaged for this operation would be 2203.8 lbs. The plate is readily usable as a structural material without further processing.
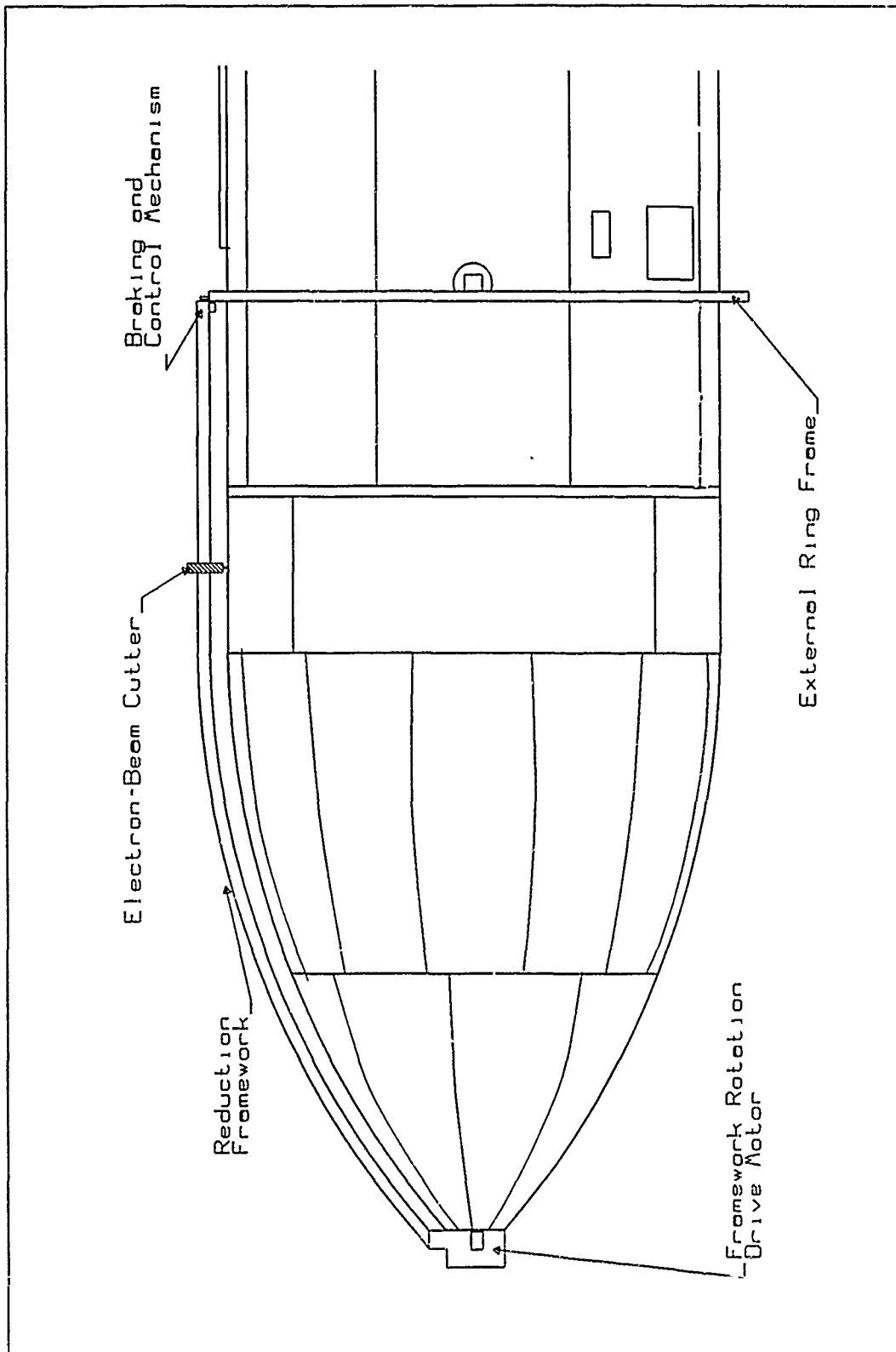
Figure 10.2. LO$_2$ Tank Salvage, Overall View

Since the barrel section is composed of four panels welded together, no additional I-beams will be produced.

10.3 Salvaging the Ogive Sections

If sufficient EVA time is available, it may be possible to salvage the forward and aft ogive sections of the lox tank. The forward ogive is composed of eight gore sections welded together while the aft ogive is compose of twelve gore sections welded together. Ogive salvaging is particularly EVA intensive. For this reason the forward and aft ogive can not be cost effectively cut into small pieces during salvage operations. It is estimated that sufficient EVA time exists to cut the ogive sections into 37 pieces. Since these pieces will be irregularly shaped, special consideration must be given as to how SOFI will be removed from them. One way SOFI can be removed without adversely impacting the EVA budget is to use an automated SOFI removal system. Using the same rail truss that the e-beam cutter rode to cut the LO_2 barrel, another e-beam device could move over the surface of the ogive sections, spraying a defocused electron beam. This defocused beam would remove the SOFI in 22 hours. This operation would produce a great deal of very fine SOFI debris. Estimates show, however, that this debris would deorbit on average in half a day. This ogive removal operation would require an additional 4.83 EVA hours over and above the LO_2 tank EVA already quoted. Ogive sections are not readily usable. They would have to be cut, machined or melted to be used.

The slosh baffle and vortex baffle appear to be so unique as to defy reuse. For this reason it is recommended that they be melted down and extruded or molded into other shapes or discarded.

Some interest has been expressed (28) in using ET dome covers as antennas, reflectors, mirrors, or coverings. These possibilities should be further investigated. It should be noted in passing, that these dome covers have a SOFI coating. Unless they can be used with this coating, some form of SOFI removal such as defocused

Table 10.4. LO$_2$ Tank Reduction

Products	Material	Weight (lbs)	Description
Plate	2219 Al	2203.8	104 pieces-95.65"x10"
Plate	2219 Al	4323.25	37 pieces-irregularly shaped
misc	2219 Al	190	Cover Plate & Fwd Fitting

electron beam will be needed.

10.4 Salvaging the Intertank

The next portion of the External Tank to be considered is the intertank. The intertank cylindrical structure consists of eight 45 degree mechanically joined panels (two thrust panels and six external stringer- stiffened skin panels) a main ring frame, four intermediate ring frames, and an SRB beam assembly with two forged thrust fittings.

It is difficult to see how the intertank of the External tank could be cost effectively disassembled. It is so cross hatched with stringers, longerons, ring frames, doublers, chords, and stiffeners that the work of r   oving them all in order to get at relatively small panel sections does not seem worthwhile. The intertank is the strongest part of the External Tank. Its best use would be as a strong back. If there are no buyers for this use the intertank should be discarded. Another option is that the intertank be melted all at once. Disassembling the intertank does not seem like a task which could be automated.

XI. PRODUCT APPLICATIONS

11.1 On-orbit Fabrication

With very little processing, useful structures could be built out of the I-beam and plate scavenged from the External Tank. The length and width of the secondary truss on the proposed Phase 2 Space Station Freedom (see Figure 11.1, (79)) are 673 and 344 feet respectively. The salvaged I-beams from a *single* External Tank would be sufficient to build 1526 of the required 2034 feet of truss.
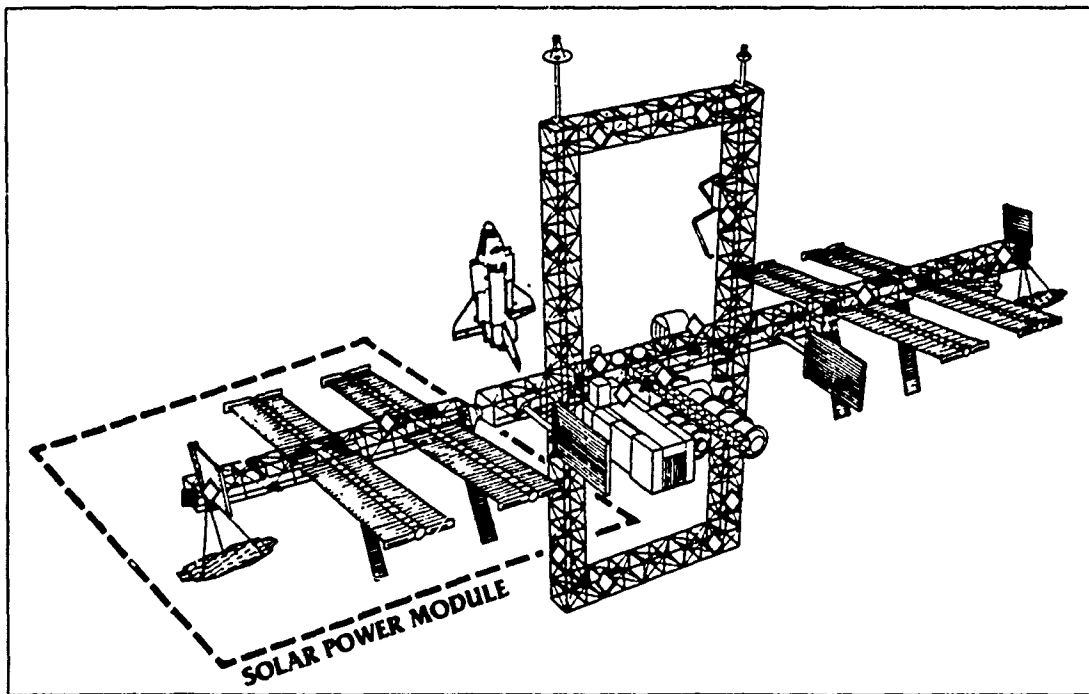
Figure 11.1. Space Station Freedom, Phase 2 Configuration

The space station truss is composed of boxes stacked atop one another. If this truss were built of I-beam scavenged from the ET, the sides of the truss could be constructed of pieces of I-beams. The design for Space Station Freedom requires diagonal reinforcements on each of the six faces of the individual boxes. If the cross sections of the boxes were 4.5 feet by 4.5 feet, four diagonals would be 19.3 feet

long and two would be 6.4 feet long. 267 pieces of 225 inch and 81 pieces of 163 inch I-beam would be required to complete a truss 1,526 feet long. If the diagonal members were composed of strips of plate 2 inches in width, 81 pieces of the 163 inch plate and 84 pieces of 225 inch plate would be required to complete the truss.

The products of an ET salvage operation can be used to build a truss for a demonstration model of a Solar Power Satellite (SPS). Many different configurations could be attempted. As an example, one could build a triangular beam structure which would be a model for the much larger structure suggested by SPS designer Peter Glaser (29). Using 228 pieces of 225 inch beam, one could build a truss 56.5 ft by 131.25 feet. The truss would be a rectangle composed of 32 triangles arranged in a 4 triangle by 8 triangle array. The triangles themselves require 96 pieces to complete. Joining eight triangles in a row requires 84 pieces to complete. Joining the 4 columns composed of eight triangles a piece requires 48 additional pieces.

11.2 Space Manufacturing

In his article on space manufacturing techniques (21), David R. Criswell points out that space production techniques should be modular. Each technique should be 'complete' by itself or in conjunction with a limited number of other techniques.

Initial technique development should draw on available Earth experience and space demonstrations should not be required. Three metal working techniques should be considered: casting, deformation, and joining.

Continuous sheet casting of aluminum is presently practiced on earth (18) and may prove adaptable to space. This method of metal forming requires that molten aluminum be forced into the roll bite of rolling machine. Continuous casting eliminates the need for reheating and multiple roll passes. Although continuous casting requires sophisticated machinery, the process takes up less space than a traditional aluminum mill. The continuous casting process could be built in a modular fash-
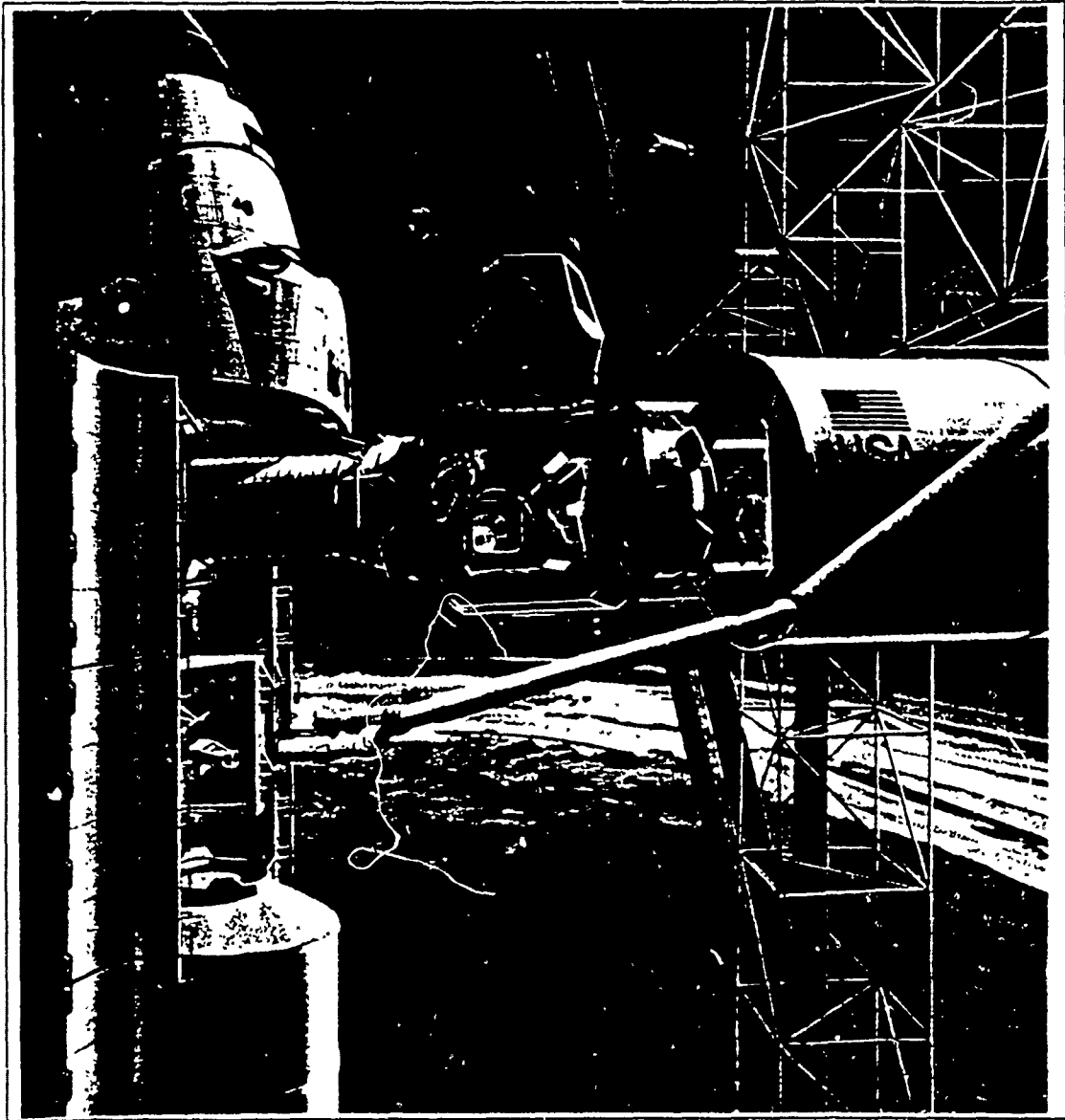
Figure 11.2. Rockwell Space Platform

ion. A solar furnace to melt the aluminum could be assembled first, then continuous casting machines could be added in a modular fashion as needed.

Many methods of metal transformation require a source of heat. The most convenient and reliable heat sources would be those brought from earth. Induction furnaces and even electron beam guns can generate heat of known quantities and qualities in convenient places and forms. As the need for greater sources of heat grows and as the competition for the use of electrical energy grows, the need for solar furnaces will grow. The first practical solar furnaces are likely to be adaptation on solar dynamic power designs. The reason for this is that although solar furnaces represent an old technology on earth, space adaptation of solar furnaces has lagged behind solar dynamic research. The basic concepts in solar dynamics and solar furnaces are the same, so it makes sense to adapt a solar dynamic design.

An existing solar dynamic design that would be reasonable to choose would be the Sunflower Collector (94). The Sunflower design has already been space hardened and the problems of packing the concentrator have already been solved. The main adaptations one might make is on the receiver. At present, the receiver is a sphere, 2.8 feet in diameter and it has a 1.2 foot opening. Since the salvage materials of the ASSET facility are much larger than the solar flux receiver, either the salvage materials will have to be cut or the receiver will have to be expanded. The solar concentrator is a collapsible parabolic form which can easily fit into the space shuttle payload pay. When fully deployed, the Sunflower Concentrator has an outer diameter of 32.2 ft and an inner diameter of 9.2 ft. The receiver temperature is $1450°F$. Since the melting point of aluminum is $1220°F$, this operating temperature will suffice.

Techniques such as injection molding, with molten aluminum as the working fluid should be considered. Pistons driven by electromotive motors could be used. Some casting technologies used on earth require expendable molds. Expendable molds would have to be produced on site in space or be brought up from earth.

Rolling metal via continuous casting has already been discussed. An alternate

11-4
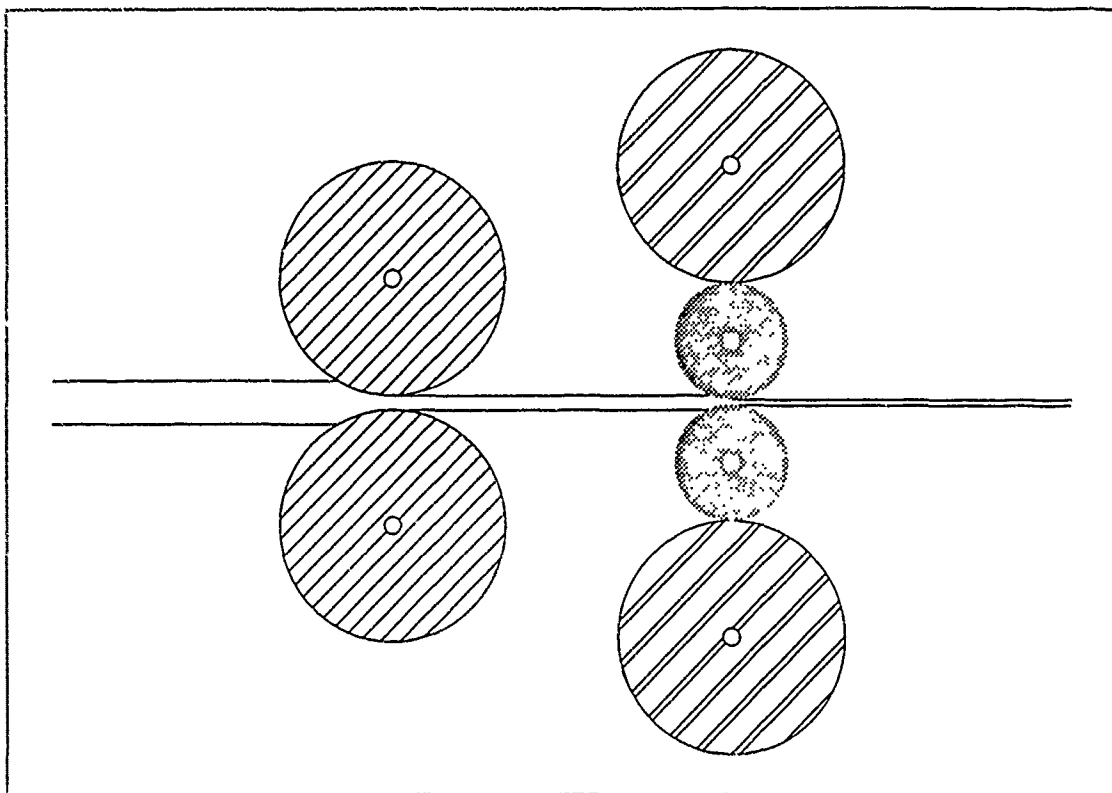
Figure 11.3. Rolling Mills

means of rolling metal would be to use 2 or 4 high reversible mills. The terms '2 high' and '4 high' refer to the number of rollers which sit atop one another in the rolling machine (see Figure 11.3). One of the most significant problems in the rolling of metals is the buckling or bending of the center of the sheet. Adding rollers to the traditional two roller design tends to lessen this effect.

The possibility of taking rolling technology into space was discussed with experts from aluminum manufacturing community (9). Recommendations from these discussions were that 2219 aluminum should probably be annealed at 775 deg Fahrenheit, and then allowed to cool at about 50 deg F/hour to 500 deg F. After this treatment the metal would be ready to roll with a two high mill. The mill rollers would be 14 inches wide and six inches in diameter. The goal would be to achieve 20% reduction per roll pass. About 8 passes would be required to reduce metal thickness

from .125 inches to .01 inches. A 40 horse power motor was recommended to run the machine even though this represents more power than the ASSET facility is likely to produce. Rolling machines can be run at less than their rated power, but throughput will be reduced. The ASSET facility manager would need to run the rolling machine at available power levels to determine throughp it. The mill would be reversible and the lengthening roll pieces would be coiled so that they would take up less space.

At this point the coiled material would be ready for the Grumman beam builder machine. The beam builder is composed of three identical machines arranged around a common axis (43). Each machine has its own coiled strip of material which is continuously formed into an open-V section as it passes through a seven-station rolling mill. Three sections emerge from one end of the machine parallel to each other, 1 meter apart, to form the longitudinal corner sections of a triangular beam. Preformed cross braces to link the section are supplied from cannisters attached to the machine, some at right angles to the sections, some inclined. These are induction welded to the longitudinal sections to form a rigid structure of the required length. Induction heating is used in the welding process because it produces good fusion welds.

One interesting way of deforming metal is called shot peening. Pieces to be worked are put into a mold and then struck by small solid pellets. The pellets deform the metal into the desired shape and the pellets can be reused. This idea might be workable in a small, confined area wherein the pellets can be recaptured and reused.

At the beginning of operations it seems likely that joints and fasteners would be specially designed and fabricated on earth for use in space. In the future it may be possible as part of molding or casting process, to manufacturing fittings and fasteners in space.

Whenever two pieces of clean, similar metal come into contact in a vacuum, cold welding can take place. The strength and resilency of such bonds does not

appear to have been studied extensively, so more research on the possible usefulness of cold welding need to be done in the future.

Another method to transform aluminum into to useful products is called the crucible melt extraction (CME) process (17). This process, developed by Batelle Columbus Labs, can be used to produce metal fibers. These fibers can be used as heat conductors or EMI shields and as components in composites. CME requires that a cold, spinning, metal wheel be brought into contact with molten metal. The process causes fibers to be thrown off by a centrifugal force. The dimensions of the fibers are determined by the the speed of the wheel, the temperature of the molten metal, and the depth of contact between the wheel and the melt.

11.3 Extended ASSET Facility

The ASSET facility could become a turnkey operation to perform casting, rolling, fabrication and assembly for space structures. Fabrication of structures, using salvaged products from the ASSET facility, is a topic worthy of an entire thesis project. The primary focus of this study was limited to ET reduction and product storage due to time constraints.

An obvious use for the extended ASSET facility is in the construction of a space facility. The 'birdcage' could be used as a construction platform from which to assemble various space structures (such as the SSF truss). By using an EPS module similar to those planned for the space station, the ASSET facility can serve as the initial power source at the start of construction. ASSET can also provide a docking facility to the shuttle until a permanent docking facility can be assembled.

XII. CONCLUSIONS & RECOMMENDATIONS

12.1 Conclusions

1. **It is clear that the external tank can be reduced to readily usable construction material.**

   - The tool design is a simple, low risk development effort. The electron beam cutters, boost/deboost modules, and photovoltaic arrays are essentially off-the-shelf purchases. There are no foreseen technical hurdles.

   - The 13,045 lbs of salvaged products (from a single LH_2 tank) are readily usable.

     (a) 6,125.8 linear feet (3,123 lbs) of I-beams.

     (b) 4,859.5 ft^2 (9,082 lbs) of plate.

     (c) A single 76.33 ft centerline track (276 lbs).

     (d) Miscellaneous other hardware (564 lbs)

2. **The external tank can be reduced in a cost effective manner.**

   - Automated scenarios are more competitive than man-tended scenarios. This trend will continue if the tool design is allowed to remain simple. The temptation to push the state of the art in the tool design should be resisted.

   - It is clear that the lower efficiency solar cell based electrical power system is more cost competitive than the higher efficiency system. The large DDT&E expenses paid early in the program cannot be offset by reduced fuel resupply costs recovered within a 10 year operational life.

   - It is clear that Scenario 1, with the less efficient array, is the most cost competitive method of operation. Scenario 3-1 is a close second and may

warrant consideration. The principal reason Scenario 3-1 is not more competitive (which may be somewhat of a surprise due to the increased revenue stream realized by the sale of power) is due to the risks associated with rendezvous at SSF. The operations costs have been skewed to the high end in the cost model, which is a conservative approach.

3. **LO_2 barrel salvage appears to be well worth the effort.** Table 9.10 and Table 9.11 show that when LO_2 barrel salvage is included, one becomes 90% confident that the salvage operation is cheaper than the alternative of launching similar products from earth.

4. **Under the assumption of four LH_2 tanks salvaged per year, ASSET could provide the equivalent of a dedicated STS launch on a yearly basis.**

   - This effectively increases the NASA launch rate, with minimal impact on current launch schedules, and can be done profitably over a 10 year operational life.

   - The facility is aptly named.

12.2 Suggested Improvements

12.2.1 SLAM Simulation. The current SLAM models are largely deterministic in nature, although some probabilistic modelling was incorporated in Scenario 2. Although the current models served their intended purpose, the activity durations (work or tool rates) could be modified to update the model for a complete probabilistic model.

SLAM models could also be developed for any phase of LO_2 tank reduction. Care should be exercised so that modular activities can be desegregated. This would allow LO_2 barrel salvage to be considered separate from LO_2 ogive salvage.

12.2.2 Electrical Power Subsystem (EPS). The current EPS designs are essentially derivatives of the SSF EPS. At the time our design was developed, the SSF EPS incorporated both AC and DC interfaces to the user. The latest SSF EPS has been redesigned (largely motivated by weight savings) to provide DC distribution only (67). Unfortunately, the ASSET design team did not become aware of the changes until the mid-October time frame.

The ASSET EPS should be redesigned to reflect the latest changes in the SSF EPS. This would also help the ASSET facility from a weight standpoint, but the current tool set (which incorporates AC motors) would have to be redesigned.

12.2.3 Orbits. The possibility of having different rates of orbital precession between SSF and ASSET requires further investigation. If, in fact, this problem is verified, the impacts for fuel resupply (and the associated costs) would need to be incorporated.

The assumption that the boost/deboost module will adequately compensate for attitude changes could also warrant further investigation. This area would need to be incorporated with a hard look at how the actual rendezvous with subsequent tanks (even with the presence of a cargo transfer vehicle) would be effected.

The next iteration should modify the orbit calculations to quantify the savings realized as a result of changed assumptions. The current model assumes the solar arrays always present maximum drag to the velocity vector. The cost numbers generated for fuel resupply costs are, therefore, extremely conservative.

12.2.4 Product Applications. This area could clearly drive an entire thesis project. The topic of how this construction material could impact the design of future space structures was discussed at some length at CDR (92). Our sponsor suggested that the salvaged products from this study be used as a given for a future design effort. The University of Houston has an architecture department which

incorporates a specialty sequence for space architecture and they were identified as the probable candidate for the follow-on study. Clearly, the structural rigidity which could be accomplished by utilizing ASSET byproducts offers many new interesting applications which previously could not have been considered due to the ruinous cost of delivering such structures to LEO.

12.2.5 Communications. This area could probably stand another iteration to firm up several factors associated with weights, power consumption, and data rates. The actual hardware used for masts and antennas could also be firmed up and more definitive cost numbers could then be generated.

12.2.6 Cost Model. The cost model itself is probably more than adequate at this point. However, the input parameters to the cost model could probably be updated and cost numbers with higher confidence levels could be generated. It would be nice if a more recent version of the cost data base for NASA CER's could be obtained. Current costs are projected in 1978 dollars and then updated to 1990 dollars.

12.2.7 Tools. The tools could be iterated another time to incorporate the changes forced by an EPS redesign to a DC distribution system. The same iteration could also incorporate another level of controls, vibration effects, and sensoring to improve the overall tool design.

12.2.8 Thermal. The thermal model could be expanded to a finite element model. The outputs from such an expanded model should probably be cross-checked against a TRASYS run at Martin Marietta.

Appendix A. *TOOLS*

A.1 *Motors*

Specifications for space-rated motors are not readily available for generic design
applications, so an aircraft rated motor has been selected. This selection is used for
rough size, weight, and, power calculations. The primary difference would be cooling
(or heating) and lubrication.

Table A.1. Motor Specifications

Motor Selection	Datron Inc. FEMCO 5068D100
Output Power	.05 hp
Angular Velocity	14 rpm
Voltage	115 VAC
Current	.98 amps
Frequency	400 hz
Input Power	112.7 watts
Torque	180 in-lb
Efficiency	13.5%
Heat Generated	75.5 watts
Max. Output Power	.058 hp (@ 12.3 rpm)
Max. Ang. Velocity	16 rpm (no load)
Max. Current	1.3 amps (@ stall)
Max. Input Power	149.5 watts (@ stall)
Max. Torque	470 in-lb (@ stall)
Max. Efficiency	17% (@ 12.5 rpm)
Max. Heat Generated	149.5 watts (@ stall)
Weight	4.75 lbs
Length	5.05 in
Diameter	3.00 in
Shaft Length	1.660 in

Using the nominal motor specifications, calculations for tool power are as fol-
lows:

A.1.1 Radial Motor Calculations. The angular velocity of the centerline trolley arm (ω_l) is 4π radians per minute (2 rpm) with an 11 in. gear radius (r_l). The radius of the drive motor gear (r_m) is given by:

$$r_m = \frac{\omega_l r_l}{\omega_m} = \frac{(2 \ rpm)(11 \ in)}{(14 \ rpm)} = 1.5714 \ in \qquad (A.1)$$

The load force (F_l) available at the 11 inch gear is given by (assuming a 95% gear efficiency):

$$F_l = \frac{\omega_m T_m}{\omega_l r_l} = \frac{(14)(180 \ in\text{-}lb)}{(2)(11 \ in)}(.95) = 108.8 \ lbs \qquad (A.2)$$

The torque required (T_r) to accelerate the arm with a plate section to 2 rpm in 1 sec. $(.2094 \ rad/sec^2)$ is: The required force (R_r) is then given by:

$$
\begin{aligned}
T_i &= & \omega_i m_i r_i^2 & \\
T_{arm} &= (0.5905 \ slugs)(0.2094 \ rad/sec^2)(48 \ in)^2 &= 23.92 \ in\text{-}lbs \\
T_{extension} &= (0.3036 \ slugs)(0.2094 \ rad/sec^2)(63 \ in)^2 &= 21.03 \ in\text{-}lbs \\
T_{plate} &= (1.195 \ slugs)(0.2094 \ rad/sec^2)(96 \ in)^2 &= 192.18 \ in\text{-}lbs \\
T_{effector} &= (.3106 \ slugs)(0.2094 \ rad/sec^2)(96 \ in)^2 &= \underline{49.95 \ in\text{-}lbs} \\
& T_r \ (total) &= 287.14 \ in\text{-}lbs
\end{aligned}
$$

$$R_r = \frac{T_r}{r_l} = \frac{287.14 in\text{-}lbs}{11 in} = 26.10 lbs \qquad (A.3)$$

Since the available load force is nearly four times the required force. we can conclude that a motor of this size and weight could easily operate the radial motion of the trolley/arm. The controls necessary to ensure accurate acceleration have not been addressed, but need to be developed before implementation.

A.1.2 Plate Stacker Drive Motor Calculations. The ET is subject to a worst case acceleration of .98 ft/sec² due to the 2000 pound thrusters during which the plate stacker must be able to restrain the 9082 lbs (282.05 slugs) of total aluminum

plate. The resulting restraint force (F_r) is (.98 ft/sec^2 X 282.05 $slugs$) 276.41 lbs. The restraint force is provided by springs pushing normal to the plates. The spring force (normal) is given by:

$$F_s = \frac{F_r}{f} = \frac{276.41 \ lbs}{1.4} = 197.4 \ lbs \qquad \text{(A.4)}$$

Where the coefficient of dry sliding friction (f) for aluminum on aluminum is 1.40.

The plates must stack at a rate equal to the electron beam cutting rate (40 in/min). Assuming a 1 inch drive wheel radius (r_d), the drive wheel angular velocity (ω_d) is given by:

$$\omega_d = \frac{V}{2\pi r_d} = \frac{40 \ in/min}{2\pi \ (1 \ in)} = 6.37 \ rads/min \qquad \text{(A.5)}$$

Assuming a 95% gear efficiency, the force exerted by the drive wheels is:

$$F = \frac{\omega_m T_m}{\omega_d r_d} = \frac{(14)(180 \ in\text{-} \ lbs)}{(6.37)(1 \ in)}(0.95) = 376 \ lbs \qquad \text{(A.6)}$$

Since the available force is nearly two times the required force we can conclude that a motor of this size and weight should be more than adequate to drive the plate stacker.

A.2   Centerline Track Deflections

Arm Bending Due to Angular Acceleration:

$$y = \frac{\alpha}{3EI_a}\left[2m_a\left(\frac{L_a}{2}\right)^4 + (m_e + m_p)L_a^4\right] \qquad \text{(A.7)}$$

Plate End Deflection Due to Longitudinal Acceleration:

$$pd = \frac{AL_p}{6EI_a}\left[2m_a\left(\frac{L_a}{2}\right)^2 + (m_e + m_p)L_a^2\right] \qquad \text{(A.8)}$$

Table A.2. Deflection Calculation Variables

ω = *angular velocity*

α = *angular acceleration*

A = *longitudinal acceleration*

E = *modulus of elasticity*

G = *modulus of rigidity*

t = *material thickness*

S_t = *effective circumference*

L_t = *track length*

a = *effective area*

I_t = *moment of inertia, track*

m_t = *mass of track*

L_a = *length of arm*

I_a = *moment of inertia, arm*

m_a = *mass of arm*

m_e = *mass of end effector*

L_p = *length of plate*

m_p = *mass of plate section*

y = *deflection of the arm due to arm bending*

pd = *deflection at the end of the plate due to longitudinal acceleration*

tw = *deflection of the arm due to track twist*

b = *deflection of the arm due to track bending*

Track Twist:

$$tw = \frac{\alpha S_t L_t L_a}{16a^2 Gt} \left[m_a \left(\frac{L_a}{2}\right)^2 + (m_e + m_p)L_a^2 \right] \qquad (A.9)$$

Track Bending:

$$b = \frac{\omega^2 L_t^3}{48EI_t} \left[m_a \left(\frac{L_a}{2}\right) + (m_e + m_p)L_a \right] \qquad (A.10)$$

Table A.3 shows the results of these calculations in a spreadsheet format. The results demonstrate the small amount of deflection at the end of the arm. In all cases the arm is moved only in its retracted position (8 ft). The deflections relate directly to the amplitude of the oscillations that would occur if the arm were left totally undamped. The two primary areas of concern are feeding the I-beam/plate combinations into the SOFI workstation and placing the primary cutter onto the stringers. In both cases the engagement tolerances are more than enough to accept the worst case summation of these deflections.

The combination of radial arm bending and track twisting, due to the angular acceleration of the trolley system, create deflections in the radial direction. Track bending is a result of central directed forces on the track due to the constant angular velocity of trolley system. Track bending creates deflections in the lateral direction. Plate deflection is a result of the longitudinal acceleration of the trolley system, which creates deflections in both the longitudinal and lateral directions. The length of each piece determines the total amount of lateral deflection. All calculations assume that the arm attaches to the object at its center of gravity.

A.3 Cutter Selection

Selecting a cutting technology capable of cutting aluminum in a space environment was a fundamental step in developing feasible ET reduction scenarios. A

Table A.3. Centerline Track Calculations

Angular Velocity (rad/sec) 4 Pi per minute	0.2094
Acceleration Time (sec)	1.0000
Angular Acceleration (rads/sec^2)	0.2094
Longitudinal Velocity (ft/sec)	1.0000
Acceleration Time (sec)	1.0000
Longitudinal Acceleration (ft/sec^2)	1.0000
Material: 2219-T87	
Rigidity (G) (psi)	4.00E+06
Elasticity (E) (psi)	1.06E+07
Density (slugs/in^3)	3.20E-03
Track Thickness (in)	0.1250
Track Height (in)	6.0000
Effective Circumference (S) (in)	23.5000
Track Length (in)	912.0000
Effective Area (A) (in^2)	34.5156
Moment of Inertia (I) (in^4)	16.9059
Mass (slugs)	8.5695
Arm Height (in)	4.0000
Arm Length (in) (8.0 ft)	96.0000
Moment of Inertia (I) (in^4)	4.8538
Mass (slugs)	0.5950
Actuator Mass (slugs)	0.3106

Number of Slabs	1	3	5	10	Cutter
Mass (slugs)	1.1954	3.5862	5.977	11.954	0.8981
Slab Length (in)	225.95	225.95	225.95	225.95	
Deflection (in)					
Arm Bending	0.0152	0.0381	0.0611	0.1185	0.0123
Track Twist	0.0575	0.1405	0.2235	0.4310	0.0471
Total Radial	0.0726	0.1786	0.2846	0.5495	0.0595
Track Bending	0.0558	0.1298	0.2038	0.3887	0.0466
Plate Deflection	0.0122	0.0283	0.0444	0.0847	

wide variety of metal cutting technologies were investigated to determine the best type of cutter for our application. The primary factors used in selecting a cutter were power required and maintainability of the cutter. Our goal was to minimize the power required for the cutter while maximizing its maintainability. Initially, cutter power was limited to a maximum of 10 kW. The maintainability goal was for the facility to operate for one complete ET reduction before any scheduled maintenance of the cutter was required.

A.3.1 Cutting Technologies. Several types of cutting technologies were eliminated after an initial technology review. Saw or blade type cutters were eliminated for several reasons. First, these type of cutters require more frequent routine service to replace the blades. A second problem associated with this type of cutting device is the requirement to contain the metal filings produced in making a cut. This debris is be a hazard to any type of optical equipment on the facility, as well as a hazard to any other vehicle in a similar orbit, in particular the orbiter. Astronaut safety was also a consideration; this type of cutter is more likely to leave sharp edges on the metal products than other cutting methods. Since only plate is cut by the secondary cutter, a rotary shear type cutter is feasible. A shear cutter is inexpensive and simple in design, but its wearout rate would have to be quantified; a minimum of one ET reduction per blade is desired. Oxygen - fuel type cutters are not effective for cutting non - ferrous metals and, therefore would not be feasible for ET reduction since it is constructed almost exclusively from aluminum(11:54). Plasma Arc Cutting (PAC) was also researched. PAC is attractive because it is less expensive and less exacting a process than electron beam or laser beam cutting. It also can cut at very high speeds(42:41). The primary drawback for PAC is the power required; in order to cut 0.125 inches of aluminum plate using PAC, more than 30 kW of power is needed. This would make PAC power prohibitive for our application. A second problem associated with PAC, is that these cutters require a supply of plasma gas. In the case of aluminum plate, 110 cubic feet of nitrogen is needed per hour of cut. The cutting

A-7

torch also requires active cooling. Typically, for cutting aluminum plate, 0.43 gallons of water is required per minute of cut (58:916-917). Supplying the plasma gas and coolant on a continued basis is a logistic problem we want to avoid.

A.3.2 Cutter Capabilities. The choice of cutter technologies was eventually narrowed down to electron beam (EB) and laser beam (LB) cutters. These high energy density type cutters have some common traits that make their use advantageous. Both EB and LB cutters produce a very localized heat affected zone. This means the properties of the metal are essentially unchanged, except in the area very close to the cut. The thermal distortion of the metal is also minimized. Electron beam and LB cutters also have a high depth to width ratio which translates to a capability to cut very deep while maintaining a narrow cut in the metal. The capability to cut at very high speeds is also a benefit(74:26).

A.3.3 Cutter Comparison. Although EB and LB cutters have some common characteristics, there are fundamental differences. Electron beam cutters require high operating voltages (greater than 30 kV), while LB cutters need low operating voltages, (less than 30 kV). The EB cutter is a direct energy conversion type device with an efficiency of 65 percent, it is therefore more efficient than a LB cutter. One problem with using an EB cutter is that it produces x-rays when it strikes the workpiece, therefore an x-ray shield is required if personnel are to work nearby. Laser beams have a similar problem in that they can be reflected. This can be eliminated by using a simple opaque shield. More accurate beam focus control is available with the EB cutter. This is the most important factor in assuring quality control over the width and depth of the cut. Since the EB is focused using a magnetic coil which can be adjusted electrically it can be adjusted more accurately than the LB, which is focused using a conventional optical type lens. An EB type cutter is more reliable than a LB device. The only consumable item on the EB cutter is the gun filament, which will last for several hundred hours of cutting in a total vacuum. A LB cutter

requires regular cleaning of the beam exit window and the optical components. This is important because the LB efficiency is greatly reduced by smoke, dust, and vapor which will be present in our application. These will foul the LB cutter optical components, reducing its efficiency. The electron beam cutter is not significantly affected by this debris(74:26-29). Comparing electron beam cutters with laser beam cutters, EB cutters are the best choice for our use.

Appendix B. *EXTERNAL TANK REDUCTION MODEL*

B.1 Purpose

The purpose of our reduction model is to simulate the reduction of the liquid hydrogen (LH_2) tank for each scenario in order to:

- Quantify the power requirements of the reduction facility.

- Develop reduction timelines for one tank.

B.2 General

The ET consists of an LH_2, intertank, and LO_2 tank. Our ET reduction model portrays only the reduction of the LH_2 tank. The model uses the SLAM II simulation language (75) with FORTRAN subroutines to describe the movement of the tools and the movement and storage of the I-beam and plate product. The reduction model allows for variable tool work rates and tool power consumption. The two primary outputs of the model are: the peak power requirements of the total ASSET facility and the total time required to reduce the ET to a 'bird cage' configuration. Peak power requirements are used as input into the design of the facility's power system. They are the primary design variables used to determine the size of the solar arrays, which in turn has a direct impact on the orbital model of the facility. This is due to the significant drag associated with the solar arrays. Reduction timelines are used as input to the orbital model and affect the initial facility altitude. Additional outputs from the reduction model include: peak and mean power requirements for each tool and tool utilization rates.

B.3 Assumptions

The reduction model assumes, for both scenario one (automated reduction) and Scenario 2 (manned reduction), that the initial setup of the ASSET facility has

been accomplished by EVA. This includes removal of the intermediate ring frames, installation of all tools, setup and test of all monitoring, control, and communication equipment, and installation of the facility power system. The facility is fully operational at the start of the simulation. The reduction model also assumes that the LH_2 tank is reduced in one continuous operation; reduction takes place during both daylight and night time operations, with no change in work rates. This implies that there are no equipment breakdowns. The facility power system is designed to provide a steady state power during both day and night. The simulation does not account for the required sixteen hour breaks taken by the astronauts between each EVA for Scenario 2. Deterministic work rates were used to describe all machine driven activities. Human activities were described as normally distributed random variables.

B.4 Liquid Hydrogen Tank Layout

It is important to be familiar with the general layout of the LH_2 tank in order understand the interaction of the tools used in reducing the tank and how they were portrayed by the reduction model. The liquid hydrogen tank consists of four barrel sections. Each barrel section consists of 96 stringers and plates, with the exception of the aft barrel section, which has 90 stringers and 88 plates. The remaining stringer/plate sections in the aft barrel are replaced by two longerons located at the orbiter attach points. They provide the necessary structural support to the tank. Stringers are centered 10.832 inches apart with 9.582 inches of plate between each stringer. Figure B.1 shows the nominal dimensions for a typical skin panel with stringers and plate. The geometry of the LH_2 tank makes it the best possible ET component for reduction. The tank is conveniently indexed radially by the stringers and longitudinally by the five major ring frames. The stringers provide a feasible means of longitudinal transport for a cutting device between the major ring frames. This facilitates an automated cutting operation.
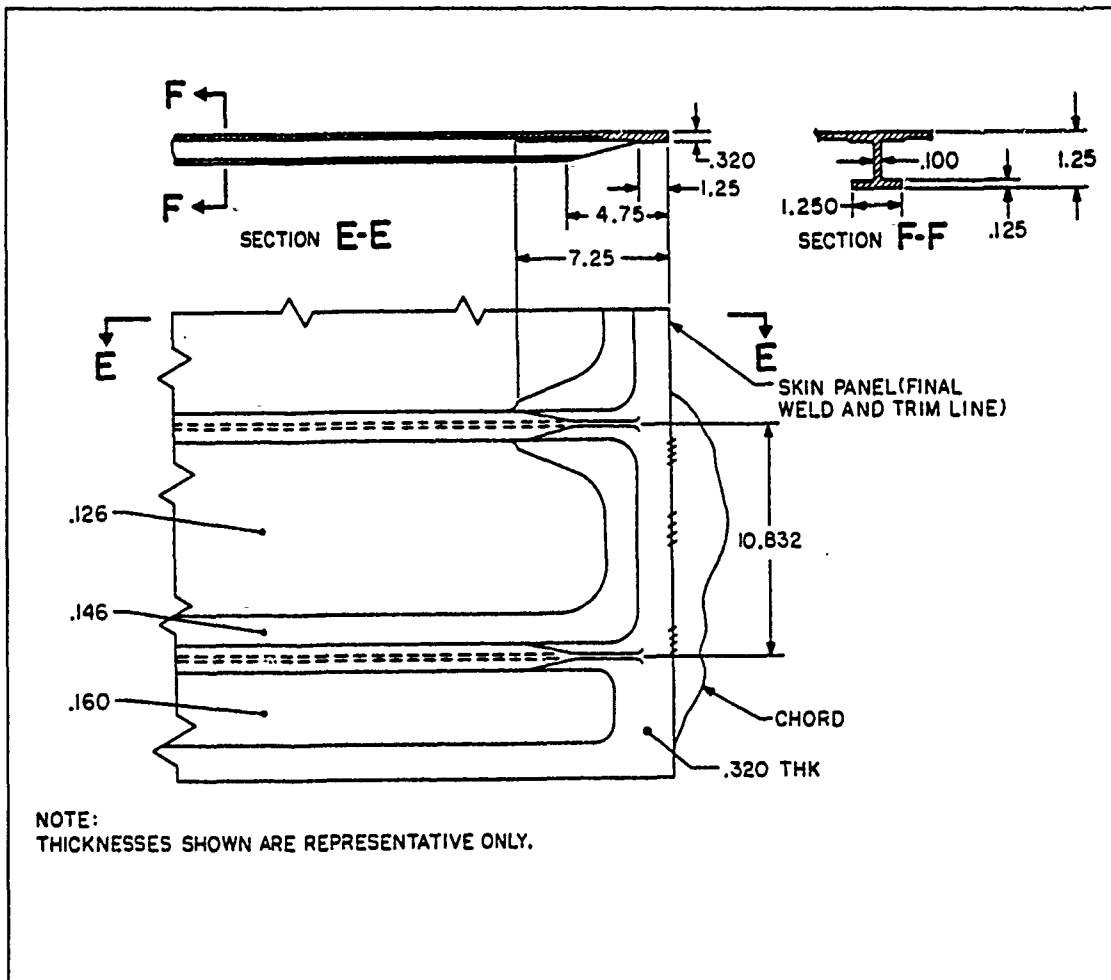
Figure B.1. Skin Panel Geometry

B.5 Cutter Transport

We designed a cutter transport mechanism to take advantage of the favorable layout of the LH_2 tank. For both scenarios, the primary cutting device is an electron beam cutter (EBC). The EBC is mounted on a mobile platform that rides on two stringers while cutting off to one side of the platform. The platform moves the cutter between major ring frames while making longitudinal cuts in the barrel section. To make radial cuts, the platform remains stationary and the cutter itself moves. The cutter platform cannot traverse the longerons in the aft barrel section. This requires that the cutter be capable of cutting on either side of the platform. This is accomplished by rotating the cutter 180 degrees. The platform cannot traverse closer than 4.75 inches on either side of the major ring frames. This is a result of the geometry of the stringers depicted by Figure B.1; stringers taper off adjacent to the major ring frames and the skin panel thickens. The cutter is designed to leave 7.25 inches of skin panel (plate and stringer) intact on either side of each major ring frame. This keeps the resulting plate at a nominal thickness of 0.126 inches.

B.6 Cut Sequence

The cutter and platform are automated to make two types of cuts, c - cuts and box - cuts. A c - cut is a radial cut through one stringer and plate combination, followed by a longitudinal cut the length of the barrel section, finished by a radial cut through one stringer and plate combination. The cut ends at the opposite end of the barrel section it began. Figure B.2 depicts a c - cut; the path of the cutter is labeled A, B, and C. A box-cut is a c-cut followed by a longitudinal cut the length of the barrel section. The cut ends at the point it began. The box - cut is also shown in Figure B.2; the path of the cutter is labeled A, B, C, D. While making radial cuts, the cutter platform remains stationary and the cutter moves. Longitudinal cuts are made by moving the cutter platform with the cutter stationary. The reason a combination stringer/plate section is cut by each pass of the cutter, rather than
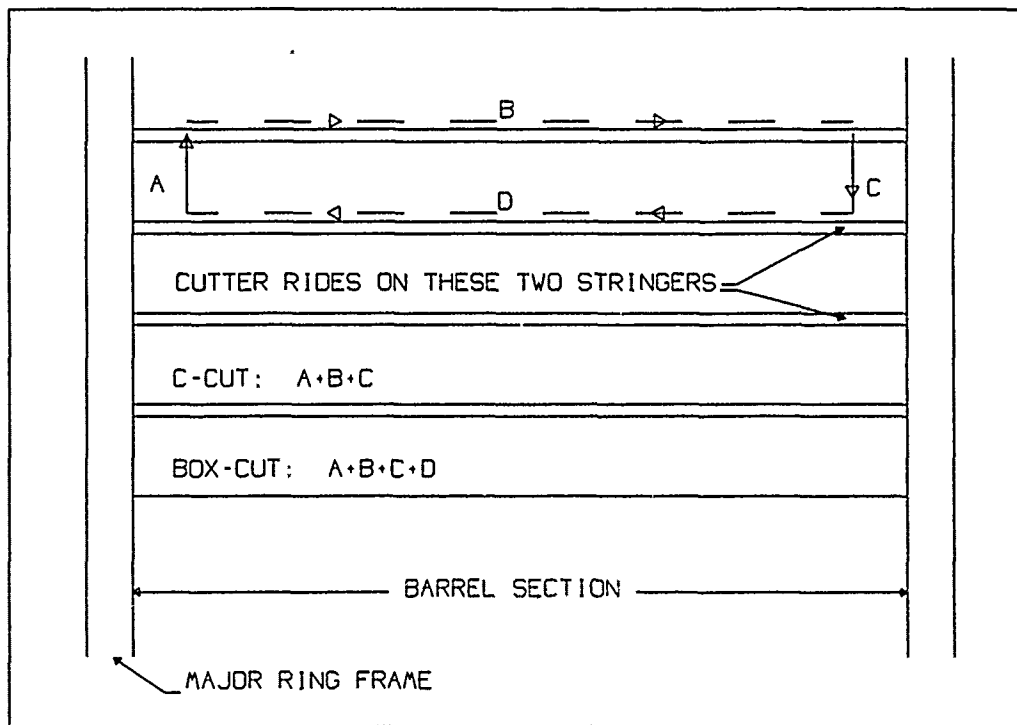
Figure B.2. General Cutting Sequence

individual plates and stringers, is to facilitate handling of the product. Plate sections alone would be difficult to handle, especially the first piece removed from each barrel section. With an I - beam attached to the plate it is easier for both astronauts and machines to handle.

B.7 Barrel Section Reduction - Scenario 1

In Scenario 1, each barrel section is reduced one at a time, working from the aft barrel forward. Each barrel section is reduced in three stages. Figure B.3 depicts the cutting sequence for the aft barrel. First, a series of seventeen c-cuts, followed by a box - cut, is made. This is shown as 1. After each cut, the cutter is moved one stringer clockwise. Once the first series of cuts is completed, the cutter is moved and a second set of thirty two cuts is made, thirty one c-cuts and a box-cut; this is shown as 2. The cutter is moved clockwise one stringer after each cut. Following the second set of cuts, the cutter is rotated 180 degrees and moved to begin the third set

of cuts. This is depicted as 3 in Figure B.3. The final series of cuts consists of thirty c-cuts and one box-cut. Once again, the cutter is moved one stringer after each cut, this time counter clockwise. After the third series of cuts has been completed, the cutter is moved to the next barrel section and the process continues. The second, third, and fourth barrel sections are reduced in a similar manner. Figure B.4 shows the sequence of cuts for the forward barrel sections. The first series of cuts consists of thirty seven cuts made with the cutter moving clockwise. The second and third set of cuts consist of nineteen and thirty three cuts respectively; the cutter moves counter clockwise for these.

B.8   Scenario 1 Reduction Model

SLAM II is a simulation language that allows a system to be represented as a stream of entities which flow through a network of nodes and activities(75:97). An activity represents the path an entity follows as it travels through the network from one node to another. An entity may require a particular resource in order to accomplish a specific activity. SLAM allows for these resources to be modeled also. In the Scenario 1 reduction model, three items are modeled as entities; the cutter, the transport arm, and the stringer/plate pieces. Three items are also modeled as resources; the transport arm, the stringer/plate pieces, and power. Each of these will be discussed separately.

B.8.1   Cutter.   The primary cutter is modeled as an entity. The cutter's initial position is at the aft end of the aft barrel section. At the start of the simulation, the cutter begins its initial c - cut. The general sequence of activities for the cutter is:

1. An initial c - cut is made.

2. The cutter is moved to the next stringer by the transport arm.
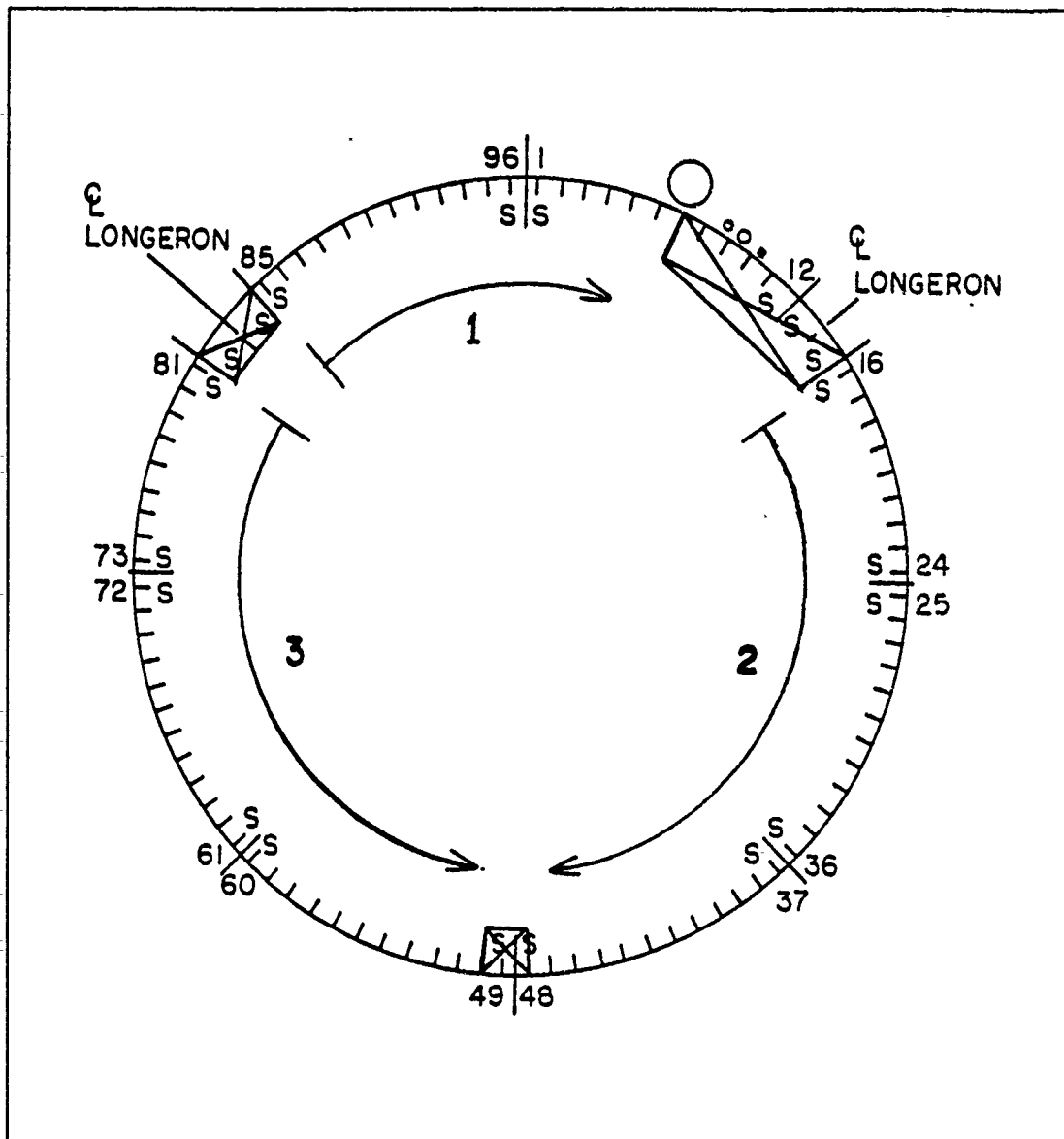
Figure B.3. Aft Barrel Section - Scenario 1
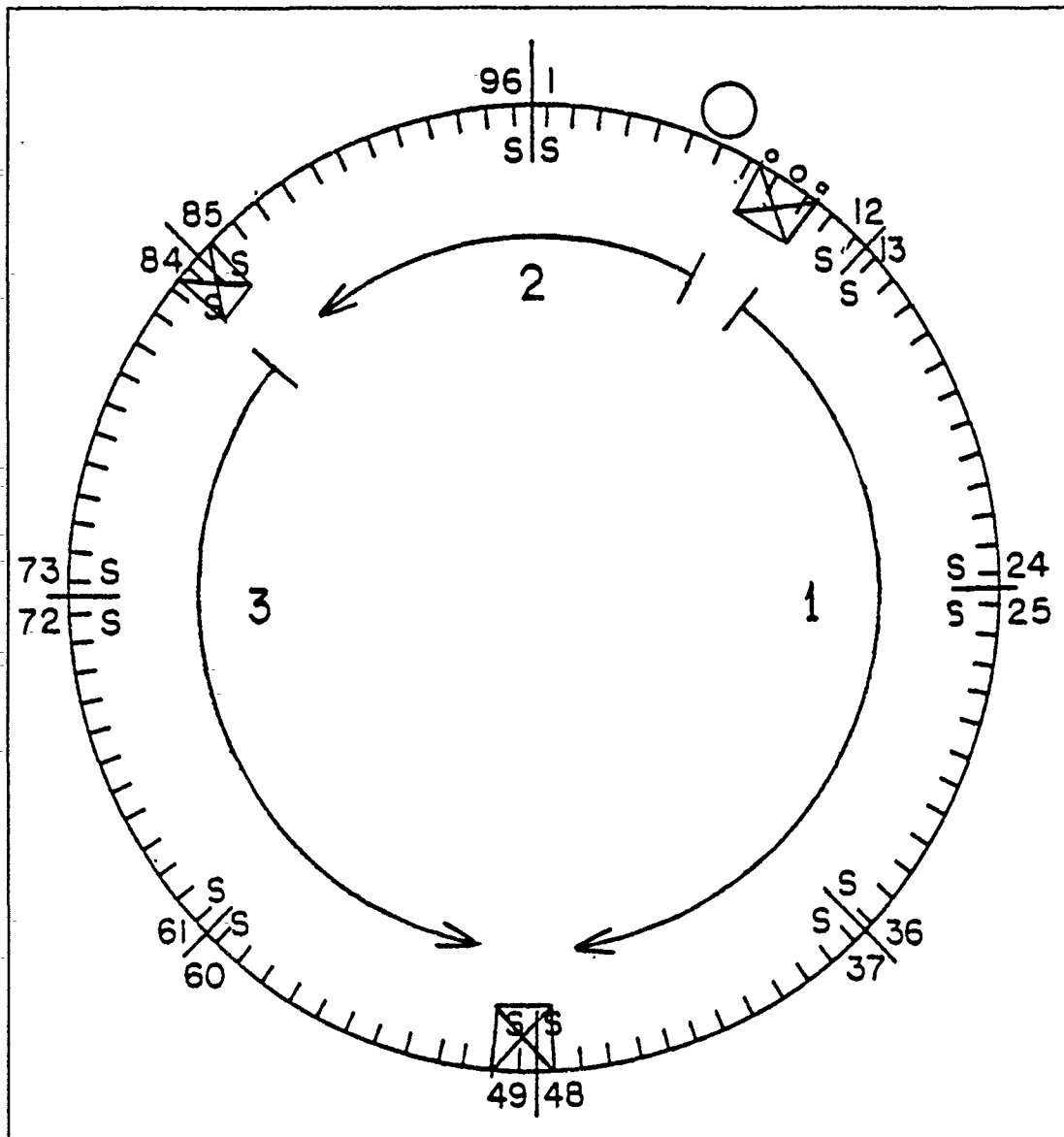
Figure B.4. Forward Barrel Section - Scenario 1

3. Subsequent c - cuts are made and the cutter is moved by the transport arm each time.

4. A box c - cut is made to finish a series of cuts.

5. The cutter is moved by the transport arm to the next section of cuts and continues as above.

6. Once an entire barrel section is reduced, the cutter is moved by the arm to the next barrel section and the process continues as above.

B.8.2 Transport Arm. The transport arm is modeled as an entity and as a resource. The arm's initial position is at the forward end of the aft barrel. The transport arm begins moving at the end of the cutter's initial c - cut; no stringer/plate pieces have been created. The general sequence of activitie; for the transport arm is:

1. The transport arm moves the cutter one stringer.

2. The arm moves to the center of the barrel section to grab the stringer/plate piece.

3. Once the piece has been cut free, the arm transports the stringer/plate piece to the SOFI work station.

4. The transport arm returns to the cutter and the process continues as above.

5. The cutter makes a box-cut to end a series of cuts; two stringer/plate pieces are produced. At the end of the c-cut portion of the box-cut, the arm grabs and transports the first stringer/plate piece to the SOFI work station.

6. The transport arm returns to the center of the barrel section and grabs the second stringer/plate piece.

7. When it is cut free, the second piece is transported to the SOFI work station.

8. The arm returns to the cutter and moves it to the next section of cuts.

9. Once an entire barrel section is reduced, the transport arm moves the cutter to the next barrel section and reduction continues as above.

The transport arm is a resource for the cutter and for the stringer/plate pieces. Both compete for its use. The pieces use the arm to move them to the SOFI work station. They have priority for the use of the arm. The rationale for this is that unless the arm grabs them, the pieces will float free once they are cut from the barrel section. The reduction model requires that transport arm grasp each stringer/plate piece before it is cut free. Following each cut, the cutter must wait for the arm to return from the SOFI work station before it can be moved to its next cut.

B.8.3 Stringer and Plate Pieces. The stringer/plate pieces are modeled as entities and as resources. The first piece is created when the cutter makes its second c - cut. Another piece is created each time the cutter makes a subsequent c - cut in that series of cuts. A box - cut creates two pieces. The general sequence of activities for the stringer/plate pieces is:

1. The piece is transported to the SOFI work station by the arm.

2. SOFI is stripped from the piece.

3. The stringer and plate are separated by the secondary cutter.

4. The products are stored.

The stringer/plate pieces are modeled as a resource for the transport arm. The arm must wait for the pieces to be cut free before it can transport them to the SOFI work station. Power is modeled as a resource for the SOFI work station. The work station cannot operate while the primary cutter is cutting an I - beam. This allows the facility's peak power to be regulated. Cutting I - beams is the most power intensive activity; limiting the power used by the work station keeps the peak power within the design constraints, without significantly affecting the tank reduction time.

Table B.1. Tool Work Rates and Power Use

TOOL	RATE	POWER
Primary Cutter	10 in/min (stringer)	7.05 kW
Primary Cutter	80 in/min (plate)	4.05 kW
Secondary Cutter	80 in/min (plate)	4.00 kW
SOFI Stripper	80 in/min	1.25 kW
Transport Arm	720 in/min (longitudinally) 720 deg/min (radially)	0.20 kW
Communications, Cameras, Lights		2.00 kW

B.8.4 Simulation Input.   The tool work rates and power requirements shown in Table B.1 were used in the final version of the Scenario 1 reduction model.

B.8.5 Results The total time required to reduce the ET for Scenario 1 is 2446 minutes or 1.70 days. The peak power required by the facility is 11.50 Kilowatts.

B.9 Barrel Section Reduction - Scenario 2

Two cutters are employed simultaneously in Scenario 2. Barrel sections are reduced two at a time. Each barrel section is reduced in three stages. The two forward barrel are reduced first. Figure B.5 depicts the cutting sequence for one forward barrel section. First, a box - cut is made, followed by a series of thirty six c - cuts. This is shown as 1. After each cut, the cutter is moved one stringer clockwise. Once the first series of cuts is completed, the cutter is moved and a second set of cuts, consisting of one box - cut and thirty two c - cuts is made; this is shown as 2. The cutter is moved clockwise one stringer after each cut. Following the second set of cuts, the cutter is moved and begins the third set of cuts. This is depicted as 3 in Figure B.5. The final series of cuts consists of one box-cut and nineteen c-cuts. Once again the cutter is moved one stringer clockwise after each cut. After the third series of cuts has been completed, the cutter is moved to the next barrel section and the process continues. The aft barrel section is reduced in a similar manner.

B-11

Figure B.6 shows the sequence of cuts for the aft barrel section. The first series of cuts consists of thirty two cuts. The second and third set of cuts consist of thirty one and nineteen cuts respectively; the cutter moves clockwise for all three sets of cuts. Since there are fewer cuts to be made in the aft barrel compared to the second barrel section, the aft barrel cutter must be delayed in order to stay in sync with the second cutter; this occurs two times. The aft cutter is delayed from making its first set of cuts until the second cutter has made five and one half cuts. A second delay occurs following the second series of cuts. Once the second cutter has cut halfway through its first cut, the aft cutter begins its third series of cuts.

B.10 Scenario 2 Reduction Model

The Scenario 2 reduction model is similar to Scenario 1. For the Scenario 2 model, both mobile cutters are portrayed by entities, as well as the stringer/plate pieces. Astronauts take the place of the transport arm; they move the cutters and transport the pieces. No resources were modeled for scenario two.

B.10.1 Primary Cutters. The two mobile cutters are portrayed as entities. At the beginning of the simulation, the cutters are positioned on either side of the fourth major ring frame (station point 1377.35), as shown in Figure 6.1, along with an astronaut who controls the cutters. The general sequence of activities for the two cutters is:

1. The first cutter begins a box - cut.

2. The second cutter begins a box - cut, once the first cutter has cut half way.

3. The first cutter is moved by an astronaut to the next stringer, once its box - cut is complete.

4. The first cutter begins a c - cut.

5. Once its box - cut is complete, the second cutter is moved by an astronaut to the next stringer.

B-12
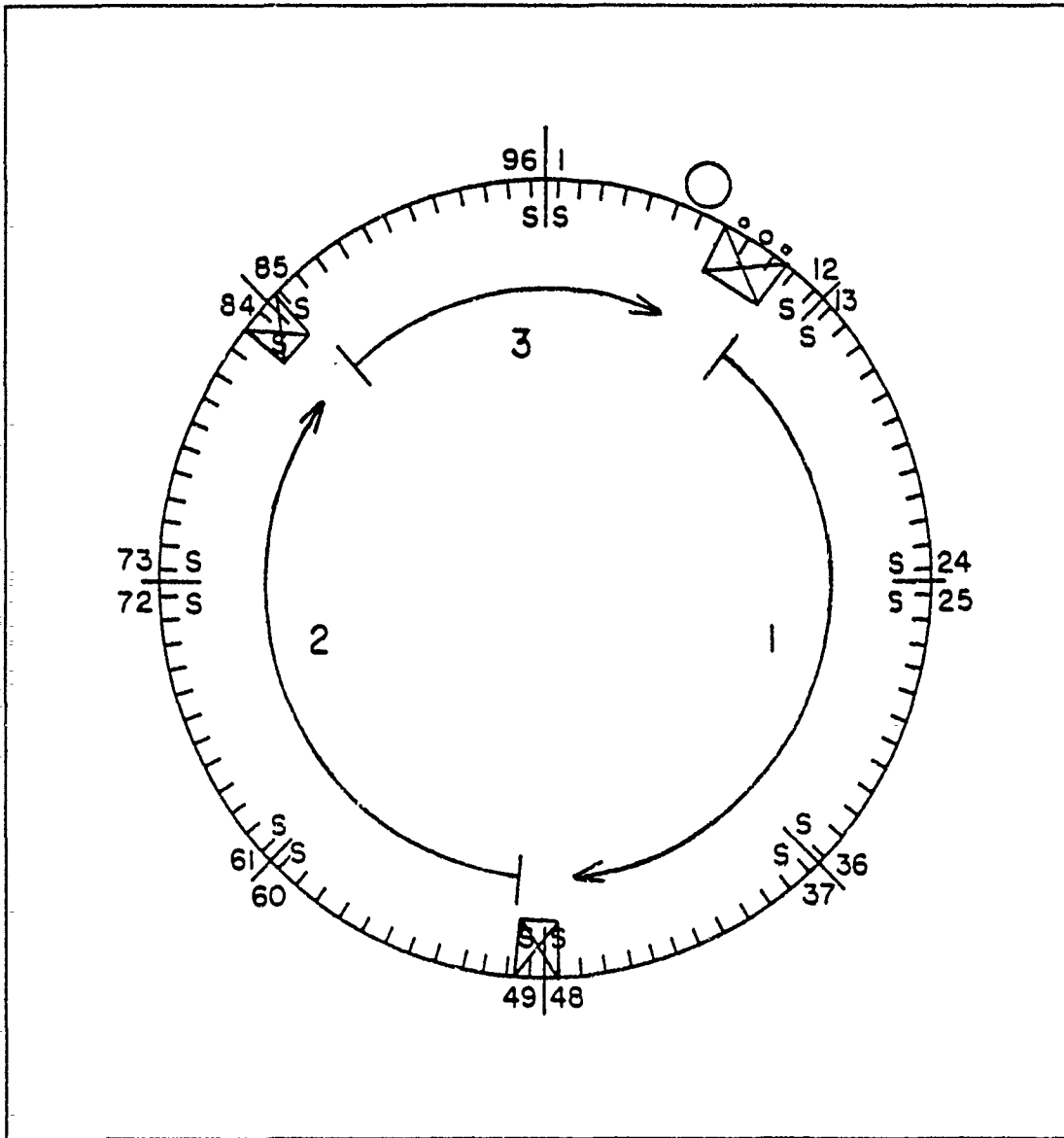
Figure B.5. Forward Barrel Section - Scenario 2

Figure B.6. Aft Barrel Section - Scenario 2

6. When the first cutter has cut half way, the second cutter begins a c - cut.

7. At the end of the first cutter's c - cut, the stringer/plate piece is moved by the astronaut to the SOFI work station. The cutter travels back to the major ring frame and is moved by an astronaut to the next pair of stringers and continues cutting.

8. At the end of its c - cut, the second cutter travels back to the major ring frame while the stringer/plate piece is moved by the astronaut to the SOFI work station. The second cutter is then moved by an astronaut to the next set of stringers and continues cutting.

9. Both cutters continue to make c - cuts and be moved until the entire series of cuts has been made.

10. When the series of cuts is completed, both cutters are moved to the new cut location and tank reduction continues as above.

11. When the entire barrel section is reduced, both cutters are moved by an astronaut to the second major ring frame (station point 1871) and the process continues as above until completion.

B.10.2 Stringer and Plate Pieces. Stringer and plate pieces are depicted as entities for scenario two. The pieces are created each time a cutter completes a cut. The general sequence of activities for a stringer/plate piece is:

1. The piece is created as it is cut free from the barrel section.

2. The piece is transported by an astronaut to the SOFI work station.

3. The stringer and plate are separated by the secondary cutter.

4. The products are stored.

Table B.2. Tool Work Rates and Power Use - Scenario 2

TOOL	RATE	POWER
Primary Cutters	10 in/min (stringers)	7.05 kW
Primary Cutters	50 in/min (plate)	3.55 kW
Primary Cutters	120 in/min (travel)	0.50 kW
Secondary Cutter	100 in/min (plate)	5.00 kW
SOFI Stripper	100 in/min	1.25 kW
Communications, Cameras, Lights		2.00 kW

B.10.3 Simulation Input. The tool work rates and power requirements shown in Table B.2 were used in the final version of the Scenario 2 reduction model.

B.10.4 Results. The total time required to reduce the ET to the 'bird cage' configuration using Scenario 2 is 1383 minutes or 0.96 days. The peak power required by the facility is 18.85 Kilowatts.

B.11 SLAM Program and FORTRAN Subroutines

The following pages are the SLAM programs, FORTRAN subroutines, and output for the Scenario 1 and Scenario 2 reduction models.

This SLAM program models the SCENARIO ONE reduction scheme.
```
;
GEN,ASSET,SCENARIO 1,6/12/90,,,,,N,,72;
LIM,6,6,700;
;CONT,0,6,.1,1,.1;
;TIMST,XX(2),CUTTER USE,150/0/50;
;TIMST,XX(5),ARM USE,20/0/5;
;TIMST,XX(6),STRIPPER USE,60/0/25;
TIMST,XX(7),TOTAL EQUIP USE,15/5000/500;
;REC,TNOW,TIME,,P,.1,0;
;VAR,XX(2),C,CUTTER;
;VAR,XX(5),A,ARM;
;VAR,XX(6),S,STRIPPER;
;VAR,XX(7),T,TOTAL;
;VAR,SS(1),C,CUTTER,0,12000;
;VAR,SS(2),A,ARM,0,12000;
;VAR,SS(3),S,STRIPPER,0,12000;
;VAR,SS(4),T,TOTAL,0,12000;
;
;      XX1 = barrel section to be cut
;      XX2 = flag showing cutter power consumption
;      XX3 = # cuts completed on current section
;      XX4 = section #
;      XX5 = flag showing arm power consumption
;      XX6 = flag showing stripper power consumption
;      XX7 = flag showing total power consumption
;      XX8 = flag showing base power (lights, cameras, & comm)
;      XX9 = flag showing second cutter power consumption
;
NETWORK;
      RES/ARM(1),2,1/PIECE(0),3,P1(0),4,P2(0),5;
      CREATE;
      ASS,XX(1)=0,XX(2)=1,XX(5)=0,XX(6)=0,
          XX(8)=2000,XX(9)=0;                   Base power 2 kW
      ASS,XX(7)=XX(2)+XX(5)+XX(6)+XX(8)+XX(9);   Total power
;
BRL   ASS,XX(1)=XX(1)+1,XX(3)=0,XX(4)=1;
```

SCENARIO ONE SLAM PROGRAM (continued)
```
;
;***************************************************************
;************     MAKE INITIAL C-CUT FOR EACH SECTION   ********
;***************************************************************
SEC   EVENT,1;
      ASS,XX(2)=7050.;                            Cutter power 7 kW
      ASS,XX(7)=XX(2)+XX(5)+XX(6)+XX(8)+XX(9);    Total power
      ACT/1,XX(20);                               Cut 1st beam
      ASS,XX(2)=4050.;                            Cutter power 4 kW
      ASS,XX(7)=XX(2)+XX(5)+XX(6)+XX(8)+XX(9);    Total power
      ACT/2,XX(21)+XX(22);                        L-cut plate
      GOON,1;
      ACT/3,XX(22);                               End cut plate
      ASS,XX(2)=7050.;                            Cutter power 7 kW
      ASS,XX(7)=XX(2)+XX(5)+XX(6)+XX(8)+XX(9);    Total power
      ACT/4,XX(20);                               Cut 2d beam
      ASS,XX(2)=0.;                               Not cutting
      ASS,XX(7)=XX(2)+XX(5)+XX(6)+XX(8)+XX(9);    Total power
;                                                 Wait for arm
CA1   AWAIT(1),ARM/1;                             to move cutter
      ASS,XX(5)=200.;                             Arm power 200 W
      ASS,XX(7)=XX(2)+XX(5)+XX(6)+XX(8)+XX(9);    Total power
      ACT/5,XX(10) + 0.43333;                     Move cutter
      ASS,XX(5)=0;                                Arm idle
      ASS,XX(7)=XX(2)+XX(5)+XX(6)+XX(8)+XX(9);    Total power
CF1   FREE,ARM/1;
      ASS,XX(3)=XX(3)+1;                          Count # cuts
;
;***************************************************************
;**************     CUT INDIVIDUAL PIECES     ******************
;***************************************************************
;
CUT   EVENT,1;                                    Decide brl & sec
;                                                 to be worked on
      GOON,2;
        ACT,,,SKP1;
        ACT/17,,,PA1;                             Create piece
```

SCENARIO ONE SLAM PROGRAM (continued)

```
;
;       ×*********      make one c - cut
SKP1   GOON,1;
       ASS,XX(2)=7050.;                                  Cutter power 7 kW
       ASS,XX(7)=XX(2)+XX(5)+XX(6)+XX(8)+XX(9);  Total power
       ACT/1,XX(20);                                     Cut 1st beam
       ASS,XX(2)=4050;                                   Cutter power 4 kW
       ASS,XX(7)=XX(2)+XX(5)+XX(6)+XX(8)+XX(9);  Total power
       ACT/2,XX(21)+XX(22);                              L-Cut of plate
       ALTER,PIECE,+1;                                   Piece cut free
       ACT/3,XX(22);                                     Make end cut
       ASS,XX(2)=7050;                                   Cutter power 7 kW
       ASS,XX(7)=XX(2)+XX(5)+XX(6)+XX(8)+XX(9);  Total power
       ACT/4,XX(20);                                     Cut 2nd beam
       ALTER,P1,+1;
       ASS,XX(2)=0;                                      Not cutting
       ASS,XX(7)=XX(2)+XX(5)+XX(6)+XX(8)+XX(9);  Total power
;
;       ***·******      move cutter to next stringer
;                                                        Wait for arm to
CA2    AWAIT(1),ARM/1;                                   move cutter
       ASS,XX(5)=200.;                                   Arm power 200 W
       ASS,XX(7)=XX(2)+XX(5)+XX(6)+XX(8)+XX(9);  Total power
       ACT/5,XX(10) + 0.43333;                           Move cutter
CF2    FREE,ARM/1;                                       Free arm
       ASS,XX(3)=XX(3)+1,XX(5)=0;                        Count # of cuts
       ASS,XX(7)=XX(2)+XX(5)+XX(6)+XX(8)+XX(9);  Total power
       GOON,2;
          ACT,,,G1;
          ACT,XX(20);
          ALTER,P2,+1;
          TERM;
;
G1     GOON,1;
          ACT,,XX(3).LE.XX(23),CUT;                      Continue cutting or
          ACT;                                           make box cut
       EVENT,1;
       GOON,2;
          ACT,,,SKP2;
          ACT/17,,,PA3;                                  Create piece
```

```
SCENARIO ONE SLAM PROGRAM (continued)
;
;      *********     make box cut
SKP2  GOON,1;
      ASS,XX(2)=7050.;                          Cutter power 7 kW
      ASS,XX(7)=XX(2)+XX(5)+XX(6)+XX(8)+XX(9);  Total power
      ACT/1,XX(20);                             Cut 1st beam
      ASS,XX(2)=4050;                           Cutter power 4 kW
      ASS,XX(7)=XX(2)+XX(5)+XX(6)+XX(8)+XX(9);  Total power
      ACT/2,XX(21)+XX(22);                      L-cut of plate
      ALTER,PIECE,+1;                           Piece cut free
      ACT/6,XX(21)+XX(22);                      2nd L-cut of plate
      ASS,XX(2)=7050.;                          Cutter power 7 kW
      ASS,XX(7)=XX(2)+XX(5)+XX(6)+XX(8)+XX(9);  Total power
      ACT/4,XX(20);                             Cut 2d beam
      ALTER,P1,+1;
      ASS,XX(3)=XX(3)+1,XX(2)=0;                Count cuts complete
      ASS,XX(7)=XX(2)+XX(5)+XX(6)+XX(8)+XX(9);  Total power
CA3   AWAIT(1),ARM/1;                           Wait for arm
      ASS,XX(5)=200.;                           Arm power 200 W
      ASS,XX(7)=XX(2)+XX(5)+XX(6)+XX(8)+XX(9);  Total power
;*****************************************************************
;**********   MOVE CUTTER BETWEEN SECTIONS OR BARRELS   ********
;*****************************************************************
      GOON,1;
        ACT/9,,XX(1).GE.4 .AND. XX(4).GE.3,DONE;   Done cutting
        ACT/7,XX(24),XX(4).LT.3,SKP3;      Move cutter to next sec
        ACT/8,XX(25),XX(4).GE.3;           Move cutter to next brl
CF3   FREE,ARM/1;
      ASS,XX(5)=0;                              Arm idle
      ASS,XX(7)=XX(2)+XX(5)+XX(6)+XX(8)+XX(9);  Total power
      GOON,2;
        ACT,,,BRL;                              Cut next barrel
        ACT,XX(20)+XX(20);
        ALTER,P2,+1;
        TERM;
SKP3  FREE,ARM/1;
      ASS,XX(3)=0,XX(4)=XX(4)+1,XX(5)=0;        Count barrel #
      ASS,XX(7)=XX(2)+XX(5)+XX(6)+XX(8)+XX(9);  Total power
```

```
SCENARIO ONE SLAM PROGRAM (continued)
;
      GOON,2;
          ACT,,,SEC;                                  Cut next section
          ACT,XX(20)+XX(20);
          ALTER,P2,+1;
          TERM;
DONE  ALTER,P2,+1;
      TERM;
;
;************       TRANSPORT PIECE TO STRIPPER     ****************
;************            (normal c-cut)             ****************
******************************************************************
;                  Wait for arm to
PA1   AWAIT(2),ARM/1;                                 move to piece
      ASS,XX(5)=200.;                                 Arm power 200 W
      ASS,XX(7)=XX(2)+XX(5)+XX(6)+XX(8)+XX(9); Total power
      ACT/11,XX(11) + 0.21666;         Move arm to center of brl
      ASS,XX(5)=0;                                    Arm idle
      ASS,XX(7)=XX(2)+XX(5)+XX(6)+XX(8)+XX(9); Total power
      ACT,4.1666;                                     Wait for cutter
PA2   AWAIT(3),PIECE/1;                               Wait for piece
      ASS,XX(5)=200.;                                 Arm power 200 W
      ASS,XX(7)=XX(2)+XX(5)+XX(6)+XX(8)+XX(9); Total power
      ACT/12,XX(12) + 0.63333;                        Move piece
      GOON,1;
      ACT/13,XX(13);                                  Rtn to cutter
      ASS,XX(5)=0;                                    Arm idle
      ASS,XX(7)=XX(2)+XX(5)+XX(6)+XX(8)+XX(9); Total power
PF1   FREE,ARM/1;                                     Arm available
      ACT,,,STRP;                                     To stripper
;
;*************       TRANSPORT PIECE TO STRIPPER     *************
;*************              (box cut)                *************
;****************************************************************
;                                                    Wait for arm to
PA3   AWAIT(2),ARM/1;                                 move to piece
      ASS,XX(5)=200.;                                 Arm power 200 W
      ASS,XX(7)=XX(2)+XX(5)+XX(6)+XX(8)+XX(9); Total power
      ACT/11,XX(11) + 0.21666;         Move arm to center of brl
      ASS,XX(5)=0;                                    Arm idle
      ASS,XX(7)=XX(2)+XX(5)+XX(6)+XX(8)+XX(9); Total power
      ACT,4.1666;                                     Wait for cutter
```

```
SCENARIO ONE SLAM PROGRAM (continued)
;
PA4    AWAIT(3),PIECE/1;                            Wait for piece
       ASS,XX(5)=200.;                              Arm power 200 W
       ASS,XX(7)=XX(2)+XX(5)+XX(6)+XX(8)+XX(9);     Total power
       ACT/12,XX(12) + 0.63333;                     Move piece
       GOON,1;
       ACT/14,XX(14);                               Return to piece
       GOON,1;
       ACT,0.41666;                                 Extend arm, grab
       GOON,1;                                       retract
       ACT/15,XX(14);                               Piece to stripper
       GOON,1;
       ACT,0.43333;                                 Extend arm, feed,
       GOON,1;                                      release, retract
       ACT/16,XX(15);                               Return to cutter
       ASS,XX(5)=0;                                 Arm idle
       ASS,XX(7)=XX(2)+XX(5)+XX(6)+XX(8)+XX(9);     Total power
PF2    FREE,ARM/1;                                  Arm available
       ACT,,,STRP;                                  Piece to stripper
;****************     STRIP SOFI OFF PIECES     ****************
;**************************************************************
STRP   AWAIT(4),P1/1;                               Wait for the I-beams to
       AWAIT(5),P2/1;                               be cut before stripping
       GOON,2;
       ACT,,,CUT2;
       ACT;
       ASS,XX(6)=1250;                              Stripper power 1250 W
       ASS,XX(7)=XX(2)+XX(5)+XX(6)+XX(8)+XX(9);     Total power
       ACT/20,XX(30);                               Strip sofi
       ASS,XX(6)=200.;                              Secondary drive motor
       ASS,XX(7)=XX(2)+XX(5)+XX(6)+XX(8)+XX(9);     Total power
       ACT/21,2.0;                                  Push piece thru cutter
       ASS,XX(6)=0.;                                Motor off
       ASS,XX(7)=XX(2)+XX(5)+XX(6)+XX(8)+XX(9);     Total power
       TERM;
CUT2   ASS,XX(9)=4000;                              Secondary cutter
       ASS,XX(7)=XX(2)+XX(5)+XX(6)+XX(8)+XX(9);     Total power
       ACT/22,XX(22);                               Cut beam from plate
       ASS,XX(9)=0.;                                2d cutter idle
       ASS,XX(7)=XX(2)+XX(5)+XX(6)+XX(8)+XX(9);     Total power
       TERM;
       END;
FIN;
```

```
C       These FORTRAN subroutines determine activity
C       durations for the SCENARIO ONE reduction model.
        PROGRAM MAIN
        DIMENSION NSET(100000)
        INCLUDE 'SLAM$DIR:PARAM.INC'
        COMMON/SCOM1/ATRIB(MATRB),DD(MEQT),DDL(MEQT),DTOW,
       1II,1MFA, MSTOP,NCLNR,NCRDR,NPRNT, NNRUN,NNSET NTAPE,
       2SS(MEQT), SSL(MEQT),TNEXT, TNOW, XX(MMXXV),XVEL,
       3RVEL, CUTRAT1, CUTRAT2, STRPRATE
C
        COMMON QSET(100000)
        EQUIVALENCE (NSET(1),QSET(1))
        NNSET=100000
        NCRDR=5
             NPRNT=6
        NTAPE=7
        NPLOT=2
        CALL SLAM
        STOP
        END
C
        SUBROUTINE EVENT(I)
        INCLUDE 'SLAM$DIR:PARAM.INC'
        COMMON/SCOM1/ATRIB(MATRB),DD(MEQT),DDL(MEQT) DTNOW,
       1II,MFA, MSTOP,NCLNR, NCRDR,NPRNT,NNRUN,NNSET, NTAPE,
       2SS(MEQT), SSL(MEQT),TNEXT, TNOW, XX(MMXXV), XVEL,
       3RVEL, 3RVEL, 3RVEL, CUTRAT1, CUTRAT2, STRPRATE
C
C       Activity durations are determined by the barrel,
C       section, and cut being worked on.
C       NB = # BARREL        NC = # CUT        NS = # SECTION
C
     1  NB=XX(1)
        NC=XX(3)
        NS=XX(4)
        ANG = .065449846
        A1  = .0083333
        A2  = .0166666
        XVEL = 720.
        RVEL = 12.56637
        CUTRAT1 = 80.
        CUTRAT2 = 10.
        STRPRATE = 80.
```

```fortran
C     SCENARIO ONE FORTRAN subroutines (continued)
C
C     Move cutter one stringer
      XX(10) = ANG/RVEL +A1
C
C     Cut I beam
      XX(20) = 1.25/CUTRAT2
C
C     Cut end of panel (w/o beam)
      XX(21) = 9.852/CUTRAT1
***************************************************************
********************   Barrel one     ************************
***************************************************************
      IF (NB .EQ. 1) THEN
        XX(11) = 76.75/XVEL + 0.1308997/RVEL + A2
        XX(22) = 163.0/CUTRAT1
        XX(25) = 185.3/XVEL + 2.487094/RVEL + A2 + 0.233333
        XX(30) = 163/STRPRATE
C
C     Barrel one / Section one
C
      IF (NS .EQ. 1) THEN
      XX(12) = 171.45/XVEL+(1.3417218-(NC-1)*ANG)/RVEL +A2
      XX(14) = 171.45/XVEL + 0.2290745/RVEL + A2
      XX(15) =  94.70/XVEL + 0.1636246/RVEL + A2
      XX(23) = 17.
      XX(24) = 0.6544985/RVEL + A1 + 0.233333
C
        IF (-1**NC .LT. 0) THEN
        XX(13) = 248/XVEL +(1.210822 -(NC-1)*ANG)/RVEL +A2
        ELSE
        XX(13) = 94.7/XVEL +(1.210822 -(NC-1)*ANG)/RVEL +A2
        END IF
C
C     Barrel one / Section two
C
      ELSE IF (NS .EQ.2) THEN
      XX(12) = 171.45/XVEL+(0.425424+(NC-1)*ANG)/RVEL + A2
      XX(14) = 171.45/XVEL + 2.4543693/RVEL + A2
      XX(15) =     248/XVEL + 2.519819/RVEL + A2
      XX(23) = 31.
      XX(24) = 2.0943951/RVEL + A1 + 0.233333
```

```fortran
C       SCENARIO ONE FORTRAN subroutines (continued)
C
        IF (-1**NC .LT. 0) THEN
        XX(13) = 94.7/XVEL +(0.425424 +(NC -1)*ANG)/RVEL +A2
        ELSE
        XX(13) = 248/XVEL +(0.425424 +(NC -1)*ANG)/RVEL +A2
        END IF
C
C       Barrel one / Section three
C
        ELSE
                XX(14) = 171.45/XVEL + 2.7161687/RVEL + A2
                XX(15) = 248/XVEL + 2.650719/RVEL + A2
                XX(23) = 30.
                XX(24) = 0.
C
                IF (NC .LE. 24) THEN
                XX(12) = 171.45/XVEL +(1.603521+(NC-1)*ANG)/RVEL +A2
                ELSE
                XX(12) = 171.45/XVEL+(3.108868-(NC-24)*ANG)/RVEL +A2
                END IF
                  IF (NC .LE. 22) GO TO 11
                  IF (NC .GT. 22) GO TO 12
C
   11   IF (-1**NC .LT. 0) THEN
        XX(13) = 248/XVEL +(1.603513 +(NC-1)*ANG)/RVEL +A2
        ELSE
        XX(13) = 94.7/XVEL +(1.603513 +(NC-1)*ANG)/RVEL+A2
        END IF
        GO TO 13
C
   12   IF (-1**NC .GT. 0) THEN
        XX(13) = 248/XVEL+(3.108868 -(NC-22)*ANG)/RVEL +A2
        ELSE
        XX(13) = 94.7/XVEL+(3.108868-(NC-22)*ANG)/RVEL+A2
        END IF
C
   13     CONTINUE
          END IF
          RETURN
```

```fortran
C       SCENARIO ONE FORTRAN subroutines (continued)
C

        **********************************************************
        *****************   Barrel two    ********************
        **********************************************************
                ELSE IF (NB .EQ. 2) THEN
                XX(11) = 108.1/XVEL + 0.1308997/RVEL + A2
                XX(22) = 225.7/CUTRAT1
                XX(25) = 246.2/XVEL + 2.487094/RVEL + A2 + 0.233333
                XX(30) = 225.7/STRPRATE
C
C       Barrel two / Section one
C
        IF (NS .EQ. 1) THEN
                XX(12) = 76.75/XVEL +(0.0981748 +(NC-1)*ANG)/RVEL+A2
                XX(14) = 76.75/XVEL + 2.4543693/RVEL + A2
                XX(15) = 31.35/XVEL + 2.519819/RVEL + A2
                XX(23) = 36.
                XX(24) = 2.6834437/RVEL + A1 + 0.233333
                IF (-1**NC .LT. 0) THEN
                XX(13)= 31.35/XVEL +(0.2290745 +(NC-1)*ANG)/RVEL +A2
                ELSE
                XX(13)= 184.85/XVEL+(0.2290745+(NC-1)*ANG)/RVEL +A2
                END IF
C
C       Barrel two / Section two
C
        ELSE IF (NS .EQ.2) THEN
                XX(12) = 76.75/XVEL+(0.0981748 +(NC -1)*ANG)/RVEL +A2
                XX(14) = 76.75/XVEL + 1.276272/RVEL + A2
                XX(15) = 31.35/XVEL + 1.341722/RVEL + A2
                XX(23) = 18.
                XX(24) = 0.1963495/RVEL + A1 +0.233333
C
                IF (-1**NC .LT. 0) THEN
                XX(13)= 31.35/XVEL +(0.2290745 +(NC-1)*ANG)/RVEL +A2
                ELSE
                XX(13)= 184.85/XVEL+(0.2290745 +(NC-1)*ANG)/RVEL +A2
                END IF
```

```fortran
C     SCENARIO ONE FORTRAN subroutines (continued)
C     Barrel two / Section three
C
      ELSE
              XX(14) = 76.75/XVEL + 2.7161687/RVEL + A2
              XX(15) = 31.35/XVEL + 2.650719/RVEL + A2
              XX(23) = 32.
              XX(24) = 0.
              IF (NC .LE. 26) THEN
              XX(12) = 76.75/XVEL+(1.47262 +(NC-1)*ANG)/RVEL+A2
              ELSE
              XX(12) = 76.75/XVEL +(3.108868-(NC-26)*ANG)/RVEL+A2
              END IF
C
              IF (NC .LE. 24) GO TO 21
              IF (NC .GT. 24) GO TO 22
   21         IF (-1**NC .LT. 0) THEN
               XX(13) = 31.35/XVEL+(1.6035213+(NC-1)*ANG)/RVEL+A2
               ELSE
               XX(13) =184.85/XVEL+(1.6035213+(NC-1)*ANG)/RVEL+A2
               END IF
               GO TO 23
       22     IF (-1**NC .GT. 0) THEN
               XX(13) = 31.35/XVEL+(3.108868-(NC-24)*ANG)/RVEL+A2
               ELSE
               XX(13) =184.85/XVEL+(3.108868-(NC-24)*ANG)/RVEL+A2
               END IF
   23    CONTINUE
         END IF
         RETURN
*************************************************************
***************** Barrel three    ********************
*************************************************************
         ELSE IF (NB .EQ. 3) THEN
              XX(11) = 108.2/XVEL + 0.1308997/RVEL + A2
              XX(22) = 225.95/CUTRAT1
              XX(25) = 246.45/XVEL + 2.487094/RVEL + A2
              XX(30) = 225.95/STRPRATE
```

```fortran
C       SCENARIO ONE FORTRAN subroutines (continued)
C
C       Barrel three / Section one
C
        IF (NS .EQ. 1) THEN
        XX(12) = 323.2/XVEL+(0.0981748+(NC-1)*ANG)/RVEL+A2
        XX(14) = 323.2/XVEL + 2.4543693/RVEL + A2
        XX(15) = 214.95/XVEL + 2.519819/RVEL + A2
        XX(23) = 36.
        XX(24) = 2.6834437/RVEL + A1 + 0.233333
        IF (-1**NC .LT. 0) THEN
        XX(13) = 214.95/XVEL+(0.2290745 +(NC-1)*ANG)/RVEL+A2
        ELSE
        XX(13) = 431.4/XVEL +(0.2290745 +(NC-1)*ANG)/RVEL+A2
        ENDIF
C
C       Barrel three / Section two
C
       ELSE IF (NS .EQ. 2) THEN
       XX(12) = 323.2/XVEL +(0.0981748 +(NC-1)*ANG)/RVEL+A2
       XX(14) = 323.2/XVEL + 1.276272/RVEL + A2
       XX(15) = 214.95/XVEL + 1.341722/RVEL + A2
       XX(23) = 18.
       XX(24) = 0.1963495/RVEL + A1 + 0.233333
       IF (-1**NC .LT. 0) THEN
       XX(13) = 214.95/XVEL +(0.2290745+(NC-1)*ANG)/RVEL+A2
       ELSE
       XX(13) = 431.4/XVEL +(0.2290745 +(NC-1)*ANG)/RVEL+A2
       END IF
C
C       Barrel three / Section three
C
        ELSE
        XX(14) = 323.2/XVEL + 2.7161687/RVEL + A2
        XX(15) = 214.95/XVEL + 2.650719/RVEL + A2
        XX(23) = 32.
        XX(24) = 0.
        IF (XX(3) .LE. 26) THEN
        XX(12) = 323.2/XVEL +(1.47262+(NC-1)*ANG)/RVEL +A2
 ELSE
        XX(12) = 323.2/XVEL +(3.108868-(NC-26)*ANG)/RVEL+A2
        END IF
```

```fortran
C     SCENARIO ONE FORTRAN subroutines (continued)
C
      IF (XX(3) .LE. 24) GO TO 31
      IF (XX(3) .GT. 24) GO TO 32
C
   31 IF (-1**NC .LT. 0) THEN
      XX(13) =214.95/XVEL+(1.6035213 +(NC-1)*ANG)/RVEL+A2
      ELSE
      XX(13) = 431.4/XVEL+(1.6035213 +(NC-1)*ANG)/RVEL+A2
      END IF
      GO TO 33
C
   32 IF (-1**NC .GT. 0) THEN
      XX(13) =214.95/XVEL+(3.108868-(NC -24)*ANG)/RVEL+A2
      ELSE
      XX(13) = 431.4/XVEL +(3.108868-(NC-24)*ANG)/RVEL+A2
      END IF
C
   33 CONTINUE
      END IF
      RETURN
C
***************************************************************
********************  Barrel four   ***************
***************************************************************
      ELSE
          XX(11) = 108.2/XVEL + 0.1308997/RVEL + A2
          XX(22) = 225.95/CUTRAT1
          XX(25) = 246.45/XVEL + 2.487094/RVEL + A2
          XX(30) = 225.95/STRPRATE
C
C     Barrel four / Section one
C
      IF (NS .EQ. 1) THEN
      XX(12) = 569.2/XVEL+(0.0981748+(NC-1)*ANG)/RVEL +A2
      XX(14) = 569.2/XVEL + 2.4543693/RVEL + A2
      XX(15) = 461.4/XVEL + 2.519819/RVEL + A2
      XX(23) = 36.
      XX(24) = 2.6834437/RVEL + A1 + 0.233333
```

```fortran
C       SCENARIO ONE FORTRAN subroutines (continued)
C
        IF (-1**NC .LT. 0) THEN
        XX(13) = 461.4/XVEL+(0.2290745+(NC-1)*ANG)/RVEL+A2
        ELSE
        XX(13) = 677.85/XVEL+(0.2290745+(NC-1)*ANG)/RVEL+A2
        END IF
C
C       Barrel four / Section two
C
        ELSE IF (NS .EQ. 2) THEN
        XX(12) = 569.2/XVE +(0.098174 +(NC-1)*ANG)/RVEL + A2
        XX(14) = 569.2/XVEL + 1.276272/RVEL + A2
        XX(15) = 461.4/XVEL + 1.341722/RVEL + A2
        XX(23) = 18.
        XX(24) = 0.1963495/RVEL + A1 + 0.233333
        IF (-1**NC .LT. 0) THEN
        XX(13) = 461.4/XVEL +(0.2290745+(NC-1)*ANG)/RVE +A2
        ELSE
        XX(13) = 677.85/XVE +(0.2290745+(NC-1)*ANG)/RVE +A2
        END IF
C
C       Barrel four / Section three
C
        ELSE
        XX(14) = 569.2/XVEL + 2.7161687/RVEL + A2
        XX(15) = 461.4/XVEL + 2.650719/RVEL + A2
        XX(23) = 32.
        XX(24) = 0.
        IF (NC .LE. 26) THEN
        XX(12) = 569.2/XVEL+(1.4726 +(NC-1)*ANG)/RVEL+A2
        ELSE
        XX(12) = 569.2/XVEL+(3.108868-(NC-26)*ANG)/RVEL+A2
        END IF
        IF (NC .LE. 24) GO TO 41
        IF (NC .GT. 24) GO TO 42
41      IF (-1**NC .LT. 0) THEN
        XX(13) = 461.4/XVEL +(1.603521 +(NC-1)*ANG)/RVEL +A2
        ELSE
        XX(13) = 677.85/XVEL +(1.603521 +(NC-1)*ANG)/RVEL +A2
        END IF
        GO TO 43
```

```fortran
C SCENARIO ONE FORTRAN subroutines (continued)
C
   42         IF (-1**NC .GT. 0) THEN
              XX(13) = 461.4/XVEL +(3.108868 -(NC-24)*ANG)/RVEL +A2
              ELSE
              XX(13) = 677.85/XVEL +(3.108868 -(NC-24)*ANG)/RVEL +A2
              END IF
C
   43         CONTINUE
C
           END IF
         RETURN
       END IF
       RETURN
       END
C
     SUBROUTINE INTLC
     INCLUDE 'SLAM$DIR:PARAM.INC'
     COMMON/SCOM1/ATRIB(MATRB), DD(MEQT),DDL(MEQT),DTNOW, II, MFA,
    1MSTOP,NCLNR, NCRDR, NPRNT, NNRUN, NNSET, NTAPE, SS(MEQT),
    2SSL(MEQT),TNEXT, TNOW, XX(MMXXV),XVEL, RVEL,CUTRAT1, CUTRAT2,
    3STRPRATF
     OPEN (1,FILE='PWR1A.DAT',STATUS='NEW')
     RETURN
     END
C
     SUBROUTINE STATE
     INCLUDE 'SLAM$DIR:PARAM.INC'
     COMMON/SCOM1/ATRIB(MATRB), DD(MEQT), DDL(MEQT),DTNOW,II,MFA,
    1MSTOP,NCLNR, NCRDR, NPRNT, NNRUN, NNSET, NTAPE, SS(MEQT),
    2SSL(MEQT),TNEXT, TNOW, XX(MMXXV), XVEL, RVEL,CUTRAT1,CUTRAT2,
    3STRPRATE
C
       SS(1)=XX(2)
       SS(2)=XX(5)
       SS(3)=XX(6)
       SS(4)=XX(2)+XX(5)+XX(6)+XX(8)+XX(9)
       SS(5)=XX(8)
       SS(6)=XX(9)
       WRITE(1,5) TNOW,SS(4)
    5  FORMAT(1X,2F20.8)
       RETURN
       END
```

S L A M   I I   S U M M A R Y   R E P O R T

SIMULATION PROJECT SCENARIO ONE
DATE   6/12/1990
CURRENT TIME   0.2446E+04
STATISTICAL ARRAYS CLEARED AT TIME   0.0000E+00

STATISTICS FOR VARIABLES BASED ON OBSERVATION

	MEAN VALUE	STANDARD DEVIATION	COEFF. OF VARIATION	MINIMUM VALUE	MAXIMUM VALUE	NO.OF OBS
BRL COMPLETE	0.250E+01	0.117E+01	0.467E+00	0.100E+01	0.400E+01	12
SEC COMPLETE	0.200E+01	0.853E+00	0.426E+00	0.100E+01	0.300E+01	12
CUTS COMPLETE	0.300E+02	0.783E+01	0.261E+00	0.190E+02	0.380E+02	12

STATISTICS FOR TIME-PERSISTENT VARIABLES

	MEAN VALUE	STANDARD DEVIATION	MINIMUM VALUE	MAXIMUM VALUE	TIME INTERVAL	CURRENT VALUE
TOTAL EQUIP USE	7586.524	3301.536	0.00	11500.00	2446.055	2200.00

FILE STATISTICS

FILE NUMBER	LABEL/TYPE		AVERAGE LENGTH	STANDARD DEVIATION	MAXIMUM LENGTH	CURRENT LENGTH	AVERAGE WAIT TIME
1	CA1	AWAIT	0.100	0.300	1	0	0.678
2	PA1	AWAIT	0.000	0.000	1	0	0.000
3	PA2	AWAIT	^.000	0.000	1	0	0.000
4	STRP	AWAIT	0.013	0.113	1	0	0.091
5		AWAIT	0.082	0.274	1	0	0.574
6			0.000	0.000	0	0	0.000
7		CALENDAR	2.845	1.107	4	0	0.637

REGULAR ACTIVITY STATISTICS

ACTIVITY INDEX/LABEL	AVERAGE UTILIZATION	STANDARD DEVIATION	MAX UTIL	CURRENT UTIL	ENTITY COUNT
1 Cut 1st beam	0.0184	0.1344	1	0	360
2 L-cut of pla	0.4067	0.4912	1	0	360
3 Make end cut	0.3757	0.4843	1	0	348
4 Cut 2d beam	0.0184	0.1344	1	0	360
5 Move cutter	0.0636	0.2440	1	0	348
6 2nd L-cut of	0.0135	0.1154	1	0	12
7 Move cutter	0.0012	0.0341	1	0	8
8 Move cutter	0.0008	0.0290	1	0	3
9 Done cutting	0.0000	0.0000	1	0	1
11 Move arm to	0.0546	0.2272	1	0	348
12 Move piece t	0.1674	0.3734	1	0	348
13 Rtn to cutte	0.0648	0.2462	1	0	336
14 Return to pi	0.0028	0.0531	1	0	12
15 Piece to str	0.0028	0.0531	1	0	12
16 Return to cu	0.0024	0.0493	1	0	12
17 Create piece	0.0000	0.0000	1	0	348
20 Strip sofi	0.3760	0.4844	1	0	348
21 Push piece t	0.2845	0.4512	1	0	348
22 Cut beam fro	0.3760	0.4844	1	0	348

RESOURCE STATISTICS

RESOURCE NUMBER	RESOURCE LABEL	CURRENT CAPACITY	AVERAGE UTIL	STANDARD DEVIATION	MAX UTIL	CURRENT UTIL
1	ARM	1	0.96	0.197	1	1
2	PIECE	348	179.71	101.472	348	348
3	P1	348	179.45	101.430	348	348
4	P2	348	179.37	101.435	348	348

RESOURCE NUMBER	RESOURCE LABEL	CURRENT AVAILABLE	AVERAGE AVAILABLE	MINIMUM AVAIL	MAXIMUM AVAIL
1	ARM	0	0.0405	0	1
2	PIECE	0	0.2364	0	1
3	P1	0	0.0998	0	1
4	P2	0	0.0000	0	0

SCENARIO ONE SLAM SUMMARY (continued)

TIME-PERSISTENT HISTOGRAM NUMBER 1
TOTAL EQUIP USE

```
CELL RELA   UPPER
TIME FREQ CELL LIM 0       20        40        60      80      100
 407. 0.17 0.500E+04 +********                                  +
   0. 0.00 0.550E+04 +        C                                 +
   0. 0.00 0.600E+04 +        C                                 +
 *** 0.42 0.650E+04 +********************         C             +
   0. 0.00 0.700E+04 +                            C             +
   3. 0.00 0.750E+04 +                            C             +
   0. 0.00 0.800E+04 +                            C             +
   0. 0.00 0.850E+04 +                            C             +
   0. 0.00 0.900E+04 +                            C             +
  90. 0.04 0.950E+04 +**                             C          +
   0. 0.00 0.100E+05 +                               C          +
   0. 0.00 0.105E+05 +                               C          +
   0. 0.00 0.110E+05 +                               C          +
 917. 0.37 0.115E+05 +*******************                       C
   0. 0.00 0.120E+05 +                                          C
   0. 0.00 0.125E+05 +                                          C
   0. 0.00   INF     +                                          C
 ----                 +  +  +  +  +  +  +  +  +  +  +
 ****                 0    20   40   60   80   100
```


STATISTICS FOR TIME-PERSISTENT VARIABLES

	MEAN VALUE	STANDARD DEVIATION	MINIMUM VALUE	MAXIMUM VALUE	TIME INTERVAL	CURRENT VALUE
TOTAL EQUIP USE	7586.524	3301.536	0.00	11500.00	2446.055	2200.00

B-34

This SLAM program models the SCENARIO TWO reduction scheme

```
;
GEN,ASSET,SCENARIO 2,9/06/90,,,,,N,,72;
LIM,5,5,5000;
;CONT,0,6,.1,1,.1;
;TIMST,XX(1),CUTTER USE,150/0/50;
;TIMST,XX(2),CUTTER 2,150/0/50;
;TIMST,XX(3),CUTTER 3,150/0/50;
;TIMST,XX(4),STRIPPER USE,60/0/25;
TIMST,XX(9),TOTAL EQUIP USE,31/5000/500;
;REC,TNOW,TIME,,P,.1,;
;VAR,XX(1),1,CUTTER 1;
;VAR,XX(2),2,CUTTER 2;
;VAR,XX(3),3,CUTTER 3;
;VAR,XX(4),S,STRIPPER;
;VAR,XX(9),T,TOTAL;
;VAR,SS(1),1,CUTTER 1,0;
;VAR,SS(2),2,CUTTER 2,0;
;VAR,SS(3),3,CUTTER 3,0;
;VAR,SS(4),S,STRIPPER,0;
;VAR,SS(9),T,TOTAL,0;
;
;       xx1 = cutter 1 on/off
;       xx2 = cutter 2 on/off
;       xx3 = cutter 3 on/off
;       xx4 = stripper on/off
;       xx5 = base power on/off
;       xx9 = total power use
;
NETWORK;
;
        CREATE;
        ASS,XX(5)=2000;                                 Base power 2 kW
        ASS,XX(9)=XX(1)+XX(2)+XX(3)+XX(4)+XX(5);
;
  G1    ASS,XX(41)=0.,XX(42)=0.;
        GOON,2;
        ACT,,,B2;
        ACT
```

SCENARIO TWO SLAM PROGRAM (continued)

```
;
;!!!!!!!!!!!!!!!!!!!!!!        first cutter     !!!!!!!!!!!!!!!!!!!!!!!!!!!!
;!!!!!!!!!!!!!!!!!!!!!!!!!!!!!!!!!!!!!!!!!!!!!!!!!!!!!!!!!!!!!!!!!!!!!!!!!!!!!
  B1   ASS,XX(51)=XX(51)+1
  S1   ASS,XX(31)=0,XX(41)=XX(41)+1;
       EVENT,1;
;
;!!!!!!!!!!!!!!!!!!!!!!        make box cut      !!!!!!!!!!!!!!!!!!!!!!!!!!!!
;
       ASS,XX(1)=7050.;                          Cutter power 7 kW
       ASS,XX(9)=XX(1)+XX(2)+XX(3)+XX(4)+XX(5);  Total power
       ACT/10,XX(10);                            Cut 1st beam
       ASS,XX(1)=3550.;                          Cutter power 3.5 kW
       ASS,XX(9)=XX(1)+XX(2)+XX(3)+XX(4)+XX(5);  Total power
       ACT/11,XX(11);                            C-cut plate
       ASS,XX(1)=7050.;                          Cutter power 7 kW
       ASS,XX(9)=XX(1)+XX(2)+XX(3)+XX(4)+XX(5);  Total power
       ACT/12,XX(10);                            Cut 2d beam
       ASS,XX(1)=3550.;                          Cutter power 3.5 kW
       ASS,XX(9)=XX(1)+XX(2)+XX(3)+XX(4)+XX(5);  Total power
       ACT/13,XX(13);                            Straight cut
       ASS,XX(1)=0.,XX(31)=1;                    1st cut complete
       ASS,XX(9)=XX(1)+XX(2)+XX(3)+XX(4)+XX(5);  Total power
       ACT/15,RNORM(.5,.15);                     Move cutter
       GOON,2;
          ACT,RNORM(1.,.3),,STRP;                Handoff piece to strpr
          ACT;                                   Continue cutting
;
;!!!!!!!!!!!!!!!!!!!!!!        make c cut        !!!!!!!!!!!!!!!!!!!!!!!!!!!!
;
  C1   ASS,XX(1)=7050.;                          Cutter power 7 kW
       ASS,XX(9)=XX(1)+XX(2)+XX(3)+XX(4)+XX(5);  Total power
       ACT/10,XX(10);                            Cut 1st beam
       ASS,XX(1)=3550.;                          Cutter power 3.5 kW
       ASS,XX(9)=XX(1)+XX(2)+XX(3)+XX(4)+XX(5);  Total power
       ACT/11,XX(11);                            C-cut plate
       ASS,XX(1)=7050.;                          Cutter power 7 kW
       ASS,XX(9)=XX(1)+XX(2)+XX(3)+XX(4)+XX(5);  Total power
       ACT/12,XX(10);                            Cut 2d beam
       ASS,XX(1)=50.;                            Cutter platform 50 W
       ASS,XX(9)=XX(1)+XX(2)+XX(3)+XX(4)+XX(5);  Total power
```

SCENARIO TWO SLAM PROGRAM (continued)
;
```
      GOON,2;
         ACT,RNORM(1.,.03),,STRP;               Handoff piece to strpr
         ACT/14,XX(14);                         Cutter rtn to MRF
      ASS,XX(1)=0.,XX(31)=XX(31)+1;             Count cut
      ASS,XX(9)=XX(1)+XX(2)+XX(3)+XX(4)+XX(5); Total power
      GOON,1;
;           continue cutting
      ACT/15,RNORM(.5,.01),XX(31).LT.XX(35),C1;
;             move to next section
      ACT/16,RNORM(.75,.02),XX(31).GE.XX(35).AND.XX(41).LT.3,S1;
;               stop, wait for 2d cutter
      ACT/17,,XX(41).GE.3,DONE;
 DONE    TERM;
;!!!!!!!!!!!!!!!!!!!!!!     second cutter      !!!!!!!!!!!!!!!!!!!!!!!!!!
;!!!!!!!!!!!!!!!!!!!!!!!!!!!!!!!!!!!!!!!!!!!!!!!!!!!!!!!!!!!!!!!!!!!!!!!!!
  B2 ASS,XX(52)=XX(52)+1
  S2 ASS,XX(32)=0,XX(42)=XX(42)+1;
     EVENT,1;
     EVENT,2;
     ACT/8,XX(28);                             Delay for 2d cutter
     GOON,1;
;!!!!!!!!!!!!!!!!!!!!!!!     make box cut      !!!!!!!!!!!!!!!!!!!!!!!!!!
     ACT/5,XX(25);                             Stagger 2d cutter
     ASS,XX(2)=7050.;                          Cutter power 7 kW
     ASS,XX(9)=XX(1)+XX(2)+XX(3)+XX(4)+XX(5); Total power
     ACT/20,XX(20);                            Cut 1st beam
     ASS,XX(2)=3550.;                          Cutter power 3.5 kW
     ASS,XX(9)=XX(1)+XX(2)+XX(3)+XX(4)+XX(5); Total power
     ACT/21,XX(21);                            C-cut plate
     ASS,XX(2)=7050.;                          Cutter power 7 kW
     ASS,XX(9)=XX(1)+XX(2)+XX(3)+XX(4)+XX(5); Total power
     ACT/22,XX(20);                            Cut 2d beam
     ASS,XX(2)=3550.;                          Cutter power 3.5 kW
     ASS,XX(9)=XX(1)+XX(2)+XX(3)+XX(4)+XX(5); Total power
     ACT/23,XX(23);                            Straight cut
     ASS,XX(2)=0.,XX(32)=1;                    Count 1st cut
     ASS,XX(9)=XX(1)+XX(2)+XX(3)+XX(4)+XX(5); Total power
     GOON,1;
     ACT/25,RNORM(.5,.01);                     Move cutter
```

SCENARIO TWO SLAM PROGRAM (continued)

```
;
        GOON,2;
            ACT,RNORM(1.,.03),,STRP;                    Handoff piece to strpr
            ACT;                                        Continue cutting
;
;!!!!!!!!!!!!!!!!!!!!!      make c cut       !!!!!!!!!!!!!!!!!!!!!!!!!
;
 C2     ASS,XX(2)=7050.;                                Cutter power 7 kW
        ASS,XX(9)=XX(1)+XX(2)+XX(3)+XX(4)+XX(5);        Total power
        ACT/20,XX(20);                                  Cut 1st beam
        ASS,XX(2)=3550.;                                Cutter power 3.5 kW
        ASS,XX(9)=XX(1)+XX(2)+XX(3)+XX(4)+XX(5);        Total power
        ACT/21,XX(21);                                  C-cut plate
        ASS,XX(2)=7050.;                                Cutter power 7 kW
        ASS,XX(9)=XX(1)+XX(2)+XX(3)+XX(4)+XX(5);        Total power
        ACT/22,XX(20);                                  Cut 2d beam
        ASS,XX(2)=50.;                                  Cutter platform 50 W
        ASS,XX(9)=XX(1)+XX(2)+XX(3)+XX(4)+XX(5);        Total power
;
        GOON,2;
            ACT,RNORM(1.,.03),,STRP;                    Handoff piece to strpr
            ACT/24,XX(24);                              Cutter rtn to MRF
;
        ASS,XX(2)=0.,XX(32)=XX(32)+1;                   Count cut
        ASS,XX(9)=XX(1)+XX(2)+XX(3)+XX(4)+XX(5);        Total power
        ACT/7,XX(27);                                   Keep cutters in sync
;
        GOON,1;
;               continue cutting
        ACT/25,RNORM(.5,.01),XX(32).LT.XX(36),C2;
;               move cutter to next section
        ACT/26,RNORM(.75,.02),XX(32).GE.XX(36).AND.XX(42).LT.3,S2;
;               move both cutters to next 2 barrels
        ACT/27,RNORM(7.5,.2),XX(42).GE.3.AND.XX(52).LT.2,G1;
;               done cutting ET
        ACT,,XX(41).GE.3.AND.XX(52).GE.2,QUIT;
 QUIT   TERM;
```

SCENARIO TWO SLAM PROGRAM (continued)

```
;
;!!!!!!!!!!!!!!!!!!!!!!    STRIP SOFI OFF PIECES    !!!!!!!!!!!!!!!!!!!
;
STRP  GOON,2;
      ACT,,,C3;
      ACT;
      ASS,XX(4)=1250;                            Stripper power 1250 W
      ASS,XX(9)=XX(1)+XX(2)+XX(3)+XX(4)+XX(5);   Total power
      ACT/30,XX(30);                             Strip sofi
      ASS,XX(4)=200.;                            Secondary drive motor
      ASS,XX(9)=XX(1)+XX(2)+XX(3)+XX(4)+XX(5);   Total power
      ACT/31,2.0;                                Push piece thru cutter
      ASS,XX(4)=0.;                              Motor off
      ASS,XX(9)=XX(1)+XX(2)+XX(3)+XX(4)+XX(5);   Total power
      TERM;
;
  C3  ASS,XX(3)=5000;                            Cutter 100 ipm
      ASS,XX(9)=XX(1)+XX(2)+XX(3)+XX(4)+XX(5);   Total power
      ACT/32,XX(30);                             Cut beam off
      ASS,XX(3)=0.;                              Cutter idle
      ASS,XX(9)=XX(1)+XX(2)+XX(3)+XX(4)+XX(5);   Total power
      TERM;
      END;
FIN;
```

```
C      These FORTRAN subroutines determine activity durations for
C      the SCENARIO TWO reduction model.
       PROGRAM MAIN
       DIMENSION NSET(100000)
       INCLUDE 'SLAM$DIR:PARAM.INC'
       COMMON/SCOM1/ATRIB(MATRB), DD(MEQT), DDL(MEQT), DTNOW, II, MFA,
      1MSTOP,NCLNR, NCRDR, NPRNT, NNRUN, NNSET, NTAPE, SS(MEQT),
      2SSL(MEQT),TNEXT, TNOW, XX(MMXXV), CUTRAT1,CUTRAT2,CUTRAT3,
      3STRPRATE, TRVLRATE
C
       COMMON QSET(100000)
       EQUIVALENCE (NSET(1),QSET(1))
       NNSET=100000
       NCRDR=5
       NPRNT=6
       NTAPE=7
       NPLOT=2
       CALL SLAM
       STOP
       END
C
       SUBROUTINE EVENT(I)
       INCLUDE 'SLAM$DIR:PARAM.INC'
       COMMON/SCOM1/ATRIB(MATRB), DD(MEQT), DDL(MEQT), DTNOW, II, MFA,
      1MSTOP,NCLNR, NCRDR, NPRNT, NNRUN, NNSET, NTAPE, SS(MEQT),
      2SSL(MEQT),TNEXT, TNOW, XX(MMXXV), CUTRAT1, CUTRAT2, CUTRAT3,
      3STRPRATE, TRVLRATE
C
       CUTRAT1 = 50.
       CUTRAT2 = 10.
       CUTRAT3 = 100.
       STRPRATE = 100.
       TRVLRATE = 120.
C
C      Cut I beam
C
       XX(10) = 1.25/CUTRAT2
       XX(20) = XX(10)
```

SCENARIO TWO FORTRAN subroutines (continued)
```
C
      GO TO (1,2),I
C
C     Number of cuts per section:
C
   1  IF (XX(41) .LE. 1) XX(35) = 37
      IF (XX(41) .EQ. 2) XX(35) = 33
      IF (XX(41) .GE. 3) XX(35) = 19
      IF (XX(51) .LE. 1) THEN
          XX(11) = 245.65/CUTRAT1
          XX(13) = 225.95/CUTRAT1
          XX(14) = 225.95/TRVLRATE
          XX(30) = 225.95/STRPRATE
      ELSE
          XX(11) = 245.4/CUTRAT1
          XX(13) = 225.7/CUTRAT1
          XX(14) = 225.7/TRVLRATE
          XX(30) = 225.7/STRPRATE
      END IF
      RETURN
C          SECOND CUTTER
C
   2  IF (XX(52) .LE. 1) THEN
          XX(21) = 245.65/CUTRAT1
          XX(23) = 225.95/CUTRAT1
          XX(24) = 225.95/TRVLRATE
          XX(30) = 225.95/STRPRATE
          XX(25) = XX(10) + (XX(11)+XX(14))/2.
          XX(27) = 0.
          XX(28) = 0.
C
C          Number of cuts per section:
C
          IF (XX(42) .LE. 1) XX(36) = 37
          IF (XX(42) .EQ. 2) XX(36) = 33
          IF (XX(42) .GE. 3) XX(36) = 19
C
```

SCENARIO TWO FORTRAN subroutines (continued)

```
C
      ELSE
          XX(21) = 182.7/CUTRAT1
          XX(23) = 163/CUTRAT1
          XX(24) = 163/TRVLRATE
          XX(30) = 163/STRPRATE
          XX(25) = 0.
          XX(27) = XX(11)+XX(14)-XX(21)-XX(24)
C
C        Number of cuts per section:
C
        IF (XX(42) .LE. 1) THEN
        XX(36) = 32
        XX(28) = 2.5+10*(XX(10))+5*(XX(11))+4*(XX(14))+XX(13)+2.977
        END IF
        IF (XX(42) .EQ. 2) THEN
         XX(36) = 31
         XX(28) = 0.
         XX(25) = XX(10)+ (XX(11)+XX(14))/2.
        END IF
        IF (XX(42) .GE. 3) THEN
         XX(36) = 19
         XX(28) = 1.+4*XX(10)+2*(XX(11))+XX(14)+XX(13)
        END IF
      END IF
      RETURN
      END
```

SCENARIO TWO FORTRAN subroutines (continued)

```fortran
C
      SUBROUTINE INTLC
      INCLUDE 'SLAM$DIR:PARAM.INC'
      COMMON/SCOM1/ATRIB(MATRB), DD(MEQT), DDL(MEQT), DTNOW, II, MFA,
     1MSTOP,NCLNR, NCRDR, NPRNT, NNRUN, NNSET, NTAPE, SS(MEQT),
     2SSL(MEQT),TNEXT, TNOW, XX(MMXXV), CUTRAT1, CUTRAT2, CUTRAT3,
     3STRPRATE, TRVLRATE
      OPEN(1,FILE='POWER2A.DAT',STATUS='NEW')
      RETURN
      END
C
      SUBROUTINE STATE
      INCLUDE 'SLAM$DIR:PARAM.INC'
      COMMON/SCOM1/ATRIB(MATRB), DD(MEQT), DDL(MEQT), DTNOW, II, MFA,
     1MSTOP,NCLNR, NCRDR, NPRNT, NNRUN, NNSET, NTAPE, SS(MEQT),
     2SSL(MEQT),TNEXT, TNOW, XX(MMXXV), CUTRAT1, CUTRAT2, CUTRAT3
     3STRPRATE, TRVLRATE
C
      SS(1)=XX(1)
      SS(2)=XX(2)
      SS(3)=XX(3)
      SS(4)=XX(4)
      SS(5)=XX(5)
      SS(9)=XX(1)+XX(2)+XX(3)+XX(4)+XX(5)
      WRITE(1,5) TNOW, SS(9)
    5 FORMAT(1X,2F20.8)
      RETURN
      END
```

SIMULATION PROJECT SCENARIO 2   CURRENT TIME   0.1383E+04
                    STATISTICAL ARRAYS CLEARED AT TIME   0.0000E+00

                STATISTICS FOR TIME-PERSISTENT VARIABLES
                   MEAN   STANDARD MIN   MAXIMUM TIME   CURRENT
                   VALUE   DEVIATION VALUE VALUE   INTERVAL VALUE
TOTAL EQUIP USE 9301.383 3252.369 0.00 18850.00 1382.903 2000.00

                FILE STATISTICS
FILE   AVERAGE STANDARD   MAXIMUM CURRENT AVERAGE
NUMBER LABEL/TYPE   LENGTH   DEVIATION LENGTH   LENGTH   WAIT TIME
  1   0.000   0.000   0   0   0.000
  2   0.000   0.000   0   0   0.000
  3   0.000   0.000   0   0   0.000
  4   0.000   0.000   0   0   0.000
  5   CALENDAR   3.819   0.995   7   0   1.304

                REGULAR ACTIVITY STATISTICS
ACTIVITY   AVERAGE   STANDARD   MAX CURRENT ENTITY
INDEX/LABEL   UTILIZATION   DEVIATION   UTIL UTIL   COUNT
  5 Stagger 2d c   0.0102   0.1004   1   0   6
  7 Keep cutters   0.1016   0.3022   1   0   165
  8 Delay for 2d   0.0441   0.2054   1   0   6
 10 Cut 1st beam   0.0161   0.1258   1   0   178
 11 C-cut plate   0.6321   0.4822   1   0   178
 12 Cut 2d beam   0.0161   0.1258   1   0   178
 13 Straight cut   0.0196   0.1386   1   0   6
 14 Cutter rtn t   0.2341   0.4234   1   0   172
 15   0.0622   0.2415   1   0   172
 16   0.0022   0.0470   1   0   4
 17   0.0000   0.0000   1   0   2
 20 Cut 1st beam   0.0155   0.1234   1   0   171
 21 C-cut plate   0.5329   0.4989   1   0   171
 22 Cut 2d beam   0.0155   0.1234   1   0   171
 23 Straight cut   0.0169   0.1288   1   0   6
 24 Cutter rtn t   0.1947   0.3960   1   0   165
 25   0.0597   0.2369   1   0   165
 26   0.0022   0.0465   1   0   4
 27   0.0054   0.0730   1   0   1
 30 Strip sofi   0.5409   0.5870   2   0   349
 31 Push piece t   0.5047   0.5676   2   0   349
 32 Cut beam off   0.5409   0.5870   2   0   349

                              B-44

TIME-PERSISTENT HISTOGRAM NUMBER 1
TOTAL EQUIP USE

```
CELL RELA   UPPER
TIME FREQ  CELL LIM 0        20       40       60       80       100
  31. 0.02 0.500E+04 +*                                           +
   0. 0.00 0.550E+04 +C                                           +
 408. 0.29 0.600E+04 +***************C                            +
   0. 0.00 0.650E+04 +              C                             +
   1. 0.00 0.700E+04 +              C                             +
   0. 0.00 0.750E+04 +              C                             +
   0. 0.00 0.800E+04 +              C                             +
  72. 0.05 0.850E+04 +***           C                             +
   0. 0.00 0.900E+04 +               C                            +
 305. 0.22 0.950E+04 +***********          C                      +
   0. 0.00 0.100E+05 +                     C                      +
   0. 0.00 0.105E+05 +                     C                      +
 139. 0.10 0.110E+05 +*****                     C                 +
   0. 0.00 0.115E+05 +                          C                 +
 244. 0.18 0.120E+05 +*********                       C           +
   0. 0.00 0.125E+05 +                                C           +
  41. 0.03 0.130E+05 +*                                 C         +
   0. 0.00 0.135E+05 +                                  C         +
   0. 0.00 0.140E+05 +                                  C         +
  69. 0.05 0.145E+05 +**                                  C       +
   0. 0.00 0.150E+05 +                                    C       +
  46. 0.03 0.155E+05 +**                                     C+
   0. 0.00 0.160E+05 +                                       C+
   0. 0.00 0.165E+05 +                                       C+
   0. 0.00 0.170E+05 +                                       C+
   0. 0.00 0.175E+05 +                                       C+
  12. 0.01 0.180E+05 +                                       C+
   0. 0.00 0.185E+05 +                                       C+
  15. 0.01 0.190E+05 +*                                       C
   0. 0.00 0.195E+05 +                                        C
   0. 0.00 0.200E+05 +                                        C
   0. 0.00 0.205E+05 +                                        C
   0. 0.00   INF      +                                        C
****                  0        20       40       60       80       100
```

STATISTICS FOR TIME-PERSISTENT VARIABLES

	MEAN VALUE	STANDARD DEVIATION	MIN VALUE	MAXIMUM VALUE	TIME INTERVAL	CURRENT VALUE
TOTAL EQUIP USE	9301.383	3252.369	0.00	18850.00	1382.903	2000.00

Appendix C. *ELECTRICAL POWER SUBSYSTEM (EPS)*

C.1 Initial Trade Study

The first task undertaken to support the EPS design was to survey various energy alternatives to identify candidate sources. Ten alternatives (and their associated derivatives) were explored.

C.1.1 Solar Arrays.

Solar arrays have been the most frequently used space power system since the early 1970's. They have the inherent advantage of supporting multiple configurations, coupled with low launch weights, and minimal EVA installation requirements. Their disadvantages include the need for drive mechanisms to track the sun, batteries to augment the array during the eclipse portion of the orbit, and repair or replacement of the batteries and/or blankets every 5 to 15 years. For the last 20 years, the advantages have continued to outweigh the disadvantages.

Solar arrays have demonstrated the capability to continually adjust to meet the increasing growth demands for spacecraft power. In the 1960's, power needs grew from tens of watts up to kilowatt levels and the solar cells adapted well. Unfortunately, the ability to adapt during this period was also marked by a lack of standardization in satellite solar cell panels. Solar cell arrays continue to be mostly custom designed for specific needs.

Flexibility and modularity to meet increasing power demands has kept photovoltaic (PV) power as the major satellite power source. As other power generating technologies matured for space use, the use of solar cells has been predicted to decline. However, solar cells have continued to flourish under that same threat for 30 years.

In the last 30 years, cell efficiency has doubled for silicon cells and is between 21 - 35% for galium arsenide (GaAs) cells (31, 60, 69, 71, 87, 88, 95, 97, 99). Cell

sizes have also increased by thirty fold and now approach 100 square centimeters. The cell weight per unit area has also been reduced to 1/4 to 1/8 of previous values. Degradation after cell exposure has been reduced 3 to 5 fold (37).

It is not easy to predict when (or if) other power generation technologies will advance to the point where their reliability and possible safety and political advantages can be offset. Solar cell technology has proved to be very reactive to new demands and solar arrays will continue to present a moving target to competitive technologies.

C.1.2 Organic Rankine Cycle (ORC). The ORC system is similar to conventional steam Rankine cycle systems. ORC power conversion systems can be couple to various heat sources (isotopes, solar collectors, or reactors). In addition to the heat source, the major system components consist of a boiler, turbopump-generator, regenerator, and radiator as shown in Figure C.1 (16). A working fluid is selected (toluene and RC-1 are typical) to achieve high cycle efficiencies at moderate peak cycle temperatures. Efficiencies of 18 - 25% are projected (16).

A ground demo unit has been developed by Sunstrand Corp. for the Department of Energy (DOE). The heat source is an isotope (Pu 238) and output power levels up to 1.3 kW have been demonstrated. Currently, a 7 year development program is planned by the DOE and the goal is to demonstrate the necessary technology required to provide space power in the 1 to 10 kW range for use in the early 1990's and beyond (16).

The technology issues for the isotope driven ORC EPS include two- phase boiling and condensing in a zero gravity environment, possible decomposition of the working fluid, isotope availability and cost, and safety. A Grumman Corporation design for a condenser and heat pipe radiator developed for Space Station's solar dynamic power system has eliminated the uncertainties associated with two- phase conditioning (16). The DOE has determined that the other areas of concern are
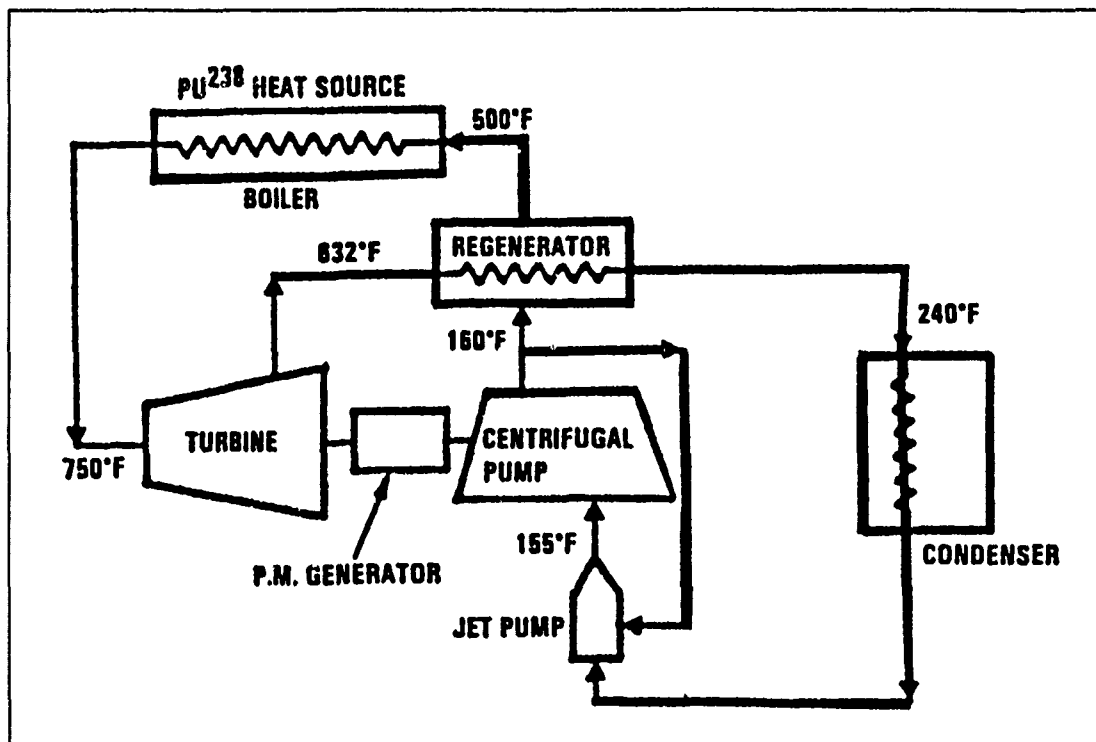
Figure C.1. ORC EPS Components and Typical Cycle Conditions

workable.

The technology issues for the solar collector driven ORC EPS include the additional requirement for an LiOH thermal energy storage subsystem (to provide heat during the eclipse portion of the orbit), collector concentration ratio and pointing accuracy, peak and part load operating characteristics, receiver aperture optimization, and structural dynamic interactions. Various derivatives of this system are currently being investigated by TRW (3 kW solar dynamic mercury rankine cycle), Sunstrand/USAF (ASTEC 15 kW solar dynamic rubidium rankine cycle), and JPL in conjunction with Barber-Nichols (25 kW system for the DOE) (16).

Reactor driven ORC EPS systems are also in various stages of development. A considerable technology base exists for these reactors from the earlier 3 kW SNAP-2

program and the 35-50 kW SNAP-8 program. Los Alamos National Lab (LANL) is developing a compact nuclear power source (CNPS) to deliver 25 kW with an advertised 20 year life and 20 - 30% cycle efficiency. LANL is also pursuing lithium cooled reactor (LCR) technology for SP-100 applications between 100 - 300 kW with the goal to achieve technology readiness by 1995 (16).

Nuclear power, in general, seems to be plagued by problems of a political rather than technological nature. Nuclear power offers the advantages of providing adjustable power loads over wide ranges, hardened structures, low visible signatures, and long life operation. Their disadvantages include the safety concerns (during fabrication, launch, accident, and reentry), higher thermal signatures, higher weight at lower power levels, (38, 76) and more demanding analysis and testing. To date, the U.S. has launched only nuclear isotope power systems (Pu 238) allowing the generation of about 1 kW (6).

C.1.3 Closed Brayton Cycle (CBC). The closed Brayton cycle (CBC) system is similar to conventional gas turbine heat engines except that the working fluid is recirculated in a closed-loop fashion rather than being emitted as exhaust to the atmosphere. The major components of a CBC system are shown in Figure C.2 (16). The same heat sources (isotope, solar collector, or reactor) may be used in this application as well. The technology issues remain the same as for the ORC.

Garrett-AiResearch Corp. has developed a 1.3 - 2.0 kW demonstrator. It is Pu-238 isotope driven (10 kW is believed to be the upper limit for this heat source) and is advertised at 25 - 28% cycle efficiency (16).

C.1.4 Free Piston Stirling Engine (FPSE). Power is produced in Free Piston Stirling Engines much like conventional gas cycle engines. Helium is a very common working fluid and a separate lubrication system is required. Engine weight and operating life were primary concerns in early designs (working fluid was frequently contaminated by the lubrication fluid). Common heat sources (isotopes, solar collec-
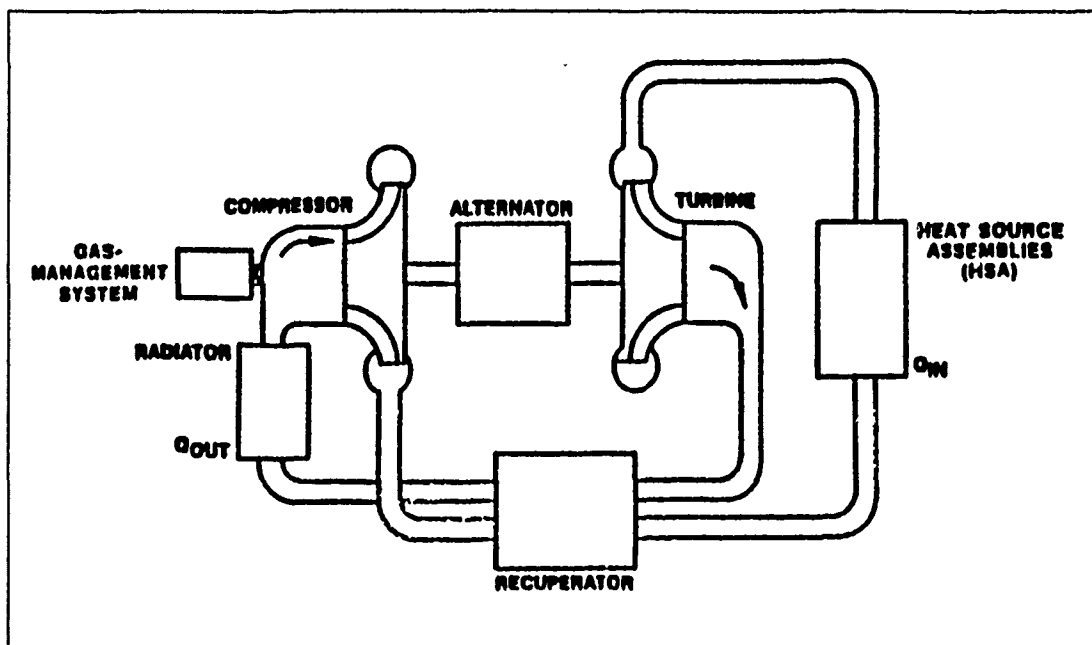
Figure C.2. Typical Closed Brayton Cycle Flow Diagram

tors, and reactors) are also applicable (along with their associated set of technology problems).

General Electric (GE) has built a Stirling Isotope Power System (SIPS) for the DOE which delivers 1.112 kW and operates at approximately 25% cycle efficiency. Mechanical Technology Inc. has designed the Space Power Demonstration Engine (SPDE) which delivers 12.5 kW (collector or reactor driven) and operates at approximately 25% cycle efficiency. Rockwell and JPL are working on a 100 kW reactor driven variant for SP-100 applications (16).

C.1.5 Potassium Rankine Cycle (PRC). This form of power system is also known as the liquid metal potassium rankine cycle (LMKRC). Liquid metal is the working fluid for this power system. GE and Pratt & Whitney conducted preliminary research for this device in the early 1960's. A SNAP- 50 reactor driven 300 kW system was the design goal with 20% cycle efficiency (16). The lack of a mission

coupled with high temperature corrosion problems led to program termination in the 1960's. However, the Strategic Defense Initiative (SDI) has revived interest in possible applications.

C.1.6 Alkaline Metal Thermionic Conversion (AMTEC). AMTEC, sometimes referred to as the Sodium Heat Engine (SHE) has the potential fro providing direct energy conversion for a space nuclear power system. An efficiency of 19% has been demonstrated in the lab and calculations indicate that 25 - 30% conversion efficiency may be achieved with an optimized design (16). Research is ongoing at JPL, but is geared toward SP-100 applications.

C.1.7 Supercritical Cycle Power Systems. This variant of power system uses regeneration to increase the efficiency of the more common Rankine, Brayton, of Stirling closed cycle power systems. Supercritical Cycle systems are so named because their working fluid must work in the supercritical region (that regime above it's critical pressure and temperature). In that region, the density of liquid and vapor at any given state is the same (which nicely resolves the problem of two phase boiling and condensing in a zero gravity environment).

Most of the work in this area is on the development of a suitable working fluid; the most common being $CO-2$, SO_2, or NH_3 (16). To date, most of the work has been done with CO_2 (also referred to as the Feher cycle). A typical schematic of the closed form of the supercritical cycle is shown in Figure C.3 (16). Note that this is a high pressure cycle, and because of this the performance characteristics of the turbomachinery are not suitable for power levels below 25 kW.

C.1.8 Thermoelectric Conversion (TEC). Thermoelectric conversion (TEC) cycles have had extensive application in space power systems. The primary use has been in the area of low power generation (5 - 150 Watts). Current research is centered on using collector or reactor driven TEC which has been hardened to meet
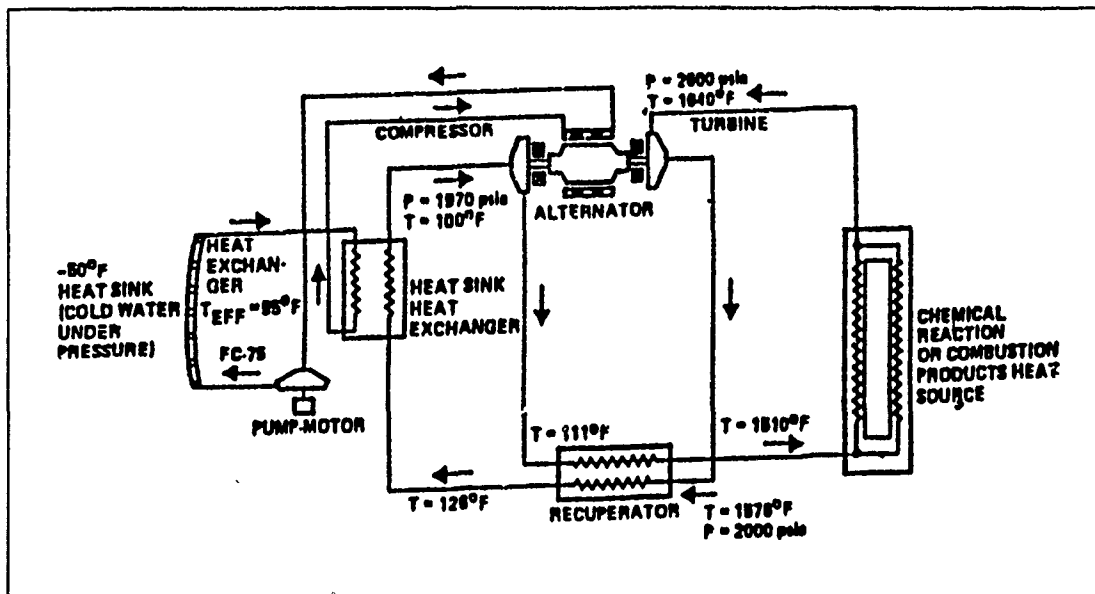
Figure C.3. Typical Closed Form Supercritical Cycle

the various military space threats.

C.1.9 Thermionic Conversion Systems. Thermionic power conversion is based upon the use of a vacuum diode utilizing a temperature difference, and employs electrons as the working fluid. Thermionic converters (like thermoelectric converters) are subject to Carnot cycle efficiency limitations, the maximum efficiency being limited by the absolute temperature of the source and sink. Most of the work in this area is geared toward reactor driven variants with an eye toward SP-100 applications.

C.1.10 Tethers. Drag compensation and orbit altitude changes are the main propulsive mission identified for tethers. Power generation in a stand-alone mode with rocket make-up has been shown to offer potential fuel savings when compared to fuel cells, but the system mass and complexity are increased due to large magnetic field and electron density fluctuations over one orbit. Energy storage for solar array systems is also a possibility, but is not by itself mass-competitive with conventional

battery systems (over dimensioning is required for tether voltage fluctuations) (32).

Important uncertainties still exist that make it difficult to arrive at definitive design decisions and performance estimations at this time. The ionospheric circuit impedance is unknown, the performance of contactors is unknown, and the high voltage insulation technology for this purpose has not been tested (32). The uncertainties involved with tether dynamics will also require further testing and verification.

C.1.11 Conclusion. This trade study turned out to be somewhat diluted. A full-blown trade was initially envisioned where specific power densities, system masses, and development costs would be traded against each other to determine the optimum power source for the ASSET facility. Low cost and low risk were always considered as prime drivers. If one were to limit the ASSET power to 25 kW, and then ask how many of the candidate systems have a demonstrated capability to deliver 25 kW, one would find that solar arrays are the only viable alternative. Other alternatives could clearly be developed, but it is clear that such development carries both an increased cost and risk.

Our sponsor specifically asked that we quantify the tradeoffs between PV arrays and the solar dynamic option (since that is the intended growth mode for SSF) (13). The contrasts between the two are provided in Table C.1.

Table C.1. Solar Dynamic vs. PV Array Comparisons

	Solar Dynamic	PV Array
Overall sun to user efficiency	18 - 20%	6 - 7%
Drag impacts on ASSET	276 m^2	714 m^2
Weight (75 kW systems, lbs)	42,858	26,936
Sun Tracking Rqmts (degrees)	0.1	2.0
EVA Set-Up Time (hours)	>8	<2

C.2 Battery Trade Study

C.2.1 Evolution. When we originally started this effort, it was not clear whether we even wanted batteries to augment the solar array. Preliminary work was conducted and it was found that batteries are a major contributor to total EPS weight (16). Furthermore, they are probably the first component of the EPS to require maintenance actions (67). By the same token, batteries can provide power during the eclipse portion of the orbit, provide emergency power during primary failure, and normally impact the total EPS cost by < 10% (68).

The question of batteries vs. no batteries was basically overcome by events once we discovered we needed to salvage the tank as quickly as possible. Thus, operation during the eclipse portion of the orbit became a given. Once it was known that batteries would be used, the focus shifted to the type of battery which should be selected for ASSET applications.

C.2.2 Alternatives Evaluated. Nickel-cadmium (NiCd) and nickel-hydrogen (NiH$_2$) are both viable candidates within the current state of the art. Both NiCd and HiH$_2$ batteries have a proven space heritage and examples of each are shown in Figure C.4 (16) and Figure C.5 (16). NiCd has the chief advantage of having 40% smaller volume than NiH$_2$ (16). On the other hand, NiH$_2$ batteries have a longer cycle life (5, 22, 59, 83, 96), a higher energy density (72), and 15% lower weight (16) than their NiCd counterparts.

The current trend in technology is to provide higher energy densities (measured in watt hours per kilogram, Wh/kg, or in Wh/lb). Two battery technologies have been identified and are currently being developed under the auspices of the High Energy Density Rechargeable Battery (HEDRB) development program (16).

Gould is developing a HEDRB using lithium iron disulfide (LiFeS$_2$) technology. Eagle-Picher Corp. is developing a HEDRB using sodium sulfur (NaS) technology. The goal is a 110 Wh/kg battery with a ten year life length. Meeting the HEDRB
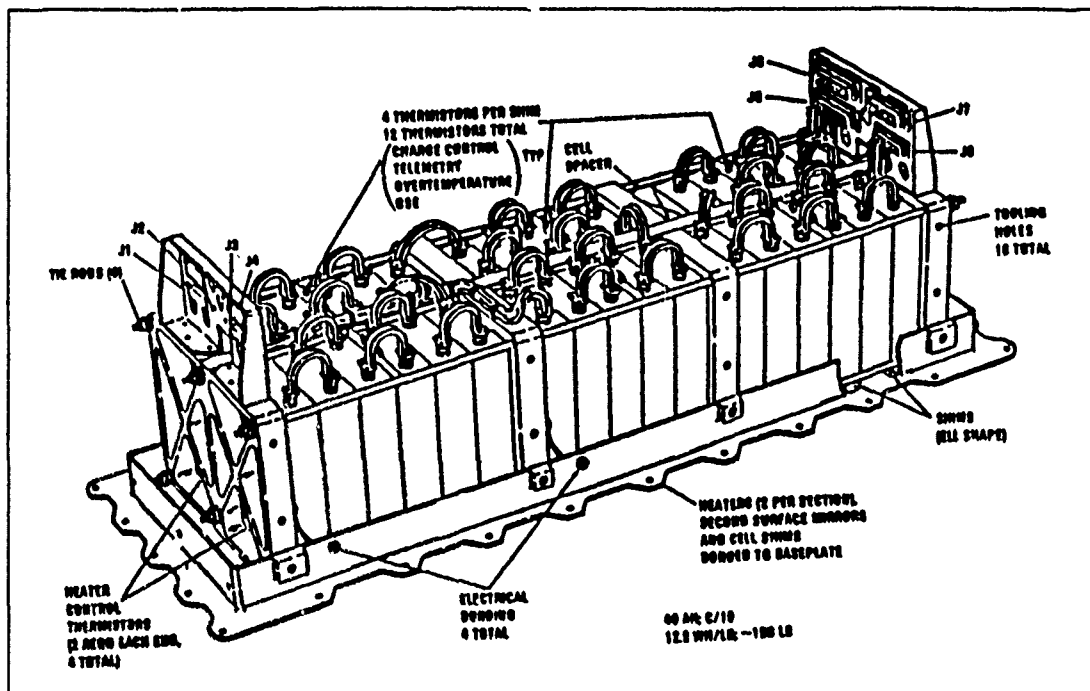
Figure C.4. Typical Nickel-Cadmium Battery

energy density goal would reduce battery weight by 80% as compared to NiCd batteries and by 60% as compared to NiH$_2$ batteries (16). This translates to a saving of 1250 kg (versus NiCd) for a 25 kW system.

Operating on the assumption the shuttle orbiter is weight limited rather than volume limited, NiH$_2$ was selected as the baseline ASSET battery. SSF batteries are also NiH$_2$ (86) and are rated at 81 amp hours (AH; a fully charged battery could deliver 81 amps for 1 hour). We decided to adopt the same type of battery rather than try to develop a battery with higher energy density and corresponding lower weight. Again, lower cost and risk were the primary drivers which led to the selection.

C.2.3 Impacts On The ASSET Facility. Aside from the weight factor previously mentioned, batteries have a significant impact on the thermal control sys-

C-10
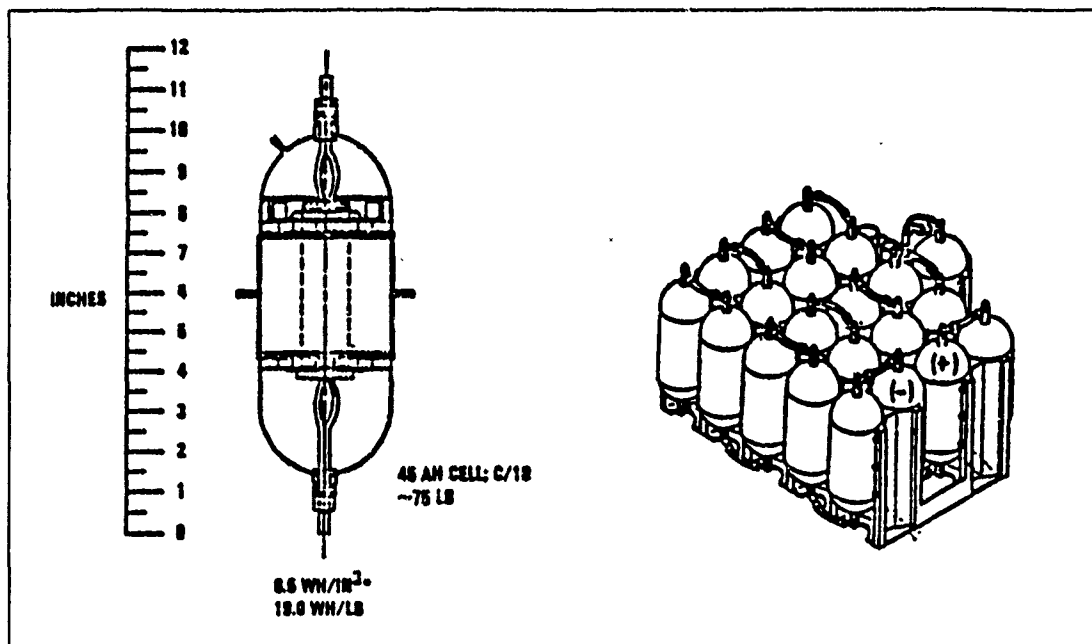
Figure C.5. Typical Nickel-Hydrogen Battery

tem (98). ASSET will demand battery power when the eclipse starts. The battery generates a large amount of heat during its discharge (even with a well designed heat removal system, the battery temperature is expected to rise rapidly during this discharge).

At the end of the eclipse and as soon as the solar array can provide power, the battery is charged to be ready for the next eclipse discharge. The beginning of the battery charge cycle results in a brief period of endothermic operation during which the battery cools rapidly. Battery heaters are required to prevent the battery from reaching an undesirably low temperature.

As the battery approaches overcharge it becomes exothermic and its temperature increases again. It is desirable to fully charge the battery well before the next eclipse begins and its temperature controlled to prevent overheating during the eclipse discharge.

A good battery design must satisfy 4 constraints:

1. Maximum temperature must remain below a set value to avoid damage to the battery of shortening its life.

2. Minimum temperature must not be too low to reduce its efficiency of even freeze the battery and render it inoperable.

3. As the battery nears full charge, its voltage must be lower than the available solar array charge voltage so that the charge can continue.

4. Charge current must be sufficiently high so full charge can be achieved before the next eclipse.

Batteries are normally operated and maintained at $0 \pm 5°C$ (with contingency ops of -5 to +15 °C) (86:290). The baseline Space Station Freedom batteries (see Figure C.6 (78:269)) are designed for an orbital replacement unit (ORU) which is installed in a free space environment. Batteries may be left in the free space environment (if we adopt a concept similar to SSF integrated equipment assembly (IEA)) or could be installed in the intertank area.

C.3 Space Station Freedom (SSF) EPS Baseline

C.3.1 Introduction. Since the initial power budget estimates called for a 25 kW system, once the decision to incorporate a photovoltaic (PV) array augmented with batteries had been reached, the next logical step seemed to be to gain an understanding of the SSF EPS. The SSF EPS design is governed by several competing factors. The foremost is the power requirement, which demands 75 kW of power at the end of Phase I (23, 93). Only slightly less important are the factors of initial and life cycle costs, total mass, maintainability, reliability, and safety (36). When SSF's EPS is compared with previous space power designs, two major differences stand out.
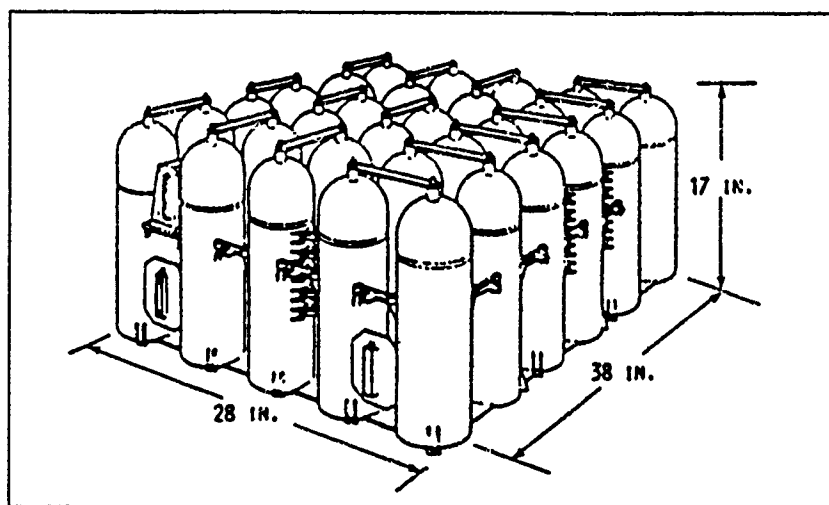
Figure C.6. SSF Battery ORU, November 1987 Baseline

The first is the size of the EPS, which is larger than any previously launched system. Satellites typically have power systems on the order of 1 kW. Skylab generated 12 kW and the Space Shuttle Orbiter generates 22 kW from it's fuel cells, although only a third of this is usually in use (93). The Soviets are credited with testing at least two nuclear powered satellites of around 10 kW each, while Mir, their largest space structure, has been augmented to supply around 12 kW of power through it's solar arrays (93).

The second major difference between the EPS and other space power designs is the expected life length of SSF. The station is intended to be capable of an indefinite life (although 30 years has been used for life cycle cost calculations) (23, 48). To maintain life indefinitely, maintenance and resupply of the system must become an integral factor in assessing the design. The EPS must be able to grow and adapt to greater user needs and future technological advances.

C.3.2 Power Generation. Phase I power will be generated by eight PV wings 34.7 m long by 10.3 m wide (113.7 ft x 33.8 ft) (93:246) as shown in Figure C.7 (78:268). Each wing will consist of two solar blankets made up of 84 panels of 200 large (8

cm x 8 cm) silicon solar cells each. Each solar cell produces approximately 2.4 amps when operated at 0.4 volts. The 400 cells of every two panels are connected in series and controlled by a sequential shunting unit to produce the nominal 160 Vdc output voltage.

The size of these solar cells is larger than any previously used silicon solar cells. Because of the large surface areas, the cells are more efficient, less expensive to manufacture, weigh less, and have a longer life than previous cells. The solar arrays themselves will be automatically deployed by a retractable mast made from coilable continuous longerons (see Figure C.8 (67:2-5)). The solar arays can be folded together in an accordion-like fashion when the mast is stowed, producing a light and compact storage configuration (see Figure C.9 (67:2-6)) that will fit into the Space Shuttle cargo bay (see Figure C.10 (67:1-54)).

The technology used on the Space Station Freedom Solar Array (SSFSA) design is based largely on the Solar Array Flight Experiment (SAFE) (8, 45, 46) while taking advantage in advances in large solar cell design and adding protection for the array from the LEO atomic oxygen (AO) environment. (2, 62, 63, 80, 89)

When directly facing the sun, each solar array wing will be capable of generating 23.4 kW of power (measured 4 years after initial deployment) (8). All eight wings combined will generate 187.2 kW, over twice the required 75 kW (93). However, nearly half of this power will be used to charge batteries for use during the eclipse portion of the orbit. At the planned orbit altitude of 335 to 460 km (180 - 250 nmi) the orbit period will be 91 to 94 minutes and the eclipse period will vary between 28 and 36 minutes, depending on the season of the year and the angle between the sun's ecliptic plane and the orbit plane (93).

Due to stringent power requirements and weight limitations, nickel- hydrogen (NiH_2) batteries were selected to supply power during the eclipse (78). NiH_2 batteries have accumulated over 28,000,000 on-orbit cell hours over the last 6 years. For a
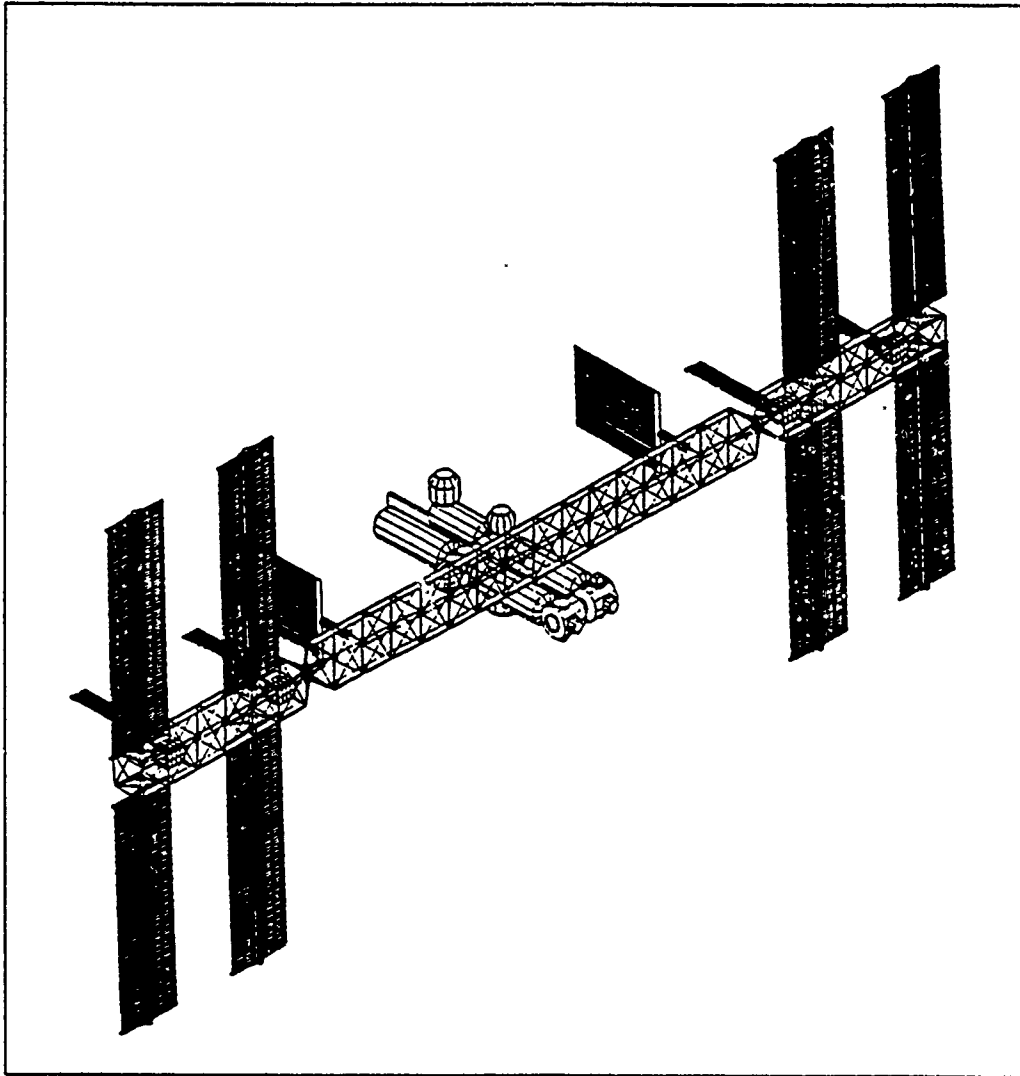
Figure C.7. Space Station Phase I Baseline Configuration
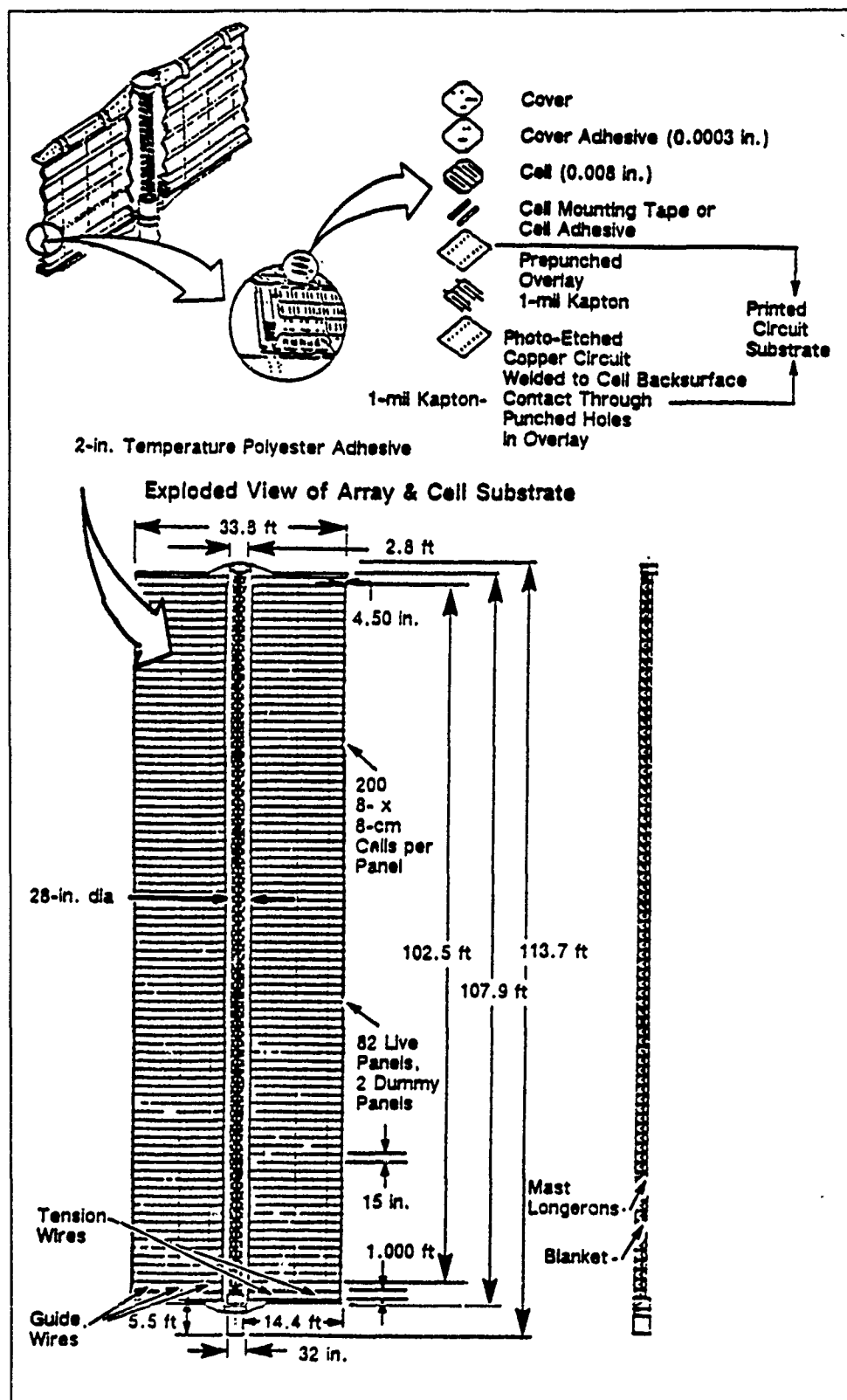
Figure C.8. Space Station PV Array Assembly

C-16
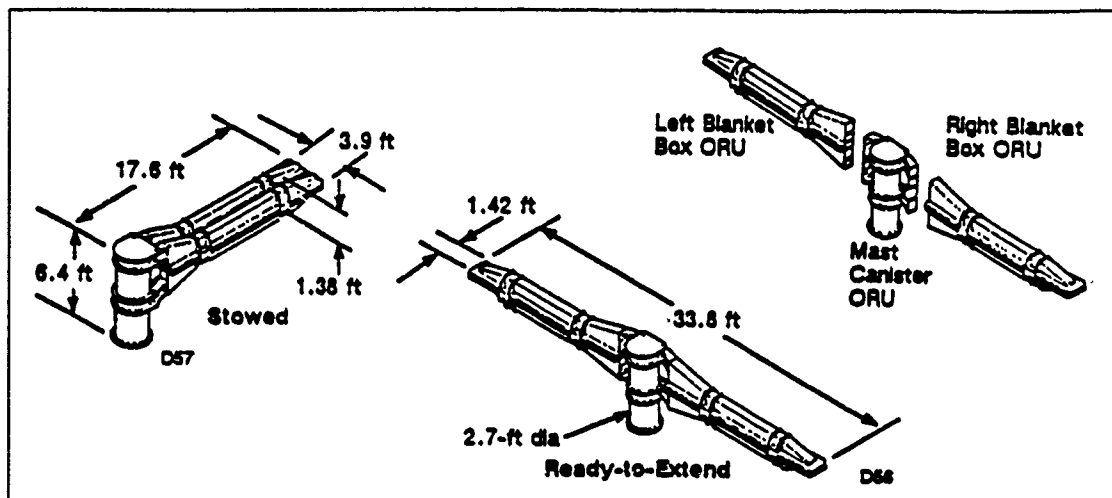
Figure C.9. Space Station Solar Array Assembly ORU's
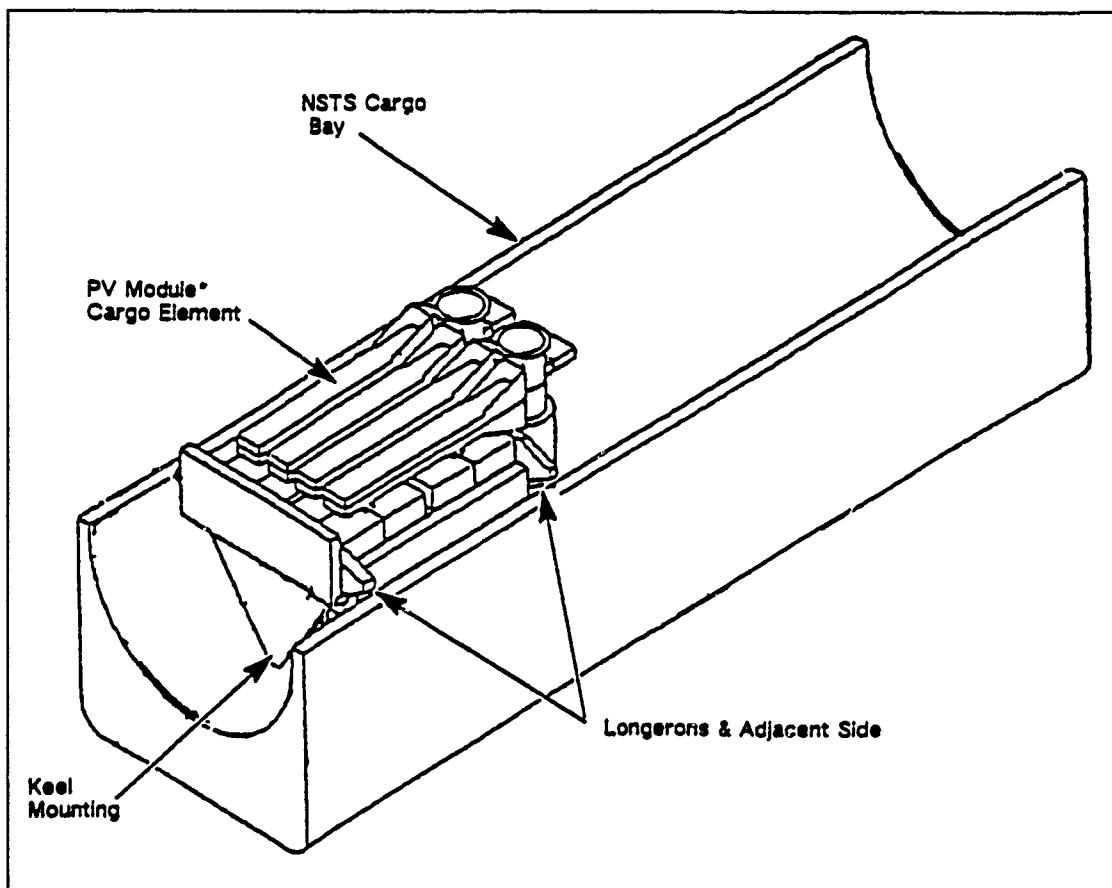
Figure C.10. PV Module Launch Configuration
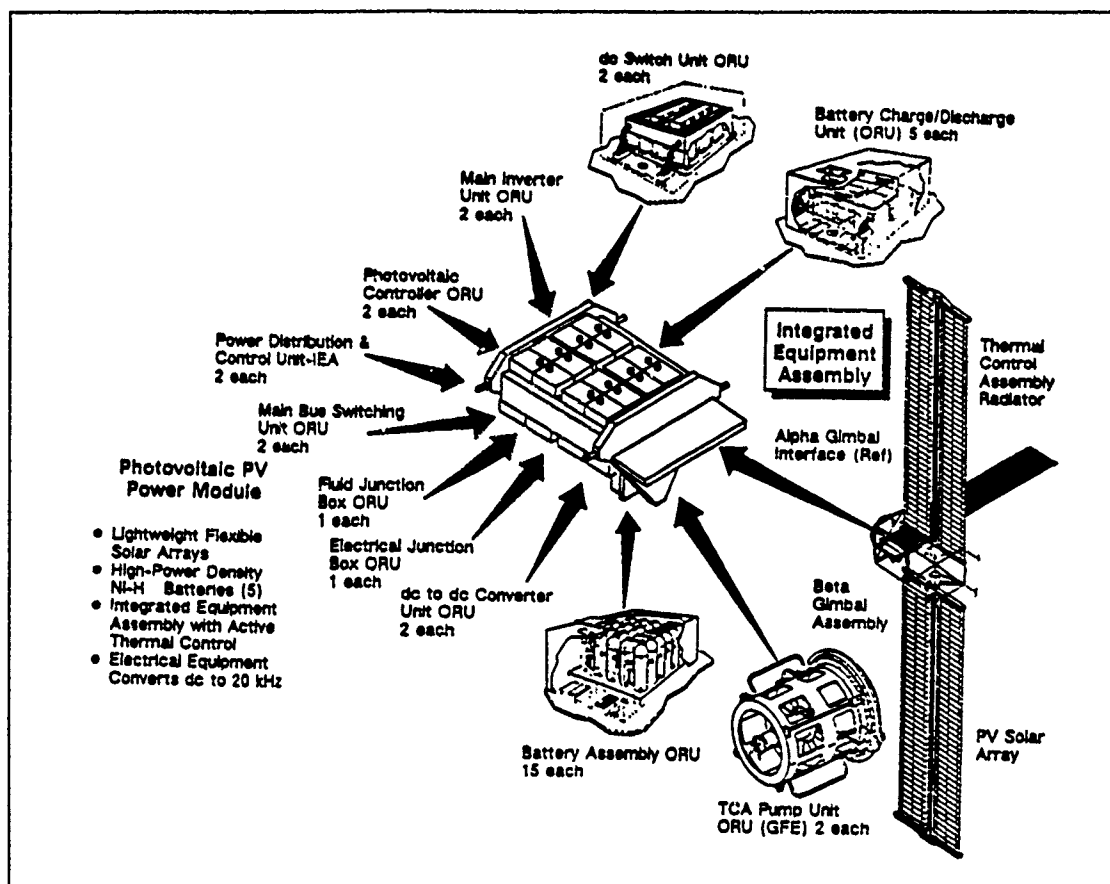
Figure C.11. PV Module Description

Weibull distribution with a 45,000 cycle mean cell life and a beta (shape factor) of 12, the 5 year battery probability of success is 0.9997 (86).

A twenty battery complement, consisting of 90 cells each and having a nominal capacity of 81 amp-hr will be used (40, 93). This system was chosen because of it's good discharge characteristics, light weight, and inherent overcharge protection. The configuration of a PV module, complete with arrays, batteries, and supporting hardware is shown in Figure C.11 (93:247).

It is instructive to consider just what makes up a 'battery' at this point. Figure C.11 points out that there are 15 battery assembly ORU's per PV power module. An individual battery 'ORU' (86) has the following characteristics:

- ORU is comprised of 30 81 amp-hr cells

- Cells are connected in series to produce 37.5 volt output

- Dimensions = 38" x 28" x 17"

- Weight = 81.5 kg (179.3 lb)

- Normal eclipse depth of discharge (DOD) = 35%

- Contingency DOD = 80%

The actual ORU enclosure functions to transport heat from the assembly baseplate to the thermal bus, provides electrical connections, and provides structural support.

An individual 'battery' is comprised of 3 ORU's connected in series (40) and has the following characteristics:

- 3 ORU's in series produce 112.5 volt outputs

- Nominal discharge power = 112.5 volts x (35% x 81 amp-hr) = 3189.4 Watts

- Total battery weight per PV module = 2689.5 lbs

C.3.3 Power Distribution. The overall system architecture is shown in Figure C.12 (39:309). The output from the energy collection, storage and conversion portion will be 160 Vdc. The system protection and distribution provides both DC to DC and DC to AC converters and delivers power in the form of 208 Vac or 120 Vdc at the standard user connection. The Standard user connections can be further downconverted, but the user will be charged for conversion inefficiencies.

C.3.4 Power Management and Control. As shown in Figure C.12, the management and control subsystem has global coordination responsibility for the end-to-end power system. The functional responsibilities of resource management, power scheduling, network analysis, state estimation, and contingency planning are all contained with this subsystem. The design effort for this subsystem will drive approximately 50% of the DT&E costs (68).
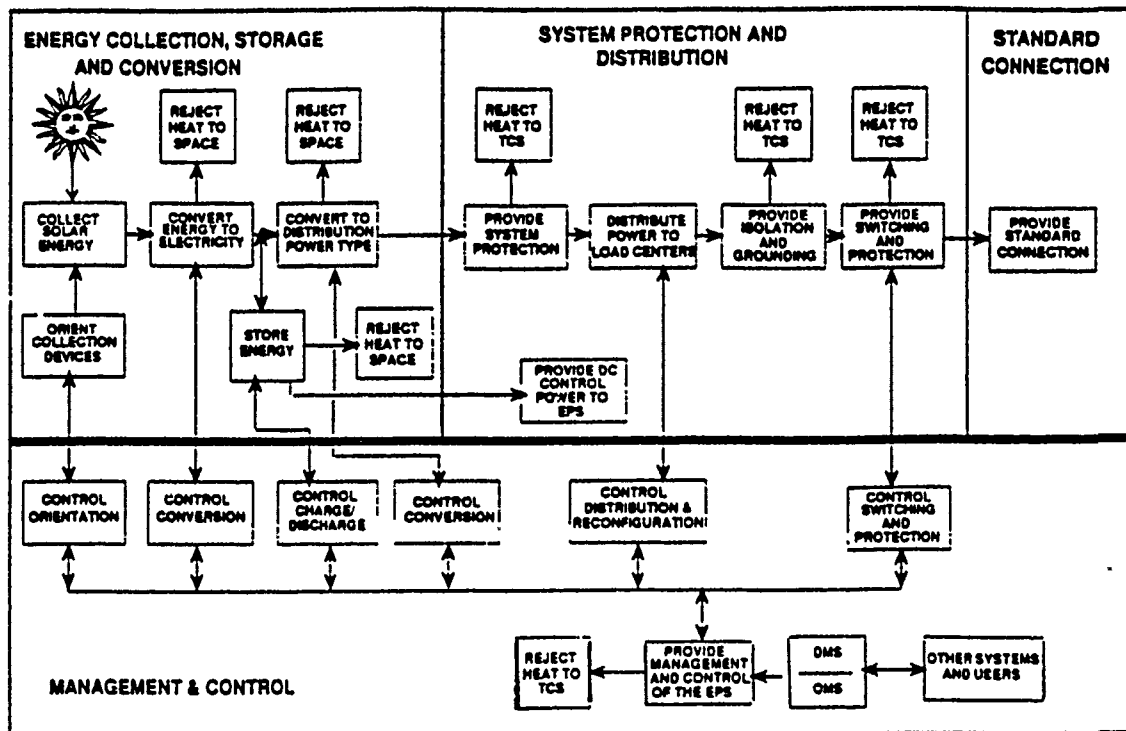
Figure C.12. EPS Top Level Functional Diagram

C.4 Power Flow per PV Module

C.4.1 Orbital Average Power. Orbital averaging is the normal mode of operation for SSF (86:289). This concept will be explained in more details by two different methods. The first is a 'brute force' method and is shown, at a very high level, in Figure C.13. The term 'brute force' is derived from the method from which the base of array (BOA) power is calculated:

$$\text{BOA Power} = \psi A_{bl} p_f \eta_{array} X_{degr}$$
$$= \psi A_{active} \eta_{array} X_{degr}$$
$$= 60.2294 kW$$

where

ψ = solar flux = 1.35 kW/m^2

A_{bl} = solar blanket area = 566 m^2
single panel = 153.32" by 14.2' = 1.6842 m^2
84 panels/blanket = 141.4741 m^2
4 blankets/PV module = 566 m^2

p_f = packing factor
single circuit (2 panels) require 400 cells
cells are 8cm x 8cm
$(400)(8)(8) = 2.56$m^2
cell area/panel area $= \frac{2.56}{2(1.6842)} = 0.7600$

A_{active} = active array surface area
2 dummy panels/blanket
8 dummy panels/PV module
8 panels x 1.6842 = 13.4736 m^2
= (packing factor)(blanket area - dummy area)
= (0.7600)(566-13.5)
= 419.9 m^2

η_{array} = solar cell efficiency = 12.5%

X_{degr} = degradation factor = 85%
(Array will decrease 15% over 5 years)

The 60.2294 kW at the base of the array (BOA), shown in Figure C.13 at the junction of the PV arrays, is routed to two places. 51% of the BOA power is routed to the electrical equipment subsystem (EES) where DC to DC and DC to AC conversion takes place. The conversion losses leave the EES with an efficiency of 0.8431 (40). The power management and distribution (PMAD) equipment accounts for the distribution losses and has an efficiency of 0.8953 (40). Thus, the 30.7170 kW delivered to the EES ends up as 23.1860 kW delivered to the user for 54.8 minutes of the orbit.

The remaining 49% of BOA power is routed to the battery charge/discharge units (BCDU's) to charge the batteries during the sunlit portion of the orbit. The charge and discharge efficiencies of the BCDU's are slightly different because the batteries work in different temperature regimes during the two operations.

The complement of 5 batteries, operated at 35% DOD, (86) will deliver 15.9469 kW to the BCDU's during the eclipse portion of the orbit. Tracing this power

23.1860 kW System

11.5833 kW Loads

ORBIT ALTITUDE = 180 nm
SUNLIGHT = 54.8 min.
ECLIPSE = 36.4 min.

PMAD
.8953

25.8975kW
12.9379kW

EES
.8431

BCDU
$n = .9623$

30.7170
15.3457

N_1H_2
Batteries

15.9469

29.1524

$n = .9357$

27.6148

60.2294

PV ARRAY

PV ARRAY
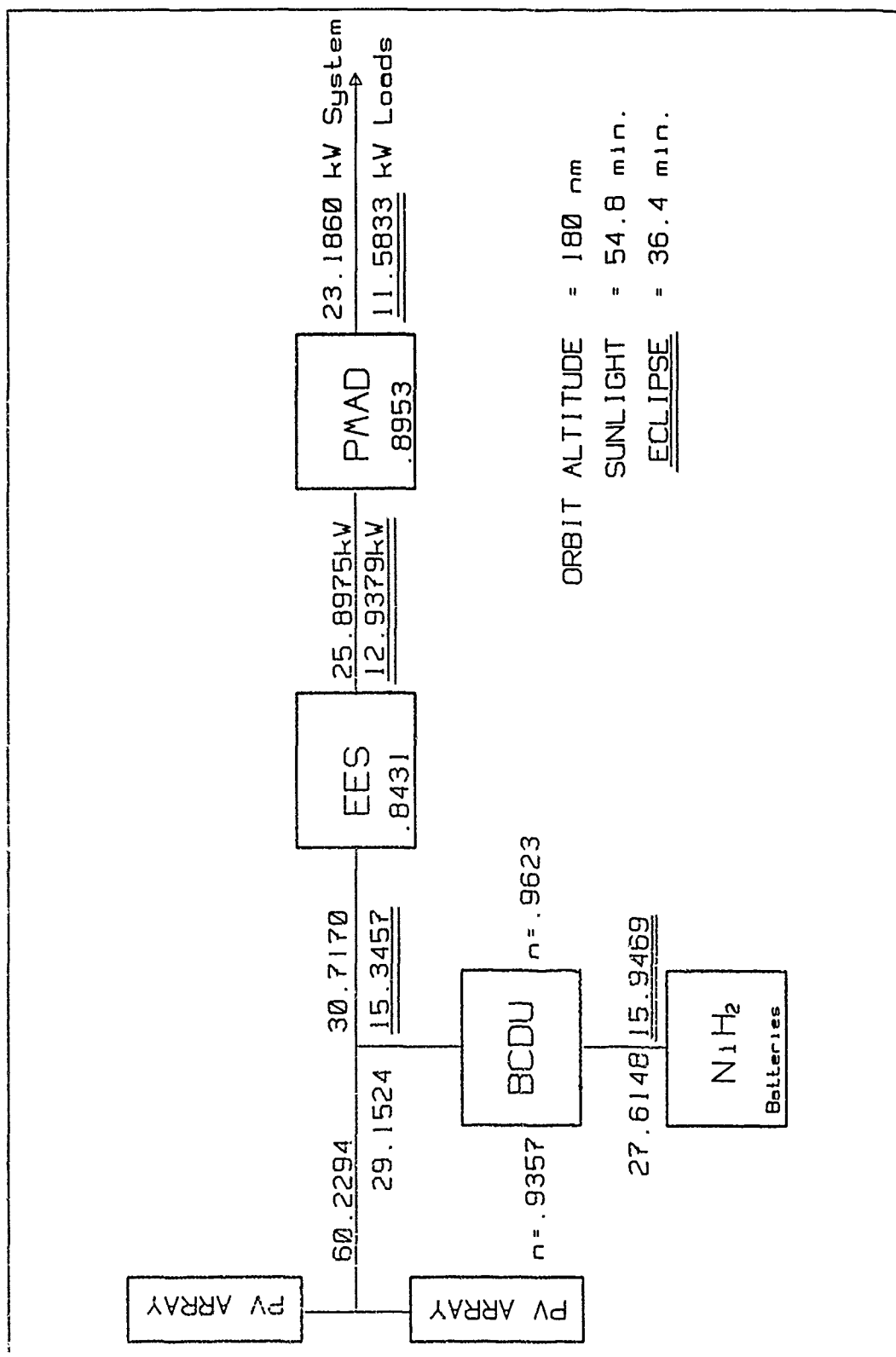
Figure C.13. 'Brute Force' Orbital Average Power Flow Diagram

C-22

through the various inefficiencies in the system results in 11.5833 kW delivered to the user during the eclipse portion of the orbit. One begins to appreciate the difficulties involved with load scheduling (12) since the power available during the sunlit portion of the orbit is more than twice that available during the eclipse portion of the orbit.

The orbital average power is calculated as shown below:

$$\text{Orbital Avg. Power} = \frac{54.8}{91.2}(23.1860) + \frac{36.4}{91.2}(11.5833) = 18.5551\text{kW}.$$

Using the 'brute force' method, one finds that 4 PV modules x 18.5551 kw/module yields a SSF power of 74.22 kw at the 5 year life point.

A very similar method can be used, as shown in Figure C.14. This method was revealed during telephone conversations with NASA Lewis (34) and is a shortcut method (thus referred to as the NASA shortcut method) for finding the BOA power. The NASA shortcut method is built on the following:

- There are 65,600 cells per PV module

- Each cell operates at 0.4V & 2.4A at the 4 year life point

- 1 circuit is comprised of 2 solar array panels

- 400 cells per circuit yield 160 Vdc @ 2.4A

- 65,600 cells/400 cells per circuit = 164 circuits

- 164 circuits @ 160V & 2.4A = 62.9760 kW at 4 years life

This new BOA power can be traced through Figure C.14 in the same fashion as before. Using the NASA shortcut method, one finds that 4 PV modules/SSF x 19.1905 kW/module = 76.76 kW at the 4 year life point. As before, the power available during the sunlit portion of the orbit is more than twice the value of the available power during the eclipse portion of the orbit.
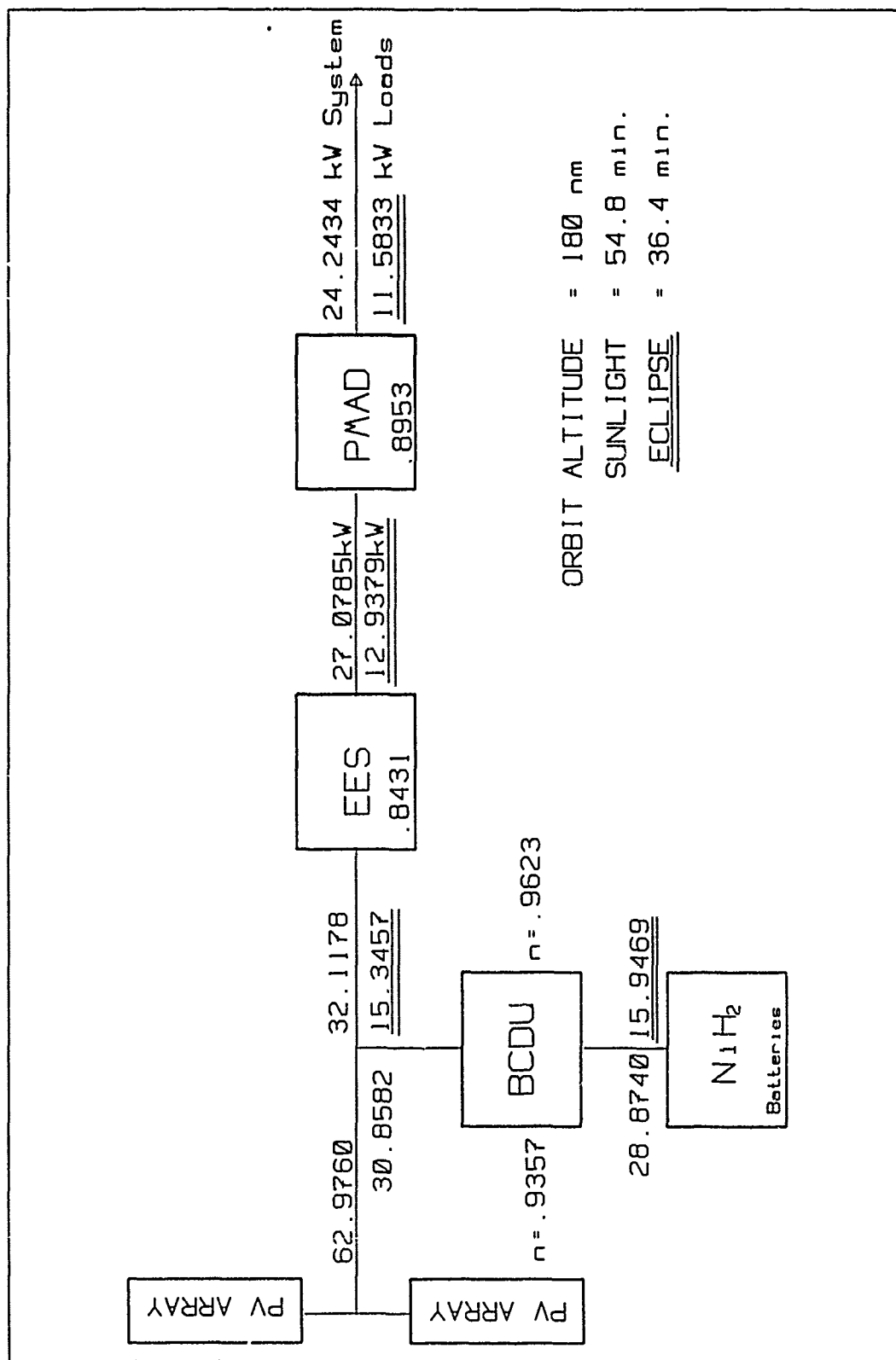
Figure C.14. 'NASA Shortcut' Orbital Average Power Flow Diagram

C.4.2 Alternative Constant Power System. One might ask whether the EPS system could be driven such that the available load power is constant during all portions of the orbit. The answer is yes, as shown in Figure C.15, but the impacts of operating in such a fashion must be clearly understood. The same BOA power as was used in the NASA shortcut method is used again for explanation purposes. The only difference from before is the power that must be delivered from the batteries during the eclipse portion of the orbit.

As previously pointed out, the complement of 5 batteries is operated at 35% DOD to deliver 15.9469 kW to the BCDU's during the eclipse portion of the orbit. To supply the required power shown in Figure C.15, a 5 battery complement would have to be operated at 73.25% DOD. Driving the batteries at this DOD has severe impacts on the battery life length. One could provide more batteries, but at 537.9 lbs per battery (which excludes a 400 lb utility plate), the weight penalty adds up very quickly.

The bottom line is that constant load power can be delivered (which simplifies the load scheduling problem), but only at the expense of increased weight (more batteries) or life length of the current battery complement.

C.4.3 %DOD vs. Life Length. Battery life length is very sensitive to DOD. A plot used to calculate life lengths as a function of DOD is provided as Figure C.16 cite[294]array8. The shaded region of the figure shows that NiH_2 batteries are normally operated between 35 - 50% DOD. The vertical axis represents the expected number of charge/discharge cycles which may be experienced prior to failure. One then calculates the number of charge discharge cycles per year for a given orbit (5,840 per year for our purposes) and computes a life length (hopefully in years) for the battery in question.

There is almost no data available on life length for batteries operated at DOD above 50%. Conversations with NASA Lewis (85) revealed that some lim-

24.2434 kW System

24.2434 kW Loads

ORBIT ALTITUDE = 160 nm
SUNLIGHT = 54.8 min.
ECLIPSE = 36.4 min.

PMAD
.8953

27.0785kW
27.0859kW

EES
.8431

32.1178
32.1178

BCDU
n = .9623

33.3761

62.9760
30.8582

n = .9357

28.8740

N_1H_2
Batteries

PV ARRAY

PV ARRAY
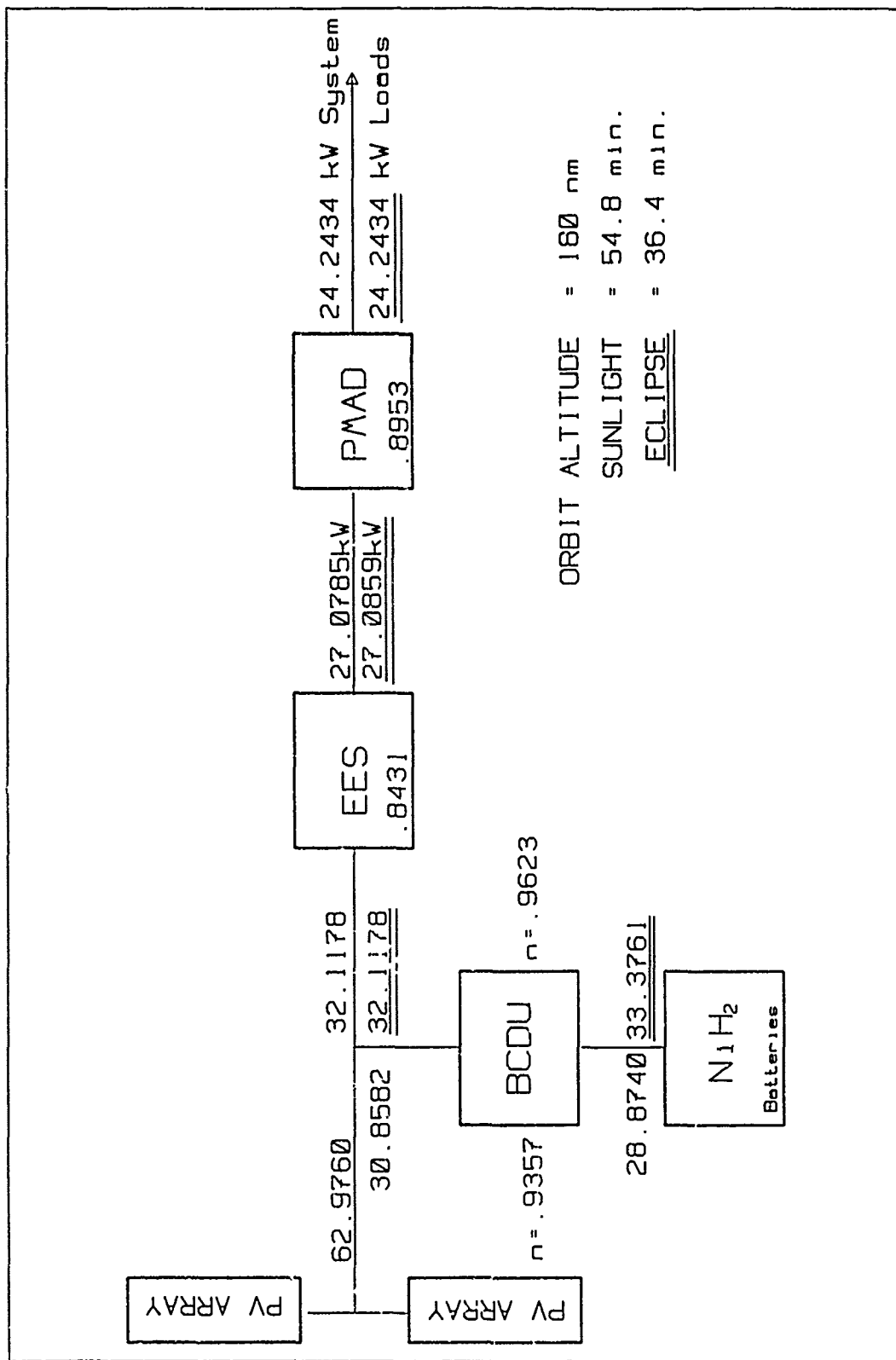
Figure C.15. Alternative Constant Power EPS
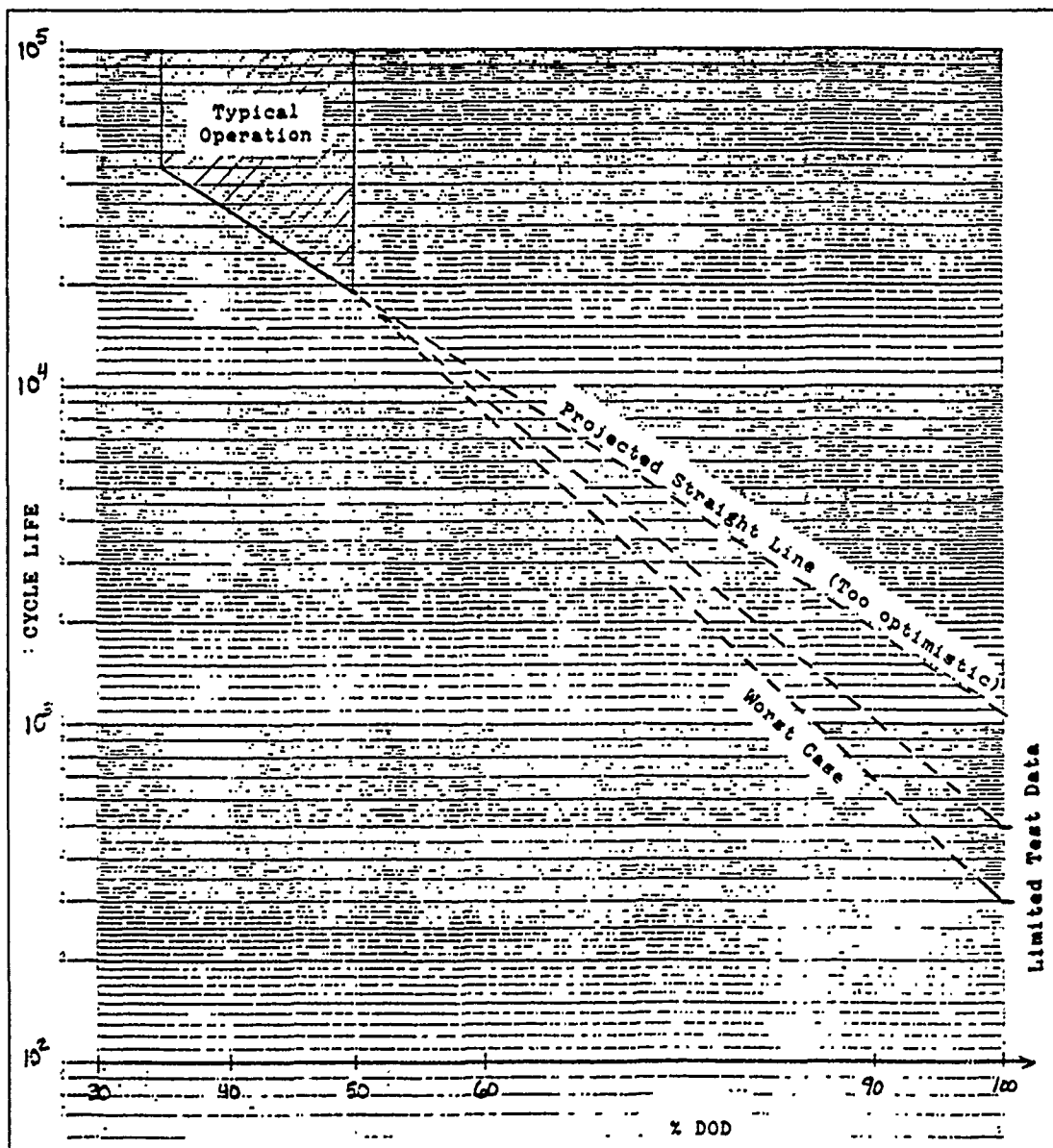
Figure C.16. Cycle Life vs. %DOD

ited testing has been carried out at 100% DOD resulting in cycle lifes of 300 to 500 charge/discharge cycles. Using the lower value, conservative life projections can be made via linear projection. This is precisely the method used to generate the data used to determine the optimum number of batteries required for various scenarios (as presented in sections 5.6 and 6.6)

Appendix D. *ORBIT ANALYSIS*

The orbital analysis model serves as a mission planning tool for this thesis by

- determining the fuel requirements for ASSET orbital maintenance,
- tracking the altitude loss of the different facility configurations,
- and addressing orbital debris issues.

Increased interest in adapting spent STS External Tanks for on-orbit applications has prompted several studies dealing with the low Earth orbit dynamics of the ET (54), (90). Major Dennis D. Miner, a recent AFIT graduate, studied the orbital characteristics of a passive, gravity-gradient stabilized external tank (61). Miner searched for the minimum altitude at which an ET could be deployed without exceeding an altitude-loss tolerance of 25 km over a 90 day period. The analysis of the ASSET facility orbit dynamics is essentially an adaptation of Miner's work.

The *Artificial Satellite Analysis Program (ASAP)* (47), the primary analytical tool used in this portion of our study, is a general orbit prediction software package. Its application produces time histories of all the classic Keplerian orbital elements, the vehicle altitude, and other items of interest to space mission planners. As an adjunct to ASAP, two short subroutines have been written to determine the ΔV's required to perform the proposed orbital maneuvers, and to quantify the amount of fuel consumed during those maneuvers.

D.1 Simplifications/Assumptions

The following assumptions greatly simply the analysis, yet allow sufficient accuracy to meet the requirements of this study:

1. ASSET facility is deployed in a 'nose-on' (bullet) attitude

2. ASSET avionics module maintains 'nose-on' orientation by use of magnetic dampers and RCS motors within some small tolerance

3. Solar panels remain perpendicular to freestream atmosphere

4. Orbital maintenance managed by ET GRIT Boost/Deboost Module derivative

5. Solar flare activity ignored

6. Static Earth 1977 standard atmosphere

7. Solar and lunar third-body perturbations ignored

8. Solar radiation pressure ignored

9. Hohmann transfers used for altitude changes

10. Space Station *Freedom* deployed, fully operational

11. ASSET facility remains in same orbital plane as *Freedom*

12. 90 day resupply cycle for *Freedom*

We have made the assumption that the ASSET facility's longitudinal axis will remain aligned with the body's velocity vector. This minimum drag orientation has the typical drag profile shown in Figure D.1. The second statement asserts that the attitude control problem has been solved by an avionics module designed specifically for this application. Therefore, the attitude dynamics issues have not been addressed in this study. We have assumed that the External Tank is deployed and *maintained* in a minimum drag orientation. Consequently, a constant spacecraft drag area (AREAD)[1] was assumed for each data run. AREAD, however, did vary from scenario to scenario.

The third item makes the assumption that the solar panels are always perpendicular to the freestream airflow. This will not be the case in practice, as the panels will be designed to track the sun for maximum electrical power output. The effective planform area will therefore vary in some sinusoidal fashion as the facility orbits the Earth. The planform area could have been adjusted by a scale factor to account for this sinusoidal change in AREAD:

$$AREAD_{eff} = AREAD_{ET} + (.707)AREAD_{SP}$$

------

[1]FORTRAN variable for drag area.
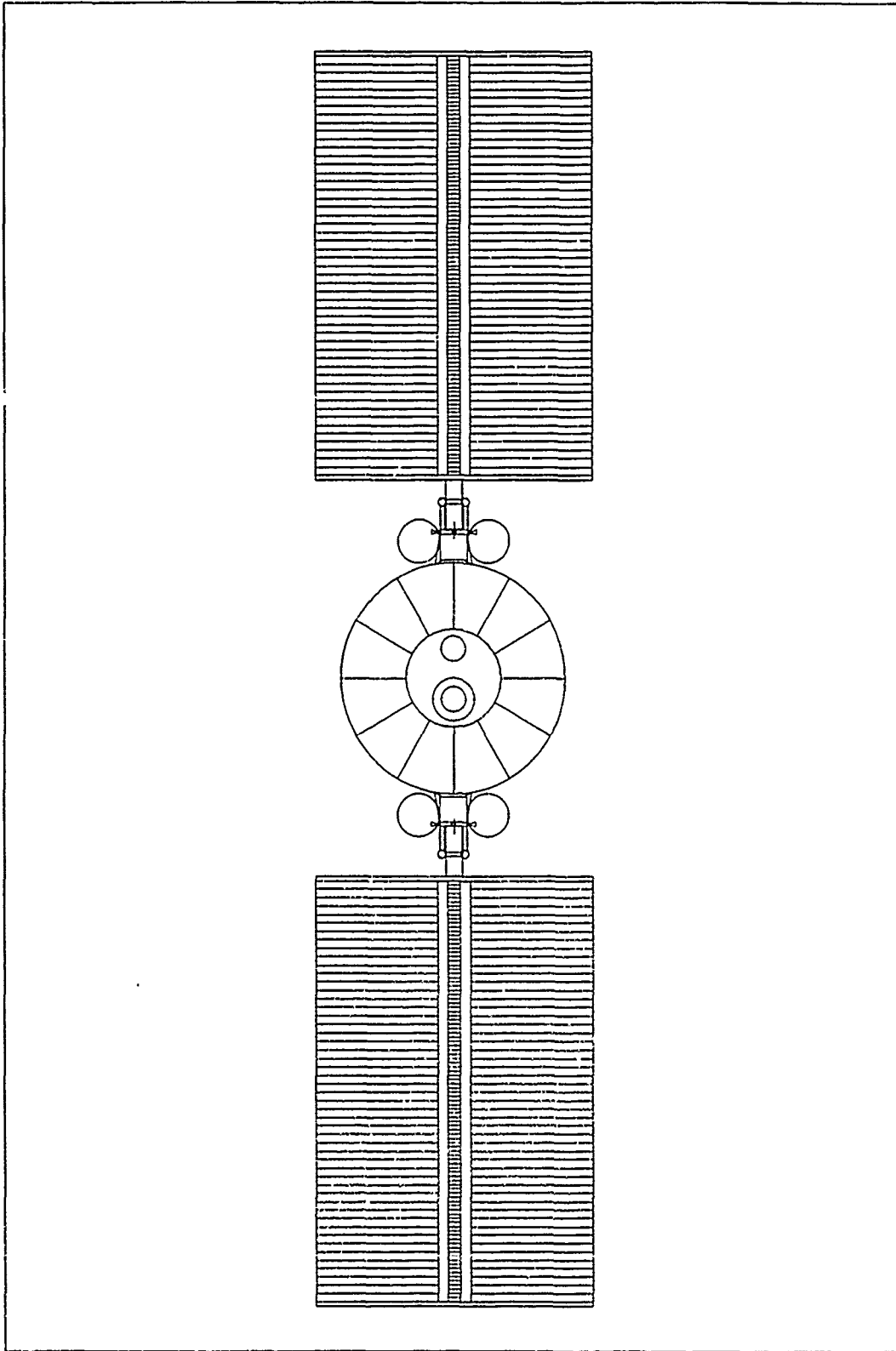
Figure D.1. Typical Facility Drag Profile (Aft View)

where

$$AREAD_{eff} = \text{effective spacecraft drag area}$$
$$AREAD_{ET} = \text{maximum planform area of ET}$$
$$AREAD_{SP} = \text{maximum planform area of Solar Panels}$$

and where the .707 scale factor indicates some sort of RMS scale factor which could be used to account for the varying orientation of the panels with respect to the body of the tank. However, since $AREAD_{SP}$ represents roughly 85% of the total planform area, the orbital decay rate will be very sensitive to any planform area calculation errors. Additionally, any changes in the attitude of the structure from its equilibrium position will increase $AREAD_{eff}$. Therefore a more conservative approach is taken, namely that the sinusoidal changes to the magnitude of the solar panel planform area are ignored. This represents the worst case scenario, incorporating the uncertainties due to both the orientation of the ASSET facility and the orientation of the solar panels with respect to the facility.

The fourth assumption simply chooses a candidate boost/deboost module for altitude and attitude control. One of the initial constraints imposed on the ASSET design was that it could not rely on outside stationkeeping support. Deciding on a propulsion unit conveniently sets the performance characteristics needed for burn time and fuel consumption calculations: I_{sp} and thrust.

Ignoring or underestimating solar flare activity (*ala SKYLAB*) could prove disastrous. However, Martin Marietta has already studied the effects of the solar cycle on the proposed ET Gamma Ray Imaging Telescope's (ET GRIT) orbital life (54). Their study shows that for a minimum drag ET GRIT facility deployed at an initial altitude of 160 nautical miles, an orbit lifetime ranging from 15 to 50 days can result, depending upon the year of the launch. It is clear then that any facility at low Earth orbit using an external tank as its structural frame should account for variations in the density of the atmosphere due to solar activity. For simplicity's sake though, solar flare activity has been ignored in this study. The fuel consumption results are, therefore, probably optimistic and must be regarded

D-4

as rough approximations only.

The effects of third-body perturbations and solar radiation pressure on the facility should have little impact on its orbital decay rate. There are a couple of good reasons for ignoring these effects. First, the third-body and solar radiation forces acting on a facility located 160-170 nautical miles above the Earth are small relative to the aerodynamic forces at those altitudes. Additionally, these perturbations tend to have more of an impact on the attitude dynamics of a space structure than on its orbital decay rate (especially at high altitudes). Since we have already assumed that any perturbations to the attitude of the facility can be corrected with the on-board stabilization and control hardware, these assumption appear to be reasonable.

Figure D.2 shows a typical mission profile for the ASSET facility. After the initial tank setup and reduction (A), the facility if boosted up (B) to an altitude such that after 90 days on orbit (C), atmospheric drag brings the facility back down to the 170 nmi rendezvous altitude (D). The second tank is salvaged, the scrap deorbited (D), and the ASSET facility (with the salvaged products from the second tank) reboosted to an appropriate altitude to repeat the process. Hohmann transfer maneuvers have been assumed for the reboosts (B and E).

From an economic standpoint, the high cost of designing, deploying, and operating ASSET requires that large numbers of tanks be salvaged. The operation of Space Station *Freedom* will require roughly 4-5 resupply missions per year (49); these crew-exchange missions could potentially provide a space-based aluminum salvage station with a regular supply of spent external tanks.

These missions can be designed such that the spent ETs are released in the same orbital plane as *Freedom*. Therefore, if the ASSET platform can somehow remain within the same orbital plane as *Freedom*, the facility will be able to rendezvous with the expended tanks without requiring expensive plane-change ΔV's. Relatively simple timing maneuvers should then be sufficient to rendezvous with the spent tanks.
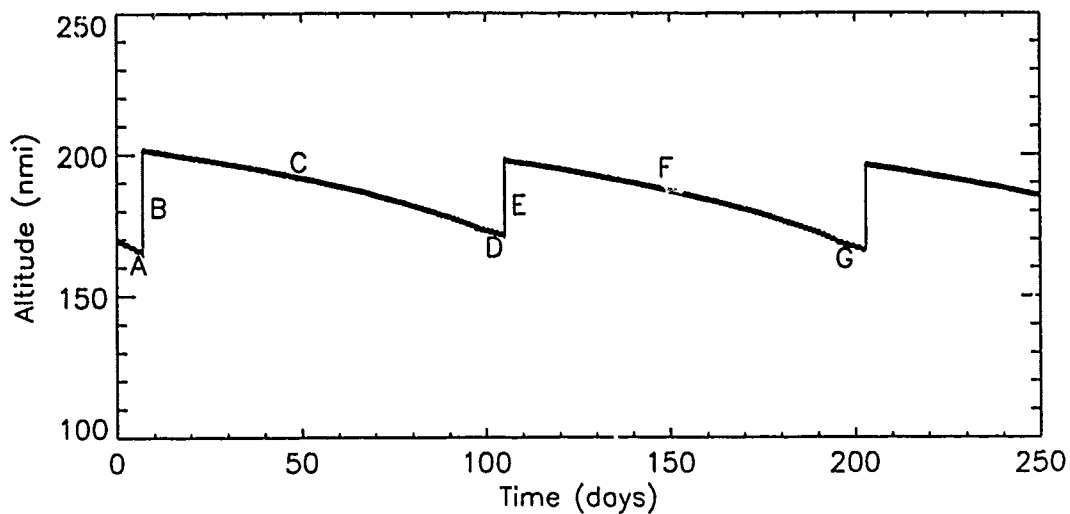
Figure D.2. Typical Mission Profile

However, the assumption that the ASSET facility can remain within the same orbital plane as *Freedom* is questionable at best. One of the primary concerns of NASA Space Station mission planners (49) involves the accommodation of free-flying platforms. As soon as the free-flyers begin to operate at different altitudes than *Freedom*, the orbit of the free-flyer will precess at a different rate than will the *Freedom* orbit. (Due primarily to the differences in the ballistic coefficients and geometries of the structures.) This phenomenon could make the rendezvous operations with the free-flyers extremely complicated and fuel intensive. Since the ASSET facility could be operating at substantially different altitudes (averaging 30-50 nautical miles on any given day), this effect will be even more profound. Quantifying the differences in the precession rates was not addressed in this study; further investigation is recommended.

D.2 Software Tools (Orbit Prediction)

The *Artificial Satellite Analysis Program (ASAP)*, developed several years ago by Johnny H. Kwok of NASA JPL (47), is a general orbit prediction program that

includes sufficient orbit modeling accuracy for mission design, maneuver analysis, and mission planning. Chapter 3 of the ASAP manual (47:3-1) describes the mathematical theory behind the program.

ASAP uses Cowell's method to numerically integrate the equations of motion. It includes perturbations on the spacecraft orbit due to the non-sphericity of the central body (Earth in this case), luni-solar third body effects, drag and solar radiation pressure. An 8th order Runge-Kutta integration routine with variable step-size control is used to propagate the state equations.

D.2.1 ASAP Input Over 60 variables make up the input file for ASAP. Since the program has been designed to incorporate lunar and solar perturbations, many of the input variables deal with the sun/moon orbital elements. These variables are ignored since we have assumed minimal effects due to third-body perturbations on the attitude of the ASSET facility. The following list identifies the variables that are of primary interest in this study:

$$
\begin{array}{lcl}
\text{ORB(1)} & = & a, \text{semi-major axis (km)} \\
(2) & = & e, \text{eccentricity} \\
(3) & = & i, \text{inclination (deg)} \\
(4) & = & \Omega, \text{longitude of ascending node (deg)} \\
(5) & = & \omega, \text{argument of periapsis (deg)} \\
(6) & = & M, \text{mean anomaly (deg)} \\
\text{TINT(1)} & = & \text{Initial calendar date of run} \\
(2) & = & \text{Initial time of day of run} \\
\text{TFIN} & = & \text{Final calendar date and time of run} \\
\text{TREF} & = & \text{Time, date corresponding to prime meridian location} \\
\text{GE} & = & \text{Product of gravitational constant and mass of planet, } \mu \\
\text{RE} & = & \text{Equatorial radius of the planet (km)} \\
\text{RATE} & = & \text{Rotation rate of the planet (deg/sec)} \\
\text{PM} & = & \text{Location of prime meridian at TREF} \\
\text{AREAD} & = & \text{Effective spacecraft area for drag (km}^2 \\
\text{SCMASS} & = & \text{Effective spacecraft mass for length of the propagation (kg)} \\
\text{CDRAG} & = & \text{Drag coefficient}
\end{array}
$$

where $ORB(i)$, $i = 1, \ldots, 6$ is recognized as the classic orbital element set (see Figure D.3). A typical STS orbit insertion is assumed, establishing the following

initial orbital element set:

$$
\begin{aligned}
a &= RE + h_{\circ} \\
e &= 0.0 \\
i &= 28.5° \\
\Omega &= 10.0° \\
\omega &= 0.0° \\
M &= 0.0°
\end{aligned}
$$

where RE, the equatorial radius of the Earth, is a known constant (6378.145 km (10:429)), and $h_{\circ}$, the initial altitude of the facility, is case dependent.

AREAD, SCMASS, and CDRAG are the three most critical variables used in this analysis. The equation of motion due to drag can be expressed as

$$
\ddot{\bar{r}} = -\frac{1}{2}\frac{C_D A}{M}\rho v_b \bar{v}_b, \tag{D.1}
$$

where C_D is the coefficient of drag, A is the effective drag area, M is the mass of the facility, and ρ is the density of the atmosphere (47:3-4). The velocity of the facility relative to the rotating atmosphere is given by

$$
\bar{v}_b = (v_x + y\omega)\bar{\imath} + (v_y - x\omega)\bar{\jmath} + v_z \bar{k} \tag{D.2}
$$

where ω is the Earth's rate of rotation, and $\bar{\imath}$, $\bar{\jmath}$, and $\bar{k}$ are the unit vectors representing the Earth centered 'inertial' reference frame shown in Figure D.3 (10:59).

Equation D.1 can also be expressed as follows:

$$
\ddot{\bar{r}} = -\frac{1}{2}\frac{1}{\beta}\rho v_b \bar{v} \tag{D.3}
$$

D-8
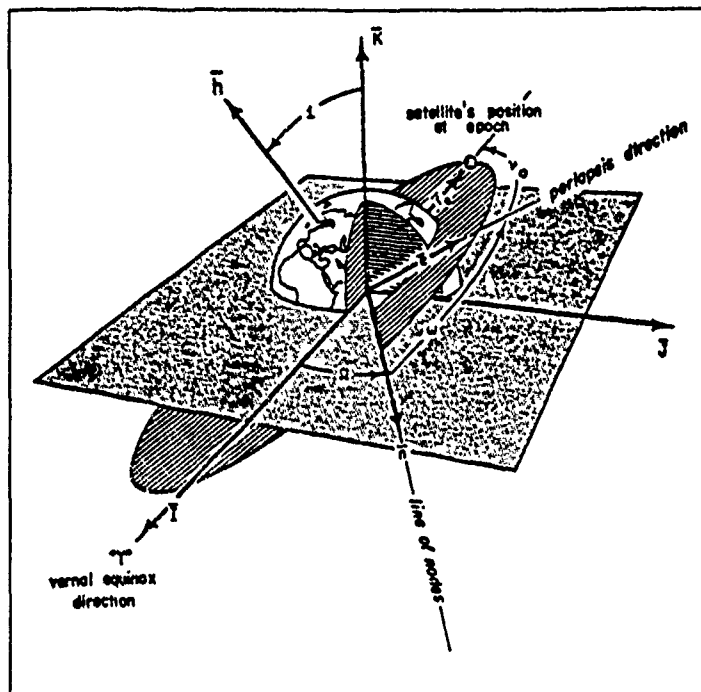
Figure D.3. Classical Orbital Elements

where

$$\beta = \frac{M}{C_D A}$$

the ballistic coefficient, can be regarded as a measure of a body's ability to overcome drag. Here we see the importance of AREAD, SCMASS, and CD. As β increases, the acceleration due to drag decreases. This implies that when comparing the ballistic coefficients of two facilities, the facility with the largest ballistic coefficient would tend to stay in a given orbit longer than the facility with the smaller ballistic coefficient.

For a given C_D, one can increase β by either decreasing the drag profile (A) or increasing the mass M of the body. (C_D has been set to a value of 2.2 for all phases of the analysis. Miner (61:33) used a value of 2.4; however, Martin Marietta recommends the slightly lower value (7)). A trade study between two types of solar arrays was performed on the basis of improving the ASSET facility's ballistic coefficient. The decreased surface area of the higher efficiency solar arrays meant a larger ballis-

tic coefficient, with a subsequent increase in the orbital lifetime of the facility. This increased orbital life can be equated with decreased fuel costs. However, this savings may or may not offset the added costs of deploying the advanced technologies. This is addressed in more detail in Chapter IX.

Note also that as each tank is reduced to I-beams and plate, this additional mass is transferred to the ASSET facility, thereby increasing β. These changes in the ASSET ballistic coefficient are accounted for throughout the analysis.

D.2.2 Sample ASAP Input File The following listing is a representative example of the ASAP input file:

```
2                       L
0                       M
0                       IRES
0                       ISUN
0                       IMOON
1                       IEPHEM
1                       IDRAG
1                       IDENS
0                       ISRP
1                       IORB
0                       IPRINT
0                       INODE
1                       IPLOT
6674.46D0               ORB(1), A
0.D0                       (2), E
28.5D0                     (3), I
10.D0                      (4), NODE
0.D0                       (5), W
0.D0                       (6), M
1.D-8                   RELERR
1.D-8                   ABSERR
3600.D0                 STEP
19940101.D0             TINT(1)
0.D0                       (2)
19940106.D0             TFIN(1)
0.D0                       (2)
```

```
19940101.D0            TREF(1)
0.D0                      (2)
3.9860045D5            GE
6378.140D0             RE
.4178074216D-2         RATE
99.652865509D0         PM
.8182D-1               ELLIP
6468.14D0              RATM
0.D0                   RDENS
0.D0                   RHT
0.D0                   SHT
1000.D0                ALTMAX
1.D0                   WT
3.32D-4                AREAD
3.32D-4                AREAS
34400.D0               SCMASS
2.2D0                  CDRAG
6.6D-3                 CSRP
.13271244D12           GS
0.D0                   ES(1)
0.D0                   ES(2)
0.D0                   ES(3)
0.D0                   ES(4)
0.D0                   ES(5)
0.D0                   ES(6)
0.D0                   ES(7)
.490279D4              GM
0.D0                   EM(1)
0.D0                   EM(2)
0.D0                   EM(3)
0.D0                   EM(4)
0.D0                   EM(5)
0.D0                   EM(6)
0.D0                   EM(7)
     2     0         -.10826271D-2                    0.D0
```
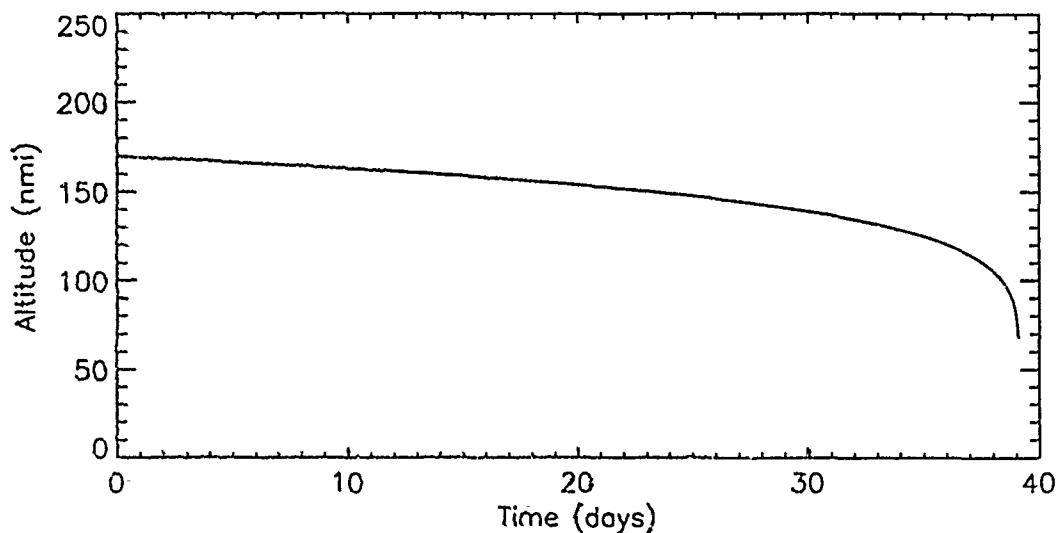
Figure D.4. Typical Orbit Lifetime Plot

D.2.3   ASAP Output The following ASAP output parameters are written to a plotfile every STEP seconds (specified at the input file):

ANODE	=	longitude of ascending node
NREV	=	revolution number
DAY	=	cumulative run time (days)
A	=	semi-major axis
E	=	eccentricity
I	=	inclination
NODE	=	nodal crossing number
W	=	argument of periapsis
MA	=	mean anomaly
LONG	=	longitude
LAT	=	latitude
PER ALT	=	periapsis altitude
ALT	=	geocentric altitude $(r - R)$

The variables DAY and ALT are stripped out of the plotfile to produce plots of altitude versus time. The mission profile and orbit lifetime plots (see Figure D.4) are generated in this fashion.
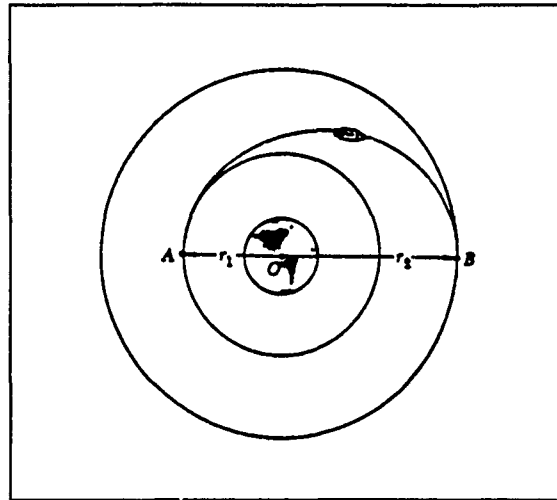
Figure D.5. Hohmann Transfer.

D.3 Software Tools (Fuel Consumption)

D.3.1 Derivation. The fuel consumed by the ASSET facility during its orbital maneuvers can be estimated by quantifying the total ΔV required for each Hohmann transfer. Given the performance specifications of the propulsion module, one can then find the burn time required for each propulsive maneuver.

The Hohmann transfer orbit is the minimum ΔV transfer between two coplanar orbits, and is achieved by using a doubly-tangent transfer ellipse. A typical Hohmann maneuver is depicted in Figure D.5. At point A, the main thruster of the satellite imparts a change in velocity tangential to the circular orbit of radius r_1. This increased velocity places the satellite on an elliptical transfer orbit. Upon reaching apogee on the transfer ellipse (point B), the thruster is fired again. The second motor firing places the satellite in a circular orbit of radius r_2. Assuming that the thrusters impart an instantaneous ΔV, the magnitudes of the required ΔV's can readily be found (14). The eccentricity of the transfer ellipse can be expressed as

$$e = \frac{r_2 - r_1}{r_1 + r_2}.$$

D-13

The velocity at perigee of the transfer ellipse can be shown to be

$$V_1 = \sqrt{\frac{\mu(1+e)}{a(1-e)}}$$

where

$$a = \frac{r_1 + r_2}{2}$$

is the semi-major axis of the transfer ellipse, and μ is the product of the gravitational constant and the mass of the Earth. The velocity at apogee has a similar form:

$$V_2 = \sqrt{\frac{\mu(1-e)}{a(1+e)}}.$$

The velocity of a satellite in the circular orbits of Figure D.5 can be found by

$$V_{c_i} = \sqrt{\frac{\mu}{r_{c_i}}}, \quad i = 1, 2.$$

The magnitude of the change in velocity required at point A for the Hohmann transfer is simply

$$\Delta V_1 = V_1 - V_{c_1},$$

and for point B,

$$\Delta V_2 = V_{c_2} - V_2.$$

These calculations are coded in the subroutine HOHXFR listed below.

Once the ΔV's are known, one can then make use of the following relationships to calculate the fuel consumed during these maneuvers for a given propulsion unit. The exhaust velocity of a rocket motor can be expressed as a function of the motor's specific impulse, I_{sp}, and the acceleration due to gravity:

$$v_e = I_{sp} g. \tag{D.4}$$

The mass flow rate of the propellants can be expressed as a function of the motor thrust, T, and the exhaust velocity:

$$\dot{m} = \frac{T}{v_e}. \tag{D.5}$$

Now, the acceleration of a particle can be approximated by

$$a \approx \frac{\Delta v}{\Delta t}, \tag{D.6}$$

assuming that the total mass of the body remains constant during the time interval Δt (a good approximation here since the mass $\sim$ the ASSET facility is $\gg$ than the mass of the fuel consumed). Then, making use of Newton's Second Law of motion, $F = ma$, and rearranging terms, equation D.6 becomes

$$\Delta t = t_b \approx \frac{M}{T} \Delta v \tag{D.7}$$

where M is the total mass of the facility, and Δv is the change in velocity calculated for the Hohmann transfer burn. Knowing the approximate burn time t_b for the motors, the mass of the fuel consumed can be approximated by making use of equation D.5:

$$m_f = \dot{m} t_b.$$

These relationships are coded in the subroutine BURNT, listed below.

D.3.2 FORTRAN Code. A main calling program was developed to facilitate the processing of the fuel consumption data. The printout of this calling program was used as the data source for the fuel consumption discussions in the scenario descriptions.

```
      PROGRAM BT
C
C *** Main calling program for subroutines HOHXFR, BURNT.
C *** Reads initial and final altitudes, specific impulse,
C *** thrust, and spacecraft mass from file 'BT.IN'.
C *** Prints results in file 'BT.OUT'
C
      OPEN(5,FILE='BT.IN')
      OPEN(7,FILE='BT.OUT')
      READ(5,1000) H1,H2,AISP,TH,SCM
1000  FORMAT(1P,BN,E15.10)
      CALL HOHXFR (H1,H2,DV1,DV2)
      CALL BURNT (AISP,TH,SCM,DV1,DV2,TB1,TB2,FUEL1,FUEL2)
      WRITE(7,100)
100   FORMAT(5X,'***First Burn***'/)
      WRITE(7,110) DV1,TB1,FUEL1
110   FORMAT(5X,'Delta-V1 = ',E12.4,' (ft/sec)'/,5X,'Burn Time = ',
     $E12.4,' (sec)',/,5X,'Fuel Consumed = ',E12.4,' (lbs)',//)
      WRITE(7,120)
120   FORMAT(5X,'***Second Burn***'/)
      WRITE(7,130) DV2,TB2,FUEL2
130   FORMAT(5X,'Delta-V2 = ',E12.4,' (ft/sec)'/,5X,'Burn Time = ',
     $E12.4,' (sec)',/,5X,'Fuel Consumed = ',E12.4,' (lbs)',//)
      WRITE(7,10)
10    FORMAT(2X,' Initial Alt  ','   Final Alt    ',
     $' Tot Delta-V  ',' Burn Time    ',' Fuel Consumed ')
      WRITE(7,20)
20    FORMAT(2X,'   (n.mi.)     ','   (n.mi.)    ',
     $'      (ft/sec)  ','   (sec)      ','     (lbs)    '/)
      DV=DV1+DV2
      TB=TB1+TB2
      FUEL=FUEL1+FUEL2
      WRITE(7,30) H1,H2,DV,TB,FUEL
30    FORMAT(2X,5(2X,E12.4),//)
```

```fortran
      WRITE(7,40) AISP,TH
40    FORMAT(5X,'For Isp = ',F8.1,' (sec)'/,5X,' Thrust = ',F8.1,
     $' (lbf)')
      CLOSE(5)
      CLOSE(7)
      END



      SUBROUTINE HOHXFR(H1,H2,DV1,DV2)
C
C Purpose:  This subroutine computes the amount of Delta-V
C required to perform a Hohmann transfer between two coplanar
C circular orbits.
C
C Input Parameters:
C       H1 - Altitude of lower orbit (n.mi.)
C       H2 - Altitude of higher orbit (n.mi.)
C Output Parameters:
C       DV1 - Delta-V at H1 (ft/sec)
C       DV2 - Delta-V at H2 (ft/sec)
C
C Note:  MU is in ft**3/sec**2 and RE is in ft.
C        H1 and H2 are converted from n.mi. to ft.
C
      REAL MU
      H1=H1*6.076E+3
      H2=H2*6.076E+3
      MU=1.40785E+16
      RE=2.092657E+7
      R1=H1+RE
      R2=H2+RE
      AT=(R1+R2)/2.
      VC1S=MU/R1
      VC2S=MU/R2
      VC1=SQRT(VC1S)
      VC2=SQRT(VC2S)
      VT1S=MU*((2.*R2)/((R1+R2)*R1))
      VT2S=MU*((2.*R1)/((R1+R2)*R2))
      VT1=SQRT(VT1S)
      VT2=SQRT(VT2S)
      DV1=VT1-VC1
      DV2=VC2-VT2
```

```fortran
      DV=DV1+DV2
      H1=H1/6.076E+3
      H2=H2/6.076E+3
      RETURN
      END


      SUBROUTINE BURNT(AISP,TH,SCM,DV1,DV2,TB1,TB2,FUEL1,FUEL2)
C
C  Purpose:  This routine calculates the burn time and total
C  fuel consumed for a given Delta-V and motor Isp, assuming
C  constant spacecraft mass.  Accuracy decreases with increasing
C  fuel flow rates and burn times.
C
C  Input parameters:
C        AISP - Specific Impulse (Isp) of motors (sec)
C        TH - Thrust of motors (lbf)
C        SCM - Spacecraft mass (lbs)
C        DV1 - Delta-V for first burn
C        DV2 - Delta-V for second burn
C
C  Output parameters:
C        TB1 - First burn time (sec)
C        TB2 - Second burn time (sec)
C        FUEL1 - Mass of fuel consumed during first burn (lbs)
C        FUEL2 - Mass of fuel consumed during second burn (lbs)
C
      REAL MDOT
      G=32.174
      SCM=SCM/G
C
C  Compute exhaust velocity
C
      VE=AISP*G
      MDOT=TH*G/VE
      TB1=SCM*DV1/TH
      TB2=SCM*DV2/TH
      FUEL1=TB1*MDOT
      FUEL2=TB2*MDOT
      RETURN
      END
```

The following are sample outputs from program BT:

```
ASSET Facility (25KW System)

***First Burn***

Delta-V1 =    0.1218E+03 (ft/sec)
Burn Time =   0.1774E+03 (sec)
Fuel Consumed =    0.1542E+04 (lbs)


***Second Burn***

Delta-V2 =    0.1212E+03 (ft/sec)
Burn Time =   0.1765E+03 (sec)
Fuel Consumed =    0.1535E+04 (lbs)


Initial Alt    Final Alt    Tot Delta-V    Burn Time    Fuel Consumed
   (n.mi.)       (n.mi.)      (ft/sec)       (sec)          (lbs)

 0.1385E+03    0.2080E+03    0.2430E+03    0.3539E+03     0.3077E+04


   For Isp =    230.0 (sec)
    Thrust =   2000.0 (lbf)




ASSET Facility + 12,200 lbs salvaged aluminum

***First Burn***

Delta-V1 =    0.9413E+02 (ft/sec)
Burn Time =   0.1549E+03 (sec)
Fuel Consumed =    0.1347E+04 (lbs)
```

Second Burn

Delta-V2 =   0.9378E+02 (ft/sec)
Burn Time =   0.1543E+03 (sec)
Fuel Consumed =   0.1342E+04 (lbs)

Initial Alt (n.mi.)	Final Alt (n.mi.)	Tot Delta-V (ft/sec)	Burn Time (sec)	Fuel Consumed (lbs)
0.1512E+03	0.2050E+03	0.1879E+03	0.3092E+03	0.2689E+04

For Isp =   230.0 (sec)
Thrust =   2000.0 (lbf)

Appendix E. *THERMAL ANALYSIS*

E.1 Thermal Modeling

The rate of change of temperature for any object is proportional to the rate the object is heated (1:280-285). For an object in space the heat balance is :

$$MC\frac{dT}{d\tau} = \alpha S\mu a + P - \epsilon A\sigma T^4 \qquad (E.1)$$

M = Mass

C = Specific Heat

T = Temperature

τ = Time

α = Thermal Absorption Coefficient

S = Solar Flux

μ = Solar Aspect Ratio = (effective surface area)/(total surface area)

a = Surface Area

P = Internal Heat Dissipation

ϵ = Thermal Emissivity

A = Radiator Area

σ = Steffan Boltzman Constant

Just after the hydrogen tank is vented and before the astronauts enter, the temperature of the LH$_2$ portion of the External Tank will be $-423°F$. There are no internal power sources at this point so $P = 0$. The only remaining terms of the right hand side of equation E.1 are the solar flux term and the term for the radiative loses.

In their study on propellant scavenging (51), Martin Marietta estimated the rate of orbital heating of the LH$_2$ tank. The depiction of this estimation appears in Figure E.1. This figure was used to calculate an effective average orbital flux. To do this, the curve was integrated over one orbit. This gave the total orbital heat in BTUs that was received in a single orbit. This total orbital energy was then divided by the period of the interval (1.5 hours) to give an average orbital heating rate. This rate was then divided by the surface area of the LH$_2$ tank in order to derive the effective average orbital flux. This number was used as S in equation E.1.
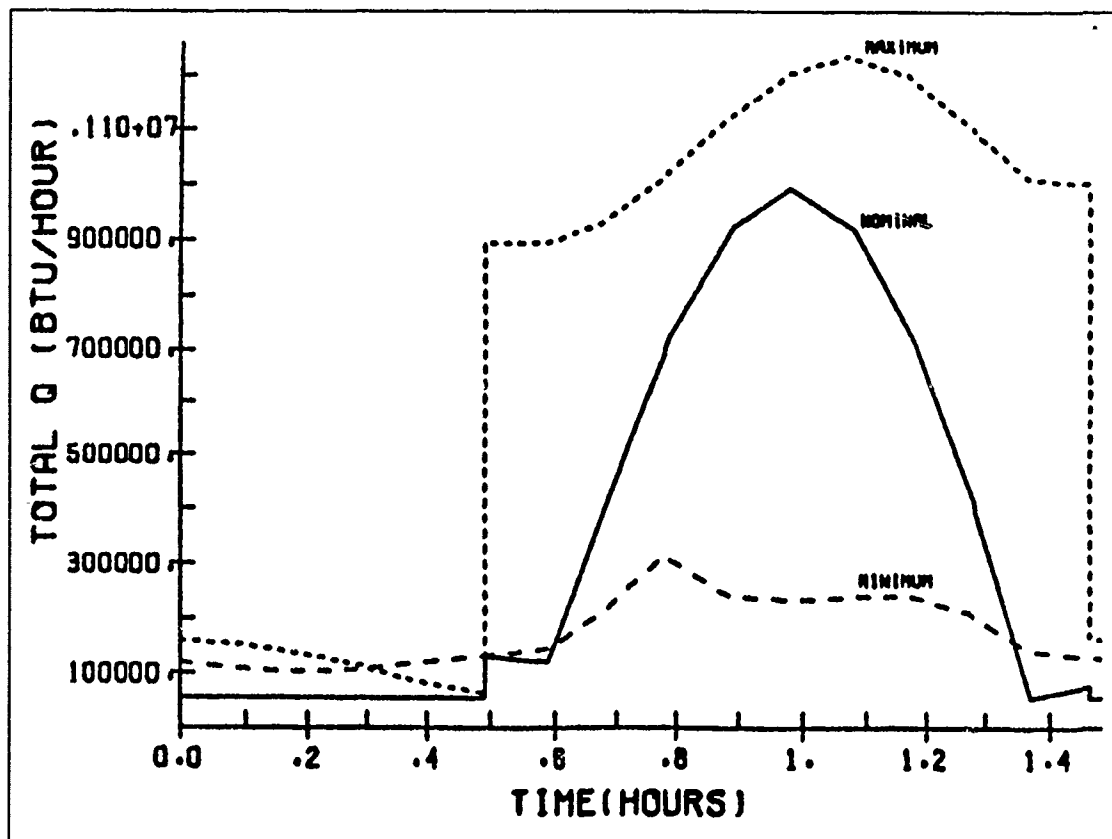
Figure E.1. LH$_2$ Tank Orbital Heating

The Nominal orbital heating curve represented in Figure E.1 is roughly two step functions joined by a parabola. The parabolic portion of the curve can be estimated via the following formula:

$$y - a = c(x - b)^2$$

y represents the heat in Btu/hour and x stands for the time in hours. The maximum of the Nominal orbital heating curve is approximately $(x, y) = (1.0, 10^6)$. This fixes the constants a and b at $a = 10^6$ and $b = 1.0$. Another point on the Nominal curve is $(x, y) = (1.375, 50,000)$. Since one of these points represents the maximum on the parabola they are sufficient to estimate the constants:

$$y = 10^6 - 6,755,555(x - 1)^2 \tag{E.2}$$

As a check on this estimate, consider a point on the side of parabola opposite of the point $(x, y) = (1.375, 50,000)$ Such as the point $(x, y) = (.8, 700,000)$. If $x = .8$ is substituted into equation E.2, y is estimated to be 729,777. The error involved in using the parabolic approximation is then:

$$\left| \frac{700,000 - 729,777}{700,000} \right| = 4\%.$$

This represents an acceptable level of error. Using the Nominal orbital heating curve, the total orbital heating is:

$$Q = .7 * 50,000 + \int_{.6}^{1.4} \left\{ 10^6 - 6,755,555(x - 1)^2 \right\} dx$$

Over a 1.5 hour period, this results in an effective average orbital heating rate of 364,508 Btu/hr. For the purposes of this calculation the effective surface area of the LH$_2$ tank was set equal to the radiator area so that $a = A$. This assumption

has the effect of averaging the heat leaking into the LH$_2$ tank over the entire tank. Given the assumption of no internal power dissipation equation E.1 becomes:

$$MC\frac{dT}{d\tau} = \alpha S\mu A - \epsilon\sigma AT^4 \tag{E.3}$$

Which can be transformed to the form:

$$\int_{T_0}^{T_1}\left\{MC\frac{dT}{\alpha S\mu A - \epsilon\sigma AT^4}\right\} = \int_{t_0}^{t_1} d\tau \tag{E.4}$$

This general solution to this differential equation can be found in the CRC tables as:

$$\frac{k}{2a}\left\{.5\log\frac{x+k}{x-k} + \arctan(x/k)\right\} \tag{E.5}$$

$$ab < 0, k = (-a/b)^{1/4} \tag{E.6}$$

The problem at hand was cast into the form above. The required log was evaluated at the absolute value of the indicated quotient so that the mathematics would be meaningful. The problem of boundary conditions on the integral remained. Integrating the right hand side of equation E.4 results in a linear function of time. This time, call it $\Delta\tau$, was the total time required to change from one temperature to another given the rates of cooling and heating. The lower limit of an integral of the left hand side of equation E.4, T_0, is $-423°F$. By varying the upper limit of integration, T_1, one could, after integration, find the time required to reach a specified upper limit. It was desirable to find the heat of the LH$_2$ tank 24 hours after the liquid hydrogen was vented, i.e. $\Delta\tau = 24$. With the lower limit of the temperature integral fixed at $-423°F$ (46 degrees Rankine) the upper limit was raised from $-423°F$ until twenty-four hours was reached. All actual calculations were done in degrees Rankine. When the upper limit of the integral was set to $-117°F$, the value of twenty-four hours was reached. It was estimated that after 24 hours, the temperature of the LH$_2$ portion of the external tank would be $-117°F$.

The next question to be answered was, what was the worst case internal temperature of the LH$_2$ tank? If the tank were cut open so that heat could escape and it was then plunged into the darkness of an eclipse period, this would equate to a worst case thermal scenario. In addition, if the tank started the eclipse period at $-117°F$, it would reach its coldest temperature. Referring to equation E.1 once more, it can be seen that under these conditions $P = 0$ (no internal power), $S = 0$, no solar flux. The equation describing these conditions is :

$$MC\frac{dT}{d\tau} = -\epsilon\sigma AT^4$$

Once integrated, this differential equation yields:

$$-1/3(\frac{1}{T_1^3} - \frac{1}{T_0^3}) = -\frac{\Delta t\epsilon A\sigma}{MC} \qquad (E.7)$$

Which can be rewritten as:

$$T_1 = \left\{ \frac{1}{\frac{1}{T_0^3} + \frac{3\Delta t\epsilon A\sigma}{MC}} \right\}^{1/3} \qquad (E.8)$$

This equation states that give an initial temperature at the start of the eclipse ($T_0 = -117$ degree Fahrenheit, for instance), and duration of the eclipse ($\Delta t = 40$ minutes, for instance), one could calculate the coldest temperature reached, T_1. For the LH$_2$ tank, this temperature was $-131°F$. Since the astronauts suits can handle temperatures as low as $-180°F$ (66), they will have no trouble with the cold. Motors and joints of machinery which require higher ambient temperatures should be heated with small electrical heating coils when the cold becomes too severe for them. The heaters should be driven by thermostats which would turn the heaters on and off when conditions warrant.

Equation E.1 can also be used to determine whether problems would arise from direct solar heating. The temperature of a surface in sunlight in space can not rise indefinitely. Either the surface reaches equilibrium or it changes state. When a surface reaches equilibrium the rate of change of temperature is zero. $\frac{dT}{d\tau} = 0$. If we assume that the solar aspect ratio $\mu = 1$ and if the surface has no internal power source, equation E.1 becomes:

$$0 = \alpha\mu a S - \epsilon\sigma A T^4$$

For a sphere, a convenient reference object, $a = \pi R^2$ and $A = 4\pi R^2$. When these values were substituted and the equation solved for T:

$$T = (\frac{\alpha S}{4\epsilon\sigma})^{1/4}$$

For an orbit at 28.5° inclination, the maximum solar flux is fixed at about $450 BTU/hr/(ft^2)$. The Steffan-Boltzman constant σ is fixed at $.1714 * 10^{-8} \frac{Btu}{hr ft^2 R^4}$. The only factors that can vary in equation E.1 are α and ϵ. Equilibrium temperatures for surfaces in direct sunlight in space are determined by the ratio of the thermal absorptivity to the thermal emissivity, α/ϵ . [This ratio is 1.0 for both 2219 Aluminum and SOFI, which comprise the only exposed surface areas of the External Tank (7).] A surface composed of either substance would achieve the same equilibrium temperature in sunlight in space. This temperature is 40.85°F. An important principle in heat transfer is that heat flows only when a difference in temperature exists. What this means is that the External Tank would get no hotter than 40.85°F, if the sun were its only source of heat.

Once substantial portions of the External Tank are cut away the solar thermal equilibrium temperature would be 40.85 deg F. Using equation E.8 the coldest temperature reached by the External tank during the eclipse period would be -12.92

deg F. This calculation was made assuming the mass of the External Tank to be 69,000 lbs, specific heat $.206Btu/(lbF)$, surface area $16,750 ft^2$, emissivity .8, and it temperature at the beginning of the eclipse at $40.85°F$. Calculations were also made concerning the coldest temperature an individual piece of aluminum plate might get during an eclipse period. As equation E.8 shows, the ratio of its surface area to its mass determines an object's temperature profile. For this reason, a piece of free plate would achieve a different eclipse temperature than the External Tank as a whole. For a piece of plate that was 163 inches by 9.582 inches, density of $177.984 lbs/ft^3$, emissivity of .8, and a specific heat of $.206Btu/(lbF)$, the coldest eclipse temperature would be $-55.77°F$. This temperature will not represent a hazard to astronauts or to machinery.

The heat generated by the electron beam cutter is an element unique to the thermal environment of the ASSET facility. The electron beam cutter cuts 2219 aluminum by melting completely through a strip of aluminum .125 inches wide. The total length of the actual cuts to made would be 157,079 inches. The surface area directly heated by electron bombardment was $136.35 ft^2$. If one neglects the surface area of the dome caps, the surface area of the interior of the LH_2 tank is $8,384 ft^2$. To form an average tank temperature these areas must be multiplied by their respected temperatures. The two resulting products are then summed and this sum is divided by the interior surface area of the LH_2 tank. The melting point of aluminum is $1220 \deg F$. The worst case temperature of the rest of the tank would the the solar thermal equilibrium temperature: $40.85 \deg F$. The worst case average temperature combining solar and electron beam cutter effects is $60.02 \deg F$.

The foregoing discussion ignores the problem of re-radiation from hot objects. The following analysis shows that there is no significant re-radiation problem.

Only two types of surfaces need to be considered as potential sources of re-radiation. 2219 aluminum and SOFI. Both of these substances have a α/ϵ ratio of 1.0. Therefore both 2219 aluminum and SOFI have solar thermal equilibrium

temperatures of $40.85° F$. Whether one is discussing conduction or radiation, the fact remains that heat will not flow if no difference in temperature exists. Therefore, from either radiative and conductive aspects, solar energy can do no worse than heat the entire tank to $40.85° F$.

The only remaining source of re-radiation problems are those areas heated by the electron beam cutter. If none of heat from the electron beam cutter can escape the tank and all of the heat is concentrated in one area. This heated area would be $136.35 ft^2$. This hot spot would be entirely enclosed by the LH$_2$ tank so the equation for radiation would be :

$$Q'' = \left\{ \frac{\sigma(T_h^4 - T_c^4)}{1.0/\epsilon + (1.0/\epsilon - 1.0)(A_h/A_c)} \right\} (A_h/A_c) \qquad (E.9)$$

$Q'' = Btu/hr/ft^2$

σ = Steffan-Boltzman constant$= .1714 * 10^{-8} Btu/hr/ft^2$

T_h = Temperature of the hot spot: $1220 \deg F$.

T_c = Temperature of the LH$_2$ tank: $40.85 \deg F$.

$\epsilon = .8$, thermal emissivity for 2219 aluminum

A_h = Area of the hot spot: $136.35 ft^2$

A_c = Area of LH$_2$ tank sans dome caps: $8,384 ft^2$

The thermal flux from the hot spot to the LH$_2$ tank is then $179.74 Btu/hr/ft^2$. This is certainly smaller than the solar flux of $450 Btu/hr/ft^2$. If one combined the flux from the hot spot and the flux from the sun and concentrated them on an area one would have a total flux of $629.74 Btu/hr/ft^2$. The equilibrium temperature this flux would produce on a reference sphere is $90.52° F$. This would not be a problem for astronauts or machinery.

Another source of potential thermal problems is the SOFI Workstation. The purpose of the SOFI Workstation is to remove SOFI and to separate plate from I-

beam. Plate and I-beam come in two sizes: 163 inches long and 225 inches long. The calculations that follow concern the 163 inch long pieces, however, similar results are obtained if the 225 inch pieces are used. Once separated from an I-beam, a typical plate section would measure 9.582 by 163 inches. To separate plate from I-beam the electron beam cutter heated a .125 inch by 163 inch strip of metal to $1220°F$. If this strip of metal were considered part of the separated plate, then its area weighted average temperature would be 56.23 degrees (assuming its initial temperature were $40.85°F$).

For the I-beam, consider a strip of metal .125 inches wide and 163 long connected to the I-beam. The I-beam is 1.25 inches wide, 163 inches long, with an initial temperature of $40.85°F$. The area weighted average temperature of the I-beam is $148.4°F$. This I-beam calculation took into account only the top surface of the I-beam. The sides and bottom, which would reduce an area weighted average, were not taken into account. Space suits are designed to handle temperatures up to $235°F$ (66) so the astronauts will still have a margin of safety. All of the stripper mechanisms that handle the I-beam and all of the stacking machinery should take into account the elevated temperature of the I-beams. No special problems would be anticipated since $150°F$ is well within the operative range of industrial machinery. All surfaces which contact the I-beams should be insulated.

Since heat will not flow without a difference of temperatures, the I-beams and plate will produce no special re-radiation problems. The worst they would do is to bring objects near them closer to their temperatures. The I-beams in particular have very small surface area compared to objects in their environment. For enclosed objects, the heat flux they radiate to their colder enclosures is proportional to the ratio of the surface area of the inner body to the outer (see equation E.9).

Inside the SOFI Workstation, where the I-beam is cut from the plate, the electron beam cutter develops a hot spot of about $.0052ft^2$. The exposed surface area of the interior of the stripper machine would be at least $3.61ft^2$. The heat

E-9

flux that would be generated would be $15.61Btu/hr/ft^2$. The reference equilibrium temperature that would be achieved by a sphere experiencing such a flux would be $-241.54°F$. Since it was already assumed that the SOFI Workstation was $40.85°F$, the temperature rise due to re-radiation from the SOFI Workstation hot spot was ignored. If the internal radiation and solar flux did combine, the spherical reference equilibrium temperature would be $50.59°F$.

The final thermal consideration comes into play in the manual reduction scenario. Astronauts would have to move freshly cut plate/I-beam combinations in this scenario. The question was, therefore, how soon could an astronaut touch the hot edge of a cut piece? Spacesuits as currently designed can withstand temperatures up to $235°F$. Since only a thin strip of the metal piece is actually heated, and both conduction and radiation are involved, this is a transient thermal problem. This problem was solved using a finite differencing scheme developed by Benjamin Gebhart (27).

The partial differential equation describing heat flow is:

$$\frac{\partial^2 T}{\partial X^2} + \frac{\partial^2 T}{\partial Y^2} + \frac{\partial^2 T}{\partial Z^2} + \frac{q'''}{k} = \frac{\partial T}{\alpha \partial \tau}$$

T = Temperature

τ = Time

$q''' = Btu/ft^3$

k = Thermal Conductivity

α = Thermal Diffusivity

The discretized version of the above equation is:

$$\frac{T_1 + T_3 - 2T_0}{\Delta X^2} + \frac{T_2 + T_4 - 2T_0}{\Delta Y^2} + \frac{T_5 + T_6 - 2T_0}{\Delta Z^2} + \frac{q'''}{k} = \frac{T(\Delta \tau) - T_0}{\Delta \tau \alpha}$$

For the two dimension case one has:

$$T(\Delta\tau) = \frac{T_1 + T_2 + T_3 + T_4}{M} + (1 - \frac{4}{M})T_0 + \frac{q'''\Delta X^2}{kM}$$

$$M = \frac{\Delta X^2}{\alpha\Delta\tau}$$

M = Fourier number

For heuristic purposes, the transient thermal problem was solved without considering radiation, i.e, $q''' = 0$. This resulted in a conservative estimate. M, the Fourier number was chosen to be 5. The larger M is, the more accurate the estimate. Setting $M = 5$ has the advantage of reducing estimates of future temperatures to the average of known past temperatures. For a two dimensional square, the average was taken of five equally weighted temperatures. The five temperatures were the temperatures of each of the adjacent sides of a square and the temperature of the square itself. A computer program was written for a 100 by 100 grid containing 10,000 such squares. Each square was chosen to be .125 inches by .125 inches in area, since the width of the electron beam is .125 inches. The squares were initialized at $40.85°F$. Ten squares on edge were set to $1220°F$ and the program was iterated until the hottest square in the 10,000 square grid was below $235°F$, via conduction. The program estimated that in 1.1 seconds the hottest spot on the grid would be $231.1°F$. At two seconds the hottest spot would be $162°F$.

Approximately four minutes will elapse before an astronaut would be be required to grasp a freshly cut piece of metal. Therefore heated metal will not pose a problem for the astronauts.

There remain some general recommendations to be made for the thermal environment of the LH$_2$ portion of the External Tank. All motors and robotic joints to be used in the ASSET facility should be thermally insulated from conductive sources

of heat. Motors and joints should be joined to other components by insulated connectors with thermal resistances as large as possible. Radiated heat will pose no problem. All housings for motors and robotic joints should be coated on their exterior surfaces with an $\alpha/\epsilon = 1$ coating such as black paint. This will ensure that the solar thermal equilibrium temperature is $40.85°F$. The interior surfaces of motor and robotic joint housings should be coated so that the motors or joints can maintain a benign thermal environment. Heating coils controlled by thermostats should be used to compensate when more passive methods will not suffice. Brij N. Agrawal (1) detailed how to use equations such as equation E.1 to size motor housings or exploit the waste heat produced by a motor.

E.2 Computer Program

ASSET

Thermal Analysis Program for the External Tank

```
This program uses a finite differencing scheme to estimate when
the hottest spot on a piece of 2219 aluminum is cool enough for
an astronaut to touch it.  The finite difference algorithm is
documented in Benjamin Gebhart ; book 'HEAT TRANSFER' in
Chapters 3 and 11.  The genera`. thrust of the methodology is to
average the effects of current temperatures in order to predict
future temperatures.  This computer program assumes no
radiation effects.  Only transient conduction is modeled.


t(i,j) = current temperature of a point i,j in degrees F
t2(i,j) = future temperature of a point i,j in degrees F
m= Fourier number, dimensionless
ck= thermal conductivity of 2219 aluminum in Btu/hr/deg F/ft
cp= specific heat of 2219 aluminum in Btu/lb/deg F
p= density of 2219 aluminum in lb/(ft**3)
alpha= thermal diffusivity of 2219 aluminum in ft*ft/hr
delx= differential distance in feet
deltau= iteration time step in hours
```

```
program conduct
dimension t(100,100),t2(100,100)
real m

ck= 75.1
cp=.206
p= 177.984
alpha= ck/(cp*p)
m=5.0
delx = .125/12.0
deltau= delx*delx/(m*alpha)
area= delx*delx

Set background temperature to 40.85 deg F.

do 10 j=1,100
do 5    i=1,100
t(i,j)= 40.85
t2(i,j)= 40.85

   5 continue
  10 continue
do 222 jj= 45,55
t(1,jj)=1220.0
  222 continue

do 400 k=1,144
do 301 j2 = 1,100
do 301 i2 = 1,100
call finite(1,100,1,100,i2,j2,t,t2)
  301 continue

do 436 j=1,100
do 436 i=1,100
t(i,j) = t2(i,j)
  436 continue
  200 continue
sind= deltau*3600*k
if(sind.le..9) go to 400
if (sind.gt. 1.2 .and. sind .le.1.9) go to 400
if (sind.gt.2.1) go to 400
```

```
      print *,'run number =',k
      print *
      print *,'The hottest temperature at ',deltau*3600*k,' seconds'
      print *
      print *,' is ',t(1,50),' deg F'
      print *
      print *
  400 continue

      end
```

FINITE DIFFERENCE SUBROUTINE

```
      subroutine finite(ixs,ixl,iys,iyl,i,j,t,t2)
      dimension t(100,100), t2(100,100)
```

TEMPERATURES ARE AVERAGED ACCORDING TO THEIR POSITION IN A
100X100 ARRAY

CENTER

```
      if (i.gt.ixs.and.j.gt.iys.and.i.lt.ixl.and.j.lt.iyl)then

      t2(i,j)= t(i,j) + t(i,j-1) + t(i+1,j) + t(i,j+1) + t(i-1,j)
      t2(i,j)= t2(i,j)/5.0

      go to 39
      end if
```

LOWER LEFT HAND CORNER

```
      if (i.eq.ixs .and. j.eq.iys) then
      t2(i,j)=  ( t(i+1,j) + t(i,j) + t(i,j+1))/3.0
      go to 39
      end if
```

LEFT CENTER

```
      if(i.eq.ixs .and. j.gt.iys .and. j.lt.iyl) then
      t2(i,j) = (t(i,j) + t(i,j-1) + t(i+1,j) + t(i,j+1))/4.0
      go to 39
      end if
```

```
UPPER LEFT HAND CORNER

if (i.eq.ixs .and. j.eq.iyl) then
t2(i,j)= ( t(i,j) + t(i,j-1) + t(i+1,j))/3.0
go to 39
end if

BOTTOM CENTER

if(j.eq.iys .and. i.gt.ixs .and. i.lt.ixl) then
t2(i,j) = ( t(i,j) + t(i+1,j) + t(i,j+1) + t(i-1,j))/4.0
go to 39
end if

BOTTOM RIGHT

if (j.eq.iys .and. i.eq.ixl) then
t2(i,j) = (t(i,j) + t(i-1,j) + t(i,j+1))/3.0
go to 39
end if

RIGHT CENTER

if (i.eq.ixl .and. j.gt.iys .and. j.lt.iyl) then
t2(i,j) = ( t(i,j) + t(i,j-1) + t(i,j+1) + t(i-1,j))/4.0
go to 39
end if

TOP RIGHT

if( i.eq. ixl .and. j.eq.iyl) then
t2(i,j) = ( t(i,j) + t(i,j-1) + t(i-1,j) )/3.0
go to 39
end if

TOP CENTER

if (j.eq.iyl .and. i.gt.ixs .and. i.lt. ixl) then
t2(i,j) = ( t(i,j) + t(i-1,j) + t(i,j-1) + t(i+1,j))/4.0
end if
   39 return
end
```

Table E.1. ASSET Thermal Model Results

RUN NUMBER	ELAPSED TIME (LOCAL HOT SPOT)	PEAK TEMPERATURE
27	1.0298 seconds	240.807° F
28	1.0679 seconds	235.863° F
29	1.1061 seconds	231.163° F
52	1.9834 seconds	163.720° F
53	2.0215 seconds	161.867° F
54	2.0596 seconds	160.069° F

Appendix F. *EVA TIMELINES*

F.1 Introduction

A recognized weakness at the start of this study was the inability to forecast (with any degree of accuracy) the amount of EVA required to perform various tasks. The sponsor suggested we examine the EVA timelines from STS 61 (EASE/ACCESS experiments) (64, 65) and the External Tank Gamma Ray Imaging Telescope (ET-GRIT) Study (53). Timeline estimates were based on a linear projection of previously quantified tasks. If no quantified data for similar tasks was found, engineering judgement was used to estimate the timelines.

It should be noted that the ability to forecast timelines for an EVA task is as much a matter of luck as skill. The timeline projections for the ACCESS experiments were in error by a factor of two. During water tank training, the crew took an average of 58 minutes to build and disassemble a 45 foot truss structure composed of 93 tubular beams and 33 nodal joints. Although 2 hours were scheduled for the task in space, the task was accomplished in 55 minutes (20:22).

Similar errors were evident in the projections for the EASE experiments which involved the construction of large pyramid structures (19:69). USAF Maj. Jerry Ross was originally scheduled to assemble two structures from the top position, but, in fact, had time to construct 4 structures (20:22). These types and degrees of error appear to be quite common and thus, our projections for EVA timelines will not be significantly better or worse.

We also needed to address the issue of whether EVA tasks could be sustained over a period of several days. The EASE/ACCESS astronauts were tasked to work as long and as hard as possible. In spite of the workload, the astronauts felt they could sustain a workload at that level, on an every other day basis, for an extended period of time (4:20). It is assumed that the ASSET workloads will be no more (and

probably less) severe than the EASE/ACCESS workloads and can be carried out over consecutive days.

It has been assumed that 8 hour EVA missions will be accommodated and this should be a safe assumption in light of recent space suit evaluations. NASA has evaluated both the AX-5, an all-hard metal suit developed at NASA-Ames Research Center, and the Zero Pre-breathe Suit (ZPS) Mk. 3, a suit using both hard and soft elements developed at Johnson Space Center (84:36). The suits are designed for 8 hours of EVA, either on a continuous 8 hour shift or for a routine SSF work day schedule, with a 4 hour shift before and after lunch (84:36). We have assumed continuous 8 hour timelines to support the ASSET mission.

F.2 Initial Mission Set-Up

INITIAL DEPLOYMENT/SCENARIO 1
EVA #1: 2 ASTRONAUTS, 480 MINUTES

Install Boost/De-orbit Modules X 2	120
Remove cable tray covers for pyro charges	20
Remove pyro charges X 2	55
Access Intertank	20
Install connectors for Solar Array in Intertank . . .	15
Install power connectors in LH2 forward dome	15
Install Solar Arrays X 2	120
Remove Aft LH2 tank manhole cover	20
Install fireman's pole	10
Remove station 1500.58 Intermediate ring frame . . .	20
Cut station 1500.58 Int. ring frame in 4 pieces . . .	10
Bundle, transport, and store 1500.58 in LH2 fwd dome . .	15
Install wiring for communications/cameras/lights . . .	20
Install wiring for center arm and cutter	10
Install wiring for SOFI workstation	10

TOTAL = 480

INITIAL DEPLOYMENT/SCENARIO 1
EVA #2: 2 ASTRONAUTS, 480 MINUTES

Install lights	60
Install camera mounts/cameras	40
Remove/cut/store 7 more intermediate ring frames . . .	200
Note: 1 of the remaining 7 ring frames is bolted in and can be removed by 1 astronaut while the other is using the E-beam cutter.	
Install center arm trolley	30
Install SOFI stripper table	20
Install secondary cutter on SOFI stripper table . . .	10
Install SOFI bag	10
Install I-beam storage/containment	20
Install plate storage/containment	20
Install primary cutter	10
Install spares: primary and secondary cutters . . .	10
Store umbilical cables for subsequent tanks	10
Install control masts and antennas	40

TOTAL = 480

F.2.1   Scenario 1 At the conclusion of the first 2 EVA's, the initial tank is now in a position to be reduced. The orbiter would (in theory) be free to leave at this time for the 1.7 days of automated reduction. We would recommend, however, that the orbiter remain in the vicinity in the event problems arise and EVA intervention is required to correct the problem.

F.2.2   Scenario 2

INITIAL DEPLOYMENT/SCENARIO 2
EVA #1: 2 ASTRONAUTS, 470 MINUTES

```
Install Boost/De-orbit Modules X 2      .     .     .     .     .     .     120
Remove cable tray covers for pyro charges .     .     .     .     .      20
Remove pyro charges X 2      .     .     .     .     .     .     .     .      55
Access Intertank      .     .     .     .     .     .     .     .     .      20
Install connectors for Solar Array in Intertank    .     .     .      15
Install power connectors in LH2 forward dome  .     .     .     .      15
Install Solar Arrays X 2      .     .     .     .     .     .     .     .     120
Remove Aft LH2 tank manhole cover      .     .     .     .     .      20
Install fireman's pole      .     .     .     .     .     .     .     .      10
Remove station 1500.58 Intermediate ring frame     .     .     .      20
Cut station 1500.58 Int. ring frame in 4 pieces     .     .     .      10
Bundle, transport, and store 1500.58 in LH2 fwd dome   .     .      15
Install wiring for communications/lights      .     .     .     .      20
Install wiring for SOFI workstation .     .     .     .     .     .      10
```

                                                   TOTAL = 470

INITIAL DEPLOYMENT/SCENARIO 2
EVA #2: 2 ASTRONAUTS, 480 MINUTES

Install lights	60
Install wiring for cutters	40
Remove/cut/store 7 more intermediate ring frames	210
Install astronaut seat on major ring frame	20
Install SOFI stripper table	20
Install secondary cutter on SOFI stripper table	10
Install SOFI bag	10
Install I-beam storage/containment	20
Install plate storage/containment	20
Install primary cutter	10
Install spares: primary and secondary cutters	10
Store umbilical cables for subsequent tanks	10
Install control masts and antennas	40

TOTALS = 480

F.3 Reduction Timelines

The EVA timelines to carry out the actual salvage operation are not included in this appendix. Recall that a SLAM simulation was developed and used to quantify reduction timelines and power requirements. The timelines for actual reduction, for both scenarios, are provided in Appendix B.

F.4 Subsequent Tank Reduction: LH₂ Tank Reduction Only

F.4.1 Scenario 1

TANK #2 & SUBSEQUENT
SCENARIO 1: EVA #1

Install docking mechanism on tank 1 (one time operation)	30
Mate the tanks	30
Access the intertank on tank N+1	20
Install power connectors in LH2 forward dome	15
Run guide rails/restraint lines between the intertank doors	20
Install umbilical cables between tank 1 and tank N+1	20
Access LH2 aft dome manhole cover on tank N+1	20
Run guide rails/restraint lines between aft dome manholes	20
Install restraint lines, over cable tray, between previously installed lines	20
Remove cable tray covers for pyro charges on tank N+1	20
Remove pyro charges for tank N+1	55
Remove, cut, bundle, transport, and store 7 (seven) intermediate ring frames in tank N+1	210

> Note: 1 of the first 7 ring frames is bolted
>   in and can be removed in parallel with
>   the other ring frames being cut out via
>   the E-beam cutter.

                                          TOTAL = 480

TANK #2 & SUBSEQUENT
SCENARIO 1: EVA #2

Remove, cut, bundle, transport, and store the last intermediate ring frame in tank N+1 . . .	30
Remove and bundle wiring for center arm trolley and SOFI workstation	10
Remove and bundle lights/cameras in tank 1	25
Remove and bundle lights/cameras wiring in tank 1 . .	25
Transport and install lights/cameras wiring in tank N+1 .	35
Transport and install lights/cameras in tank N+1 . . .	35
Transport and install wiring for center arm trolley and SOFI workstation	20
Remove old SOFI bag in tank 1 (deorbit or return to cargo bay)	10
Bundle previously salvaged I-beams from tank 1 . . .	10
and store in tank 1	20
Bundle previously salvaged plates from tank 1 . . .	10
and store in tank 1	20
Remove I-beam storage/containment equipment from tank 1 .	10
Remove plate storage/containment equipment from tank 1 .	10
Transport storage/containment equipment to tank N+1 . .	20
Install I-beam storage/containment equipment in tank N+1 .	10
Install plate storage/containment equipment in tank N+1 .	10
Egress back to tank 1	10
Remove secondary cutter from SOFI strip table in tank 1 .	10
Remove SOFI strip table from tank 1	20
Transport secondary cutter and strip table to tank N+1 . .	20
Install SOFI strip table in tank N+1	20
Install secondary cutter in tank N+1	10
Egress back to tank 1	10
Remove primary cutter from tank 1	05
Transport and install primary cutter in tank N+1 . . .	15
Egress back to tank 1	10
Remove center arm trolley from tank 1	10
Transport and install center arm trolley in tank N+1 . .	20
Install new SOFI bag in tank N+1	10

```
                                    ----------
                              TOTAL = 480
```

At this point, the reduction effort can be carried out on tank 2. The orbiter would be free to leave for the next 1.7 days. Subsequent EVA will still be required after the second tank has been reduced. The products from tank 2 need to be off-loaded to tank 1. The tools and wiring will also need to be removed and stored in tank 1 for use on subsequent tanks. Tank 2 and subsequent bird cage structures will either be sold or de- orbited.

TANK #2 & SUBSEQUENT
SCENARIO 1: EVA #3

Install tethers/restraint lines between tanks . . .	60
Bundle salvaged I-beams from tank N+1	10
Transport and store salvaged I-beams in tank 1 . . .	40
Bundle salvaged plates from tank N+1	10
Transport and store salvaged plates in tank 1 . . .	40
Egress back to tank N+1	10
Remove SOFI bag (deorbit or store in cargo bay) . . .	10
Remove I-beam storage/containment equipment from tank N+1 .	15
Remove plate storage/containment equipment from tank N+1 .	15
Bundle, transport, and store storage/containment equipment in LH2 aft dome area of tank 1	30
Egress back to tank N+1	10
Remove SOFI strip table from tank N+1 (secondary cutter need not be removed)	20
Transport and store SOFI strip table in LH2 aft dome of tank 1	20
Egress back to tank N+1	10
Remove center arm trolley from tank N+1	10
Transport and store center arm trolley in tank 1 . . .	20
Egress back to tank N+1	10
Remove primary cutter from tank N+1	05
Transport and store primary cutter in tank 1 . . .	15
Egress back to tank N+1	10
Remove and bundle lights/cameras from tank N+1 . . .	25
Transport and store lights/cameras in tank 1 . . .	10
Egress back to tank N+1	10
Remove and bundle wiring for lights/cameras from tank N+1 .	25
Transport and store wiring for lights/cameras in tank 1 .	20
Egress back to tank N+1	10
Remove and bundle wiring for SOFI workstation and center arm trolley	10

```
                                                   ------------
                                               TOTAL = 480
```

TANK #2 & SUBSEQUENT
SCENARIO 1: EVA #4

Transport and store wiring for SOFI workstation and center
    arm trolley in tank 1 20
Egress back to tank N+1 10
Remove power cables and connectors from tank N+1 . . . 30
Transport and store power connectors and cables in tank 1 . 20
Egress back to tank N+1 10
Transport and store the intermediate ring frames from
    tank N+1 to tank 1 80
Cut out the pre-installed center line track from tank N+1
    via portable E-beam cutter 60
Transport and store center line track in tank 1 . . . 30
Egress back to tank N+1 10
Remove guide rails/restraint lines between intertank doors
    and store in tank 1 intertank 20
Egress to aft LH2 dome of tank N+1 10
Remove guide rails/restraint lines between LH2 aft domes
    and store in tank 1 20
Remove tethers/restraint lines between tanks 30
Disengage docking mechanisms 30
Deorbit tank N+1   ------------

TOTALS = 380

MISSION OUTLINE: SCENARIO 1
LH2 TANK REDUCTION ONLY
TANK 2 AND SUBSEQUENT

A. From mission launch to first EVA, 72 hours must elapse under the current NASA guidelines. We would ask for a waiver to allow EVA via ASSET employees 24 hours after launch.

B. PRODUCT STORAGE (Tank #1) & TOOL TRANSFER (To Tank #2)
   - DAY 2 - EVA #1 (480 minutes)
   - DAY 3 - EVA #2 (480 minutes)
   - Reduction can commence upon completion
   - Reduction time requires 1.7 days (40.8 hours)
   - Orbiter would be free to leave for 1.7 days

C. TANK REDUCTION
   - Last 16 hours of day 3
   - All of day 4
   - First 48 minutes of day 5

D. PRODUCT & TOOL TRANSFER TO TANK #1
   - DAY 5 - EVA #3 (480 minutes)
   - DAY 6 - EVA #4 (380 minutes)

E. MISSION COMPLETE
   428 minutes into day 6, you're ready to return to earth. Thus, 6.2972 days into the mission (including the 1.7 days the orbiter was free to leave during the reduction operation), the ASSET facility would no longer need EVA support. An assumed maximum 10 day orbiter mission would, therefore, still have 5.4028 days to conduct their primary resupply mission at SSF.

NOTE: If NASA denies our waiver, this would change the scenario 1 timelines from a 6.2972 day mission to an 8.2972 day mission. An assumed maximum 10 day orbiter mission would, therefore, still leave 3.4028 days to perform their primary mission of SSF resupply.

F.4.2   Scenario 2

<div align="center">

TANK #2 & SUBSEQUENT
SCENARIO 2: EVA #1
</div>

Install docking mechanism on tank 1 (one time operation) . 30
Dock the tanks 30
Access the intertank on tank N+1 20
Install power connectors in LH2 forward dome 15
Run guide rails/restraint lines between the intertank doors . 20
Install umbilical cables between tank 1 and tank N+1 . . 20
Access LH2 aft dome manhole cover on tank N+1 . . . 20
Run guide rails/restraint lines between aft dome manholes . 20
Install restraint lines, over cable tray, between
      previously installed lines 20
Remove cable tray covers for pyro charges on tank N+1 . . 20
Remove pyro charges for tank N+1 55
Remove, cut, bundle, transport, and store 7 (seven)
      intermediate ring frames in tank N+1 210

<div align="right">

TOTAL = 480
</div>

TANK #2 & SUBSEQUENT
SCENARIO 2; EVA #2

Remove, cut, bundle, transport, and store the
    last intermediate ring frame in tank N+1   .   .   .   40
Remove and bundle wiring for primary cutters
    and SOFI workstation   10
Remove and bundle lights in tank 1   25
Remove and bundle wiring for lights in tank 1   .   .   25
Transport and install wiring for lights in tank N+1   .   .   35
Transport and install lights   35
Transport and install wiring for primary cutters and
    SOFI workstation   20
Remove old SOFI bag in tank 1
    (deorbit or return to cargo bay)   10
Bundle previously salvaged I-beams from tank 1   .   .   .   10
    and store in tank 1   20
Bundle previously salvaged plates from tank 1   .   .   .   10
    and store in tank 1   20
Remove I-beam storage/containment equipment from tank 1   .   10
Remove plate storage/containment equipment from tank 1   .   10
Transport storage/containment equipment to tank N+1   .   .   20
Install I-beam storage/containment equipment in tank N+1   .   10
Install plate storage/containment equipment in tank N+1   .   10
Egress back to tank 1   10
Remove secondary cutter from SOFI strip table in tank 1   .   10
Remove SOFI strip table from tank 1   20
Transport secondary cutter and strip table to tank N+1 .   .   20
Install SOFI strip table in tank N+1   20
Install secondary cutter in tank N+1   10
Egress back to tank 1   10
Remove primary cutters from tank 1   05
Transport and install primary cutters in tank N+1 .   .   .   15
Egress back to tank 1   10
Remove astronaut seat from major ring frame in tank 1 .   .   05
Transport and install astronaut seat in tank N+1 .   .   .   15
Install new SOFI bag in tank N+1   10

                                            TOTAL = 480

All EVA's to this point have been 2 man EVA's. EVA #3 through #5 are required for tank reduction. Recall, the 23 hour timeline for reduction is an output from the SLAM simulation presented in Appendix B. Actual tank reduction EVA's for Scenario 2 are 3 man EVA's. The 3 man EVA's still assume 8 hour duration with 16 hours of rest between EVA.

TANK #2 & SUBSEQUENT
SCENARIO 2: EVA #6

Install tethers/restraint lines between tanks . . .	60
Bundle salvaged I-beams from tank N+1	10
Transport and store salvaged I-beams in tank 1 . . .	40
Bundle salvaged plates from tank N+1	10
Transport and store salvaged plates in tank 1 . . .	40
Egress back to tank N+1	10
Remove SOFI bag (deorbit or store in cargo bay) . . .	10
Remove I-beam storage/containment equipment from tank N+1 .	15
Remove plate storage/containment equipment from tank N+1 .	15
Bundle, transport, and store storage/containment equipment in LH2 aft dome area of tank 1	30
Egress back to tank N+1	10
Remove SOFI strip table from tank N+1 (secondary cutter need not be removed)	20
Transport and store SOFI strip table in LH2 aft dome of tank 1	20
Egress back to tank N+1	10
Remove astronaut seat from tank N+1	10
Transport and store astronaut seat in tank 1	20
Egress back to tank N+1	10
Remove primary cutters from tank N+1	05
Transport and store primary cutters in tank 1 . . .	15
Egress back to tank N+1	10
Remove and bundle lights from tank N+1	25
Transport and store lights in tank 1	10

TOTAL = 415

TANK #2 & SUBSEQUENT
SCENARIO 2: EVA #7

Remove and bundle wiring for lights from tank N+1 . . . 25
Transport and store wiring for lights in tank 1 . . . 20
Egress back to tank N+1 10
Remove and bundle wiring for SOFI workstation and
      primary cutters 10
Transport and store wiring for SOFI workstation and
      primary cutters in tank 1 20
Egress back to tank N+1 10
Remove power cables and connectors from tank N+1 . . . 30
Transport and store power connectors and cables in tank 1 . 20
Egress back to tank N+1 10
Transport the removed intermediate ring frames
      from tank N+1 to tank 1 80
Remove guide rails/restraint lines between intertank doors
      and store in tank 1 intertank 20
Egress to aft LH2 dome of tank N+1 10
Remove guide rails/restraint lines between LH2 aft domes
      and store in tank 1 20
Remove tethers/restraint lines between tanks 30
Disengage docking mechanisms 30
Deorbit tank N+1

                                 TOTAL = 345

MISSION OUTLINE: SCENARIO 2
LH2 TANK SALVAGE ONLY
TANK 2 AND SUBSEQUENT

A. From mission launch to first EVA, 72 hours must elapse under the current NASA guidelines. We would ask for a waiver to allow ASSET employees to EVA 24 hours after launch.

B. PRODUCT STORAGE (Tank #1) and TOOL TRANSFER (To Tank #2)
   - DAY 2 - EVA #1 (470 minutes)
   - DAY 3 - EVA #2 (480 minutes)
   - Reduction can commence 16 hours after completion
   - Reduction time requires 23 hours (as per Appendix B)

C. TANK REDUCTION (3 MAN EVA)
   - DAY 4 - EVA #3 (480 minutes)
   - DAY 5 - EVA #4 (480 minutes)
   - DAY 6 - EVA #5 (420 minutes)

D. TOOL AND PRODUCT TRANSFER (Back to Tank #1)
   - EVA #6 (415 minutes)
      -- Last 60 minutes of day 6
      -- First 345 minutes of day 7
      -- 16 hours of required crew rest
      -- 1305 minutes into day 7 (135 minutes remaining)
   - EVA #7 (345 minutes)
      -- Last 135 minutes of day 7
      -- First 210 minutes of day 8

E. MISSION COMPLETE
   - DAY 8 - Return to earth
   - 8.2396 day mission

EVA: QUANTITY = 7 (Conducted over 7 consecutive days)
            EVA #1 = 470 minutes of 2 man EVA
            EVA #2 = 480 minutes of 2 man EVA
            EVA #3 = 480 minutes of 3 man EVA
            EVA #4 = 480 minutes of 3 man EVA
            EVA #5 = 420 minutes of 3 man EVA
            EVA #6 = 415 minutes of 2 man EVA
            EVA #7 = 345 minutes of 2 man EVA
         TOTAL DURATION = 3090 Minutes (51.5 Hours)
                        = 63.0 Equiv. hrs for Cost

F.5 Subsequent Tank Reduction: LH_2 and LO_2 Tank Reduction

F.5.1 Scenario 1

<div align="center">

TANK #2 & SUBSEQUENT
SCENARIO 1: EVA #1

</div>

```
Install docking mechanism on tank 1 (one time operation)  .  30
Dock the tanks .    .    .    .    .    .    .    .    .    . 30
Access the intertank on tank N+1   .    .    .    .    .    . 20
Install power connectors in LH2 forward dome .   .    .    . 15
Run guide rails/restraint lines between the intertank doors . 20
Install umbilical cables between tank 1 and tank N+1  .  . 20
Access LH2 aft dome manhole cover on tank N+1    .    .  . 20
Run guide rails/restraint lines between aft dome manholes  . 20
Install restraint lines, over cable tray, between
      previously installed lines    .    .    .    .    .  . 20
Remove cable tray covers for pyro charges on tank N+1 .  . 20
Remove pyro charges for tank N+1    .    .    .    .    .  . 55
Remove, cut, bundle, transport, and store 7 (seven)
      intermediate ring frames in tank N+1   .    .    . . 210
```

> Note: 1 of the first 7 ring frames is bolted
> in and can be removed in parallel with
> the other ring frames being cut out via
> the E-beam cutter.

```
                                        ------------
                                        TOTAL = 480
```

TANK #2 & SUBSEQUENT
SCENARIO 1: EVA #2

Remove, cut, bundle, transport, and store the last intermediate ring frame in tank N+1	30
Remove and bundle wiring for center arm trolley and SOFI workstation	10
Remove and bundle lights/cameras in tank 1	25
Remove and bundle lights/cameras wiring in tank 1	25
Transport and install lights/cameras wiring in tank N+1	35
Transport and install lights/cameras in tank N+1	35
Transport and install wiring for center arm trolley and SOFI workstation	20
Remove old SOFI bag in tank 1 (deorbit or return to cargo bay)	10
Bundle previously salvaged I-beams from tank 1	10
and store in tank 1	20
Bundle previously salvaged plates from tank 1	10
and store in tank 1	20
Remove I-beam storage/containment equipment from tank 1	10
Remove plate storage/containment equipment from tank 1	10
Transport storage/containment equipment to tank N+1	20
Install I-beam storage/containment equipment in tank N+1	10
Install plate storage/containment equipment in tank N+1	10
Egress back to tank 1	10
Remove secondary cutter from SOFI strip table in tank 1	10
Remove SOFI strip table from tank 1	20
Transport secondary cutter and strip table to tank N+1	20
Install SOFI strip table in tank N+1	20
Install secondary cutter in tank N+1	10
Egress back to tank 1	10
Remove primary cutter from tank 1	05
Transport and install primary cutter in tank N+1	15
Egress back to tank 1	10
Remove center arm trolley from tank 1	10
Transport and install center arm trolley in tank N+1	20
Install new SOFI bag in tank N+1	10

TOTAL = 480

Subsequent EVA will be required after the second tank has been reduced. The salvaged products must be transported from tank #2 to tank #1 along with all the tools, power cables, and associated equipment. Tank #2 and subsequent bird cage structures will either be sold or de-orbited.

<div align="center">

TANK #2 & SUBSEQUENT
SCENARIO 1: EVA #3
</div>

```
Install tethers/restraint lines between tanks        .    .    .  60
Bundle salvaged I-beams from tank N+1     .    .    .    .    .  10
Transport and store salvaged I-beams in tank 1   .    .    .  40
Bundle salvaged plates from tank N+1      .    .    .    .    .  10
Transport and store salvaged plates in tank 1    .    .    .  40
Egress back to tank N+1   .    .    .    .    .    .    .    .  10
Remove SOFI bag (deorbit or store in cargo bay)  .    .    .  10
Remove I-beam storage/containment equipment from tank N+1  .  15
Remove plate storage/containment equipment from tank N+1   .  15
Bundle, transport, and store storage/containment equipment
        in LH2 aft dome area of tank 1    .    .    .    .    .  30
Egress back to tank N+1   .    .    .    .    .    .    .    .  10
Remove SOFI strip table from tank N+1
        (secondary cutter need not be removed)   .    .    .    .  20
Transport and store SOFI strip table in LH2 aft dome
        of tank 1 .    .    .    .    .    .    .    .    .    .  20
Egress back to tank N+1   .    .    .    .    .    .    .    .  10
Remove center arm trolley from tank N+1      .    .    .    .  10
Transport and store center arm trolley in tank 1 .    .    .  20
Egress back to tank N+1   .    .    .    .    .    .    .    .  10
Remove primary cutter from tank N+1      .    .    .    .    .  05
Transport and store primary cutter in tank 1     .    .    .  15
Egress back to tank N+1   .    .    .    .    .    .    .    .  10
Remove and bundle lights/cameras from tank N+1   .    .    .  25
Transport and store lights/cameras in tank 1     .    .    .  10
Egress back to tank N+1   .    .    .    .    .    .    .    .  10
Remove and bundle wiring for lights/cameras from tank N+1  .  25
Transport and store wiring for lights/cameras in tank 1    .  20
Egress back to tank N+1   .    .    .    .    .    .    .    .  10
Remove/bundle wiring for workstation and center arm trolley .  10
                                                       -----------
                                              TOTAL = 480
```

TANK #2 & SUBSEQUENT
SCENARIO 1: EVA #4

Transport and store wiring for SOFI workstation and center arm trolley in tank 1	20
Egress back to tank N+1	10
Remove power cables and connectors from tank N+1	30
Transport and store power connectors and cables in tank 1	20
Egress back to tank N+1	10
Transport and store the intermediate ring frames from tank N+1 to tank 1	80
Cut out the pre-installed center line track from tank N+1 via portable E-beam cutter	60
Transport and store center line track in tank 1	30
Egress back to tank N+1	10
Remove guide rails/restraint lines between intertank doors and store in tank 1 intertank	20
Egress to aft LH2 dome or tank N+1	10
Remove guide rails/restraint lines between LH2 aft domes and store in tank 1	20
Remove tethers/restraint lines between tanks	30
Disengage docking mechanisms	30
Deorbit tank N+1	
	TOTAL = 380

TANK #2 & SUBSEQUENT
SCENARIO 1: EVA #5
SET-UP FOR LOX TANK SALVAGE

Remove nose cone (17 bolts) 10
Transport and store in tank N+1 10
Egress back to nose cap area 10
Remove forward ogive cover plate (92 bolts) 45
Transport and store fwd. ogive cover plate in tank 1 . . 10
Install radial supports between SRB mounts (2 pieces) . . 20
Install adapter to forward ogive fitting 15
Install structure between radial support around the
      intertank and the forward ogive fitting 25
Install structure between radial support around the
      intertank and the input to SOFI workstation . . . 20
Install LOX tank cutter 15

Set-up subtotal = 180

EXECUTE LOX BARREL SALVAGE

1st cut is box cut [(211.3")/80 IPM] = 2.641 minutes
2nd and subsequent cuts are C-cut [(116.5")/80 IPM] = 1.456 min.
2.641 + 103(1.456) = 152.609 minutes of total cutting time

Allow 147.391 minutes for piece part transport
      1.417 min./piece (85 seconds)
      25 seconds to grasp and attach to transport system
      60 seconds to transport 60 feet

SOFI stripper can easily keep up with cut/transport rate

LOX barrel salvage subtotal = 300
EVA #5 TOTAL = 480

NOTE: 36 hours required between EVA #5 and EVA #6 to allow the
       SOFI on the LOX forward and aft ogive sections to be
       cleaned via an E-beam cutter.

```
                    TANK #2 & SUBSEQUENT
                    SCENARIO 1: EVA #6
                    LOX OGIVE SALVAGE (37 cuts at 28" max. width)

Make 1st box cut (9.578 min.) + 9 C-cuts @ 4.982 min
     = 54.425 minutes plus bundling      .    .    .    .    . 60
Transport and store 1st 10 pieces in tank 1 .    .    .    . 20
Make 9 more C-cuts @ 4.982 = 44.847 + bundling   .    .    . 50
Transport and store 2nd 9 pieces in tank 1  .    .    .    . 20
Make 9 more C-cuts @ 4.982 = 44.847 + bundling   .    .    . 50
Transport and store 3rd 9 pieces in tank 1  .    .    .    . 20
Make last 9 C-cuts @ 4.982 = 44.847 + bundling   .    .    . 50
Transport and store last 9 pieces in tank 1 .    .    .    . 20
                                         ---------------------------
                                         OGIVE SALVAGE TOTAL = 290




                            TEAR DOWN


Remove LOX tank cutter and store in tank 1   .    .    .    . 20
Remove structure between radial supports and input
     to SOFI workstation and store in tank 1      .    .    . 30
Remove structure between radial support and forward
     ogive fitting .    .    .    .    .    .    .    .    . 35
Remove adapter to forward ogive fitting and store in tank 1   25
Salvage forward ogive fitting and store in tank 1      .    . 30
Remove radial supports between SRB mounts
     and store in tank 1       .    .    .    .    .    .    . 30
                                         ---------------------------
                                         TEAR DOWN TOTALS = 170

                                         EVA #6 TOTALS = 460
```

MISSION OUTLINE: SCENARIO 1
LH2 AND LOX TANK SALVAGE
TANK 2 AND SUBSEQUENT

A. From mission launch to first EVA, 72 hours must elapse under the current NASA guidelines. We would ask for a waiver to allow EVA via ASSET employees 24 hours after launch.

B. PRODUCT STORAGE (Tank #1) and TOOL TRANSFER (To Tank #2)
  - DAY 2 - EVA #1 (480 minutes)
  - DAY 3 - EVA #2 (480 minutes)
    -- Reduction can commence upon completion
    -- Reduction time requires 1.7 days (40.8 hours)
    -- Orbiter would be free to leave the area

C. TANK REDUCTION
  - Last 16 hours of day 3
  - All of day 4
  - First 48 minutes of day 5

D. PRODUCT and TOOL TRANSFER (To Tank #1)
  - DAY 5 - EVA #3 (480 minutes)
  - DAY 6 - EVA #4 (380 minutes)

E. LOX BARREL SALVAGE
  - Claims 2203.8 pounds of readily usable plate.
  - DAY 7 - EVA #5 (480 minutes)
  - End of this EVA marks 428 minutes into day 7 (7.2972 days)
  - 36 hours required for E-beam to clean SOFI off the exterior surfaces of the LOX forward and aft ogive sections
    -- Last 1012 minutes (16.8667 hours) of day 7
    -- First 1148 minutes (19.1333 hours) of day 8

F. LOX OGIVE SALVAGE and TOOL TRANSFER
  - Ogive salvage claims 4513 pounds of material that will most likely require further processing.
  - EVA #6 (460 minutes)
    -- Last 292 minutes of day 8
    -- First 168 minutes of day 9

G. MISSION COMPLETE
  - 168 minutes into day 9
  - Return to earth (9.1167 day mission)

EVA QUANTITIES: SCENARIO 1
LH2 AND LOX TANK SALVAGE
TANK #2 & SUBSEQUENT

EVA #1 = 480 minutes
EVA #2 = 480 minutes

        Break: 1.7 days (Automated reduction)

EVA #3 = 480 minutes
EVA #4 = 380 minutes
EVA #5 = 480 minutes

        Break: 1.5 days (LOX SOFI removal)

EVA #6 = 460 minutes

TOTAL EVA DURATION = 2760 Minutes (46 Hours)
                 (All EVA's are 2 man EVA)

The 9.1167 day mission includes two down periods where the orbiter would be free to leave the vicinity. These two periods included the 1.7 days required for actual LH_2 tank reduction and 1.5 days required to remove the SOFI (via an electron beam gun) from the LO_2 aft and forward ogive sections. Thus, under an assumed 10 day maximum orbiter constraint, the orbiter would still have 4.0833 days to accomplish it's primary resupply mission at SSF.

Should NASA refuse the waiver (to EVA 24 hours after launch), the Scenario 1 timelines would extend to an 11.1167 mission. Failure to obtain a waiver would probably preclude LO_2 salvage.

F.5.2   Scenario 2

TANK #2 & SUBSEQUENT
SCENARIO 2: EVA #1

Install docking mechanism on tank 1 (one time operation)   . 30
Dock the tanks 30
Access the intertank on tank N+1   20
Install power connectors in LH2 forward dome 15
Run guide rails/restraint lines between the intertank doors . 20
Install umbilical cables between tank 1 and tank N+1   .   . 20
Access LH2 aft dome manhole cover on tank N+1   .   .   . 20
Run guide rails/restraint lines between aft dome manholes   . 20
Install restraint lines, over cable tray, between
      previously installed lines   20
Remove cable tray covers for pyro charges on tank N+1 .   . 20
Remove pyro charges for tank N+1   55
Remove, cut, bundle, transport, and store 7 (seven)
      intermediate ring frames in tank N+1   210

                              TOTAL = 480

TANK #2 & SUBSEQUENT
SCENARIO 2: EVA #2

Remove, cut, bundle, transport, and store the
    last intermediate ring frame in tank N+1   .   .   . 40
Remove and bundle wiring for primary cutters
    and SOFI workstation   10
Remove and bundle lights in tank 1   25
Remove and bundle wiring for lights in tank 1   .   .   . 25
Transport and install wiring for lights in tank N+1   .   . 35
Transport and install lights 35
Transport and install wiring for primary cutters and
    SOFI workstation   20
Remove old SOFI bag in tank 1
    (deorbit or return to cargo bay)   10
Bundle previously salvaged I-beams from tank 1   .   .   . 10
    and store in tank 1 20
Bundle previously salvaged plates from tank 1   .   .   . 10
    and store in tank 1 20
Remove I-beam storage/containment equipment from tank 1   . 10
Remove plate storage/containment equipment from tank 1   . 10
Transport storage/containment equipment to tank N+1   .   . 20
Install I-beam storage/containment equipment in tank N+1   . 10
Install plate storage/containment equipment in tank N+1   . 10
Egress back to tank 1   10
Remove secondary cutter from SOFI strip table in tank 1   . 10
Remove SOFI strip table from tank 1   20
Transport secondary cutter and strip table to tank N+1 .   . 20
Install SOFI strip table in tank N+1   20
Install secondary cutter in tank N+1   10
Egress back to tank 1   10
Remove primary cutters from tank 1 05
Transport and install primary cutters in tank N+1 .   .   . 15
Egress back to tank 1   10
Remove astronaut seat from major ring frame in tank 1 .   . 05
Transport and install astronaut seat in tank N+1 .   .   . 15
Install new SOFI bag in tank N+1   10

                                                TOTAL = 480

Up to this point, all EVA's have been 2 man EVA. The EVA's required for actual tank reduction will be 3 man EVA. The standard assumptions of 8 hour EVA duration followed by 16 hours of crew rest still apply. This also assumes the orbiter can support 3 man EVA. The requirement for 23 hours of 3 man EVA is developed in Appendix B.

TANK #2 & SUBSEQUENT
SCENARIO 2: EVA #6

```
Install tethers/restraint lines between tanks        .     .     .  60
Bundle salvaged I-beams from tank N+1        .     .     .     .  10
Transport and store salvaged I-beams in tank 1      .     .     .  40
Bundle salvaged plates from tank N+1         .     .     .     .  10
Transport and store salvaged plates in tank 1       .     .     .  40
Egress back to tank N+1 .     .     .     .     .     .     .  10
Remove SOFI bag (deorbit or store in cargo bay)     .     .     .  10
Remove I-beam storage/containment equipment from tank N+1  .  15
Remove plate storage/containment equipment from tank N+1   .  15
Bundle, transport, and store storage/containment equipment
     in LH2 aft dome area of tank 1          .     .     .     .  30
Egress back to tank N+1 .     .     .     .     .     .     .  10
Remove SOFI strip table from tank N+1
     (secondary cutter need not be removed)  .     .     .     .  20
Transport and store SOFI strip table in LH2 aft dome
     of tank 1 .     .     .     .     .     .     .     .     .  20
Egress back to tank N+1 .     .     .     .     .     .     .  10
Remove astronaut seat from tank N+1          .     .     .     .  10
Transport and store astronaut seat in tank 1 .     .     .     .  20
Egress back to tank N+1 .     .     .     .     .     .     .  10
Remove primary cutters from tank N+1         .     .     .     .  05
Transport and store primary cutters in tank 1       .     .     .  15
Egress back to tank N+1 .     .     .     .     .     .     .  10
Remove and bundle lights from tank N+1       .     .     .     .  25
Transport and store lights in tank 1         .     .     .     .  10
                                                   -----------
                                             TOTAL = 415
```

TANK #2 & SUBSEQUENT
SCENARIO 2: EVA #7

Remove and bundle wiring for lights from tank N+1 . . . 25
Transport and store wiring for lights in tank 1 . . . 20
Egress back to tank N+1 10
Remove and bundle wiring for SOFI workstation and
     primary cutters 10
Transport and store wiring for SOFI workstation and
     primary cutters in tank 1 20
Egress back to tank N+1 10
Remove power cables and connectors from tank N+1 . . . 30
Transport and store power connectors and cables in tank 1 . 20
Egress back to tank N+1 10
Transport the removed intermediate ring frames
     from tank N+1 to tank 1 80
Remove guide rails/restraint lines between intertank doors
     and store in tank 1 intertank 20
Egress to aft LH2 dome of tank N+1 10
Remove guide rails/restraint lines between LH2 aft domes
     and store in tank 1 20
Remove tethers/restraint lines between tanks 30
Disengage docking mechanisms 30

                                     TOTAL = 345

TANK #2 & SUBSEQUENT
SCENARIO 2: EVA #8
SET-UP FOR LOX TANK SALVAGE

Remove nose cone (17 bolts) 10
Transport and store in tank N+1 10
Egress back to nose cap area 10
Remove forward ogive cover plate (92 bolts) 45
Transport and store fwd. ogive cover plate in tank 1 . . 10
Install radial supports between SRB mounts (2 pieces) . . 20
Install adapter to forward ogive fitting 15
Install structure between radial support around the
      intertank and the forward ogive fitting 25
Install structure between radial support around the
      intertank and the input to SOFI workstation . . . 20
Install LOX tank cutter 15

                             Set-up subtotal = 180

EXECUTE LOX BARREL SALVAGE

1st cut is box cut [(211.3")/80 IPM] = 2.641 minutes
2nd and subsequent cuts are C-cut [(116.5")/80 IPM] = 1.456 min.
2.641 + 103(1.456) = 152.609 minutes of total cutting time

Allow 147.391 minutes for piece part transport
    1.417 min./piece (85 seconds)
       25 seconds to grasp and attach to transport system
       60 seconds to transport 60 feet

SOFI stripper can easily keep up with cut/transport rate

               LOX barrel salvage subtotal = 300

                         EVA #8 TOTAL = 480

NOTE: 22 hours required between EVA #8 and EVA #9 to allow the
       SOFI on the LOX forward and aft ogive sections to be
       cleaned via an E-beam cutter.

TANK #2 & SUBSEQUENT
SCENARIO 2: EVA #9
LOX OGIVE SALVAGE (37 cuts at 28" max. width)

Make 1st box cut (9.578 min.) + 9 C-cuts @ 4.982 min
     = 54.425 minutes plus bundling   60
Transport and store 1st 10 pieces in tank 1   20
Make 9 more C-cuts @ 4.982 = 44.847 + bundling   .   .   .   50
Transport and store 2nd 9 pieces in tank 1   20
Make 9 more C-cuts @ 4.982 = 44.847 + bundling   .   .   .   50
Transport and store 3rd 9 pieces in tank 1   20
Make last 9 C-cuts @ 4.982 = 44.847 + bundling   .   .   .   50
Transport and store last 9 pieces in tank 1   20

                          OGIVE SALVAGE TOTAL = 290

TEAR DOWN

Remove LOX tank cutter and store in tank 1   20
Remove structure between radial supports and input
     to SOFI workstation and store in tank 1   .   .   .   30
Remove structure between radial support and forward
     ogive fitting   35
Remove adapter to forward ogive fitting and store in tank 1   25
Salvage forward ogive fitting and store in tank 1   .   .   30
Remove radial supports between SRB mounts
     and store in tank 1   30

                          TEAR DOWN TOTALS = 170

                          EVA #9 TOTALS = 460

MISSION OUTLINE: SCENARIO 2
LH2 AND LOX TANK SALVAGE
TANK #2 AND SUBSEQUENT

A. From mission launch to first EVA, 72 hours must elapse under the current NASA guidelines. We would ask for a waiver to allow ASSET employees to EVA 24 hours after launch.

B. PRODUCT STORAGE (Tank #1) and TOOL TRANSFER (To Tank #2)
- DAY 2 - EVA #1 (470 minutes)
- DAY 3 - EVA #2 (480 minutes)
  -- Reduction can commence 16 hours after completion
  -- Reduction time requires 23 hours of 3 man EVA

C. TANK REDUCTION (3 MAN EVA)
- DAY 4 - EVA #3 (480 minutes)
- DAY 5 - EVA #4 (480 minutes)
- DAY 6 - EVA #5 (420 minutes)

D. LH2 PRODUCT AND TOOL TRANSFER TO TANK #1
- EVA #6 (415 minutes)
  -- Actually last 60 minutes of day 6
  -- First 355 minutes into day 7
- EVA #7 (345 minutes)
  -- Last 125 minutes of day 7
  -- First 220 min of day 8
- 6 hours of crew rest takes you 1180 minutes into day 8
- 260 minutes remain in day 8

E. LOX BARREL SALVAGE
- EVA #8 (480 minutes)
  -- Last 260 minutes of day 8
  -- First 220 minutes of day 9
  -- End of this EVA marks 220 minutes into day 9
- 36 hours required for E-beam to clean SOFI off the exterior surfaces of the LOX forward and aft ogive sections
  -- Last 1220 minutes of day 9
  -- First 15.6667 hours (940 minutes) of day 10
  -- 500 minutes remain in day 10
- Marks first chance for crew rest (EVA's #1 - #8 were conducted over 8 consecutive days)

F. LOX FORWARD & AFT OGIVE SALVAGE
- EVA #9 (460 minutes)
- Includes 170 minutes for tool tear down
- 40 minutes still remain in day 10
G. MISSION COMPLETE
- 1400 minutes into day 10
- Return to earth (10.9722 day mission)

                    EVA QUANTITIES: SCENARIO 2
                    LH2 and LOX TANK SALVAGE

            EVA #1 = 470 minutes of 2 man EVA
            EVA #2 = 480 minutes of 2 man EVA
            EVA #3 = 480 minutes of 3 man EVA
            EVA #4 = 480 minutes of 3 man EVA
            EVA #5 = 420 minutes of 3 man EVA
            EVA #6 = 415 minutes of 2 man EVA
            EVA #7 = 345 minutes of 2 man EVA
            EVA #8 = 480 minutes of 2 man EVA
            EVA #9 = 460 minutes of 2 man EVA

        TOTAL DURATION = 4030 Minutes (67.1667 Hours)
                       = 78.6667 Equiv. hrs for Cost

LO_2 tank salvage to Scenario 2 requires a 10.9722 day mission even if NASA grants a waiver to allow EVA 24 hours after launch. This 10.9722 day mission only allows 1.5 days (during the time the E-beam gun is used to remove SOFI from the LO_2 aft and forward ogive sections) where the orbiter would be free to perform it's primary mission of SSF resupply. Thus, if the assumed 10 day orbiter mission is a hard constraint, LO_2 tank salvage would be precluded.

Appendix G. *COST MODEL*

In formulating the problem statement for this study, one of the primary concerns raised was whether or not salvaging an ET in space could be cost competitive with hauling the same material from the surface of the Earth. This cost model attempts to objectively address that concern.

G.1 *Model Development*

A NASA space station Life Cycle Cost Model (LCCM), developed for the George C. Marshall Space Flight Center in 1977, is used as a framework for the ASSET cost model. NASA's LCCM provides Life Cycle Costs (LCC) for all Design, Development, Test, and Evaluation (DDT&E), Flight Hardware Production (FH), and Operations expenditures.

System and subsystem LCC estimates are generated using Cost Estimating Relationships (CERs) of the form:

$$Y = \beta_0 X^{\beta_1}. \tag{G.1}$$

In general, cost is presumed to be a function of subsystem element weight. Therefore, in the equations above, X represents the weight of the subsystem and Y the LCC. For the case of estimating the LCC of the electrical power subsystem, cost is assumed to be a function of the surface area of the solar panels. The constants β_0 and β_1 can be found using linear regression techniques.

Figure G.1 portrays the six functional divisions of the NASA DDT&E system level costs:

1. Design & Development

2. Integration, Assembly, & Checkout

3. System Test & Evaluation

4. Ground Support Equipment (GSE)

5. Systems Engineering & Integration (SE&I)

6. Program Management.

Note that the Design & Development functional division is further broken out into seven subsystem cost elements:

- Structure/Environmental Protection

- Docking Adapter

- Electrical Power

- Environmental Control & Life Support (ECLS)/Crew Accommodations

- Data Management/Communications

- Stabilization & Control

- Reaction Control System (RCS)/Propulsion.

These subsystem cost elements drive the entire cost model as all other cost parameters (e. g. Program Management, GSE, etc.) are functions of these subsystem cost elements. Flight Article Production is divided into four functional areas:

1. Flight Hardware

2. Integration, Assembly & Checkout

3. SE&I

4. Program Management

Note that the Flight Hardware functional division is broken out into the same seven subsystem cost elements mentioned above.
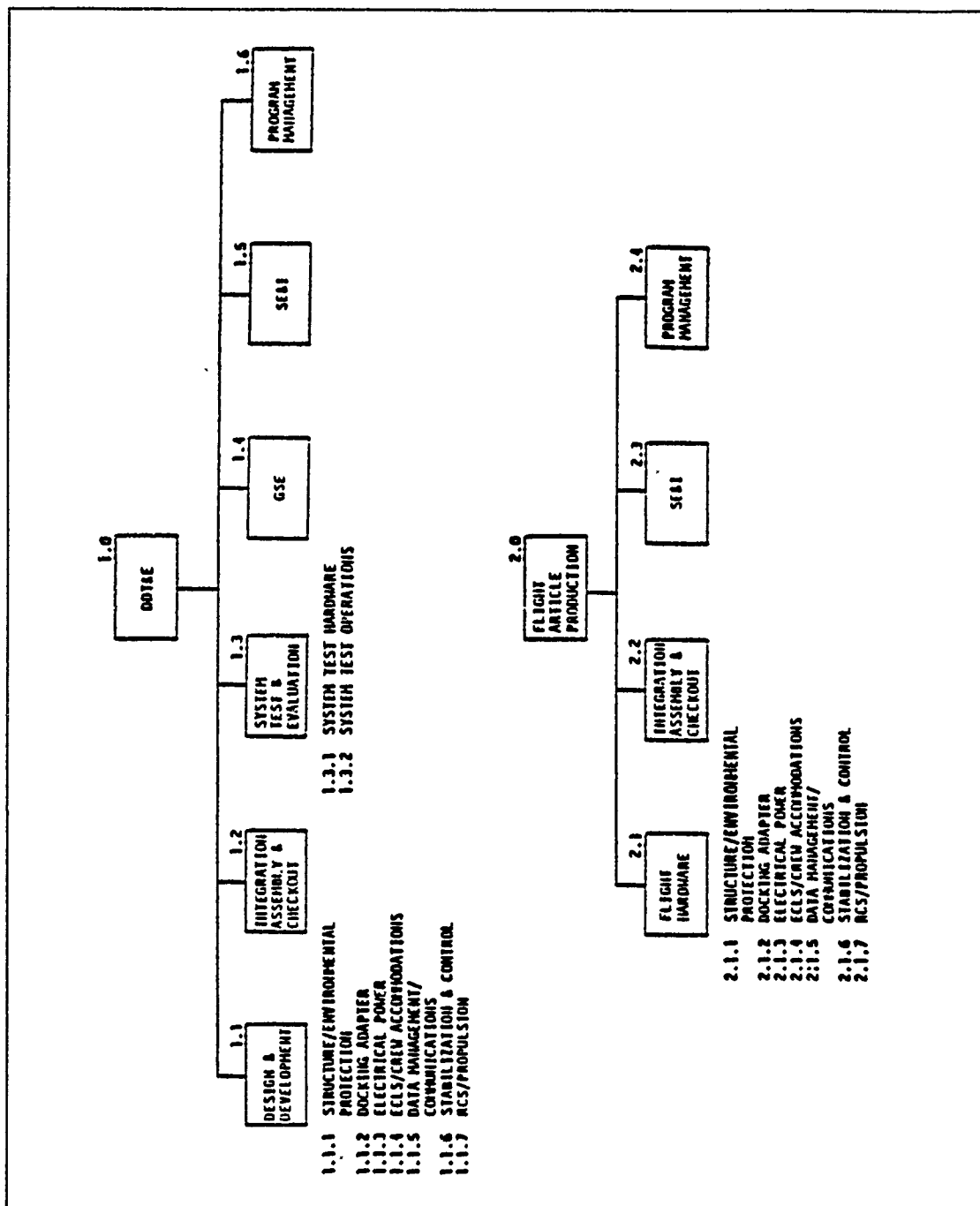
Figure G.1. Space Station Cost Model Structure

Figure G.2 depicts the six functional categories of the operations life cycle costs:

1. Operations Spares
2. Operations GSE
3. Operations Logistics
4. Ground Operations
5. Flight Operations
6. Miscellaneous Operations

The Operations Spares functional category is again subdivided into the same seven subsystem cost elements seen above. Note that the Operations LCC numbers include such elements as training, simulation, launch operations, sustaining engineering, and other logistics-type cost elements.

Once the key technologies and hardware components for the salvage operation were identified, each component had to be classified according to one of the seven subsystem cost elements. Weight estimates for these subsystem components can be found in Appendix H.

G.2 Deterministic Cost Model

Initially, the CER's developed for Space Station *Freedom* formed the basis of the ASSET cost model. A spreadsheet, making use of these CER's, was developed in order to provide a point estimate for the ASSET facility life cycle cost. Given an estimate for the weights of each Subsystem Element, this deterministic cost model provided a simple means with which to calculate a rough order of magnitude cost estimate for a given configuration.
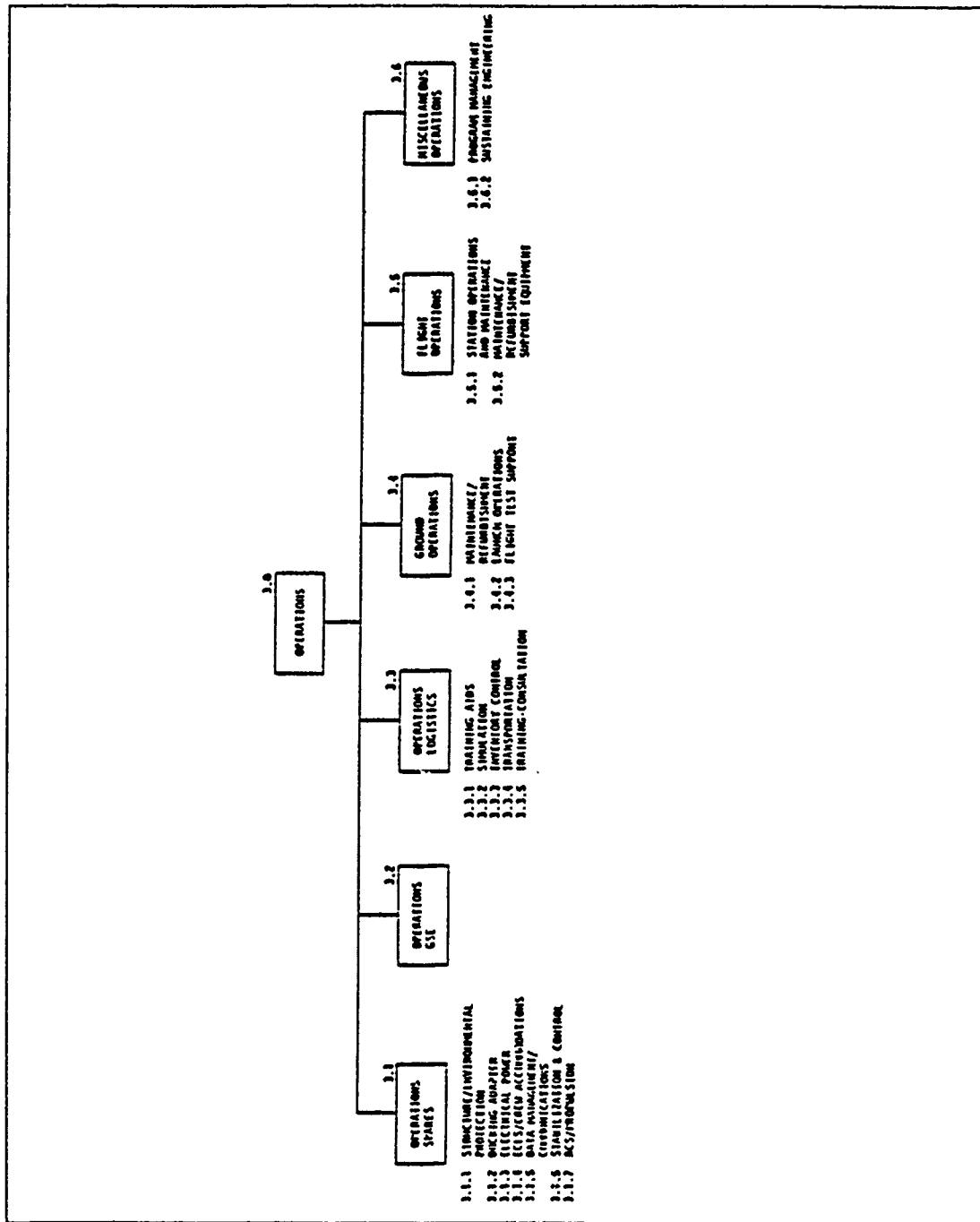
Figure G.2. Space Station Cost Model Structure (Operations)

G.2.1 LCC Point Estimate. A sample printout of this spreadsheet is found in Figure G.3. Column 2, the CER Parameter, represents the value of the independent variable for that particular CER (normally the weight of the Subsystem). Column 3 displays the forecasted DDT&E cost based upon the weight (or area) estimate provided in Column 2. The fourth column displays the 'cost complexity factor' associated with that particular Subsystem Element. Column 5 represents the product of the complexity factor and the DDT&E cost estimate, i. e. , the Adjusted DDT&E Cost projection.

The next column, labeled 'FH Cost Estimate', displays the flight hardware production cost projections. Column 7 follows with the FH complexity factors, and Column 8 portrays the Adjusted FH Cost estimate.

Following the seven Subsystem Cost Elements are the Mission Support Cost Elements (GSE, Program Management, etc.). The CER parameter of the System Test and Evaluation cost element is the sum of the adjusted flight hardware costs, while the CER parameter for Integration, Assembly & C/O cost category is simply the adjusted DDT&E costs associated with System Test and Evaluation.

The sum of the previous adjusted DDT&E cost estimates becomes the independent variable of the GSE cost element. The adjusted GSE cost estimate is then used as the CER parameter for the Systems Engineering & Integration cost element. Finally, the Program Management CER is a function of the summation of all the previous adjusted DDT&E cost estimates. Similar relationships hold for the FH Mission Support cost estimates.

The running totals of the DDT&E and FH costs (before and after adjustment) are then displayed, followed by an escalation of the cost projections. A cost escalation factor of 2.111 (73), converts the 1978$ cost estimates to 1990$.

The Operations costs follow the Mission Support Cost Elements. These cost projections are more complex than the previous cost elements, as many factors come

```
1978 $ IN MILLIONS
                                        DDT&E     DDT&E      DDT&E       FH       FH        FH
                              CER        Cost    Complexity  Adjusted   Cost   Complexity Adjusted
                           Parameter   Estimate    Factor      Cost    Estimate  Factor     Cost
Structure/Env Protection (lbs)  4518    17.840      0.1       1.784     3.436      1       3.436
Docking Adapter (lbs)            300     4.245       1        4.245     0.394      1       0.394
Electrical Power (Area)         3229   101.240      0.5      50.620     5.530      1       5.530
ECLS/Crew Accomodations (lbs)   3341    13.939      0.3       4.182     0.689      1       0.689    0.620
Data Management/Comm (lbs)       125    73.463      0.2      14.693     2.453      1       2.453
Stabilization and Control (lbs)  595     9.398      0.4       3.759     5.540      1       5.540    4.986
RCS/Propulsion (lbs)            2150    48.820      0.2       9.764     4.308      1       4.308

        SUBTOTAL                       268.944               89.046    22.349             22.349

System Test and Evaluation     22.349   57.775      0.2      11.555
Integration Assembly & C/O     11.555   15.406      0.1       1.541     2.367     0.7      1.657

        SUBTOTAL                       342.125              102.142    24.716             24.006

Ground Support Equipment      102.142   17.492      0.5       8.746

        SUBTOTAL                       359.616              110.888    24.716             24.006

Systems Engineering & Integration 110.888  15.276   0.5       7.638     3.104     0.5      1.552

        SUBTOTAL                       374.893              118.526    27.820             25.558

Program Management            118.526   12.466      0.3       3.740     2.284     0.3      0.685

    TOTAL DDT&E and FH Costs          387.359              122.266    30.105             26.244

Times Escalation Factor of =>  2.111                        258.103                      55.400


OPERATIONS                                         1978 $ (MILLIONS)          1990 $ (MILLIONS)
            Operations Spares     0.1                    2.382                      5.029
 (# of years total operation)=>    5
              Operations GSE      0.1                    0.131                      0.277
       Operations Logistics       0.1                    1.372                      2.897
           Ground Operations      0.1                    7.292                     15.393
            Flight Operations     0.1                    0.523                      1.105
   (Total crew man-years) =>        0
     Misc Operations Elements     0.1                    0.023                      0.049

Total Operations Costs                                  11.724                     24.750

                                     Total Life Cycle Cost (1990 $)             338.253
```

Figure G.3. Point Estimate Cost Projection Spreadsheet

into play here. In general, these cost projections are functions of both DDT&E and FH costs, as well as various combinations of other cost elements (68). These cost estimates are multiplied by complexity factors, the cost escalation factor, and then summed. The result is the Total (Adjusted) Operations Cost. Combining this result with the total DDT&E and FH costs yields the Total Life Cycle Cost point estimate in 1990$.

G.2.2 Limitations. As useful as the deterministic cost model proved to be for early trade studies, it had several severe drawbacks. Most notable was the lack of several key cost elements:

- the initial launch cost

- EVA costs

- consumables (Boost/Deboost Module fuel)

The inability to provide confidence levels with our forecasts, and the lack of a systematic methodology which would enable us to accommodate the uncertainties associated with weight estimates and complexity factors led to the use of a probabilistic cost model.

G.3 Probabilistic Cost Model

An AFIT developed Life Cycle Cost Model (MLCC) (15) provides the means with which to handle the weight estimate and complexity factor uncertainties. Additionally, MLCC takes into account the time value of money by calculating the present value (or, present worth) of a cash flow forecast based upon a user supplied rate of interest.

G.3.1 Cost Categories. MLCC requires that all costs be classified into one of three categories: constant cost, costs described by random variables, and costs described by CER's. A constant cost implies that the cost is known with 100% certainty. Unfortunately, not a single cost element of the ASSET facility could be classified in this manner. However, many of the ASSET cost elements can be modeled as random variables.

In general, the value of a random variable is determined by the outcome of some experiment. Due to the random nature of the various aspects of the experiment, a probability can be assigned to the possible outcomes of that experiment. W can be classified as a continuous random variable if there exists a function $f(\omega)$ defined for all ω such that for $a \leq \omega \leq b$,

$$P\{a \leq \omega \leq b\} = \int_a^b f(\omega)\, d\omega.$$

In other words, the probability that W takes on a value between a and b is equal to the area under the curve $f(\omega)$, bounded by a and b.

The function $f(\omega)$ is known as the probability density function (pdf) of the random variable W. MLCC assumes that the pdf of the cost random variables has the form (41:375):

$$f(\omega) = \frac{\Gamma(\alpha + \beta + 2)}{\Gamma(\alpha + 1)\Gamma(\beta + 1)} \omega^\alpha (1 - \omega)^\beta, \quad 0 < \omega < 1 \tag{G.2}$$

where

$$\Gamma(n) = \int_0^\infty e^{-x} x^{n-1} \, dx.$$

The function $f(\omega)$ is known as the Beta Distribution (Beta pdf). The parameters α and β determine the shape and scale of the pdf. Note that the Beta pdf is a robust distribution in that it can approximate a normal distribution, or be heavily skewed low or high depending upon the values of α and β.

Figure G.4 portrays the nine types of Beta pdf shapes available to MLCC users. A Type 1 Beta pdf implies that for $a \leq W \leq b$, W is more likely to have a value closer to b whereas for a Type 3 pdf, W is more likely to be nearer a. The Type 2 pdf is symmetric, implying that W is most likely to lie near the average of a and b. The three tiers of pdfs in Figure G.4 allow varying levels of confidence in the random variable estimates. The Type 7, 8, and 9 pdfs reflect the user's high level of confidence (low variance) whereas the lower tiered pdfs reflect the user's high level of uncertainty (high variance). MLCC also uses the Beta pdfs to describe the uncertainty associated with the cost estimating relationships.

Referring to equation G.1, a typical ASSET CER has the form

$$\ln C_i = \ln \beta_0 + \beta_1 \ln W_i \qquad (\text{G.3})$$

where

$$C_i \ = \ \text{element cost estimates}$$
$$W_i \ = \ \text{subsystem weight estimates}$$
$$\beta_i \ = \ \text{curve fit intercept and slope parameters.}$$

Since MLCC required the statistics of β_0 and β_1 (which were not readily available in the cost model literature), we were forced to analyze the historical cost data ourselves. Since the subsystem weight estimates are also subject to uncertainty, W
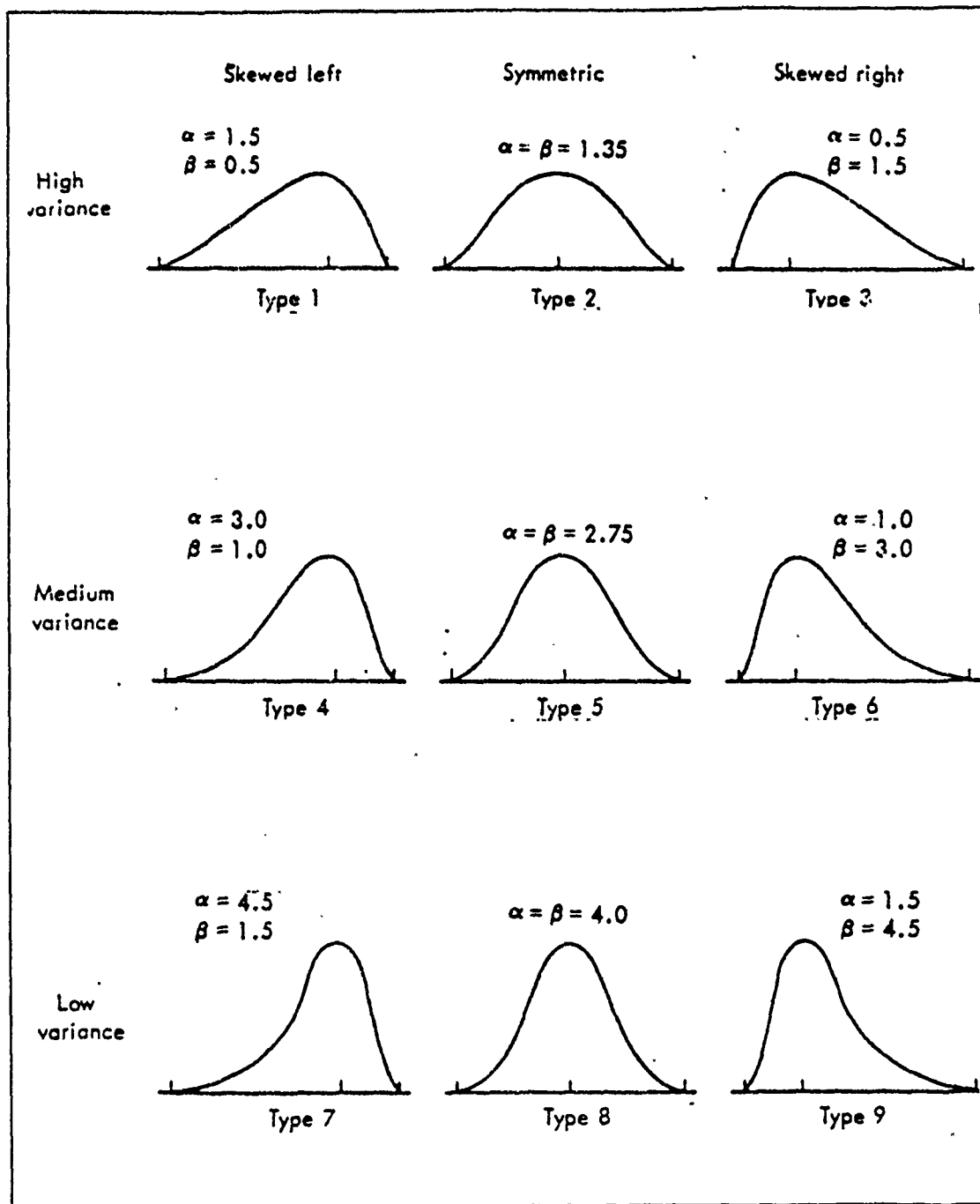
Figure G.4. Beta Distributions.

is also modeled as a random variable. MLCC assumes a Beta pdf to describe the distribution of W.

MLCC is also flexible enough to handle cost complexity factors. Taking the exponent of both sides of equation G.3 yields

$$C_i = \beta_0 W_i^{\beta_1}. \tag{G.4}$$

Letting k_i represent a cost complexity factor, then

$$C_i^* = k_i C_i = k_i \beta_0 W_i^{\beta_1}$$

represents the adjusted life cycle cost for subsystem i. The cost complexity factors are also assumed to be random variables with a Beta pdf.

G.3.2 Time Value of Money.   MLCC also incorporates the time value of money in its calculations. Figure 9.1 depicts the forecasted ASSET cash flow. Given
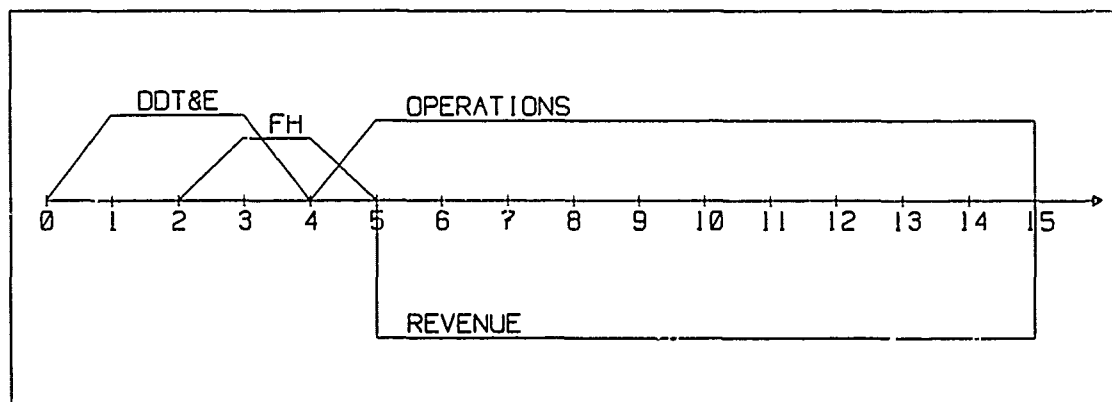

Figure G.5. Cash Flow Diagram.

the timing of all expenditures (and revenue), MLCC calculates the present value P, of the cash stream one of two ways (30:26,28):

1. Single Payment - Present Worth Factor

2. Uniform Series - Present Worth Factor

Given that

  i represents an interest rate per interest period,

  n represents a number of interest periods,

  P represents a present sum of money,

  F represents a future sum of money at the end of n periods from the present date that is equivalent to P at interest rate i, and

  A represents each end-of-period payment in a uniform series continuing for the coming n periods, the entire series equivalent to P at interest rate i,

then

$$P = F \left[\frac{1}{(1+i)^n} \right] \tag{G.5}$$

for the *single payment* to present value conversion, and

$$P = A \left[\frac{(1+i)^n - 1}{i((1+i)^n)} \right] \tag{G.6}$$

for the *annual payment* to present value conversions. The quantities in [ ]'s are the Present Worth Factors.

Referring again to Figure G.5, the revenue stream is an example of a uniform series of payments, of magnitude A_R. The DDT&E disbursements typify a mixture of future and uniform series payments. MLCC converts all of these payments to a present worth (or value) at year 0.

G.3.3 Application. A typical cost random variable is entered into MLCC using the following input statement:[1]

```
CE 2                 1.897      18.975 9 1   2   1   0
12345678901234567890123456789012345678901234567890123456789
```

where

---

[1]The second row of characters is simply a guide to help identify the columns of the formatted read statement.

Column #		Designation
1-2	⇒	cost element card
4	⇒	cost category (random variable in this case)
19-29	⇒	low value of the Beta distribution
31-41	⇒	high value of the Beta distribution
43	⇒	Beta distribution Type (1-9) [Type #9 in this case]
44-46	⇒	value of the phase in period (years) [1 year]
48-50	⇒	value of period with constant cost per year [2 years]
52-54	⇒	value of phase out period [1 year]
56-59	⇒	time period when cost element starts [year 0]

The low and high values of the DDT&E and FH random variable cost estimates are generated by applying the subsystem weight estimates to the NASA cost model CERs. The high value of the random variable represents a unity cost complexity factor, while the low value is a result of using cost complexity factors generated by the study group.

A typical CER is entered into MLCC using the following input cards:

```
CE 3                                    1    1    1    2
CER  1 1 1 1
.1
.3
9
.21674
.7064004528    -.116369248
-.116369248     .0196731538
-3.574367
.577094
1.0
1.0
1
8.517
8.594
5
```

The first card is similar to the random variable input card, and informs MLCC that the next 15 cards make up a CER:

Card #   Designator

1   =   CER card
                columns 4-6 ⇒ total number of slope parameter
                [1 for this CER]
                column 8 ⇒ presence of an intercept
                [1 ⇒ intercept present]
                column 10 ⇒ CER estimated using natural logs
                column 12 ⇒ Final cost to be multiplied by a scalar

2   =   low value of the scalar
                [.1 for this CER]

3   =   high value of the scalar
                [.3 for this CER]

4   =   type of Beta pdf
                [Type #9]

5   =   variance of the estimate
                $[S^2 = .21674]$

6,7   =   variance-covariance matrix
                $[S^2(X^TX)^{-1}]$

8   =   value of intercept
                $[b_0 = -3.574367]$

9   =   value of slope parameter
                $[b_1 = .577094]$

10-12   =   indicator that intercept is present
                [Three successive 1's]

13   =   low value of cost driver (weight, etc.)
                [8.517 - entered in Log form]

14   =   high value of cost driver
                [8.594]

15   =   type of Beta pdf describing cost driver
                [Type #5]

G.3.4 Sample Calculations. Calculations for the non-CER based random variables follow:

Consumables

Assuming a low and high value of $150M and $250M respectively for the launch cost estimate, and assuming a 53,000 lb Orbiter payload capacity for a 170 nmi orbit insertion, the launch costs per pound become

$$LC_l = \frac{\$150E6}{53E3 \ lbs} = \$2830.19 \ \$/lb$$

$$LC_h = \frac{\$250E6}{53E3 \ lbs} = \$4716.98 \ \$/lb.$$

For the Scenario 1 12% EPS system, the total annual fuel requirements were on the order of 9784 lb/yr. Assuming that a two year supply of propellants is carried onboard the dedicated setup flight[2] then eight years worth of fuel must be delivered to LEO at a cost of

$$FC_l = (9784)(8)(2830.14) = \$221.526E6 \ 1990\$$$

for the lower estimate, and

$$FC_h = (9784)(8)(4716.98) = \$369.208E6 \ 1990\$$$

---

[2]Calculations revealed that we had roughly 7,000 to 12,000 lbs of unused payload capacity. This could be put to good use by carrying along the 2nd year's supply of fuel at no additional freight costs.

for the upper estimate. Converting these values to 1978$ by dividing by the cost escalation factor of 2.111 yields

$$FC_l = \$104.938E6 \ 1978\$$$

$$FC_h = \$174.897E6 \ 1978\$$$

EVA Operations

Looking now at the EVA operations expenditures for Scenario 1, the estimated range of EVA times required to perform all required tasks was found in Appendix F. Using a low estimate of 1063.9 EVA hrs at a cost of $100,000 per hr yields

$$EVA_l = (1063.9)(100,000) = \$106.394E6 \ 1990\$$$

and using an upper estimate of 1248 EVA hrs yields

$$EVA_h = (1248.0)(100,000) = \$124.802E6 \ 1990\$$$

or, converting to 1978$,

$$EVA_l = \$50.406E6 \ 1978\$$$

$$EVA_h = \$59.120E6 \ 1978\$$$

Electron Beam Cutter

The electron beam cutter cost estimate was derived from a vendor brochure price quote (24). Adjusting the $250,000 single unit quote by 1.3^3 to accommodate enhancements for space-qualifying the cutter yield a high estimate of

---

[3]Engineering judgement.

$$EBC = (\$250,000)(1.3) = \$350,000 \text{ each.}$$

Plans call for three cutters for Scenario 1, yielding a total cost of

$$EBC_h = (350,000)(3) = \$975,000 \; 1990\$$$

or .462E6 1978\$. The low estimate for the cutter does not adjust for space qualification.

Revenue

Again, assuming a low and high launch cost of \$2830.19 and \$4716.98 per pound respectively, the 'effective' revenue stream can be calculated by multiplying these launch costs with the expected yield of aluminum. For Scenario 1, roughly 13,045 pounds of aluminum is salvaged. Therefore, the value of this aluminum has a low end worth of

$$AL_l = (2830.19)(13,045) = \$36.919E6 \; 1990\$$$

and a high end worth of

$$AL_h = (4716.98)(13,045) = \$61.532E6 \; 1990\$.$$

However, Martin Marietta recommended during our CDR to subtract roughly 3.0E6 1990\$ from each tank to finance the leasing of the Cargo Transport Vehicle.[4] There

---

[4] Used to stabilize the passive tank.

fore, assuming four tanks per year for 10 years,

$$AL_{l,10} = (36.919 - 3)(4)(10) = \$1,356.758E6 \ 1990\$$$

$$AL_{h,10} = (61.532 - 3)(4)(10) = \$2,341.280E6 \ 1990\$$$

or, in millions of 1978\$, $AL_{l,10}$ =\$642.709, and $AL_{h,10}$ =\$1,109.086.

Revenue from Selling Power

A few preliminary calculations determined that approximately 317 days out of the year would be available for selling power. Given the Scenario 3 design of an 18.75 kW orbital average power source, the consumption rate, ξ, would be

$$\xi = \frac{18.75\text{kW}}{24\text{hr}} = .7813.$$

Therefore, at NASA's current charge rate of \$11,000 per hour, we could expect to see an annual revenue stream of

$$(11,000 \ \$/\text{hr})(24 \ \text{hr/day})(317 \ \text{day/yr})\xi = \$65,385,434 \ 1990\$$$

or, \$30.974 in millions of 1978\$. This value is then adjusted by $\pm10\%$ to determine the low and high revenue estimate.

G.4 CER Parameters

The following tables document the cost complexity factors and weight (or area) estimates used for the ASSET cost model CERs:

Table G.1. Scenario 1 CER Parameters, 12% EPS.

		Weight (lbs) {†-Area (ft^2)}			Cost Complexity		
	CER	Low	High	Tendency	Low	High	Tendency
DDT&E	Electrical Power†	4564	4564	-	.05	.15	central
	Data Management	100	150	central	.05	.35	central
	RCS/Propulsion	2050	2250	central	.1	.3	central
FH	Structure	5000	5400	central	.1	.3	low
	Electrical Power†	4564	4564	-	.9	1.0	high
	Data Management	100	150	central	.9	1.0	high
	RCS/Propulsion	2050	2250	central	.9	1.0	high

Table G.2. Scenario 1 CER Parameters, 21% EPS.

		Weight (lbs) {†-Area (ft^2)}			Cost Complexity		
	CER	Low	High	Tendency	Low	High	Tendency
DDT&E	Electrical Power†	3229	3229	-	.4	.6	central
	Data Management	100	150	central	.05	.35	central
	RCS/Propulsion	2050	2250	central	.1	.3	central
FH	Structure	3420	3620	central	.1	.3	low
	Electrical Power†	3229	3229	-	.9	1.0	high
	Data Management	100	150	central	.9	1.0	high
	RCS/Propulsion	2050	2250	central	.9	1.0	high

Table G.3. Scenario 2 CER Parameters, 12% EPS.

	CER	Weight (lbs) {†-Area (ft^2)}			Cost Complexity		
		Low	High	Tendency	Low	High	Tendency
DDT&E	Electrical Power†	5682	5682	-	.05	.15	central
	Data Management	50	100	central	.05	.35	central
	RCS/Propulsion	2050	2250	central	.1	.3	central
FH	Structure	3650	3885	central	.1	.3	low
	Electrical Power†	5682	5682	-	.9	1.0	high
	Data Management	50	100	central	.9	1.0	high
	RCS/Propulsion	2050	2250	central	.9	1.0	high

Table G.4. Scenario 2 CER Parameters, 21% EPS.

	CER	Weight (lbs) {†-Area (ft^2)}			Cost Complexity		
		Low	High	Tendency	Low	High	Tendency
DDT&E	Electrical Power†	3830	3830	-	.4	.6	central
	Data Management	50	100	central	.05	.35	central
	RCS/Propulsion	2050	2250	central	.1	.3	central
FH	Structure	2975	3172	central	.1	.3	low
	Electrical Power†	3830	3830	-	.9	1.0	high
	Data Management	50	100	central	.9	1.0	high
	RCS/Propulsion	2050	2250	central	.9	1.0	high

Table G.5. Scenario 3 (Automated) CER Parameters.

	CER	Weight (lbs) {†-Area (ft^2)}			Cost Complexity		
		Low	High	Tendency	Low	High	Tendency
DDT&E	Electrical Power†	7685	7685	-	.05	.15	central
	Data Management	100	150	central	.05	.35	central
	RCS/Propulsion	2050	2250	central	.1	.3	central
FH	Structure	5080	5280	central	.1	.3	low
	Electrical Power†	7685	7685	-	.9	1.0	high
	Data Management	100	150	central	.9	1.0	high
	RCS/Propulsion	2050	2250	central	.9	1.0	high

Table G.6. Scenario 3 (Astronaut-tended) CER Parameters.

	CER	Weight (lbs) {†-Area (ft^2)}			Cost Complexity		
		Low	High	Tendency	Low	High	Tendency
DDT&E	Electrical Power†	7685	7685	-	.05	.15	central
	Data Management	50	100	central	.05	.35	central
	RCS/Propulsion	2050	2250	central	.1	.3	central
FH	Structure	4380	4580	central	.1	.3	low
	Electrical Power†	7685	7685	-	.9	1.0	high
	Data Management	50	100	central	.9	1.0	high
	RCS/Propulsion	2050	2250	central	.9	1.0	high

Appendix H. *ALLOCATED WEIGHTS*

H.1 EPS Weight and Drag Estimates

Chapters V-VII developed EPS designs to support Scenarios 1-3 respectively. Chapter IX contrasted the various drag contributions due to the EPS and computed the fuel consumption required to maintain orbit. Chapter IX showed weight and drag differences for both low (12%) and high (21%) efficiency solar arrays. The purpose of this section is to provide the weight and drag inputs (used in the Chapter IX study) as a function of the EPS design. The weight differences for the individual scenarios are not significant when compared to the external tank mass of approximately 69,000 pounds, but the drag area proved to be a significant cost driver in terms of annual fuel consumption and fuel resupply costs.

Tables H.1, H.2, H.3, H.4, and H.5 are provided for each scenario. The weights were primarily extracted from the Power System Description Document (67), but have been modified to account for smaller array sizes and fewer numbers of batteries. The cost model assumed a cost complexity factor of 0.1 for all scenario 'a' options. The weights will be lower in some areas of the 'b' tables, but only at the expense of more DDT&E dollars (cost complexity factors of 0.5 were used for 'b' options). Scenario 3 is, essentially, the EPS for Space Station Freedom. The design option of more efficient arrays was not investigated for Scenario 3.

A common table (see Table H.6) containing the total drag for all scenarios is also provided. Drag areas are provided in m^2 and ft^2 since various models which were adapted for use request the drag area to be input in different units.

Table H.1. Scenario 1a EPS Weight Estimates

Item	Total Flight Quantity	Item Weight (lbs)	Allocated Weight (lbs)
Solar Array			**2198.8**
Mast and Canister	2	490.7	981.4
PV Blanket and Box	4	285.6	1142.4
SSU	2	37.5	75.0
Thermal			**3783.0**
Pump ORU's	2	158	316
Working Fluid		101	101
Type I Utility Plates	2	334	668
Type II Utility Plates	4	299	1196
Fluid Junction Box	2	93	186
Radiator		1316	1316
EPS			**7142.8**
Batteries	4	640	2560.0
BCDU	4	168	672.0
DCSU	2	182	364.0
DDCU		167	167.0
PVCU	2	147	294.0
PV Cable Set		231	231.0
OIPU		185	185.0
SUT		225	225.0
PMAD Cable Set		1102.5	1102.5
PMAD Equipment		1342.3	1342.3
IEA Structure		2701	**2701.0**
TOTAL IEA WEIGHT			**15825.6**

Table H.2. Scenario 1b EPS Weight Estimates

Item	Total Flight Quantity	Item Weight (lbs)	Allocated Weight (lbs)
Solar Array			**1514.4**
Mast and Canister	2	417.1	834.2
PV Blanket and Box	4	151.3	605.2
SSU	2	37.5	75.0
Thermal			**3291.0**
Pump ORU's	2	158	316.0
Working Fluid		82.8	82.8
Type I Utility Plates	2	334	668.0
Type II Utility Plates	4	299	1196.0
Fluid Junction Box	2	93	186.0
Radiator		842.2	842.2
EPS			**6390.2**
Batteries	4	640	2560.0
BCDU	4	168	672.0
DCSU	2	182	364.0
DDCU		167	167.0
PVCU	2	147	294.0
PV Cable Set		231	231.0
OIPU		185	185.0
SUT		225	225.0
PMAD Cable Set		551.3	551.3
PMAD Equipment		1140.9	1140.9
IEA Structure		2304	**2304.0**
TOTAL IEA WEIGHT			**13,499.6**

Table H.3. Scenario 2a EPS Weight Estimates

Item	Total Flight Quantity	Item Weight (lbs)	Allocated Weight (lbs)
Solar Array			**2480.4**
Mast and Canister	2	490.7	981.4
PV Blanket and Box	4	356.0	1424.0
SSU	2	37.5	75.0
Thermal			**4381.0**
Pump ORU's	2	158	316
Working Fluid		101	101
Type I Utility Plates	2	334	668
Type II Utility Plates	6	299	1794
Fluid Junction Box	2	93	186
Radiator		1316	1316
EPS			**8758.8**
Batteries	6	640	3840.0
BCDU	6	168	1008.0
DCSU	2	182	364.0
DDCU		167	167.0
PVCU	2	147	294.0
PV Cable Set		231	231.0
OIPU		185	185.0
SUT		225	225.0
PMAD Cable Set		1102.5	1102.5
PMAD Equipment		1342.3	1342.3
IEA Structure			**2701.0**
TOTAL IEA WEIGHT			**18,321.2**

Table H.4. Scenario 2b EPS Weight Estimates

Item	Total Flight Quantity	Item Weight (lbs)	Allocated Weight (lbs)
Solar Array			**1767.8**
Mast and Canister	2	441.6	883.2
PV Blanket and Box	4	202.4	809.6
SSU	2	37.5	75.0
Thermal			**4185.6**
Pump ORU's	2	158.0	316.0
Working Fluid		87.1	87.1
Type I Utility Plates	2	334.0	668.0
Type II Utility Plates	6	299.0	1794.0
Fluid Junction Box	2	93.0	186.0
Radiator		1134.5	1134.5
EPS			**8006.2**
Batteries	6	640.0	3840.0
BCDU	6	168.0	1008.0
DCSU	2	182.0	364.0
DDCU		167.0	167.0
PVCU	2	147.0	294.0
PV Cable Set		231.0	231.0
OIPU		185.0	185.0
SUT		225.0	225.0
PMAD Cable Set		551.3	551.3
PMAD Equipment		1140.9	1140.9
IEA Structure			**2414.0**
TOTAL IEA WEIGHT			**16,373.6**

Table H.5. Scenario 3 EPS Weight Estimates

Item	Total Flight Quantity	Item Weight (lbs)	Allocated Weight (lbs)
Solar Array			**3177.6**
Mast and Canister	2	490.7	981.4
PV Blanket and Box	4	530.3	2121.2
SSU	2	37.5	75.0
Thermal			**4381.0**
Pump ORU's	2	158.0	316.0
Working Fluid		101.0	101.0
Type I Utility Plates	2	334.0	668.0
Type II Utility Plates	6	299.0	1794.0
Fluid Junction Box	2	93.0	186.0
Radiator		1316.0	1316.0
EPS			**8758.8**
Batteries	6	640.0	3840.0
BCDU	6	168.0	1008.0
DCSU	2	182.0	364.0
DDCU		167.0	167.0
PVCU	2	147.0	294.0
PV Cable Set		231.0	231.0
OIPU		185.0	185.0
SUT		225.0	225.0
PMAD Cable Set		1102.5	1102.5
PMAD Equipment		1342.3	1342.3
IEA Structure			**2701.0**
TOTAL IEA WEIGHT			**19,018.4**

Table H.6. Scenario Dependent Drag Characteristics as a Function of EPS Design

EPS DESCRIPTION	DRAG (m^2)	DRAG (ft^2)
1a - 12 kW Constant Load, 12 % Arrays	424	4563.8
1b - 12 kW Constant Load, 21 % Arrays	300	3229.1
2a - 20 kW Constant Load, 12 % Arrays	528	5683.0
2b - 20 kW Constant Load, 21 % Arrays	356	3832.0
3 - 23.7 kW Peak/18.75 kW Orbital Avg Load, 12 % Arrays	714	7685.5

H.2 Subsystem Weight Estimates

This section serves as a data base for subsystem weight estimates which were used both in the Orbits and Cost models. The Cost model uses (primarily) weight inputs to forecast dollars required for DDT&E and flight hardware. At NASA's request (73), the actual CER's are not published. However, one could duplicate our cost projections (if they possess a copy of the NASA Space Station Cost Model (68)) by using the appropriate weights as inputs to the appropriate CER's. The seven sets of CER input weights used in the ASSET cost model are provided below in Tables H.7, H.8, H.9, H.10, H.11, H.12, and H.13 respectively.

Table H.7. Structure Subsystem Weight Estimates, (lbs)

STRUCTURE	1a	1b	2a	2b	3-1	3-2
Solar Array Rot. Mech.	2199	1514	2480	1768	3178	3178
ET Modifications	575	575	148	148	575	148
SOFI Workstation	1157	1157	1157	1157	1157	1157
Boost-Deboost Modules	1000	1000	1000	1000	1000	1000
Robot Arm Truck	272	272			272	
TOTAL/SCENARIO	5203	4518	4785	4073	6182	5483

Table H.8. Docking Adapter Subsystem Weight Estimates, (lbs)

	1a	1b	2a	2b	3-1	3-2
DOCKING ADAPTER	300	300	300	300	500	500

Table H.9. EPS Subsystem Estimates

EPS	1a	1b	2a	2b	3-1	3-2
AREA (ft^2)	4564	3229	5683	3832	7685	7685
EQPT minus THERMAL (lbs)	7143	6390	8759	8006	8759	8759

Table H.10. ECLS Subsystem Estimates

ECLS	1a	1b	2a	2b	3-1	3-2
Lighting	25	25	25	25	25	25
EVA Restraints	25	25	25	25	25	25
Thermal Control (batts.)	3783	3291	4381	4186	4381	4381
TOTALS	**3833**	**3341**	**4431**	**4236**	**4431**	**4431**

Table H.11. Data Management/Communications Subsystem Estimates

DATA MGMT/COMM	1a	1b	2a	2b	3-1	3-2
Comm. Electronics	38	38	38	38	38	38
Antennas	12	12	12	12	12	12
TV Cameras	25	25	25	25	25	25
Robot Arm Electronics	50	50			50	
TOTALS	**125**	**125**	**75**	**75**	**125**	**75**

Table H.12. Stability and Control Subsystem Estimates

STABILITY and CONTROL	1a	1b	2a	2b	3-1	3-2
Nav. Aids	75	75	75	75	75	75
RCS Drivers	55	55	55	55	55	55
IMU & Flt. Computer	135	135	135	135	135	135
Other	330	330	330	330	330	330
TOTALS	**595**	**595**	**595**	**595**	**595**	**595**

Table H.13. RCS/Propulsion Subsystem Estimates

RCS/PROPULSION	1a	1b	2a	2b	3-1	3-2
Propulsion	150	150	150	150	150	150
Propellant Tanks	2000	2000	2000	2000	2000	2000
TOTALS	2150	2150	2150	2150	2150	2150

H.3 First Flight Manifest

Operating under the assumption that Scenario 1a is the selected method of operation, the first flight manifest would be as shown in Table H.14.

Table H.14. ASSET First Flight Manifest, (lbs)

POWER	15,826
Solar Arrays	2,199
Thermal Control System	3,783
Electrical Power Subsystem	7,143
IEA Structure	2,701
ORBITAL MAINTENANCE	**27,150**
Boost - Deboost Modules	3,150
First Year Hypergolics	12,000
Second Year Hypergolics	12,000
REDUCTION TOOLS	**2,680**
Robot Arm Truck	272
Primary Cutter	200
Spare Cutter	200
Centerline Track	276
ET Mods	575
SOFI Workstation	1157
COMM,CAMERAS,LIGHTS,AVIONICS	**770**
TOTAL FIRST FLIGHT CARGO WEIGHT	**46,426**

Appendix I. *TABLE OF ACRONYMS*

ACCESS   Assembly Concept for Construction of Erectable Space Structures
AFIT   Air Force Institute of Technology
AH   Amp Hour
AMTEC   Alkaline Metal Thermionic Conversion
AO   Atomic Oxygen
ASAP   Artificial Satellite Analysis Program
ASSET   Aluminum Salvage Station for the External Tank
BCDU   Battery Charge Discharge Unit
BOA   Base of Array
CBC   Closed Brayton Cycle
CDR   Critical Design Review
CER   Cost Estimating Relationship
CNPS   Compact Nuclear Power Source
CTV   Cargo Transfer Vehicle
DCSU   DC Switching Unit
DDCU   DC to DC Converter Unit
DDT&E   Design, Development, Test and Evaluation
DOD   Depth of Discharge
DOE   Department of Energy
EASE   Experimental Assembly of Structures in EVA
EB   Electron Beam
EBC   Electron Beam Cutter
EES   Electrical Equipment Subsystem
EMI   Electromagnetic Interference
EPS   Electrical Power Subsystem
ET   External Tank
EVA   Extra Vehicular Activity
FH   Flight Hardware
FPSE   Free Piston Stirling Engine
GFE   Government Furnished Equipment
GRIT   Gamma Ray Imaging Telescope
HEDRB   High Energy Density Rechargeable Battery
HSA   Heat Source Assemblies
IEA   Integrated Equipment Assembly
JPL   Jet Propulsion Laboratory
KW   Kilowatt
LANL   Los Alamos National Labs

LCC	Life Cycle Cost
LCCM	Life Cycle Cost Model
LCR	Lithium Cooled Reactor
LDEF	Long Duration Exposure Facility
LEO	Low Earth Orbit
LMKRC	Liquid Metal Potassium Rankine Cycle
MECO	Main Engine Cut Off
MLCC	Modified Life Cycle Cost
MTBF	Mean Time Between Failures
NPV	Net Present Value
NSTS	National Space Transportation System
OIPU	Orbital Interface Power Unit
OMS	Orbital Maneuvering System
ORC	Organic Rankine Cycle
ORU	Orbital Replacement Unit
PMAD	Power Management and Distribution
PRC	Potassium Rankine Cycle
PV	Photovoltaic
PVCU	Photovoltaic Controller Unit
RCS	Reaction Control System
RSS	Range Safety System
SAFE	Solar Array Flight Experiment
SD	Solar Dynamic
SDI	Strategic Defense Initiative
SHE	Sodium Heat Engine
SIPS	Stirling Isotope Power System
SLAM	Simulation Language for Alternative Modeling
SOFI	Spray on Foam Insulation
SPDE	Space Power Demonstration Engine
SPS	Solar Power Satellite
SRB	Solid Rocket Booster
SSF	Space Station Freedom
SSFSA	Space Station Freedom Solar Array
SSI	Space Studies Institute
STS	Space Transportation System
SSU	Shunt Switching Unit
SUT	Start Up Terminal
TCA	Thermal Control Assembly
TCS	Thermal Control System
TDRSS	Tracking and Data Relay Satellite System
TEC	Thermoelectric Conversion
ZPS	Zero Pre-Breathe Suit

Bibliography

1. Agrawal, Brij N. *Design of Geosynchronous Spacecraft.* Englewood Cliffs, NJ: Prentice-Hall, Inc., 1986.

2. Arnold, J. H. and others. "Mission Duration and Power Degradation in Photovoltaic Power Subsystems for Military Spacecraft." In *Twentieth IEEE Photovoltaic Specialists Conference - 1988, Vol. 2*, pages 848-853, New York· IEEE Press, 1988.

3. Arnold, William H. and others. "Dynamics and Design of Electromagnetic Mass Drivers." In Billingham, John and others, editors, *Space Resources and Space Settlements, NASA SP- 428*, pages 89-158, Washington D.C.: U.S. Government Printing Office, 1979.

4. "Astronauts Believe Lengthy EVA Building Sessions are Feasible," *Aviation Week & Space Technology*, pages 20-21 (16 December 1985).

5. Baggett, Randy M. and Thomas H. Whitt. "Nickel-Hydrogen Battery Testing for Hubble Space Telescope." In *24th Intersociety Energy Conversion Engineering Conference, Vol. 3*, pages 1411-1415, New York: IEEE Press, 1989.

6. Bailey, Dr. Patrick G. "A Comparison of 5 - 30 kW Space Nuclear Power Systems and Associated Requirements." In *23rd Intersociety Snergy Conversion Engineering Conference, Vol. 3*, pages 177-182, New York: The American Society of Mechanical Engineers, 1988.

7. Baillif, Faye F., Advanced Programs. Telephone interview. Martin Marietta Manned Space Systems, New Orleans LA, 17August 1990.

8. Baraona, Cosmo and others. "Space Station Freedom Solar Array Design Development." In *24th Intersociety Energy Conversion Engineering Conference, Vol. 1*, pages 283-287, New York: IEEE Press, 1989.

9. Barrie Cayless, Technical Director. Personal Correspondence. Alcan Rolled Products Company, Cleveland OH, 14August 1990.

10. Bate, Roger R. and others. *Fundamentals of Astrodynamics.* New York: Dover Publications, Inc., 1971.

11. Blankenship, G. "Plasma Arc Cutting Popularity on the Rise," *Welding Journal, 69*:53-56 (February 1990).

12. Bouzguenda, Mounir and Saifur Rahman. "A Knowledge-Based Approach to Optimize the Supply and Usage of Electricity Onboard the Space Station." In *24th Intersociety Energy Conversion Engineering Conference, Vol. 1*, pages 159-164, New York: IEEE Press, 1989.

13. Boyle, R. V. and others. "Solar Dynamic Power Option for the Space Station." In *23rd Intersociety Energy Conversion Engineering Conference, Vol. 3*, pages 319-328, New York: The American Society of Mechanical Engineers, 1988.

14. Broucke, Roger C. Lecture notes for ASE 366K, Orbital Mechanics, University of Texas at Austin, October 1983.

15. Cain, Joseph P. Class handout distributed in OPER 666, Cost Analysis for System Design. AFIT School of Engineering, WPAFB OH, August 1990.

16. Cantafio. Leopold J. *Space-Based Radar Handbook*. Norwood MA: Artech House, 1989.

17. Chern, Terry S. "Utilization of Space Shuttle External Tank Materials by Melting and Powder Metallurgy," *Acta Astronautica, 12*:693-698 (September 1985).

18. *Continuous Casting*. Product Catalog. Hunter Engineering Company, Inc., Riverside CA, undated.

19. Covault, Craig. "NASA Considers Further Tests of Space Construction Skills," *Aviation Week & Space Technology*, pages 69-71 (16 December 1985).

20. Covault, Craig. "Shuttle EVA's Utilize Techniques Planned for Space Station Assembly," *Aviation Week & Space Technology*, pages 21-23 (9 December 1985).

21. Criswell, David R. "Space Manufacturing 4." In *Proceedings of the Fifth Princeton/AIAA Conference*, pages 389-399, New York: American Institute of Aeronautics and Astronautics, 1981.

22. Donley, S. W. and others. "Nickel-Hydrogen Cell Low Earth Orbit Life Test at NWSC/Crane." In *24th Intersociety Energy Conversion Engineering Conference, Vol. 3*, pages 1417-1422, New York: IEEE Press, 1989.

23. Dunning, John W. Jr. "Space Station Power System Requirements." In *23rd Intersociety Energy Conversion Engineering Conference, Vol. 3*, pages 29-36, New York: The American Society of Mechanical Engineers, 1988.

24. *Electron Beam Welding*. Product Catalog, Wentgate Dynaweld Inc. Agawam MA, undated.

25. Engquist, Richard D. "Parameters Affecting Electron Beam Welding," *Metals Engineering Quarterly*, pages 56-63 (November 1968).

26. Fagan, Thomas L. and Myron A. Wilson. "Maintainability in Space-A Survey," *IEEE Transactions on Reliability, R-16*:52-61 (May 1967).

27. Gebhart, Benjamin. *Heat Transfer*. New York: McGraw-Hill Book Company, Inc., 1961.

28. Gimarc, J. Alex. *Report on Space Shuttle External Tank Applications*. Princeton, NJ: Space Studies Institute, December 1985.

29. Glaser, Peter E. "Space Manufacturing Facilities (Space Colonies)." In *Proceedings of the Princeton/AIAA/NASA Conference*, pages 115–128, New York: American Institute of Aeronautics and Astronautics, 1977.

30. Grant, Eugene L. and others. *Principles of Engineering Economy*. New York: John Wiley & Sons, 1990.

31. Hanak, Joseph J. and others. "Deployable Aerospace PV Array Based on Amorphous Silicon Alloys." In *NASA Conference Publication 3030, Space Photovoltaic Research and Technology 1988*, pages 162–163, NASA, 1989.

32. Hastings, D. E. and Manuel Martinez-Sanchez. "A Systems Study of a 100 kW Electrodynamic Tether." In *Advances in the Astronautical Sciences, Vol. 62: Tethers in Space*, pages 341–366, San Diego: American Astronautical Society, 1987.

33. Hill, Douglas J. and John N. Warfield. "Unified Program Planning," *IEEE Transactions on Systems, Man, and Cybernetics*, smc-2:610–621 (November 1972).

34. Hoberecht, Mark A., SSF PV Power Module Design Engineer. Telephone interview. NASA Lewis Research Center, Cleveland, OH, 7 August 1990.

35. Hofacker, Scott A. and Bernard J. Schroer. "Issues Associated with Telerobotic Systems in Space." In *3rd Conference on Artificial Intelligence for Space Applications, Part I*, pages 59–64, Washington, D. C.: U. S. Government Printing Office, November 1987.

36. Hoffman, D. and others. "Space Station Freedom Power: A Reliability, Availability, and Maintainability Assessment of the Proposed Space Station Freedom Electric Power System." In *24th Intersociety Energy Conversion Engineering Conference, Vol. 1*, pages 271–276, New York: IEEE Press, 1989.

37. Iles, P. A. "Space Solar Cells-The Moving Target." In *23rd Intersociety Energy Conversion Engineering Conference, Vol. 3*, pages 75–78, New York: The American Society of Mechanical Engineers, 1988.

38. Jaffe, L. and others. "Nuclear Reactor Power as Applied to a Space-Based Radar Mission." In *23rd Intersociety Energy Conversion Engineering Conference, Vol. 3*, pages 183–190, New York: The American Society of Mechanical Engineers, 1988.

39. Javidi, S. and others. "Space Station Freedom Power Management and Distribution Design Status." In *24th Intersociety Energy Conversion Engineering Conference, Vol. 1*, pages 309–313, New York: IEEE Press, 1989.

40. Jimenez, Amador P. and Mark A. Hoberecht. "Space Station Freedom Photovoltaic Power Module Design Status." In *24th Intersociety Energy Conversion Engineering Conference, Vol. 1*, pages 277–281, New York: IEEE Press, 1989.

41. Kaput, K. C. and L. R. Lamberson. *Reliability in Engineering Design*. New York: John Wiley & Sons, 1977.

42. Keanini, R. G. and B. Rubinsky. "Plasma Arc Welding under Normal and Zero Gravity," *Welding Journal*, *69*:41–50 (June 1990).

43. Kellock, Brian. "Rollforming That's Out of this World," *Machinery and Production Engineering*, *1*:162–164 (June 1981).

44. Koren, Yoram. *Robotics for Engineers*. New York: McGraw-Hill Book Company, 1985.

45. Kurland, Richard and Paul Stella. "Status of Advanced Photovoltaic Solar Array Program." In *23rd Intersociety Energy Conversion Engineering Conference, Vol. 3*, pages 91–95, New York: The American Society of Mechanical Engineers, 1988.

46. Kurland, Richard M. and Paul Stella. "Advanced Photovoltaic Solar Array Development." In *NASA Conference Publication 3030, Space Photovoltaic Research and Technology 1988*, pages 122–137, NASA, 1989.

47. Kwok, Johnny H. *The Artificial Satellite Analysis Program (ASAP)*. Pasadena, CA: NASA Jet Propulsion Laboratory, 1987.

48. Marshall, Matthew Fisk and others. "Evolutionary Growth for Space Station Freedom Electrical Power System." In *24th Intersociety Energy Conversion Engineering Conference, Vol. 1*, page 257=262, New York: IEEE Press, 1989.

49. Martin Marietta Aerospace. *Space Station Definition and Preliminary Design, WP-01*. Final Study Report NAS8-36525. 1987.

50. Martin Marietta Corp., Michoud Division. *Space Shuttle External Tank System Definition Handbook* (B Edition), Volume I. New Orleans, LA: Martin Marietta Manned Space Systems, August 1987.

51. Martin Marietta Denver Aerospace, Michoud Division. *STS Propellant Scavenging Systems Study*. Final Report NAS8-35614. 1985.

52. Martin Marietta Manned Space Systems. *External Tank Gamma Ray Imaging Telescope Study*. Final Report NAS8-36394. 1987.

53. Martin Marietta Manned Space Systems. *External Tank Gamma Ray Imaging Telescope (ET GRIT), Neutral Buoyancy Simulation Test*. Test Report NAS8-36394. 1988.

54. Martin Marietta Manned Space Systems. *Preliminary Data for On-orbit Utilization of the External Tank*. Preliminary Data. New Orleans, LA: NASA George C. Marshall Space Flight Center, 1988.

55. Martin Marietta Manned Space Systems. *External Tank Gamma Ray Imaging Telescope Study, Phase 4*. Final Report NAS8-36394. Huntsville, AL: NASA Marshall Space Flight Center, 1990.

56. McGraw. Technical Notes. Martin Marietta Manned Space Systems, New Orleans LA, 17July 1990.

57. Meredith, Dale D. and others. *Design and Planning of Engineering Systems.* Englewood Cliffs, NJ: Prentice-Hall, 1985.

58. Metzhower, Edward A. and others. "Electron Beam Welding." In *Metals Handbook*, (Ninth Edition), Volume 6, Metals Park, OH: American Society for Metals, 1983.

59. Miller, Lee and others. "Multi-Mission NiH_2 Battery Cells for the 1990's." In *24th Intersociety Energy Conversion Engineering Conference, Vol. 3*, pages 1387–1393, New York: IEEE Press, 1989.

60. Mills, Michael W. and Richard M. Kurland. "The Impact of Solar Cell Technology on Planar Solar Array Performance." In *NASA Conference Publication 3030, Space Photovoltaic Research and Technology 1988*, pages 111–121, NASA, 1989.

61. Miner, Maj Dennis D. *Orbital Analysis of a STS External Tank in Low Earth Orbit.* MS thesis, AFIT/GA/AA/87D-4, ENG, Wright-Patterson AFB OH, December 1987 (AD-A188829).

62. Nahra, Henry K. "Assessment of the Effects of Space Debris and Meteoroids on the Space Station Solar Array Assembly." In *Twentieth IEEE Photovoltaic Specialists Conference - 1988, Vol. 2*, pages 868–873, New York: IEEE Press, 1988.

63. Nahra, Henry K. "Review of the Environmental Effects on the Space Station Freedom Photovoltaic Power Module." In *24th Intersociety Energy Conversion Engineering Conference, Vol. 1*, pages 355–360, New York: IEEE Press, 1989.

64. NASA. *Results of the ACCESS Space Construction Shuttle Flight Experiment.* AIAA Space Systems Technology Conference Paper 86-1186 CP. jun 1986.

65. NASA. *EASE, Experimental Assembly of Structures in EVA.* Conference Publication 2490. oct 1987.

66. NASA. *EVA Catalog Tools and Equipment.* Technical Report JSC-20466 Rev A. Houston TX: NASA, apr 1989.

67. NASA. *Space Station Freedom Electric Power System, Work Package 04 (WP-04), Power System Description Document.* Technical Report Contract NAS3-25082, Document # RI/RD88-633. Canoga Park CA: Rockwell International, 13 February 1990.

68. NASA George C. Marshall Spaceflight Center. *Space Station Cost Model.* Technical Brief No. 38. Huntsville, AL: PRC Systems Services Company, 1977.

69. Negley, Gerald H. and others. "A Three Solar Cell System Based on a Self-Supporting Transparent AlGaAs Top Solar Cell." In *NASA Conference Publication 3030, Space Photovoltaic Research and Technology 1988*, pages 190–200, NASA, 1989.

70. Niswonger, C. Rollin and Philip E. Fess. *Accounting Principles*. Cincinnati OH: South-Western Publishing Co., 1977.

71. Olsen, Larry C. and others. "Investigation of High Efficiency GaAs Solar Cells." In *NASA Conference Publication 3030, Space Photovoltaic Research and Technology 1988*, pages 203–220, NASA, 1989.

72. Otzinger, Burton M. and James R. Wheeler. "Common Pressure Vessel Nickel Hydrogen Battery Development." In *24th Intersociety Energy Conversion Engineering Conference, Vol. 3*, pages 1381–1386, New York: IEEE Press, 1989.

73. Patel, Saroj, Cost Analysis Division. Facsimile message. NASA George C. Marchall Spaceflight Center, Huntsville AL, 12 July 1990.

74. Powers, D. E. and G. R. Laflamme. "EBW vs. LBW - A Comparative Look at the Cost and Performance Traits of Both Processes," *Welding Journal*, 67:25–31 (March 1988).

75. Pritsker, A. Alan B. *Introduction to Simulation and SLAM II* (Third Edition). New York: John Wiley and Sons, 1986.

76. Proust, E. and others. "Space Nuclear Power Studies in France-Overview of the ERATO Program." In *23rd Intersociety Energy Conversion Engineering Conference, Vol. 3*, pages 191–196, New York: The American Society of Mechanical Engineers, 1988.

77. Quigley, M. B. C. "High-Power Density Welding." In Lancaster, J. F., editor, *The Physics of Welding*, Oxford, England: Pergamon Press, 1986.

78. Rieker, Lorra L. and others. "Space Station Freedom Electrical Power System Hardware Commonality with the United States Polar Platform." In *24th Intersociety Energy Conversion Engineering Conference, Vol. 1*, pages 263–270, New York: IEEE Press, 1989.

79. Rocketdyne. *Electric Power System*. Specifications Bulletin 571-M-82. Rockwell International, Rocketdyne Division, Canoga Park CA, May 1990.

80. Rose, M. Frank. "Specific Issues Associated With High Power Levels In Space." In *24th Intersociety Energy Conversion Engineering Conference, Vol. 1*, pages 347–354, New York: IEEE Press, 1989.

81. Sage, Andrew P. "A Case for a Standard for Systems Engineering Methodology," *IEEE Transactions on Systems, Man, and Cybernetics*, smc-7:499–504 (1977).

82. Sage, Andrew P. *Methodology for Large Scale Systems*. New York: McGraw-Hill Book Company, 1977.

83. Schulze, N. R. "NASA Flight Cell and Battery Issues." In *24th Intersociety Energy Conversion Engineering Conference, Vol. 3*, pages 1423–1428, New York: IEEE Press, 1989.

84. Shifrin, Carole A. and others. "NASA to Evaluate Two Suit Designs for Space Station," *Aviation Week & Space Technology*, pages 36–39 (11 January 1988).

85. Simons, Stephen N., EPS Energy Storage and Thermal Control System Design Engineer. Telephone interview. NASA Lewis Research Center, Cleveland, OH, 7 August 1990.

86. Simons, Stephen N. and others. "Energy Storage and Thermal Control System Design Status." In *24th Intersociety Energy Conversion Engineering Conference, Vol. 1*, pages 289–294, New York: IEEE Press, 1989.

87. Spitzer, Mark B. and Stan M. Vernon. "Workshop Summary: Indium Phosphide Cells." In *NASA Conference Publication 3030, Space Photovoltaic Research and Technology 1988*, pages 351–352, NASA, 1989.

88. Stella, Paul M. "Workshop Summary: Ultralightweight (ULW) Photovoltaic Technology." In *NASA Conference Publication 3030, Space Photovoltaic Research and Technology 1988*, pages 356–360, NASA, 1988.

89. Stern, Theodore G. "Lightweight Solar Arrays for High Radiation Environments." In *23rd Intersociety Energy Conversion Engineering Conference, Vol. 3*, pages 127–129, New York: The American Society of Mechanical Engineers, 1988.

90. Stone, William C. and Christoph Witzgall. "Evaluation of Aerodynamic Drag and Torque for External Tanks in Low Earth Orbit." In *Proceedings of the National Institute of Standards and Technology*, pages 37–46, 1988.

91. Syomyatikov, V. S. *Spacecraft Docking Devices*. Princeton NJ: Space Studies Institute (translation), 1990.

92. Team, ASSET Design. Critical Design Review Critique. Air Force Institute of Technology, WPAFB OH, 11October 1990.

93. Thomas, Ronald L. and George J. Hallinan. "Design of the Space Station Freedom Power System." In *24th Intersociety Energy Conversion Engineering Conference, Vol. 1*, pages 245–250, New York: IEEE Press, 1989.

94. Thompson Rumo Wooldridge, Inc. *Sunflower Solar Collection*. Contract NAS 5-462, Cleveland OH: National Aeronautics and Space Administration, May 1964.

95. Tracy, John and Joseph Wise. "Space Solar Cell Performance for Advanced GaAs and Si Solar Cells." In *Twentieth IEEE Photovoltaic Specialists Conference - 19888, Vol. 2*, pages 841–847, New York: IEEE Press, 1988.

96. Vaidyanathan, H. "Effect of Design Variables on the Cycling Characteristics of NiH$_2$ Cells." In *24th Intersociety Energy Conversion Engineering Conference, Vol. 3*, pages 1405–1409, New York: IEEE Press, 1989.

97. Vernon, S. M. and others. "High Efficiency GaAs-Ge Tandem Solar Cells Grown by MOCVD." In *NASA Conference Publication 3030, Space Photovoltaic Research and Technology 1988*, pages 167–176, NASA, 1989.

98. Yang, T. M. and others. "An 83 AH Ni-H$_2$ Battery for Geosynchronous Satellite Applications." In *24th Intersociety Energy Conversion Engineering Conference, Vol. 3*, pages 1375–1379, New York: IEEE Press, 1989.

99. Yeh, Milton and others. "Status of GaAs Solar Cell Production." In *NASA Conference Publication 3030, Space Photovoltaic Research and Technology 1988*, pages 267–271, NASA, 1989.

REPORT DOCUMENTATION PAGE

Public reporting burden for this collection of information is estimated to average 1 hour per response, including the time for reviewing instructions, searching existing data sources, gathering and maintaining the data needed, and completing and reviewing the collection of information. Send comments regarding this burden estimate or any other aspect of this collection of information, including suggestions for reducing this burden, to Washington Headquarters Services, Directorate for Information Operations and Reports, 1215 Jefferson Davis Highway, Suite 1204, Arlington, VA 22202-4302, and to the Office of Management and Budget, Paperwork Reduction Project (0704-0188), Washington, DC 20503

1. AGENCY USE ONLY (Leave blank)	2. REPORT DATE December 1990	3. REPORT TYPE AND DATES COVERED Master's Thesis

4. TITLE AND SUBTITLE

An Aluminum Salvage Station for the External Tank (ASSET)

5. FUNDING NUMBERS

6. AUTHOR(S)

James N. Haislip, Jr., Capt, USAF; Roger E. Linscott, Capt, USAF; William C. Raynes, Jr., Capt, USA; Michael A. Skinner, Capt, USAF; David L. Van Matre, Capt, USAF

7. PERFORMING ORGANIZATION NAME(S) AND ADDRESS(ES)

Air Force Institute of Technology, WPAFB OH 45433-6583

8. PERFORMING ORGANIZATION REPORT NUMBER

AFIT/GSE/ENY/90D-2

9. SPONSORING/MONITORING AGENCY NAME(S) AND ADDRESS(ES)

Space Studies Institute, P.O. Box 82, Princeton, NJ 08542

10. SPONSORING/MONITORING AGENCY REPORT NUMBER

11. SUPPLEMENTARY NOTES

12a. DISTRIBUTION/AVAILABILITY STATEMENT

Approved for Public Release; Distribution Unlimited.

12b. DISTRIBUTION CODE

13. ABSTRACT (Maximum 200 words)

Abstract

The external tank is currently the only non-reusable portion of the National Space Transportation System. The tank has 98% of the energy required to be placed in orbit at the point it is jettisoned. The purpose of this study is to develop techniques which would transform this throw-away item into a source of construction material at low earth orbit.

A simulation is developed to verify the reduction timelines and peak power requirements for manual and automated reduction. The required tools to accomplish the tasks of initial cutting, product transport, spray on foam insulation removal, and product storage are developed. A trade study is conducted to determine the proposed method of power generation. Orbit models are developed to predict the orbital decay of the facility and its annual fuel requirements. A thermal model is developed and the thermal impacts of on-orbit salvage are investigated for three scenarios.

A probabilistic cost model is developed and life cycle costs are projected based upon reducing four tanks per year. It is shown that more than 52,000 lbs of readily usable construction material in the form of I-beams and plate can be salvaged annually, and is cost competitive compared to equivalent products launched from earth.

14. SUBJECT TERMS

Systems Engineering, Space Systems, Multidisciplinary Modeling, External Tank, Space Development, Space Construction, Space Platforms

15. NUMBER OF PAGES
390

16. PRICE CODE

17. SECURITY CLASSIFICATION OF REPORT	18. SECURITY CLASSIFICATION OF THIS PAGE	19. SECURITY CLASSIFICATION OF ABSTRACT	20. LIMITATION OF ABSTRACT
Unclassified	Unclassified	Unclassified	UL